

Appendix of “Integration of Preferences in Decomposition Multi-Objective Optimization”

APPENDIX A PROOF OF THEOREM 1

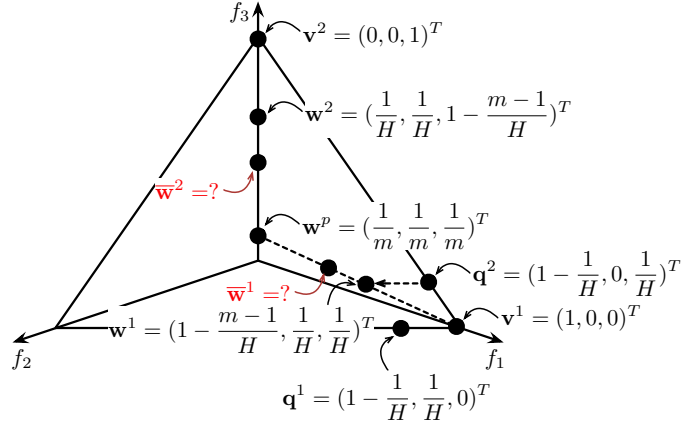


Fig. 1: Illustrative example for η computation.

Proof: Let us use a specific example shown in Fig. 1 to prove this theorem. Suppose the reference points are originally generated by the Das and Dennis’s method [1]. Therefore, reference points are distributed on an unit m -simplex. Let the centroid of this simplex, i.e., $w^p = (\frac{1}{m}, \dots, \frac{1}{m})^T$, be the pivot point. Let us consider $v^1 = (1, 0, 0)^T$ and $v^2 = (0, 0, 1)^T$ as two vertices of an edge of this simplex. Obviously, the length of each edge of this simplex is the same, i.e., $\|v^1 - v^2\| = \sqrt{2}$. Suppose w^1 and w^2 are two reference points inside this simplex and closest to v^1 and v^2 . Since reference points are generated in a structured manner, we can use a geometric method to find the coordinates of w^1 and w^2 . As shown in Fig. 1, q^1 and q^2 are two reference points lying on the two edges and closest to v^1 . Obviously, w^1 is a linear combination of v^1 , q^1 and q^2 as:

$$w_i^1 = (q_i^2 - v_i^1) + q_i^1 \quad (1)$$

where $i \in \{1, \dots, m\}$. In summary, we can have $w^1 = (1 - \frac{m-1}{H}, \dots, \frac{1}{H})^T$ and $w^2 = (\frac{1}{H}, \dots, 1 - \frac{m-1}{H})^T$. Based on our non-uniform mapping scheme, we have the new locations of w^1 and w^2 can be calculated as:

$$\bar{w}^i = w^p + t \times u^i \quad (2)$$

where $i \in \{1, 2\}$, $u^i = \frac{v^i - w^p}{\|v^i - w^p\|}$ and

$$t = d - d(\frac{d - D}{d})^{\frac{1}{\eta+1}} \quad (3)$$

where $d = \|v^i - w^p\|$ and $D = \|w^i - w^p\|$. Let $q = \frac{d-D}{d}$, we have:

$$t = d(1 - q^{\frac{1}{\eta+1}}) \quad (4)$$

In order to have the extent of ROI become size of τ of the EF, we have the following equation:

$$\frac{\|\bar{w}^1 - \bar{w}^2\|}{\|v^1 - v^2\|} = \tau \quad (5)$$

Since $\|v^1 - v^2\| = \sqrt{2}$, we have:

$$\|\bar{w}^1 - \bar{w}^2\| = \sqrt{2}\tau \quad (6)$$

Using equation (2) to substitute \bar{w}^1 and \bar{w}^2 in equation (6), we have:

$$\|t \times (u^1 - u^2)\| = \sqrt{2}\tau \quad (7)$$

Using equation (4) to substitute t in equation (7), we have:

$$d(1 - q^{\frac{1}{\eta+1}}) \times \|\mathbf{u}^1 - \mathbf{u}^2\| = \sqrt{2}\tau \quad (8)$$

By substitution, we have:

$$\begin{aligned} (1 - q^{\frac{1}{\eta+1}}) \times \|\mathbf{v}^1 - \mathbf{v}^2\| &= \sqrt{2}\tau \\ \implies q^{\frac{1}{\eta+1}} &= 1 - \tau \\ \implies \eta &= \frac{\log q}{\log(1 - \tau)} - 1 \end{aligned} \quad (9)$$

Since the coordinates of \mathbf{v}^1 , \mathbf{w}^1 and \mathbf{w}^p are known, we have:

$$\begin{aligned} d &= \sqrt{(1 - \frac{1}{m})^2 + (m - 1)\frac{1}{m^2}} \\ &= \sqrt{1 - \frac{1}{m}} \end{aligned} \quad (10)$$

and

$$\begin{aligned} D &= \sqrt{\left(1 - \frac{m-1}{H} - \frac{1}{m}\right)^2 + (m-1)\left(\frac{1}{m} - \frac{1}{H}\right)^2} \\ &= \sqrt{1 - \frac{1}{m}(1 - \frac{m}{H})} \\ &= (1 - \frac{m}{H})d \end{aligned} \quad (11)$$

Based on equation (10) and equation (11), we have:

$$\begin{aligned} q &= \frac{d - D}{d} \\ &= \frac{d - (1 - \frac{m}{H})d}{d} \\ &= \frac{m}{H} \end{aligned} \quad (12)$$

■

APPENDIX B PROOF OF COROLLARY 1

Proof: As discussed in Section III-D, we should set $\eta > 0$ in the NUMS. Thus, based on Theorem 1, we have:

$$\frac{\log \frac{m}{H}}{\log(1 - \tau)} > 1 \quad (13)$$

Since $\frac{m}{H} < 1$ and $1 - \tau < 1$, we have:

$$\log \frac{m}{H} \leq \log(1 - \tau) \implies 0 < \tau < 1 - \frac{m}{H} \quad (14)$$

■

APPENDIX C PROOF OF COROLLARY 2

Proof: The proof of this corollary is similar to the Theorem 1. Let us use Fig. 1 for illustration again. As for the reference points \mathbf{w}^1 and \mathbf{w}^2 , we should have the following relationship after the non-uniform mapping:

$$\frac{\|\bar{\mathbf{w}}^1 - \bar{\mathbf{w}}^2\|}{\|\mathbf{w}^1 - \mathbf{w}^2\|} = \tau \quad (15)$$

Since $\|\mathbf{w}^1 - \mathbf{w}^2\| = \sqrt{2}(1 - \frac{m}{H})$, we have:

$$\|\bar{\mathbf{w}}^1 - \bar{\mathbf{w}}^2\| = \sqrt{2}(1 - \frac{m}{H})\tau \quad (16)$$

Using equation (2) to substitute $\bar{\mathbf{w}}^1$ and $\bar{\mathbf{w}}^2$ in equation (16), we have:

$$\|t \times (\mathbf{u}^1 - \mathbf{u}^2)\| = \sqrt{2}(1 - \frac{m}{H})\tau \quad (17)$$

Using equation (4) to substitute t in equation (17), we have:

$$d(1 - q^{\frac{1}{\eta+1}}) \times \|\mathbf{u}^1 - \mathbf{u}^2\| = \sqrt{2}(1 - \frac{m}{H})\tau \quad (18)$$

Since $\|\mathbf{v}^1 - \mathbf{v}^2\| = \sqrt{2}$, by substitution, we have:

$$\begin{aligned} 1 - q^{\frac{1}{\eta+1}} &= (1 - \frac{m}{H})\tau \\ \implies \eta &= \frac{\log q}{\log[1 - (1 - \frac{m}{H})\tau]} - 1 \end{aligned} \quad (19)$$

where $q = \frac{m}{H}$ according to equation (12). ■

APPENDIX D PROOF OF COROLLARY 3

Proof: Since $\eta > 0$, according to equation (19), we have:

$$\frac{\log q}{\log[1 - (1 - \frac{m}{H})\tau]} > 1 \quad (20)$$

Since $\frac{m}{H} < 1$ and $1 - (1 - \frac{m}{H})\tau < 1$, we have:

$$\log \frac{m}{H} < \log[1 - (1 - \frac{m}{H})\tau] \implies 0 < \tau < 1 \quad (21) \quad \blacksquare$$

APPENDIX E
PARAMETER SETTINGS

TABLE I: Settings of Aspiration Level Vector

Problem	m	Unattainable	Attainable
DTLZ1	2	(0.3,0.5) T	(0.5,0.6) T
	3	(0.05,0.05,0.2) T	(0.3,0.3,0.2) T
	5	(0.05,0.05,0.1,0.08,0.03) T	(0.2,0.1,0.1,0.3,0.4) T
	8	(0.01,0.02,0.07,0.02,0.06,0.2,0.1,0.01) T	(0.1,0.2,0.1,0.4,0.4,0.1,0.3,0.1) T
	10	(0.02,0.01,0.06,0.04,0.04,0.01,0.02,0.03,0.05,0.08) T	(0.05,0.1,0.1,0.05,0.1,0.2,0.08,0.03,0.3,0.1) T
DTLZ2-4	2	(0.65,0.7) T	(0.75,0.75) T
	3	(0.2,0.5,0.6) T	(0.7,0.8,0.5) T
	5	(0.3,0.1,0.4,0.2,0.3) T	(0.7,0.6,0.3,0.8,0.5) T
	8	(0.3,0.1,0.4,0.25,0.1,0.15,0.4,0.25) T	(0.6,0.5,0.75,0.2,0.3,0.55,0.7,0.6) T
	10	(0.1,0.1,0.3,0.4,0.2,0.5,0.25,0.15,0.1,0.4) T	(0.3,0.3,0.3,0.1,0.3,0.55,0.35,0.35,0.25,0.45) T
WFG41	2	(0.65,0.7) T	(0.75,0.75) T
	3	(0.2,0.5,0.6) T	(0.7,0.8,0.5) T
	5	(0.3,0.1,0.4,0.2,0.3) T	(0.7,0.6,0.3,0.8,0.5) T
	8	(0.3,0.1,0.4,0.25,0.1,0.15,0.4,0.25) T	(0.6,0.5,0.75,0.2,0.3,0.55,0.7,0.6) T
	10	(0.1,0.1,0.3,0.4,0.2,0.5,0.25,0.15,0.1,0.4) T	(0.3,0.3,0.3,0.1,0.3,0.55,0.35,0.35,0.25,0.45) T
WFG42	2	(0.5,0.1) T	(0.6,0.15) T
	3	(0.05,0.05,0.2) T	(0.15,0.15,0.25) T
	5	(0.03,0.04,0.08,0.04,0.04) T	(0.1,0.05,0.1,0.05,0.05) T
	8	(0.01,0.02,0.03,0.01,0.01,0.05,0.01,0.01) T	(0.2,0.2,0.1,0.3,0.05,0.15,0.2,0.15) T
	10	(0.005,0.002,0.005,0.005,0.008,0.005,0.002,0.002,0.001,0.005) T	(0.3,0.3,0.5,0.3,0.5,0.45,0.25,0.35,0.25,0.4) T
WFG43	2	(0.9,0.8) T	(0.95,0.93) T
	3	(0.6,0.8,0.8) T	(0.95,0.95,0.85) T
	5	(0.4,0.4,0.5,0.4,0.4) T	(0.5,0.7,1,0.9,0.6) T
	8	(0.4,0.4,0.5,0.4,0.4,0.5,0.6,0.5) T	(0.95,1,1,0.95,0.8,0.95,0.95,1) T
	10	(0.5,0.2,0.4,0.3,0.4,0.5,0.6,0.7,0.6,0.7) T	(1,0.85,1,0.95,0.85,0.95,0.95,1,0.8,0.9) T
WFG44	2	(0.008,0.006) T	(0.009,0.008) T
	3	(0.0004,0.0004,0.0003) T	(0.001,0.0001,0.0005) T
	5	(5e-06,1e-05,1e-05,1e-05,5e-06) T	(0.0005,0.001,0.0003,0.0006,0.0008) T
	8	(5e-06,1e-06,1e-06,1.5e-06,5e-07,1e-06,5e-07,2e-07) T	(0.001,0.0015,0.002,0.002,0.003,0.003,0.002,0.001) T
	10	(2e-06,8e-07,3e-07,3e-07,7e-07,1e-07,2e-08,2e-07,5e-07,2e-07) T	(0.0015,0.002,0.002,0.001,0.0015,0.002,0.002,0.003,0.003,0.002) T
WFG45	2	(0.7,0.45) T	(0.75,0.5) T
	3	(0.3,0.7,0.3) T	(0.5,0.8,0.5) T
	5	(0.6,0.3,0.3,0.3,0.3) T	(0.8,0.5,0.4,0.5,0.5) T
	8	(0.2,0.3,0.3,0.3,0.3,0.2,0.1,0.2) T	(0.8,0.5,0.4,0.5,0.5,0.7,0.7,0.9) T
	10	(0.2,0.15,0.15,0.2,0.1,0.15,0.05,0.1,0.1,0.2) T	(0.9,0.65,0.6,0.5,0.55,0.8,0.8,0.9,0.5,0.55) T
WFG46	2	(0.55,0.4) T	(0.65,0.5) T
	3	(0.3,0.25,0.3) T	(0.35,0.35,0.4) T
	5	(0.1,0.1,0.2,0.1,0.15) T	(0.2,0.3,0.4,0.2,0.3) T
	8	(0.1,0.08,0.05,0.1,0.05,0.1,0.05,0.2) T	(0.2,0.5,0.3,0.2,0.3,0.1,0.1,0.2) T
	10	(0.05,0.08,0.05,0.02,0.05,0.04,0.05,0.08,0.1,0.05) T	(0.25,0.5,0.35,0.5,0.35,0.6,0.5,0.5,0.4,0.35) T
WFG47	2	(0.4,0.45) T	(0.5,0.5) T
	3	(0.7,0.4,0.4) T	(0.9,0.5,0.6) T
	5	(0.5,0.3,0.3,0.3,0.2) T	(0.8,0.4,0.5,0.4,0.6) T
	8	(0.08,0.15,0.1,0.1,0.12,0.1,0.1,0.1) T	(0.5,0.4,0.7,0.4,0.8,0.8,0.75,0.7) T
	10	(0.05,0.05,0.1,0.1,0.05,0.08,0.05,0.05,0.03,0.05) T	(0.6,0.35,0.75,0.6,0.85,0.8,0.75,0.7,0.7,0.8) T
WFG48	2	(0.6,0.4) T	(0.7,0.5) T
	3	(0.25,0.2,0.1) T	(0.35,0.3,0.2) T
	5	(0.05,0.08,0.05,0.06,0.05) T	(0.1,0.2,0.08,0.15,0.1) T
	8	(0.02,0.03,0.02,0.01,0.02,0.03,0.04,0.03) T	(0.15,0.25,0.35,0.45,0.15,0.45,0.35,0.25) T
	10	(0.005,0.008,0.01,0.01,0.02,0.03,0.04,0.03,0.02,0.01) T	(0.25,0.45,0.3,0.6,0.2,0.5,0.35,0.5,0.6,0.7) T

TABLE II: Settings of Number of Function Evaluations (FEs), N is the population size

Problem	m	# of FEs	Problem	m	# of FEs
DTLZ1	3	$400 \times N$	DTLZ3	3	$1000 \times N$
	5	$1000 \times N$		5	$1200 \times N$
	8	$1200 \times N$		8	$1500 \times N$
	10	$1500 \times N$		10	$1800 \times N$
DTLZ2	3	$250 \times N$	DTLZ4	3	$600 \times N$
	5	$800 \times N$		5	$1200 \times N$
	8	$1000 \times N$		8	$1500 \times N$
	10	$1360 \times N$		10	$1800 \times N$
WFG41-WFG48	2	$400 \times N$			
	3	$400 \times N$			
	5	$1000 \times N$			
	8	$1200 \times N$			
	10	$1500 \times N$			

APPENDIX F
DESCRIPTION OF STATISTICAL ANALYSIS FRAMEWORK

In this work, we employ the statistical analysis suggested in [2] to validate the statistical significance of the results obtained by different algorithms. Specifically, as shown in Fig. 2, we at first carry out a Kolmogorov-Smirnov test to check whether the results follow a normal distribution or not. If so, we use Levene test to check the homogeneity of the variances. Afterwards, we use ANOVA test to validate the significance if samples are with equal variance; otherwise we use Welch test instead. On the other hand, if the results do not follow a normal distribution, we use Kruskal-Wallis test to compare the median metric values obtained by different algorithms. Note that we set the confidence level as 95% (i.e., significance level of 5% or p -value under 0.05) in the statistical tests.

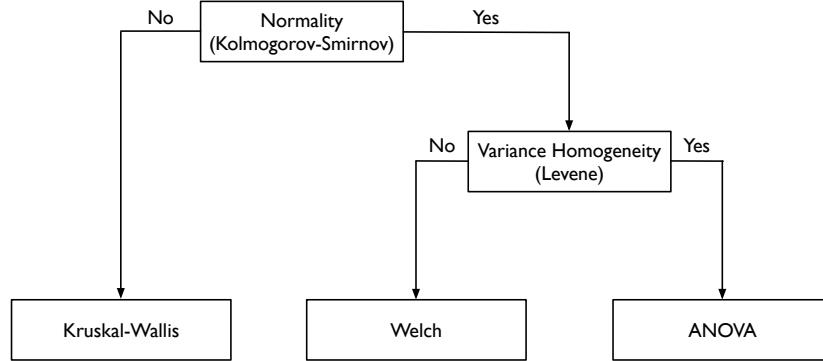


Fig. 2: Statistical analysis framework [2].

APPENDIX G

EXPERIMENTAL RESULTS ON WFG PROBLEMS

WFG41 to WFG48 problems are constructed by applying different shape functions provided in the WFG toolkit to the standard WFG4 problem [3]. Specifically, WFG41 and WFG42 problems have regular concave and convex shapes respectively. From the results shown in Table III and Table IV, and Fig. 35 to Fig. 54 in the supplementary document, we can see that three decomposition-based EMO algorithms obtain the best ROI approximation, in terms of convergence toward the PF and the diversity within the ROI. In addition, the spread of the ROI approximation is also satisfactory according to the DM's expectation. In contrast, the other three preference-based EMO algorithms are not quite comparable. In particular, for WFG42, the solutions obtained by R-NSGA-II and r-NSGA-II stray away from the ROI. Moreover, the performance of g-NSGA-II deteriorates significantly with the increase of the number of objectives.

Different from the previous two problems, WFG43 and WFG44 have strong concave and convex shapes respectively. In particular, they are built by scaling the corresponding shape function with a power $\frac{1}{4}$. As shown in Fig. 55 and Fig. 56 of the supplementary document, all three decomposition-based EMO algorithms find an appropriate ROI approximation with respect to the DM supplied aspiration level vector on WFG43. Although the solutions obtained by g-NSGA-II cover the ROI, their spread is too wide. In contrast, solutions obtained by r-NSGA-II and R-NSGA-II are away from the ROI. However, the performance of g-NSGA-II deteriorate significantly with the increase of the number of objectives. As for WFG44, due to its sharp convex property, all solutions crowded in the knee region. In this case, the extent of the ROI approximated by the three decomposition-based EMO algorithms does not meet the DM's expectation.

WFG45 has a mixed PF shape, which has both concave and convex parts simultaneously. Similar to the observations on WFG43 and WFG44, three decomposition-based EMO algorithms show the most promising performance while the solutions obtained by g-NSGA-II are acceptable when $m = 2$ whereas its performance deteriorate significantly with the increase of dimensionality.

WFG46 has a relatively simple PF shape, which is a hyperplane. All algorithms do not have difficulty in converging toward the PF when the number of objectives is small. However, g-NSGA-II cannot find well converged solutions for the attainable aspiration level vector setting when the number of objectives becomes large. In addition, we also notice that the spread of the ROI approximation obtained by g-NSGA-II is excessively wider than the other peers. Note that g-NSGA-II do not have any control on the extent of the ROI.

Both WFG47 and WFG48 have disconnected concave and convex PF shapes respectively. For the 2-objective WFG47, as shown in Fig. 95 and Fig. 96 of the supplementary document, g-NSGA-II find solutions on the PF segment which is far away from the DM supplied aspiration level vector. For the 2-objective WFG48, as shown in Fig. 105 and Fig. 106 of the supplementary document, solutions obtained by g-NSGA-II do not fully converge to the PF segment. The performance of three decomposition-based EMO algorithms is robust across different aspiration level vector settings. It is interesting to note that r-NSGA-II obtains the best R-HV value on the 2-objective WFG48 with an attainable aspiration level vector setting. As shown in Fig. 106 of the supplementary document, solutions obtained by r-NSGA-II has a slightly wider spread comparing to those obtained by the three decomposition-based EMO algorithms. However, its performance deteriorates with the increase of the number of objectives.

In summary, the experimental results fully demonstrate the effectiveness of the NUMS for assisting the decomposition-based EMO algorithms, where we use MOEA/D-STM, MOEA/D and NSGA-III as the baseline, to approximate the ROIs. In addition, we find that R-NSGA-II is also good at searching for the ROIs for DTLZ problems. However, it cannot find satisfied ROI approximation when tackling WFG problems. In addition, the spread of the preferred solutions of R-NSGA-II and r-NSGA-II is controlled in an ad-hoc manner.

TABLE III: Comparison results of median R-HV values and the IQR obtained by six preference-based EMO algorithms on WFG41 to WFG44 problems with unattainable and attainable aspiration level vectors.

Problem	m	ref	MOEA/D-STM	MOEA/D	NSGA-III	g-NSGA-II	r-NSGA-II	R-NSGA-II
WFG41	2	1	2.4298(5.07E-5)	2.4296(1.27E-6)	2.4296(6.98E-5)	4.2215(5.69E-3) [†]	4.2117(1.32E-1) [†]	4.0174(5.12E-1) [†]
		2	4.5631(2.17E-4)	4.5630(2.55E-6)	4.5630(1.67-2)	4.5628(2.66E-3) [†]	4.5271(8.27E-2) [†]	4.3848(3.33E-1) [†]
	3	1	7.6199(1.66E-2)	7.6124(0.00E+0)	7.6171(5.79E-3)	7.0242(2.20E-1) [†]	7.2876(3.08E-1) [†]	7.0602(5.12E-1) [†]
		2	10.4009(1.37E-2)	10.4005(0.00E+0)	10.3871(1.02E-2)	10.1891(1.71E-1) [†]	10.1288(1.02E+0) [†]	9.9453(3.33E-1) [†]
	5	1	23.8070(1.52E-1)	23.7453(0.00E+0) [†]	23.7291(2.46E-1) [†]	13.6383(1.17E+0) [†]	18.1798(5.23E+0) [†]	19.7685E(1.99E+0) [†]
		2	50.9815(2.50E+0)	52.4696(0.00E+0)	48.9575(2.78E-1)	24.0680(3.76E+0) [†]	33.7121(6.92E+0) [†]	42.4963(3.19E+0) [†]
	8	1	211.5465(1.21E+1) [†]	214.8829(9.02E+0) [†]	226.3126(2.64E+0)	77.3684(2.39E+1) [†]	146.1190(3.38E+1) [†]	50.8910(5.12E+0) [†]
		2	555.5724(3.81E+1) [†]	561.8469(2.98E+1)	432.7265(1.34E+1) [†]	—	325.4018(3.95E+1) [†]	121.6208(1.25E+1) [†]
	10	1	1040.2589(3.56E+1)	1013.6855(5.07E+1) [†]	923.8265(1.42E+1) [†]	304.7739(5.76E+1) [†]	704.5660(1.66E+2) [†]	—
		2	1570.5781(4.67E+1)	1357.7199(5.51E+1) [†]	1275.3521(3.24E+1) [†]	397.6032(8.63E+1) [†]	1182.4211(2.93E+2) [†]	—
WFG42	2	1	4.1574(4.96E-5)	4.1577(2.44E-6)	4.1574(1.85E-6)	4.1063(1.88E-3) [†]	3.1070(3.77E-2) [†]	4.0109(3.20E-1) [†]
		2	4.3817(1.81E-4)	4.3813(7.92E-7)	4.3811(1.23E-5) [†]	4.3431(1.99E-3) [†]	4.1510(1.19E+0) [†]	3.3759(5.56E-2) [†]
	3	1	7.7250(4.34E-3) [†]	7.7283(1.24E-3)	7.7238(1.41E-3) [†]	7.0382(2.21E-1) [†]	6.7867(1.67E-1) [†]	5.5130(3.20E-1) [†]
		2	8.8508(5.77E-3)	8.8504(1.03E-3)	8.8483(1.70E-3) [†]	8.7219(6.06E-1) [†]	7.7817(1.95E-1) [†]	8.9615(1.19E+0) [†]
	5	1	31.5611(7.61E-2)	31.5879(2.31E-2)	32.1921(6.26E-1)	28.6955(2.54E+0) [†]	30.4173(9.88E-1) [†]	25.2410(2.14E+0) [†]
		2	33.7777(6.64E-2)	33.9092(8.76E-2)	34.4050(2.15E-1)	25.6623(1.52E+0) [†]	31.9766(6.78E-1) [†]	30.4631(5.12E-1) [†]
	8	1	253.1978(1.31E+0)	254.1460(1.12E+0)	251.1147(2.80E-1)	200.0911(1.83E+1) [†]	215.1664(8.45E+0) [†]	181.5920(1.11E+1) [†]
		2	318.1471(8.21E-1)	318.9400(8.27E-1)	313.5087(3.82E-1)	—	304.6694(7.32E+0) [†]	125.2891(1.52E+0) [†]
	10	1	5012.3321(1.07E+2)	4958.7847(3.19E+1)	4911.8221(5.14E+1)	755.5785(1.19E+2) [†]	907.1323(3.58E+1) [†]	—
		2	3122.4221(1.14E+2)	3021.1282(8.12E+1)	2912.7725(9.34E+1)	2697.5424(5.80E+1) [†]	2455.2939(3.97E+2) [†]	—
WFG43	2	1	4.1409(1.02E-2)	4.1411(6.96E-6)	4.1409(2.52E-5)	4.1348(5.82E-3) [†]	4.0203(6.24E-3) [†]	3.7845(4.32E-3) [†]
		2	4.4693(6.18E-5)	4.4693(1.17E-5)	4.4692(6.85E-5)	4.3842(2.71E-3) [†]	3.9950(8.52E-2) [†]	4.0001(5.98E-2) [†]
	3	1	7.6676(2.92E-2)	7.6618(3.01E-3) [†]	7.6574(3.93E-3) [†]	7.6264(8.46E-2) [†]	6.6693(5.97E-1) [†]	5.8659(1.87E-1) [†]
		2	9.7480(5.34E-2) [†]	9.6992(4.32E-3) [†]	9.7876(3.83E-3)	9.7212(5.15E-2) [†]	8.5460(6.18E-1) [†]	8.6911(5.12E-1) [†]
	5	1	9.0901(2.29E-2) [†]	10.3782(3.91E-2) [†]	10.5747(1.29E-1)	7.9014(3.90E-1) [†]	8.6955(5.89E-1) [†]	7.6087(2.19E-2) [†]
		2	34.3411(3.09E+0) [†]	36.0054(3.79E+0)	34.3394(1.52E-1) [†]	15.3444(3.70E+0) [†]	34.0859(2.99E+0) [†]	33.4689(5.12E+0) [†]
	8	1	60.6142(2.21E+0)	60.5416(3.64E-1) [†]	60.5910(5.62E+0) [†]	12.6672(4.17E+0) [†]	50.8572(6.04E+0) [†]	15.7898(5.19E+0) [†]
		2	443.5193(5.25E+0) [†]	598.8932(3.74E+1)	497.9952(1.43E+1) [†]	—	382.9223(5.78E+1) [†]	370.8867(2.15E+1) [†]
	10	1	389.5884(9.04E+1) [†]	391.9223(7.21E+1) [†]	418.3354(1.16E+1)	20.9774(3.54E+1) [†]	283.0227(4.04E+1) [†]	—
		2	2981.7520(1.89E+1)	2268.6651(8.72E+1) [†]	2382.3351(9.01E+1) [†]	—	1637.4484(2.91E+2) [†]	—
WFG44	2	1	4.0040(3.21E-5)	4.0040(3.98E-6)	4.0039(3.60E-5)	4.0034(4.50E-5) [†]	4.0031(6.24E-3) [†]	4.0028(5.24E-5) [†]
		2	4.0096(4.60E-4)	4.0100(5.33E-7)	4.0099(4.60E-4)	4.0070(4.02E-5) [†]	4.0093(3.79E-3)	4.0098(6.31E-5)
	3	1	8.0004(1.70E-5)	8.0004(1.10E-5)	8.0004(1.50E-5)	—	7.9805(2.15E-4) [†]	8.0000(2.78E-4) [†]
		2	8.0022(9.20E-5)	8.0022(1.13E-8)	8.0022(1.36E-4)	—	7.9940(5.36E-4) [†]	—
	5	1	31.9997(2.00E-5)	31.9997(1.60E-5)	31.9999(1.36E-4)	31.9304(2.23E-1) [†]	31.9579(1.98E-3) [†]	31.0422(2.41E-5) [†]
		2	32.0239(1.46E-6)	32.0239(1.60E-5)	32.0243(6.24E-4)	—	32.0057(6.18E-3) [†]	32.0192(1.82E-4) [†]
	8	1	255.9988(3.41E-5)	255.9988(4.12E-4)	255.9988(2.15E-4)	—	245.9537(4.14E-2) [†]	—
		2	257.0258(5.12E-5)	257.0258(4.52E-4)	257.0258(4.01E-4)	—	—	—
	10	1	1023.9980(5.12E-5)	1023.9980(6.15E-5)	1023.9980(6.12E-5)	—	—	—
		2	1029.1315(4.52E-5)	1029.1315(5.17E-4)	1029.1315(6.20E-5)	—	—	—

[†] denotes the best median metric value is significantly better than the other peers according to the statistical analysis described in Appendix F of the supplementary document. ref = 1 means the unattainable aspiration level vector while ref = 2 means the attainable aspiration level vector. — means all solutions obtained by the corresponding algorithm are dominated by the other counterparts, thus no solution can be used for R-HV computation.

TABLE IV: Comparison results of median R-HV values and the IQR obtained by six preference-based EMO algorithms on WFG45 to WFG48 problems with unattainable and attainable aspiration level vectors.

Problem	m	ref	MOEA/D-STM	MOEA/D	NSGA-III	g-NSGA-II	r-NSGA-II	R-NSGA-II
WFG45	2	1	4.1226(1.84E-5)	4.1227(2.14E-6)	4.1224(1.81E-2)	4.1184(6.24E-3) [†]	3.9696(1.09E-1) [†]	3.9797(1.20E-2) [†]
		2	4.3076(9.20E-5)	4.3076(6.72E-6)	4.3075(2.51E-5)	4.3058(6.95E-3) [†]	4.1388(1.31E-1) [†]	4.1935(4.12E-2) [†]
	3	1	7.9929(4.09E-2) [†]	8.0422(1.05E-7)	8.0091(5.65E-2) [†]	7.6983(1.86E-1) [†]	6.3118(2.27E-1) [†]	6.3916(4.12E-1) [†]
		2	10.0080(2.65E-2) [†]	10.0167(1.08E-8)	10.0049(1.61E-2) [†]	9.8311(1.33E-1) [†]	8.6045(2.03E-1) [†]	8.6955(1.92E-1) [†]
	5	1	32.9969(1.57E-1)	32.5638(4.44E-1) [†]	32.4787(1.18E-1) [†]	13.9932(1.61E+0) [†]	21.4709(1.38E+0) [†]	19.0242(2.19E+0) [†]
		2	50.1882(5.22E-1)	50.0938(6.77E-1) [†]	50.1626(2.95E-1) [†]	15.1340(3.48E+0) [†]	36.7563(9.49E-1) [†]	32.8139(4.19E+0) [†]
	8	1	206.9412(7.04E+0) [†]	215.0497(9.00E+0)	208.4627(5.53E+0) [†]	55.1598(1.14E+1) [†]	85.4227(2.07E+1) [†]	65.1287(3.00E+1) [†]
		2	881.3934(1.09E+2) [†]	885.3012(9.41E+1)	762.7465(1.24E+1) [†]	—	679.4919(7.59E+1) [†]	565.8972(1.11E+1) [†]
	10	1	504.2658(2.17E+1) [†]	510.6926(3.81E+1)	502.7624(7.64E+0) [†]	136.4298(4.30E+1) [†]	229.8957(4.77E+1) [†]	—
		2	5166.8933(1.29E+2)	5127.3900(4.12E+2) [†]	5165.4071(8.31E+1) [†]	—	3862.8323(4.54E+2) [†]	—
WFG46	2	1	4.2529(1.07E-4)	4.2525(1.01E-6)	4.2529(6.04E-5)	4.2390(3.56E-3) [†]	4.2424(4.07E-2) [†]	4.1165(4.12E-2) [†]
		2	4.6540(1.77E-5)	4.6540(1.05E-6)	4.6539(1.07E-4)	4.6058(3.70E-3) [†]	4.5891(1.53E-2) [†]	4.5535(1.23E-2) [†]
	3	1	8.1923(7.69E-3) [†]	8.1943(0.00E+0)	8.1895(3.61E-3) [†]	7.9882(2.60E-1) [†]	8.0084(3.37E-1) [†]	8.0927(3.15E-1) [†]
		2	9.2414(6.06E-3) [†]	9.2460(0.00E+0)	9.2339(2.66E-3) [†]	9.0906(2.26E-1) [†]	9.1799(1.41E-1) [†]	8.3755(1.52E-1) [†]
	5	1	28.6674(1.29E-1) [†]	28.9272(3.50E-1) [†]	29.1393(8.20E-1)	20.4895(1.56E+0) [†]	25.5624(2.15E+0) [†]	19.4437(1.52E+0) [†]
		2	41.5600(1.69E-1) [†]	41.7071(3.12E-1)	41.3900(7.96E-1) [†]	20.7724(2.39E+0) [†]	35.3240(1.26E+0) [†]	33.1124(2.11E+0) [†]
	8	1	245.8676(1.82E+0) [†]	250.8208(2.91E+0)	238.0273(1.07E+0) [†]	114.1802(1.47E+1) [†]	195.0574(4.26E+1) [†]	131.5928(3.19E+1) [†]
		2	359.3627(1.64E+1) [†]	380.4842(3.16E+1)	349.0137(7.11E+0) [†]	—	333.9457(1.02E+1) [†]	285.2951(5.21E+0) [†]
	10	1	953.4312(6.86E+0)	947.1682(6.30E+0) [†]	854.2753(1.38E+0) [†]	367.5474(1.09E+2) [†]	332.0280(1.80E+2) [†]	—
		2	3565.0137(1.45E+2) [†]	3766.2139(2.36E+2)	3078.1682(1.02E+1) [†]	—	2591.9254(4.67E+2) [†]	—
WFG47	2	1	4.0063(2.81E-3) [†]	4.0091(2.84E-3) [†]	4.0114(6.01E-5)	3.9420(2.12E-3) [†]	4.0043(6.36E-3) [†]	3.9781(5.82E-3) [†]
		2	4.1728(2.09E-5) [†]	4.1729(6.03E-3) [†]	4.1794(3.82E-2)	4.0455(1.64E-3) [†]	4.1703(6.96E-3) [†]	4.1655(6.12E-3) [†]
	3	1	7.3908(1.56E-1)	7.0188(0.00E+0)	7.2178(1.89E-1)	7.0741(6.86E-1) [†]	7.1013(1.16E-1) [†]	7.0603(2.10E-1)
		2	9.7758(2.13E-1)	9.4688(0.00E+0)	9.9818(2.44E-1)	9.7088(4.74E-2) [†]	9.7477(2.04E-1) [†]	9.5621(5.12E-1) [†]
	5	1	24.8848(5.48E-1) [†]	25.3266(7.69E-1)	24.6731(3.49E-1) [†]	16.5077(1.57E+0) [†]	17.3956(1.51E+0) [†]	15.0582(1.51E+0) [†]
		2	46.6839(2.46E+0)	45.2913(1.81E+0) [†]	44.9970(1.52E+0) [†]	23.6424(3.04E+0) [†]	39.0747(8.82E-1) [†]	44.0194(6.12E-1) [†]
	8	1	92.5835(4.01E+0) [†]	92.2396(7.45E+0) [†]	92.7802(7.61E-1)	30.9631(5.45E+0) [†]	54.4934(5.33E+0) [†]	40.5829(3.15E+0) [†]
		2	690.1867(3.61E+1)	687.1738(9.76E+1) [†]	667.5491(2.24E+1) [†]	—	620.2782(5.00E+1) [†]	420.1125(4.19E+1) [†]
	10	1	179.1392(4.42E+1) [†]	169.1904(3.01E+1) [†]	207.1498(3.10E+1)	34.0169(9.29E+0) [†]	98.6983(9.57E+0) [†]	—
		2	5742.8695(5.60E+2)	5570.3522(5.82E+2) [†]	4070.0848(1.40E+2) [†]	—	3038.5789(4.47E+2) [†]	—
WFG48	2	1	3.8883(1.52E-4) [†]	3.8887(1.51E-6)	3.8884(2.97E-5) [†]	3.7947(2.99E-3) [†]	3.6997(5.75E-2) [†]	3.7239(4.23E-3) [†]
		2	4.2779(2.30E-4) [†]	4.2779(9.27E-7) [†]	4.2784(3.97E-3) [†]	4.2397(2.66E-3) [†]	4.3005(6.16E-3)	4.2501(2.12E-3) [†]
	3	1	8.2294(3.77E-3)	8.2305(3.01E-7)	8.2250(2.49E-3) [†]	8.2039(3.24E-1) [†]	8.2285(1.66E-1) [†]	7.0455(1.11E-1) [†]
		2	9.4073(4.17E-3)	9.4054(1.23E-6) [†]	9.4071(3.83E-3)	9.1336(7.11E-1) [†]	9.4050(1.03E-1) [†]	8.8295(3.02E-1) [†]
	5	1	31.3466(8.79E-2) [†]	31.3978(1.48E-1) [†]	32.2048(5.75E-1)	26.3694(2.17E+0) [†]	29.7800(8.01E-1) [†]	21.5212(7.91E-1) [†]
		2	37.2188(9.57E-2) [†]	37.1747(3.80E-1) [†]	37.9064(5.32E-1)	—	35.4740(3.96E-1) [†]	35.7858(5.12E-1) [†]
	8	1	261.2983(1.90E+0)	259.1756(1.11E+0) [†]	255.7826(2.60E-1) [†]	181.4143(4.03E+1) [†]	255.4237(9.22E+0) [†]	—
		2	459.8634(2.05E+0)	456.9066(3.10E+0) [†]	451.0410(4.22E-1) [†]	447.4523(1.79E+1) [†]	442.6764(2.25E+1) [†]	—
	10	1	422.4212(4.21E+1)	403.7712(8.224E+0) [†]	400.2181(1.28E+1) [†]	—	320.1247(6.64E+1) [†]	—
		2	1422.7213(8.21E+2)	1399.2381(9.72E+2) [†]	1391.5048(1.04E+3) [†]	—	911.9634(1.69E+2) [†]	—

[†] denotes the best median metric value is significantly better than the other peers according to the statistical analysis described in Appendix F of the supplementary document. ref = 1 means the unattainable aspiration level vector while ref = 2 means the attainable aspiration level vector. — means all solutions obtained by the corresponding algorithm are dominated by the other counterparts, thus no solution can be used for R-HV computation.

APPENDIX H
COMPARISON RESULTS ON THE QUALITY METRIC [4]

In this section, we provide the comparison results on another performance metric, i.e. Quality metric developed in [4]. Specifically, this metric is calculated by counting the number of non-dominated solutions obtained by different algorithms. It measures the convergence performance of an algorithm. The comparison results are given in Table V to Table VII. Note that when calculating the R-HV metric, the dominated solutions are also removed during the preprocessing step of the R-HV calculation. This operation further punishes the poorly converged algorithm.

TABLE V: Comparison results of median Quality Metric values and the IQR obtained by six preference-based EMO algorithms on DTLZ1 to DTLZ4 problems with unattainable and attainable aspiration level vectors.

Problem	<i>m</i>	ref	MOEAD/STM	MOEAD	NSGA-III	gNSGA-II	r-NSGA-II	R-NSGA-II
DTLZ1	3	1	106(0.00E+0)	92(7.50E-1) [†]	16(7.53E+1) [†]	0(0.00E+0) [†]	97(6.00E+0) [†]	76(3.58E+1) [†]
		2	106(0.00E+0)	92(0.00E+0) [†]	84(0.00E+0) [†]	0(0.00E+0) [†]	94(6.00E+0) [†]	100(0.00E+0) [†]
		1	211(0.00E+0) [†]	208(2.75E+0) [†]	360(0.00E+0)	9(9.00E+0) [†]	38(4.00E+1) [†]	100(0.00E+0) [†]
	5	2	211(0.00E+0) [†]	206(3.00E+0) [†]	360(0.00E+0)	6(8.00E+0) [†]	45(4.40E+1) [†]	100(0.00E+0) [†]
		1	361(0.00E+0)	360(0.00E+0) [†]	360(0.00E+0) [†]	0(2.00E+0) [†]	85(3.90E+1) [†]	100(0.00E+0) [†]
	8	2	361(0.00E+0)	360(0.00E+0) [†]	360(0.00E+0) [†]	0(1.00E+0) [†]	63(4.98E+1) [†]	100(0.00E+0) [†]
		1	661(0.00E+0)	660(0.00E+0) [†]	660(0.00E+0) [†]	0(4.00E+0) [†]	81(4.60E+1) [†]	100(0.00E+0) [†]
	10	2	650(1.38E+1) [†]	659(4.75E+0) [†]	660(0.00E+0)	11(1.13E+1) [†]	98(5.00E+0) [†]	100(0.00E+0) [†]
		1	106(0.00E+0)	76(2.00E+0) [†]	92(1.00E+0) [†]	1(2.75E+0) [†]	20(4.10E+1) [†]	98(2.75E+0) [†]
DTLZ2	3	2	106(0.00E+0)	83(1.00E+0) [†]	92(0.00E+0) [†]	74(1.18E+1) [†]	79(2.30E+1) [†]	99(3.00E+0) [†]
		1	211(0.00E+0) [†]	204(4.00E+0) [†]	360(0.00E+0)	2(2.08E+1) [†]	90(9.00E+0) [†]	100(0.00E+0) [†]
	5	2	211(0.00E+0) [†]	208(7.00E+0) [†]	360(0.00E+0)	34(1.68E+1) [†]	87(1.60E+1) [†]	100(0.00E+0) [†]
		1	361(1.75E+0)	360(0.00E+0) [†]	360(0.00E+0) [†]	1(6.00E+0) [†]	94(4.75E+0) [†]	100(0.00E+0) [†]
	8	2	361(1.00E+0)	360(0.00E+0) [†]	360(0.00E+0) [†]	6(5.75E+0) [†]	96(4.00E+0) [†]	100(0.00E+0) [†]
		1	613(2.60E+1) [†]	660(7.50E-1) [†]	660(0.00E+0)	2(0.00E+0) [†]	41(2.23E+1) [†]	100(0.00E+0) [†]
	10	2	648(1.08E+1) [†]	659(4.75E+0) [†]	660(0.00E+0)	0(9.00E+0) [†]	98(5.00E+0) [†]	0(1.00E+0) [†]
		1	106(0.00E+0)	92(0.00E+0) [†]	10(4.90E+1) [†]	0(2.75E+0) [†]	20(4.10E+1) [†]	100(2.00E+0) [†]
DTLZ3	3	2	106(0.00E+0)	92(0.00E+0) [†]	3(0.00E+0) [†]	0(1.00E+1) [†]	79(2.30E+1) [†]	95(3.00E+0) [†]
		1	211(0.00E+0) [†]	206(1.00E+0) [†]	360(7.50E-1)	3(5.00E+0) [†]	50(4.60E+1) [†]	100(0.00E+0) [†]
	5	2	211(0.00E+0) [†]	209(2.00E+0) [†]	358(6.75E+0)	3(4.00E+0) [†]	47(2.78E+1) [†]	100(0.00E+0) [†]
		1	360(1.00E+0) [†]	360(0.00E+0)	360(0.00E+0)	0(1.50E+1) [†]	70(4.60E+1) [†]	100(0.00E+0) [†]
	8	2	359(2.75E+0) [†]	360(0.00E+0)	360(0.00E+0)	0(0.00E+0) [†]	73(1.90E+1) [†]	100(0.00E+0) [†]
		1	592(3.58E+1) [†]	660(1.00E+0) [†]	660(0.00E+0)	0(0.00E+0) [†]	64(3.58E+1) [†]	100(0.00E+0) [†]
	10	2	649(5.75E+0) [†]	653(8.00E+0) [†]	660(0.00E+0)	0(2.00E+1) [†]	97(7.00E+0) [†]	0(0.00E+0) [†]
		1	106(0.00E+0)	84(2.40E+1) [†]	92(0.00E+0) [†]	98(2.75E+0) [†]	20(4.10E+1) [†]	99(2.00E+0) [†]
DTLZ4	3	2	106(0.00E+0)	84(2.40E+1) [†]	92(0.00E+0) [†]	98(2.75E+0) [†]	20(4.10E+1) [†]	99(2.00E+0) [†]
		1	211(0.00E+0) [†]	207(5.75E+0) [†]	360(0.00E+0)	55(1.53E+1) [†]	93(5.75E+0) [†]	100(0.00E+0) [†]
	5	2	211(0.00E+0) [†]	208(1.00E+0) [†]	360(0.00E+0)	51(2.70E+1) [†]	93(9.00E+0) [†]	100(0.00E+0) [†]
		1	351(1.50E+1) [†]	360(0.00E+0)	360(0.00E+0)	18(1.10E+1) [†]	96(4.75E+0) [†]	100(0.00E+0) [†]
	8	2	348(1.38E+1) [†]	360(0.00E+0)	360(0.00E+0)	5(2.75E+0) [†]	98(3.00E+0) [†]	100(0.00E+0) [†]
		1	628(1.28E+1) [†]	659(2.00E+0) [†]	660(0.00E+0)	2(3.00E+0) [†]	61(1.48E+1) [†]	100(0.00E+0) [†]
	10	2	647(1.00E+1) [†]	651(7.25E+0) [†]	660(0.00E+0)	0(9.75E+0) [†]	99(1.75E+0) [†]	0(0.00E+0) [†]

[†] denotes the best median metric value is significantly better than the other peers according to the statistical analysis described in Appendix F of the supplementary document. ref = 1 means the unattainable aspiration level vector while ref = 2 means the attainable aspiration level vector.

TABLE VI: Comparison results of median Quality Metric values and the IQR obtained by six preference-based EMO algorithms on WFG41 to WFG44 problems with unattainable and attainable aspiration level vectors.

Problem	m	ref	MOEAD/STM	MOEAD	NSGA-III	gNSGA-II	r-NSGA-II	R-NSGA-II
WFG41	2	1	100(0.00E+0)	88(0.00E+0)†	43(2.20E+1)†	6(5.50E+1)†	96(1.75E+0)†	100(0.00E+0)
		2	100(0.00E+0)	88(0.00E+0)†	23(1.10E+1)†	11(1.50E+0)†	92(4.00E+0)†	100(0.00E+0)
	3	1	106(0.00E+0)	92(0.00E+0)†	52(0.00E+0)†	3(7.50E-1)†	99(1.75E+0)†	100(0.00E+0)†
		2	106(0.00E+0)	92(0.00E+0)†	84(5.00E+0)†	5(1.50E+0)†	92(9.00E+0)†	100(2.00E+0)†
	5	1	211(0.00E+0)†	208(0.00E+0)†	360(0.00E+0)	4(0.00E+0)†	86(8.75E+0)†	99(1.00E+0)†
		2	211(0.00E+0)†	208(0.00E+0)†	360(0.00E+0)	4(1.00E+0)†	53(1.20E+1)†	96(3.00E+0)†
	8	1	361(0.00E+0)	360(0.00E+0)†	360(0.00E+0)†	1(7.50E-1)†	85(5.50E+0)†	100(0.00E+0)†
		2	361(0.00E+0)	360(0.00E+0)†	360(0.00E+0)†	0(0.00E+0)†	60(1.75E+0)†	100(0.00E+0)†
	10	1	661(0.00E+0)	660(0.00E+0)†	660(0.00E+0)†	1(0.00E+0)†	82(9.00E+0)†	0(0.00E+0)†
		2	658(1.50E+0)†	599(1.00E+0)†	660(0.00E+0)	2(1.75E+0)†	98(3.75E+0)†	0(0.00E+0)†
WFG42	2	1	100(0.00E+0)	88(0.00E+0)†	43(2.20E+1)†	1(5.50E+1)†	96(1.75E+0)†	100(0.00E+0)
		2	100(0.00E+0)	88(0.00E+0)†	23(1.10E+1)†	2(1.50E+0)†	92(4.00E+0)†	100(0.00E+0)
	3	1	106(0.00E+0)	92(5.25E+0)†	42(2.40E+1)†	3(1.75E+0)†	17(9.25E+0)†	100(0.00E+0)†
		2	106(0.00E+0)	92(1.75E+0)†	77(5.00E+0)†	2(5.00E-1)†	77(2.50E+0)†	100(0.00E+0)†
	5	1	211(0.00E+0)†	208(0.00E+0)†	358(0.00E+0)	2(0.00E+0)†	90(1.08E+1)†	87(1.10E+1)†
		2	211(0.00E+0)†	208(0.00E+0)†	360(0.00E+0)	2(2.25E+0)†	87(9.50E+0)†	100(0.00E+0)†
	8	1	361(0.00E+0)	360(2.00E+0)†	355(3.25E+0)†	4(5.00E-1)†	96(1.23E+1)†	100(0.00E+0)†
		2	361(0.00E+0)	360(0.00E+0)†	360(0.00E+0)†	0(0.00E+0)†	97(7.00E+0)†	100(0.00E+0)†
	10	1	645(1.03E+1)†	660(0.00E+0)	645(5.00E+0)†	3(5.00E-1)†	40(2.25E+0)†	0(0.00E+0)†
		2	653(1.75E+0)†	660(1.00E+0)†	660(0.00E+0)	2(1.25E+0)†	99(3.50E+0)†	0(0.00E+0)†
WFG43	2	1	100(0.00E+0)	88(0.00E+0)†	66(3.40E+1)†	5(5.50E+1)†	96(1.75E+0)†	100(0.00E+0)
		2	100(0.00E+0)	88(0.00E+0)†	26(1.40E+1)†	4(1.50E+0)†	92(4.00E+0)†	100(0.00E+0)
	3	1	106(0.00E+0)	92(0.00E+0)†	78(3.00E+0)†	4(5.00E-1)†	19(1.08E+1)†	97(2.00E+0)†
		2	106(0.00E+0)	91(1.00E+0)†	86(2.50E+0)†	4(5.00E-1)†	79(8.50E+0)†	100(0.00E+0)†
	5	1	211(0.00E+0)†	208(0.00E+0)†	360(0.00E+0)	4(1.00E+0)†	52(5.25E+0)†	100(0.00E+0)†
		2	211(0.00E+0)†	208(0.00E+0)†	356(1.75E+0)	4(1.00E+0)†	48(1.18E+1)†	100(0.00E+0)†
	8	1	361(0.00E+0)	360(0.00E+0)†	360(0.00E+0)†	4(1.25E+0)†	69(7.75E+0)†	100(0.00E+0)†
		2	361(0.00E+0)	360(1.75E+0)†	360(0.00E+0)†	0(1.25E+0)†	73(6.25E+0)†	100(0.00E+0)†
	10	1	661(0.00E+0)	660(1.50E+0)†	660(0.00E+0)†	1(2.50E-1)†	66(1.18E+1)†	0(0.00E+0)†
		2	661(0.00E+0)	655(5.00E+0)†	660(0.00E+0)†	0(0.00E+0)†	99(8.75E+0)†	0(0.00E+0)†
WFG44	2	1	100(0.00E+0)	88(0.00E+0)†	23(1.40E+1)†	2(5.50E+1)†	93(2.50E+0)†	100(0.00E+0)
		2	100(0.00E+0)	88(0.00E+0)†	64(2.40E+1)†	4(1.50E+0)†	93(4.00E+0)†	100(0.00E+0)
	3	1	106(0.00E+0)	92(0.00E+0)†	24(4.75E+0)†	0(7.50E-1)†	21(7.00E+0)†	100(0.00E+0)†
		2	106(0.00E+0)	92(0.00E+0)†	53(5.25E+0)†	0(1.00E+0)†	20(2.50E-1)†	0(0.00E+0)†
	5	1	211(0.00E+0)†	201(8.00E+0)†	360(0.00E+0)	2(1.00E+0)†	93(1.13E+1)†	100(2.50E+0)†
		2	211(0.00E+0)†	208(0.00E+0)†	360(0.00E+0)	0(0.00E+0)†	93(1.23E+1)†	100(1.00E+0)†
	8	1	361(0.00E+0)	360(0.00E+0)†	360(0.00E+0)†	0(5.00E-1)†	93(9.75E+0)†	0(0.00E+0)†
		2	361(0.00E+0)	360(0.00E+0)†	360(0.00E+0)†	0(0.00E+0)†	0(1.20E+1)†	0(0.00E+0)†
	10	1	628(1.28E+1)†	659(2.00E+0)†	660(0.00E+0)	0(3.00E+0)†	0(1.48E+1)†	0(0.00E+0)†
		2	647(1.00E+1)†	651(7.25E+0)†	660(0.00E+0)	0(9.75E+0)†	0(1.75E+0)†	0(0.00E+0)†

† denotes the best median metric value is significantly better than the other peers according to the statistical analysis described in Appendix F of the supplementary document. ref = 1 means the unattainable aspiration level vector while ref = 2 means the attainable aspiration level vector.

TABLE VII: Comparison results of median Quality Metric values and the IQR obtained by six preference-based EMO algorithms on WFG45 to WFG48 problems with unattainable and attainable aspiration level vectors.

Problem	m	ref	MOEAD/STM	MOEAD	NSGA-III	gNSGA-II	r-NSGA-II	R-NSGA-II
WFG45	2	1	100(0.00E+0)	88(2.50E+0)†	84(2.50E-1)†	88(2.50E-1)†	100(0.00E+0)	
		2	100(0.00E+0)	88(0.00E+0)†	62(4.40E+1)†	1(1.25E+0)†	87(1.75E+0)†	100(0.00E+0)
	3	1	106(0.00E+0)	92(0.00E+0)†	100(0.00E+0)†	1(1.50E+0)†	87(7.50E-1)†	100(0.00E+0)†
		2	106(0.00E+0)	92(0.00E+0)†	100(0.00E+0)†	1(1.00E+0)†	89(2.00E+0)†	100(0.00E+0)†
	5	1	211(0.00E+0)†	208(0.00E+0)†	360(0.00E+0)	1(1.50E+0)†	86(2.00E+0)†	100(0.00E+0)†
		2	211(0.00E+0)†	208(0.00E+0)†	360(0.00E+0)	5(7.50E-1)†	90(1.50E+0)†	100(0.00E+0)†
	8	1	361(0.00E+0)	360(0.00E+0)†	360(0.00E+0)†	2(2.00E+0)†	86(0.00E+0)†	100(0.00E+0)†
		2	361(0.00E+0)	360(0.00E+0)†	360(0.00E+0)†	0(0.00E+0)†	90(2.25E+0)†	100(0.00E+0)†
	10	1	661(0.00E+0)	660(0.00E+0)†	660(0.00E+0)†	5(1.50E+0)†	87(5.00E-1)†	0(0.00E+0)†
		2	658(1.50E+0)†	599(1.00E+0)†	660(0.00E+0)	0(0.00E+0)†	89(2.50E-1)†	0(0.00E+0)†
WFG46	2	1	100(0.00E+0)	88(0.00E+0)†	14(1.40E+1)†	1(7.50E-1)†	88(2.50E-1)†	100(0.00E+0)
		2	100(0.00E+0)	88(0.00E+0)†	24(3.00E+0)†	3(1.50E+0)†	87(1.75E+0)†	100(0.00E+0)
	3	1	106(0.00E+0)	92(5.25E+0)†	100(0.00E+0)†	4(1.25E+0)†	90(7.50E-1)†	100(0.00E+0)†
		2	106(0.00E+0)	92(1.75E+0)†	100(0.00E+0)†	1(1.25E+0)†	88(1.50E+0)†	100(0.00E+0)†
	5	1	211(0.00E+0)†	208(0.00E+0)†	358(0.00E+0)	3(1.25E+0)†	89(1.25E+0)†	100(0.00E+0)†
		2	211(0.00E+0)†	208(0.00E+0)†	360(0.00E+0)	4(1.25E+0)†	86(2.00E+0)†	100(0.00E+0)†
	8	1	361(0.00E+0)	360(2.00E+0)†	350(7.50E+0)†	1(1.50E+0)†	87(2.50E-1)†	100(0.00E+0)†
		2	361(0.00E+0)	360(0.00E+0)†	360(0.00E+0)†	0(0.00E+0)†	86(2.00E+0)†	100(0.00E+0)†
	10	1	645(1.03E+1)	660(0.00E+0)†	645(5.00E+0)†	3(2.50E-1)†	87(0.00E+0)†	0(0.00E+0)†
		2	655(2.50E+0)†	660(1.00E+0)†	660(0.00E+0)	0(0.00E+0)†	86(7.50E-1)†	0(0.00E+0)†
WFG47	2	1	100(0.00E+0)	88(0.00E+0)†	24(3.40E+1)†	1(1.25E+0)†	89(1.75E+0)†	100(0.00E+0)
		2	100(0.00E+0)	88(0.00E+0)†	11(1.40E+1)†	5(1.00E+0)†	86(1.25E+0)†	100(0.00E+0)
	3	1	106(0.00E+0)	92(0.00E+0)†	54(3.00E+0)†	2(2.50E-1)†	88(2.50E-1)†	97(2.00E+0)†
		2	106(0.00E+0)	91(1.00E+0)†	78(2.50E+0)†	1(7.50E-1)†	88(1.25E+0)†	100(0.00E+0)†
	5	1	211(0.00E+0)†	208(0.00E+0)†	360(0.00E+0)	1(1.50E+0)†	90(1.75E+0)†	100(0.00E+0)†
		2	211(0.00E+0)†	208(0.00E+0)†	356(1.75E+0)	1(2.25E+0)†	90(2.00E+0)†	100(0.00E+0)†
	8	1	361(0.00E+0)	360(0.00E+0)†	360(0.00E+0)†	3(2.00E+0)†	88(7.50E-1)†	100(0.00E+0)†
		2	361(0.00E+0)	360(1.75E+0)†	360(0.00E+0)†	0(0.00E+0)†	90(7.50E-1)†	100(0.00E+0)†
	10	1	661(0.00E+0)	660(1.50E+0)†	660(0.00E+0)†	2(1.25E+0)†	89(1.75E+0)†	0(0.00E+0)†
		2	661(0.00E+0)	655(5.00E+0)†	660(0.00E+0)†	0(0.00E+0)†	88(7.50E-1)†	0(0.00E+0)†
WFG48	2	1	100(0.00E+0)	88(0.00E+0)†	33(3.25E+1)†	3(7.50E-1)†	87(2.00E+0)†	98(2.00E+0)†
		2	100(0.00E+0)	88(0.00E+0)†	45(3.50E+1)†	3(2.00E+0)†	87(0.00E+0)†	100(0.00E+0)
	3	1	106(0.00E+0)	92(0.00E+0)†	100(0.00E+0)†	2(1.25E+0)†	89(1.75E+0)†	100(0.00E+0)†
		2	106(0.00E+0)	92(0.00E+0)†	100(0.00E+0)†	3(1.00E+0)†	89(2.25E+0)†	100(0.00E+0)†
	5	1	211(0.00E+0)†	201(8.00E+0)†	360(0.00E+0)	2(0.00E+0)†	88(5.00E-1)†	100(0.00E+0)†
		2	211(0.00E+0)†	208(0.00E+0)†	360(0.00E+0)	0(0.00E+0)†	88(1.25E+0)†	100(0.00E+0)†
	8	1	361(0.00E+0)	360(0.00E+0)†	360(0.00E+0)†	3(1.50E+0)†	90(0.00E+0)†	0(0.00E+0)†
		2	361(0.00E+0)	360(0.00E+0)†	360(0.00E+0)†	1(2.00E+0)†	87(1.50E+0)†	0(0.00E+0)†
	10	1	628(1.28E+1)†	659(2.00E+0)†	660(0.00E+0)	0(0.00E+0)†	89(7.50E-1)†	0(0.00E+0)†
		2	647(1.00E+1)†	651(7.25E+0)†	660(0.00E+0)	0(0.00E+0)†	90(5.00E-1)†	0(0.00E+0)†

† denotes the best median metric value is significantly better than the other peers according to the statistical analysis described in Appendix F of the supplementary document. ref = 1 means the unattainable aspiration level vector while ref = 2 means the attainable aspiration level vector.

APPENDIX I
COMPARISON OF CPU TIME COSTS

In Table VIII, we compare the average CPU time cost by the three decomposition-based EMO algorithms assisted by the NUMS and their corresponding baseline algorithms. From the comparison results, we can see that the NUMS does not incur additional computational costs to the baseline algorithm.

TABLE VIII: Comparison results of the average CPU time costs (in second) of three decomposition-based EMO algorithms assisted by the NUMS and their corresponding baseline algorithms.

Problem	m	NUMS Assisted			Baseline Algorithm		
		MOEAD/STM	MOEAD	NSGA-III	MOEAD/STM	MOEAD	NSGA-III
DTLZ1	3	1	1	2	1	1	2
	5	2	2	3	2	1	3
	8	4	4	7	3	3	7
	10	14	14	122	15	14	120
DTLZ2	3	1	1	1	1	1	1
	5	2	2	2	2	1	1
	8	4	5	8	3	4	7
	10	15	14	132	16	14	136
DTLZ3	3	2	3	3	2	3	2
	5	3	4	4	2	3	3
	8	7	8	11	6	8	11
	10	18	22	272	16	23	244
DTLZ4	3	1	1	2	1	1	2
	5	5	3	7	5	3	6
	8	6	7	11	6	6	10
	10	14	11	125	15	10	136
WFG41	3	1	1	0	1	1	1
	5	3	3	5	3	3	4
	8	5	11	12	4	10	12
	10	18	16	164	19	16	151
WFG42	3	2	2	2	1	1	1
	5	3	3	3	3	2	2
	8	6	10	12	5	9	11
	10	18	20	346	18	19	355
WFG43	3	1	1	1	1	1	1
	5	6	3	9	5	3	8
	8	8	8	11	7	8	11
	10	16	10	101	14	9	93
WFG44	3	1	1	2	1	1	1
	5	3	3	5	2	3	4
	8	5	5	7	5	5	7
	10	17	15	146	17	13	135
WFG45	3	2	2	1	1	2	1
	5	2	3	3	1	3	3
	8	5	9	12	4	8	11
	10	19	17	382	17	18	358
WFG46	3	1	1	1	1	1	1
	5	3	2	11	2	2	11
	8	5	8	13	5	8	12
	10	15	10	100	14	10	108
WFG47	3	1	1	1	1	1	1
	5	2	3	3	1	2	3
	8	2	4	7	1	4	6
	10	20	17	161	21	18	163
WFG48	3	2	2	1	1	2	1
	5	2	2	3	2	1	3
	8	4	11	11	4	10	12
	10	20	21	313	18	21	300

Moreover, in Table IX, we also show the comparisons of the average CPU time cost by the three decomposition-based EMO algorithms assisted by the NUMS with the other three preference-based EMO algorithms. From the comparison results, we can clearly see that the three decomposition-based EMO algorithms are faster.

TABLE IX: Comparison results of the average CPU time costs (in second) of three decomposition-based EMO algorithms assisted by the NUMS and the other three preference-based EMO algorithms.

Problem	m	MOEAD/STM	MOEAD	NSGA-III	g-NSGA-II	r-NSGA-II	R-NSGA-II
DTLZ1	3	1	1	2	6	8	23
	5	2	2	3	18	22	371
	8	4	4	7	43	58	1822
	10	14	14	122	323	352	10122
DTLZ2	3	1	1	1	6	7	21
	5	2	2	2	16	21	366
	8	4	5	8	51	54	2245
	10	15	14	132	347	346	11212
DTLZ3	3	2	3	3	11	13	43
	5	3	4	4	23	32	366
	8	7	8	11	51	53	2245
	10	18	22	272	421	432	15282
DTLZ4	3	1	1	2	7	6	18
	5	5	3	7	16	21	437
	8	6	7	11	37	66	1481
	10	14	11	125	382	291	9131
WFG41	3	1	1	0	6	5	19
	5	3	3	5	13	26	395
	8	5	11	12	42	69	2371
	10	18	16	164	333	406	13124
WFG42	3	2	2	2	10	11	37
	5	3	3	3	25	36	459
	8	6	10	12	58	58	1808
	10	18	20	346	369	461	10848
WFG43	3	1	1	1	8	5	17
	5	6	3	9	15	24	465
	8	8	8	11	40	59	1225
	10	16	10	101	432	310	11073
WFG44	3	1	1	2	7	5	15
	5	3	3	5	15	28	475
	8	5	5	7	41	60	2659
	10	17	15	146	412	483	14463
WFG45	3	2	2	1	11	11	36
	5	2	3	3	22	44	466
	8	5	9	12	63	74	2119
	10	19	17	382	417	376	12714
WFG46	3	1	1	1	7	5	14
	5	3	2	11	16	21	535
	8	5	8	13	35	54	1325
	10	15	10	100	367	396	15850
WFG47	3	1	1	1	8	5	12
	5	2	3	3	18	29	416
	8	2	4	7	53	69	2664
	10	20	17	161	429	536	16671
WFG48	3	2	2	1	13	10	39
	5	2	2	3	25	43	519
	8	4	11	11	65	79	1864
	10	20	21	313	462	381	11184

APPENDIX J
PLOTS OF FINAL POPULATIONS

This section provides the visual comparisons of different preference-based EMO algorithms. In particular, we plot the final solutions obtained by different algorithms that achieve the best R-HV value.

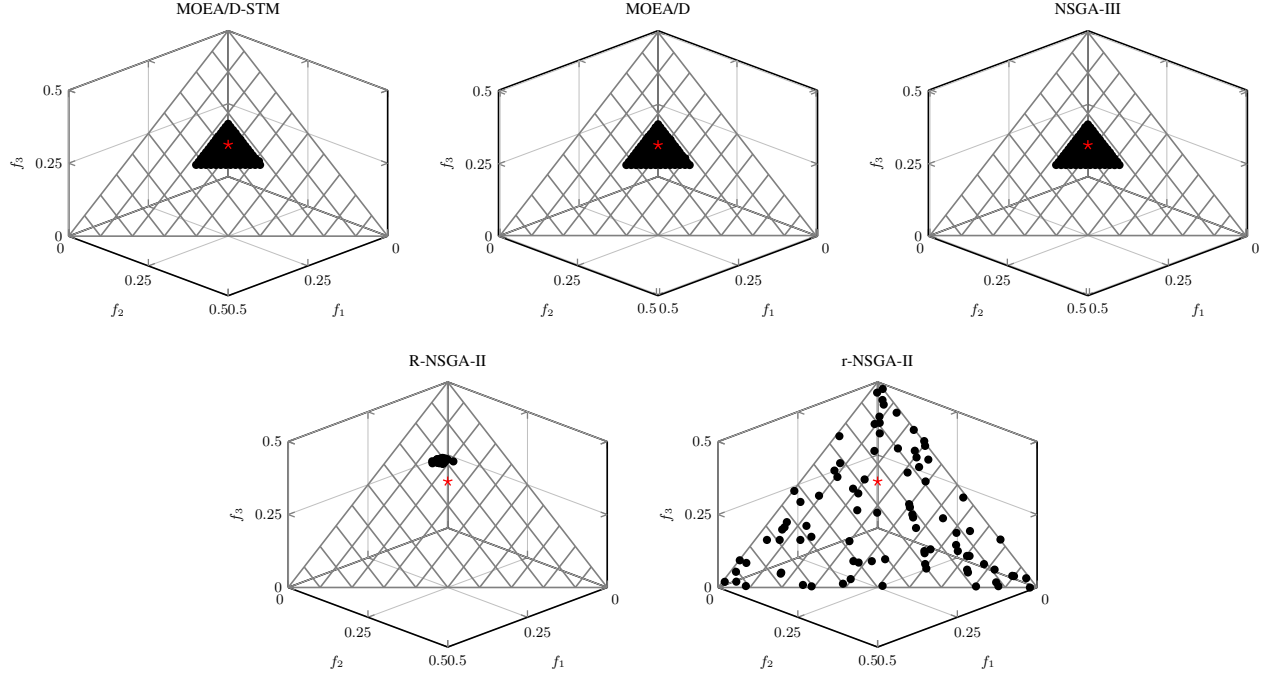


Fig. 3: Comparisons on 3-objective DTLZ1 where $\mathbf{z}^r = (0.05, 0.05, 0.2)$.

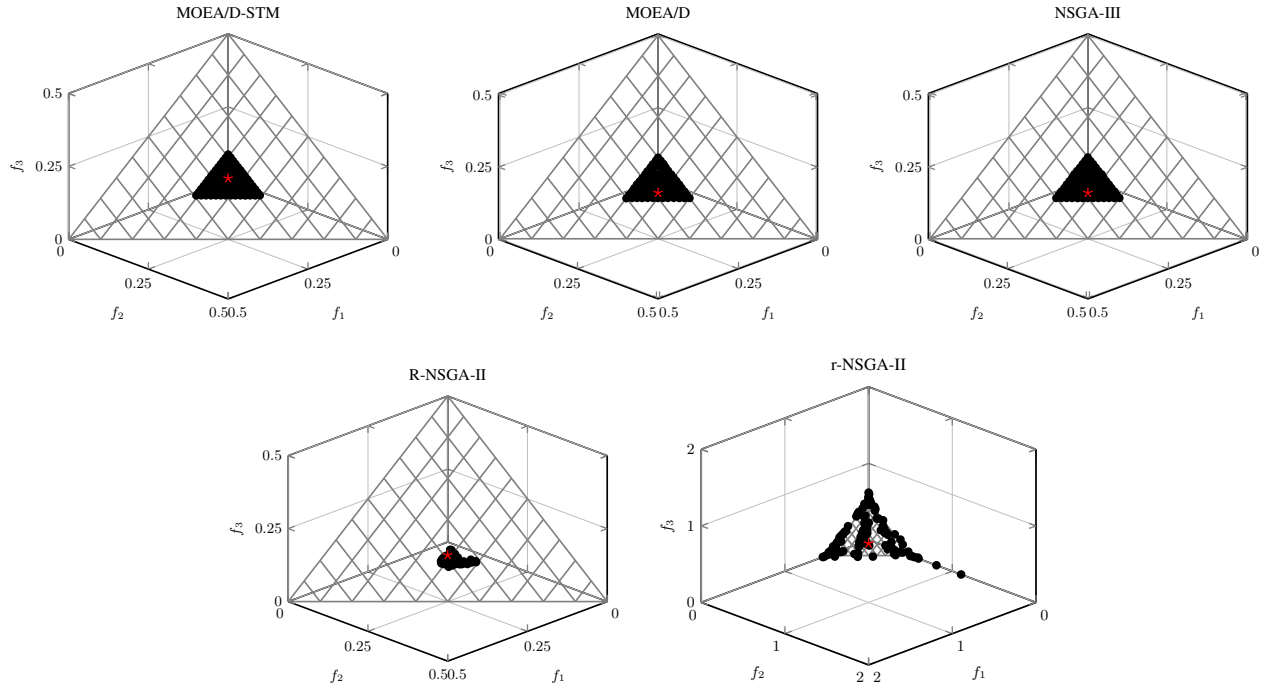
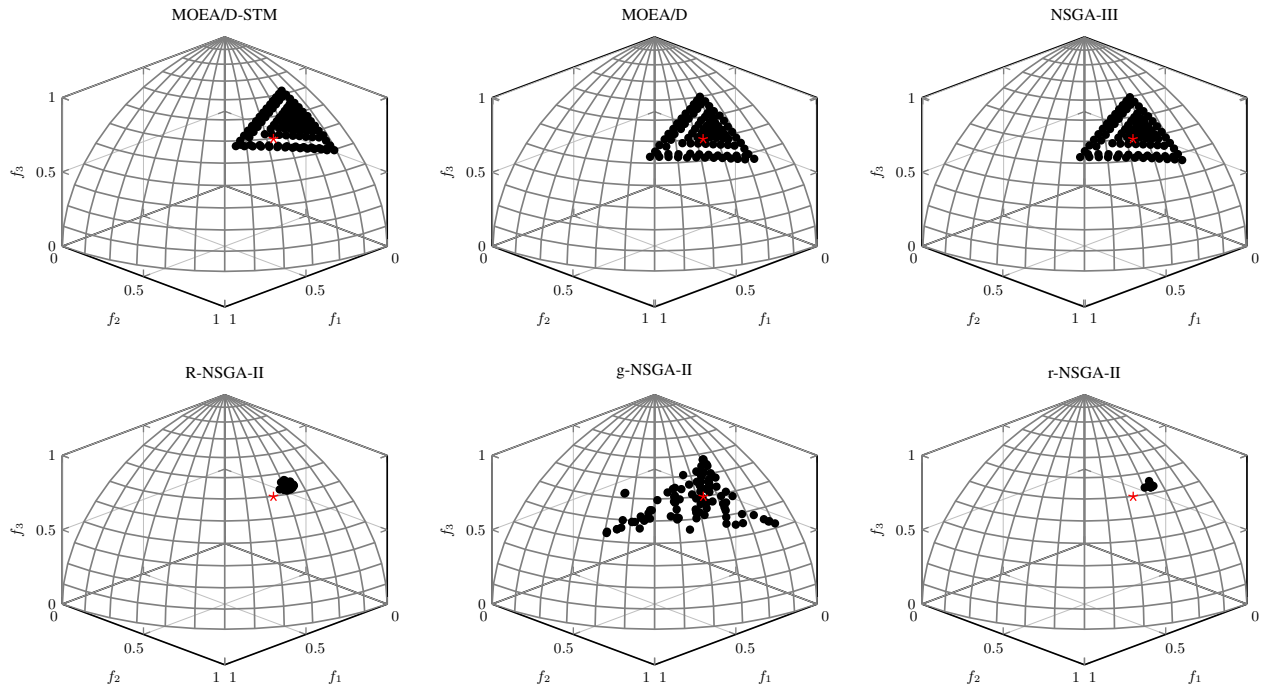
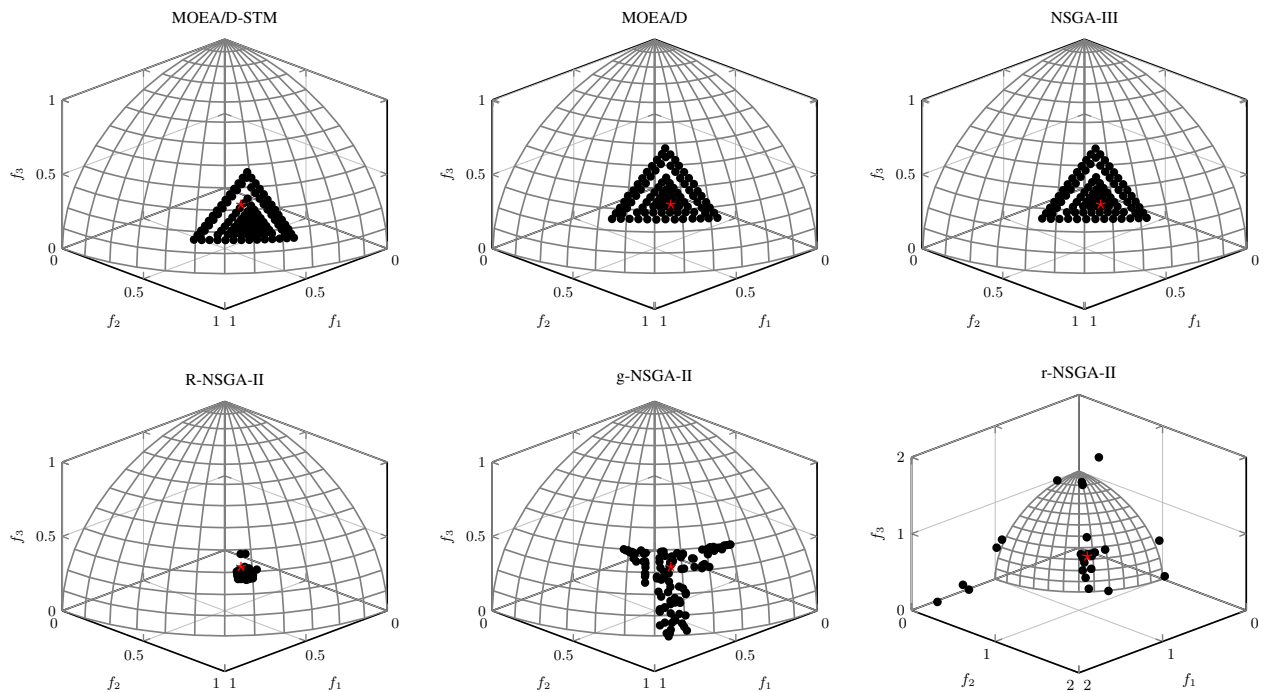


Fig. 4: Comparisons on 3-objective DTLZ1 where $\mathbf{z}^r = (0.3, 0.3, 0.2)$.

Fig. 5: Comparisons on 3-objective DTLZ2 where $z^r = (0.2, 0.5, 0.6)$.Fig. 6: Comparisons on 3-objective DTLZ2 where $z^r = (0.7, 0.8, 0.5)$.

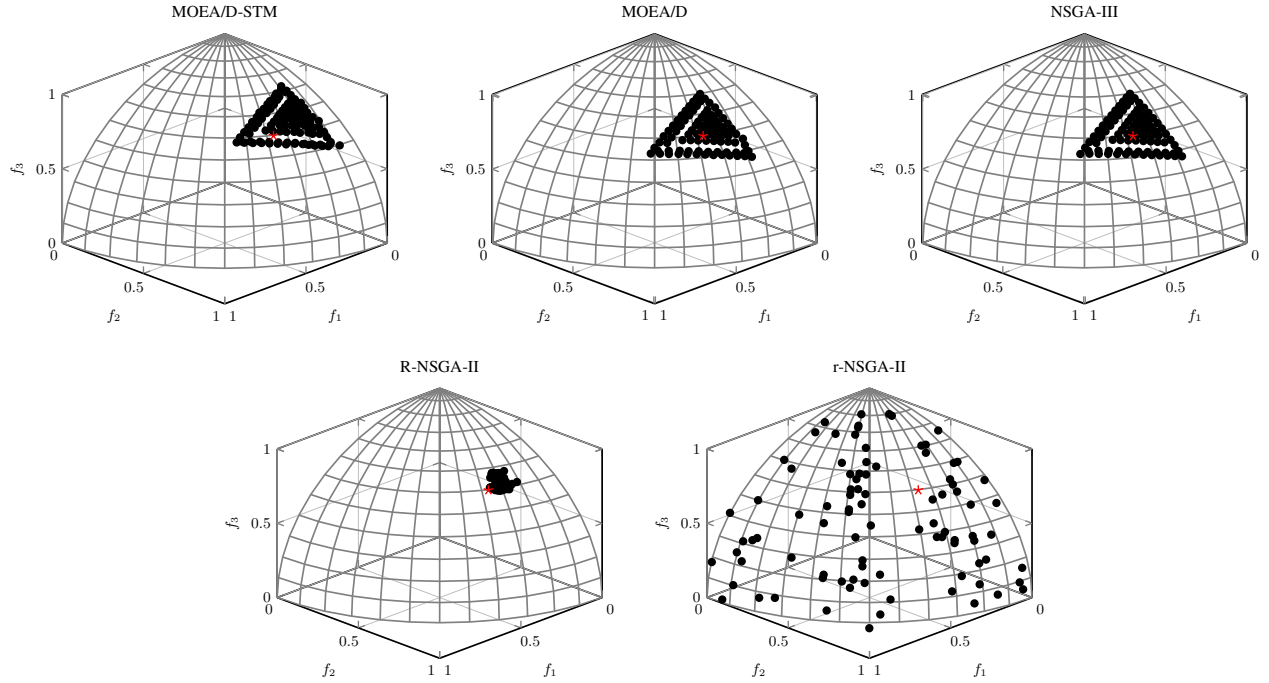


Fig. 7: Comparisons on 3-objective DTLZ3 where $\mathbf{z}^r = (0.2, 0.5, 0.6)$.

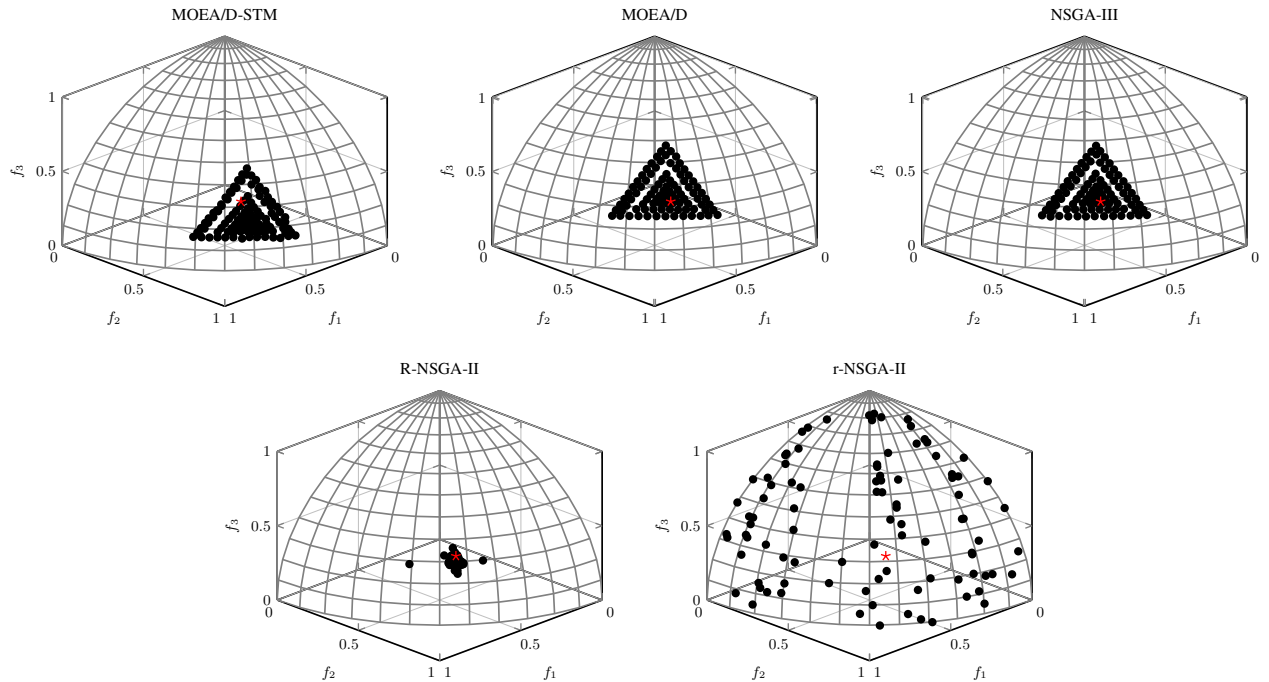
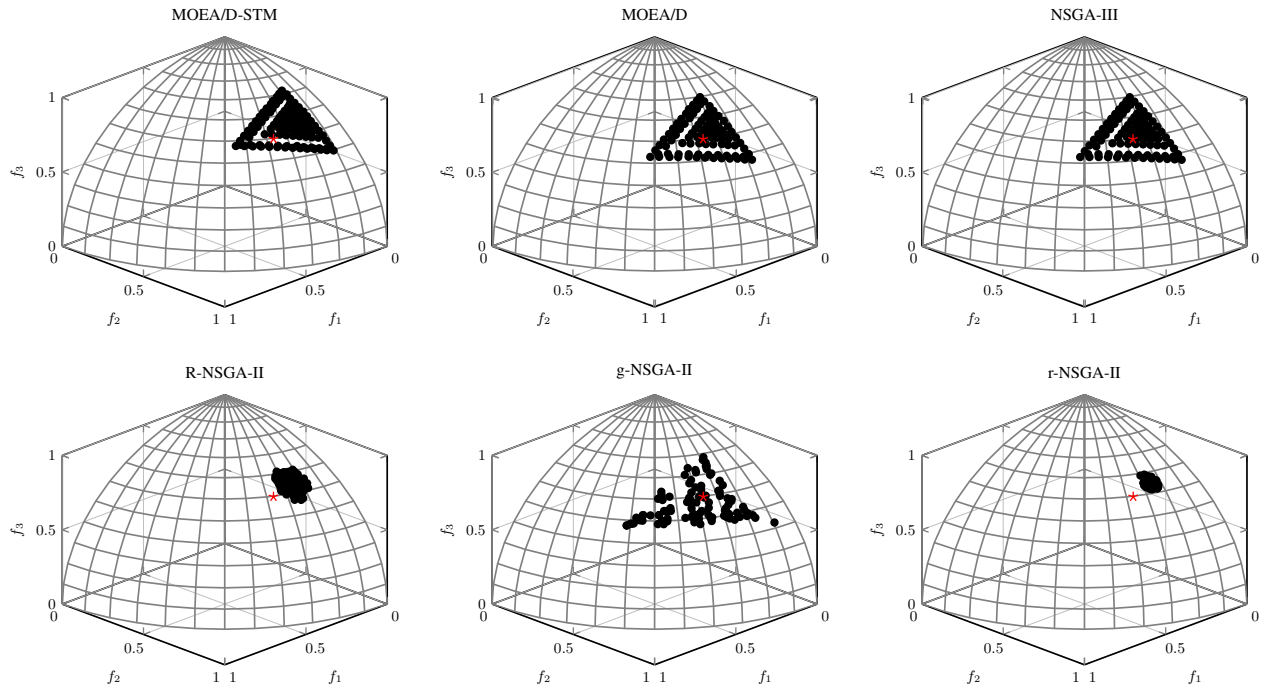
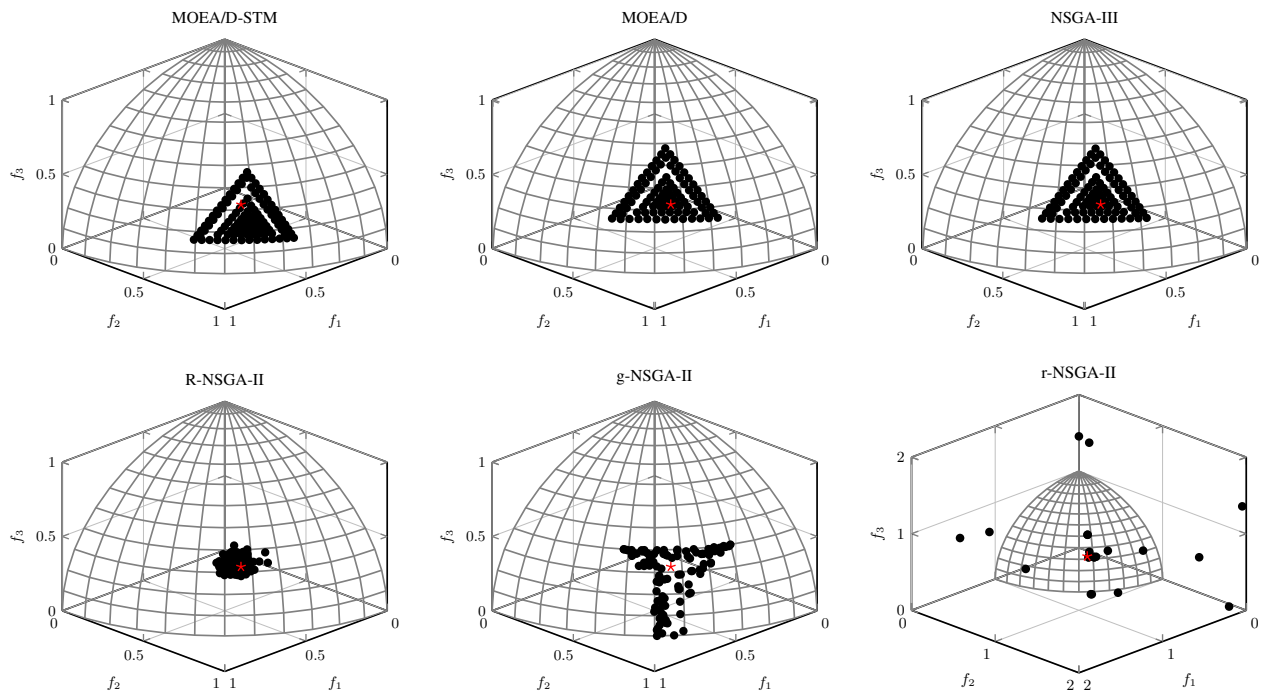


Fig. 8: Comparisons on 3-objective DTLZ3 where $\mathbf{z}^r = (0.7, 0.8, 0.5)$.

Fig. 9: Comparisons on 3-objective DTLZ4 where $z^r = (0.2, 0.5, 0.6)$.Fig. 10: Comparisons on 3-objective DTLZ4 where $z^r = (0.7, 0.8, 0.5)$.

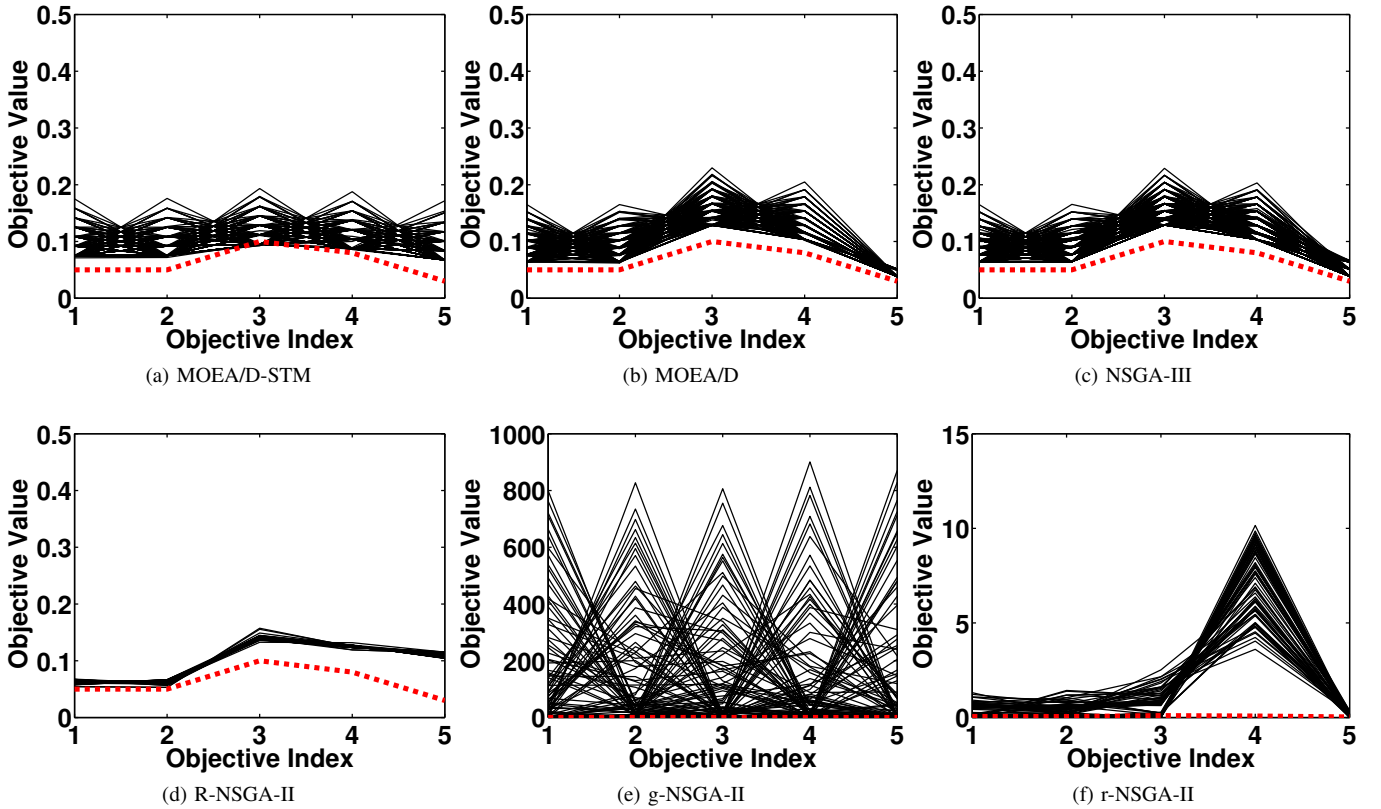


Fig. 11: Comparisons on 5-objective DTLZ1 where $\mathbf{z}^r = (0.05, 0.05, 0.1, 0.08, 0.03)^T$.

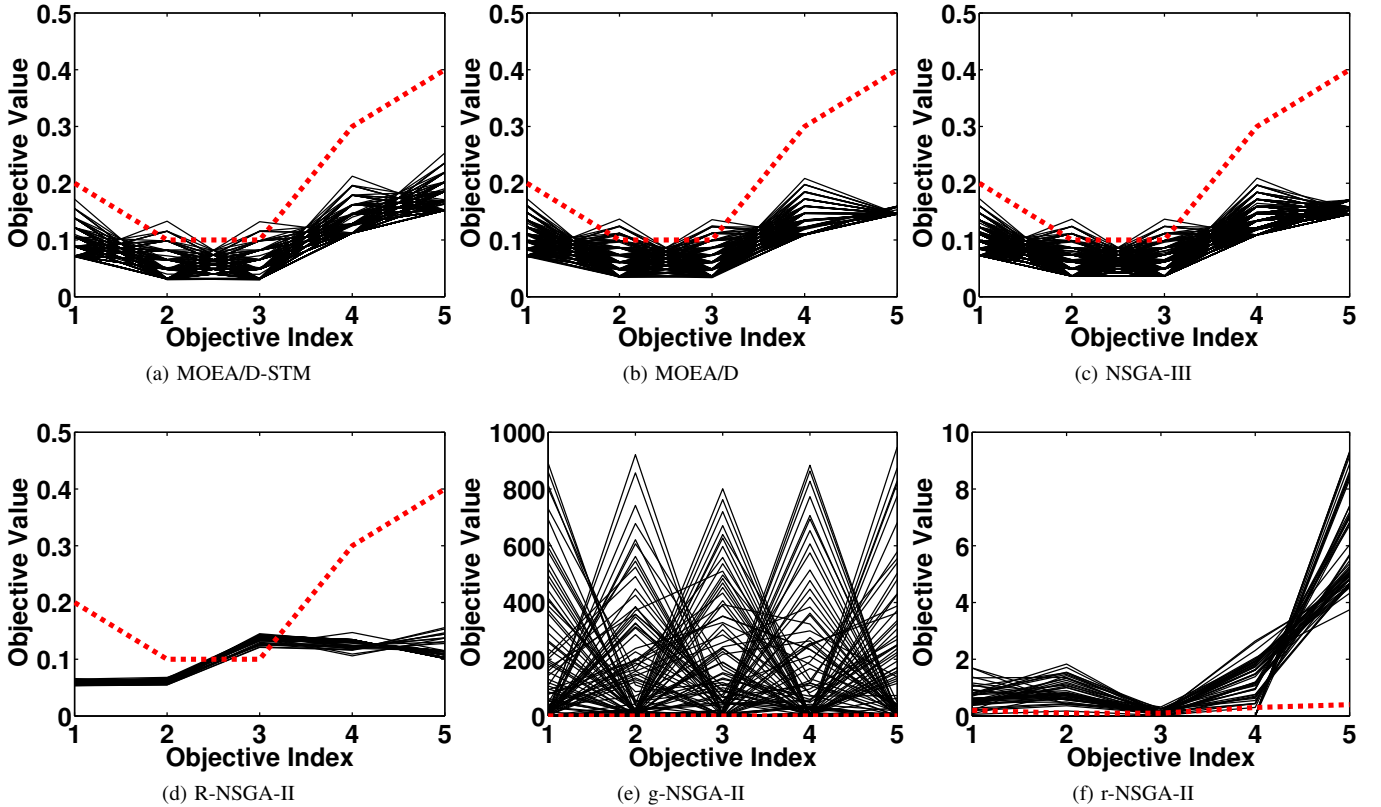
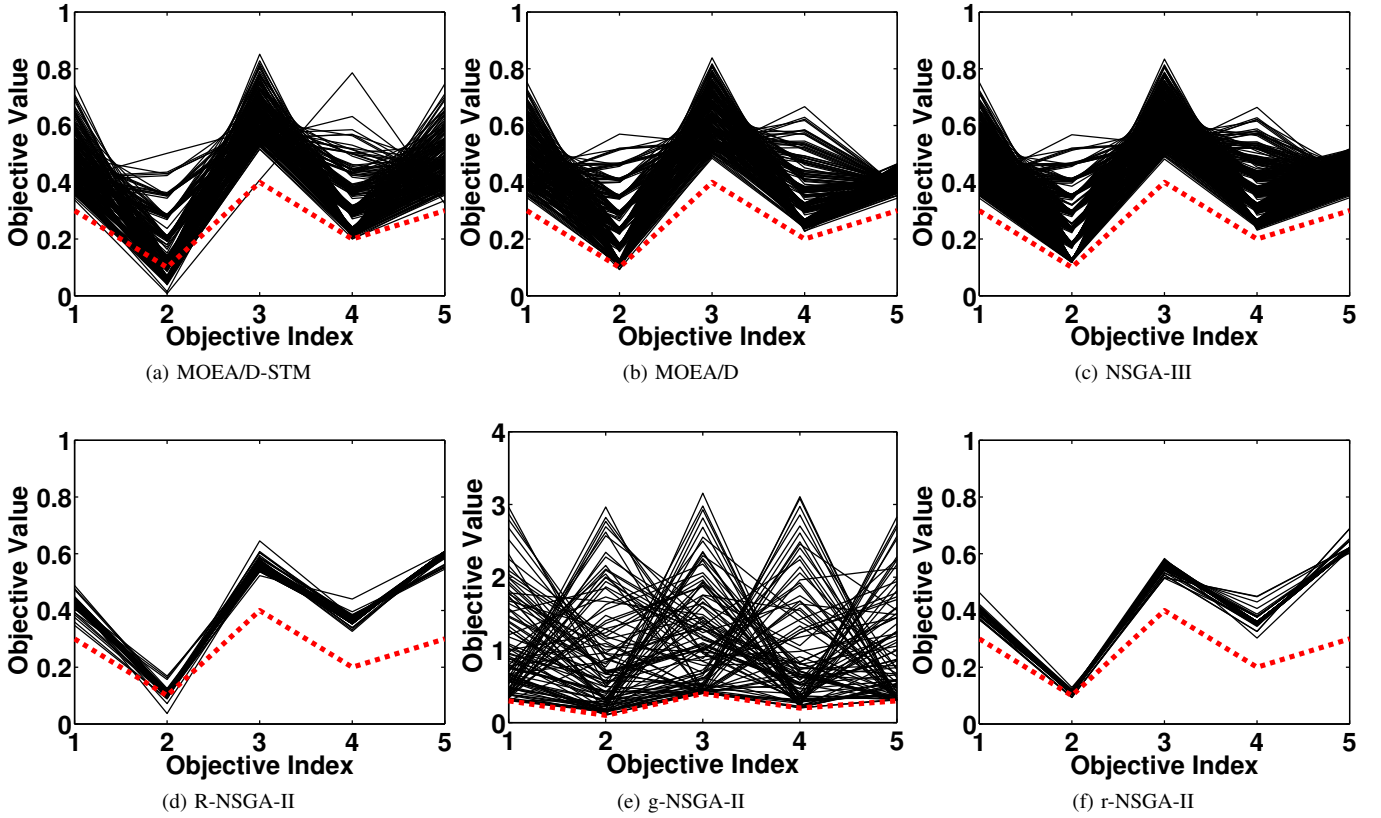
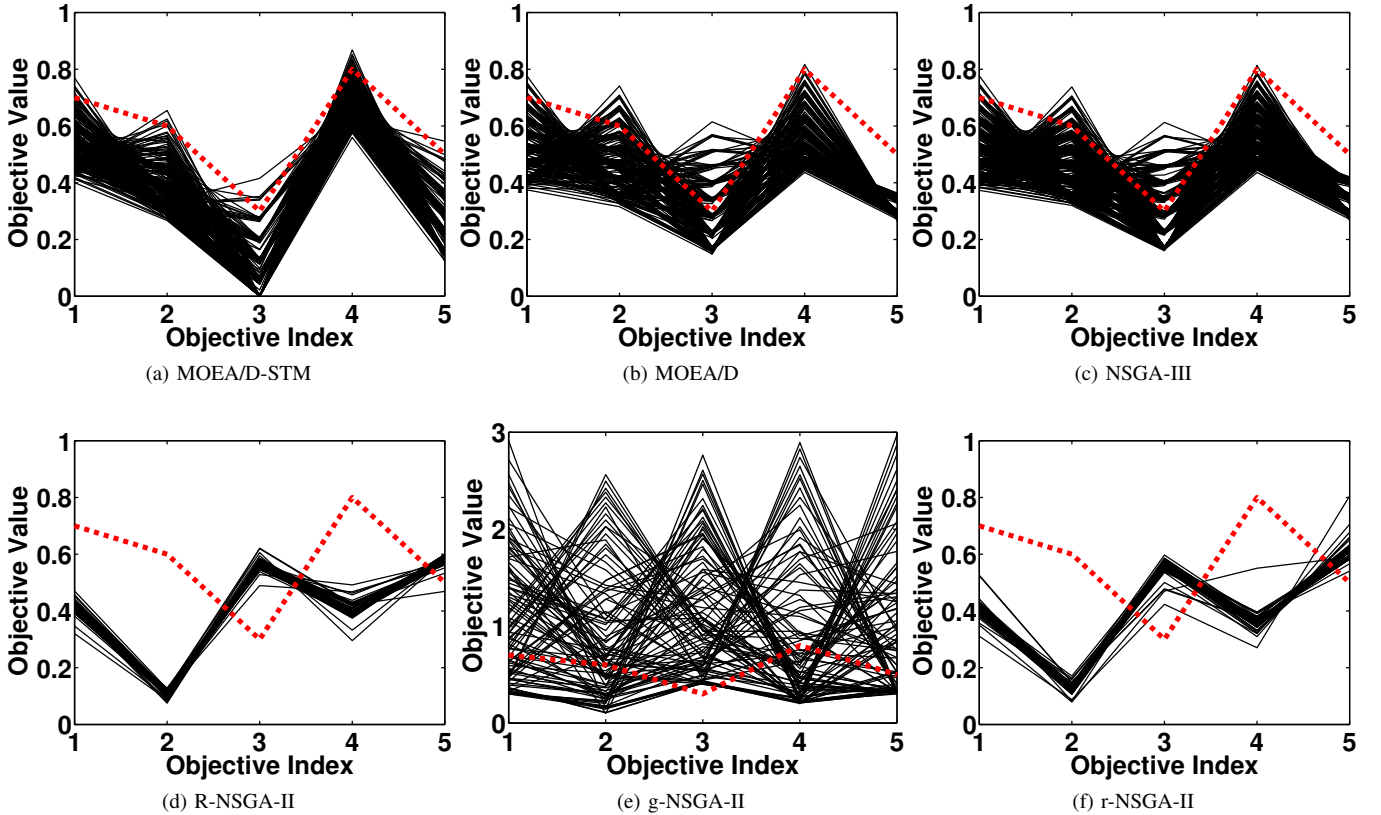
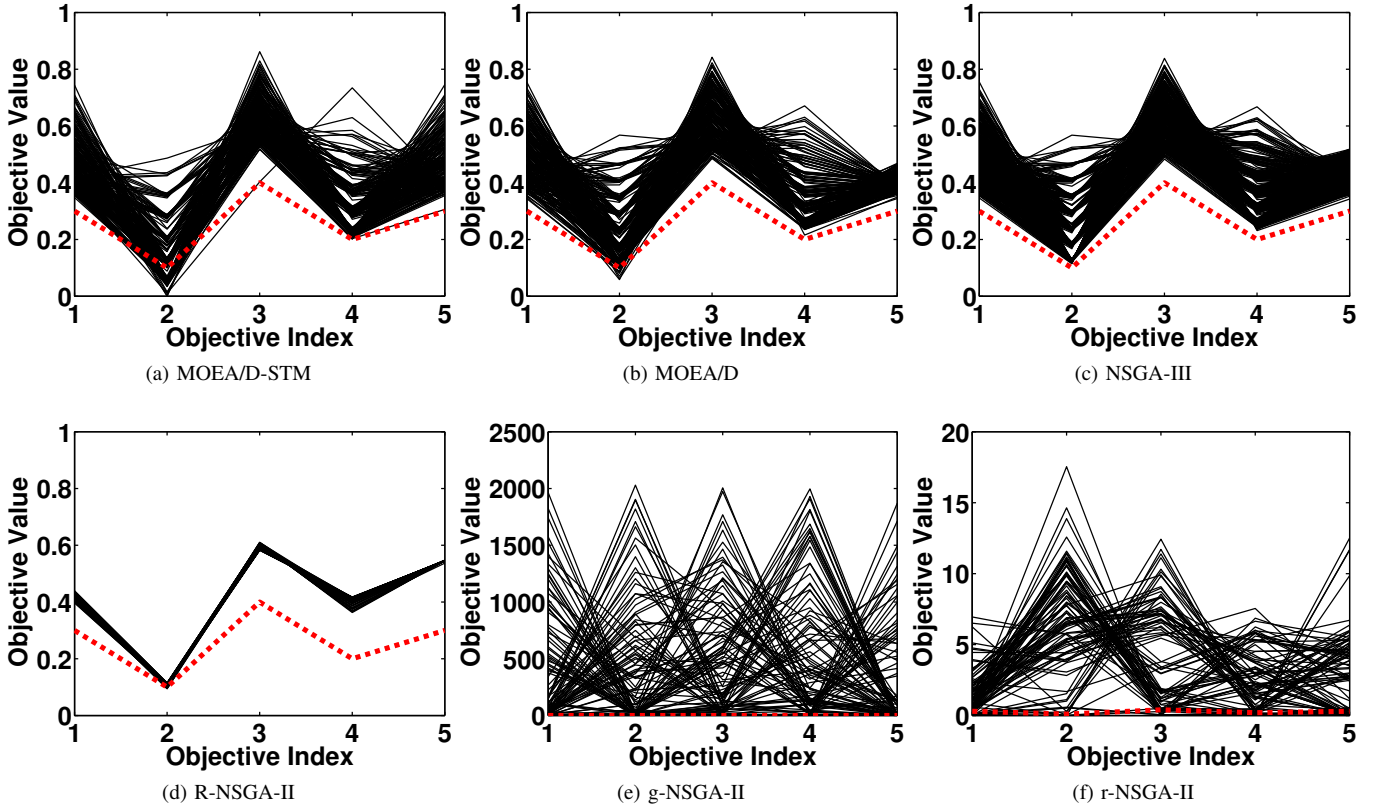
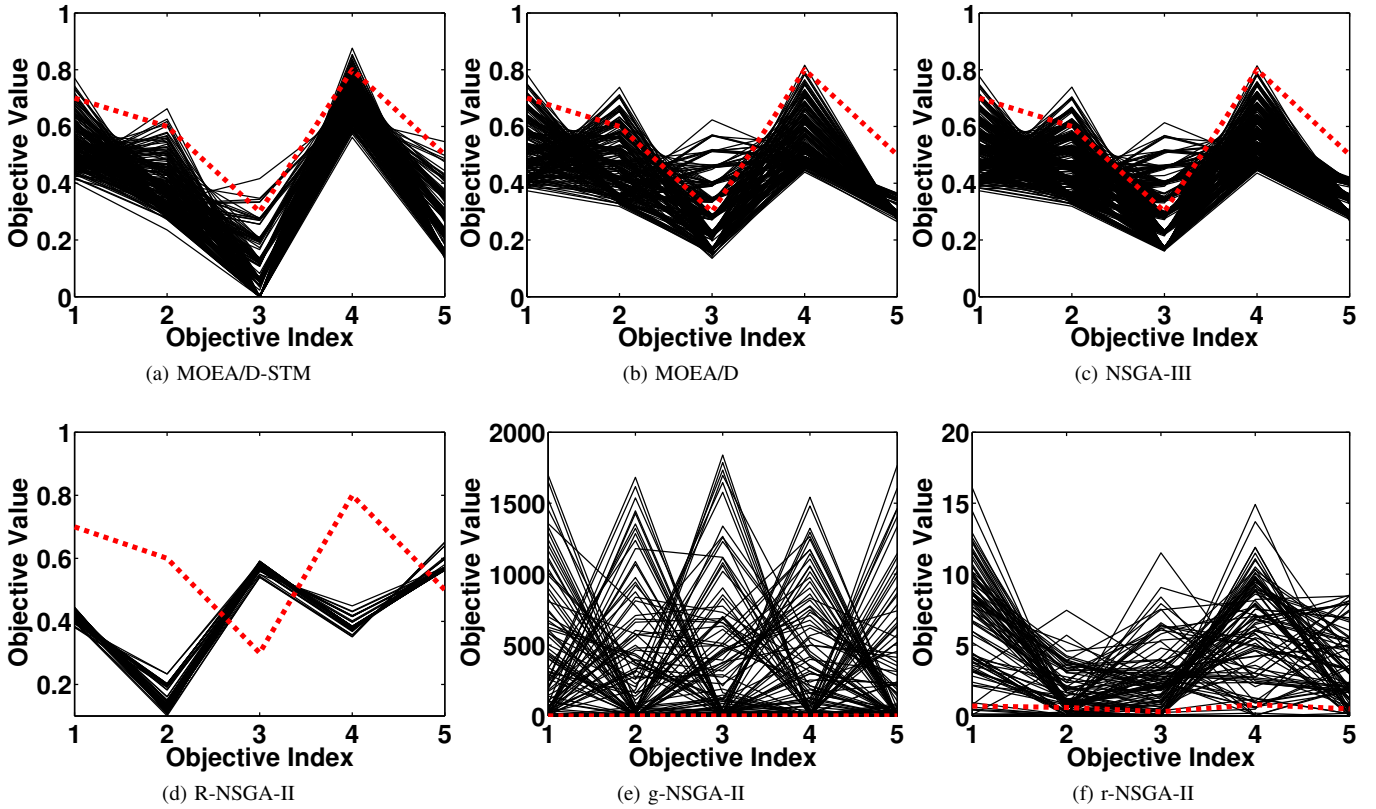
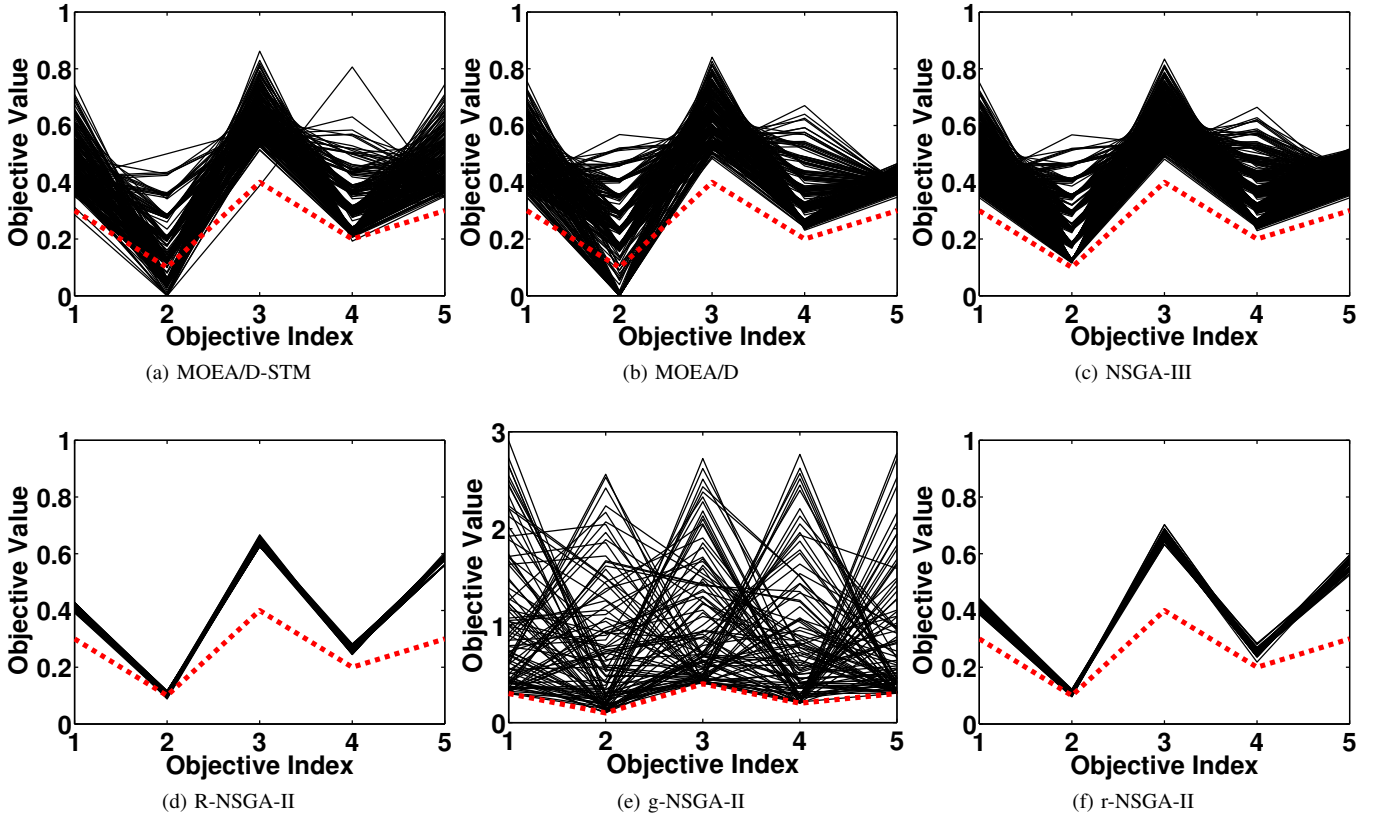
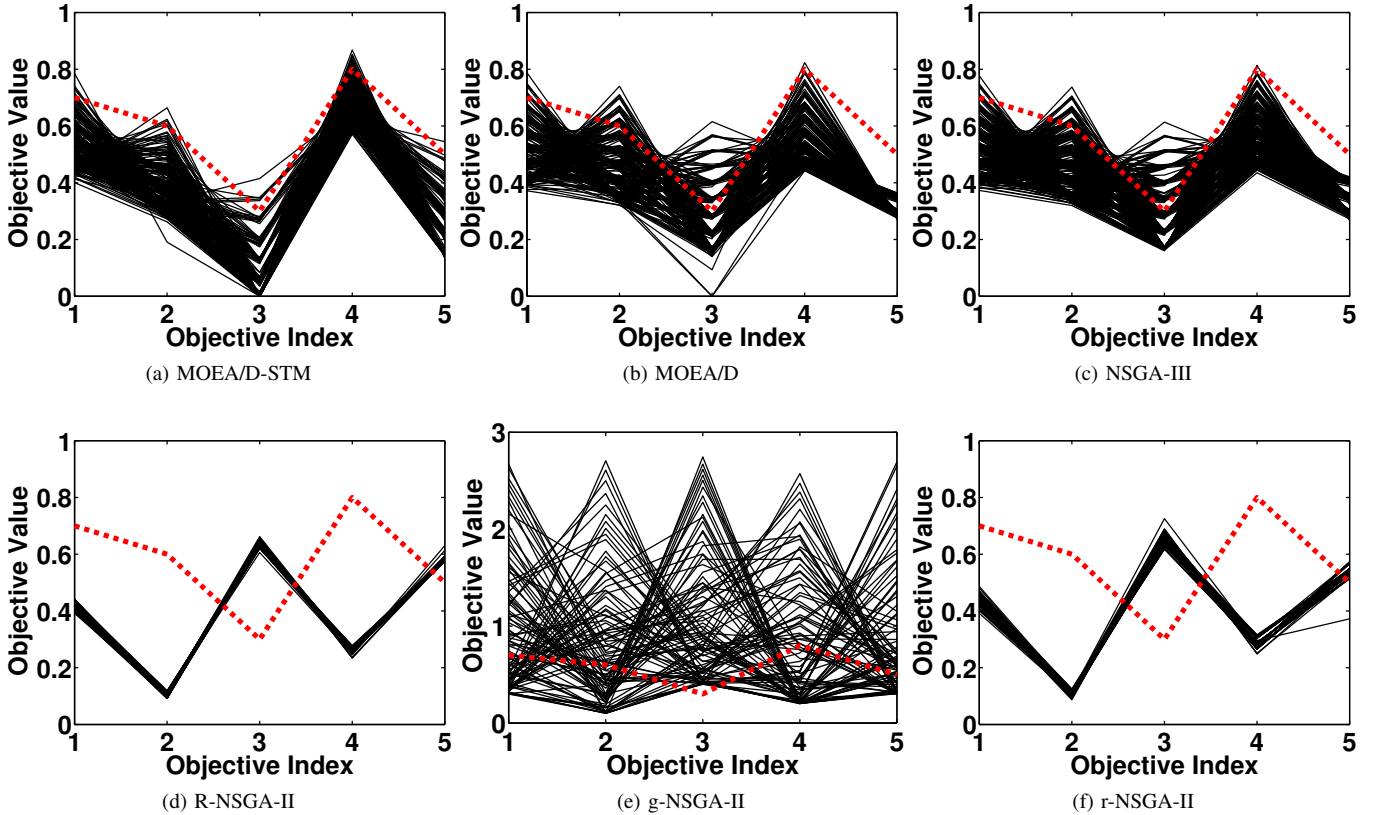


Fig. 12: Comparisons on 5-objective DTLZ1 where $\mathbf{z}^r = (0.2, 0.1, 0.1, 0.3, 0.4)^T$.

Fig. 13: Comparisons on 5-objective DTLZ2 where $\mathbf{z}^r = (0.3, 0.1, 0.4, 0.2, 0.3)^T$.Fig. 14: Comparisons on 5-objective DTLZ2 where $\mathbf{z}^r = (0.7, 0.6, 0.3, 0.8, 0.5)^T$.

Fig. 15: Comparisons on 5-objective DTLZ3 where $\mathbf{z}^r = (0.3, 0.1, 0.4, 0.2, 0.3)^T$.Fig. 16: Comparisons on 5-objective DTLZ3 where $\mathbf{z}^r = (0.7, 0.6, 0.3, 0.8, 0.5)^T$.

Fig. 17: Comparisons on 5-objective DTLZ4 where $\mathbf{z}^r = (0.3, 0.1, 0.4, 0.2, 0.3)^T$.Fig. 18: Comparisons on 5-objective DTLZ4 where $\mathbf{z}^r = (0.7, 0.6, 0.3, 0.8, 0.5)^T$.

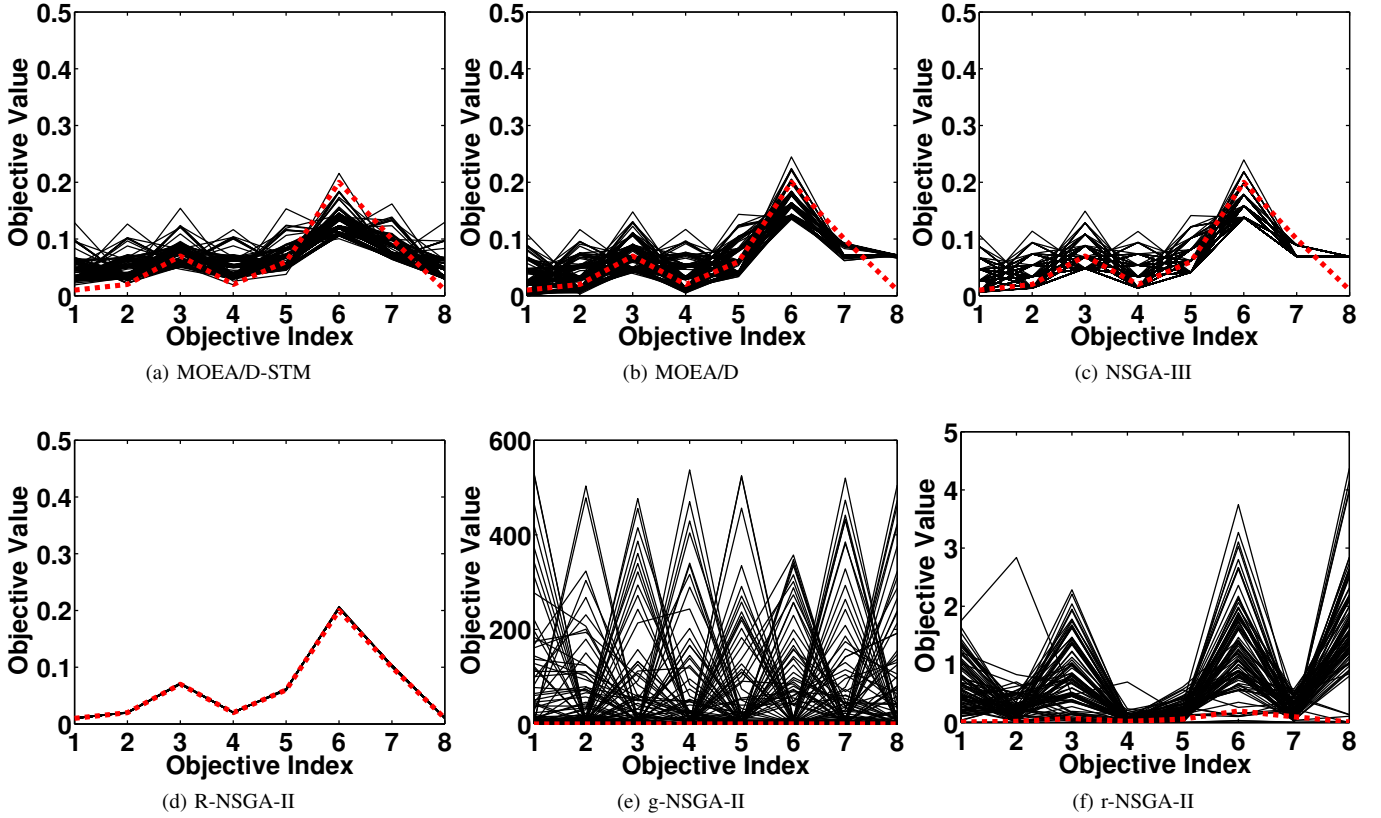


Fig. 19: Comparisons on 8-objective DTLZ1 where $\mathbf{z}^r = (0.01, 0.02, 0.07, 0.02, 0.06, 0.2, 0.1, 0.01)^T$.

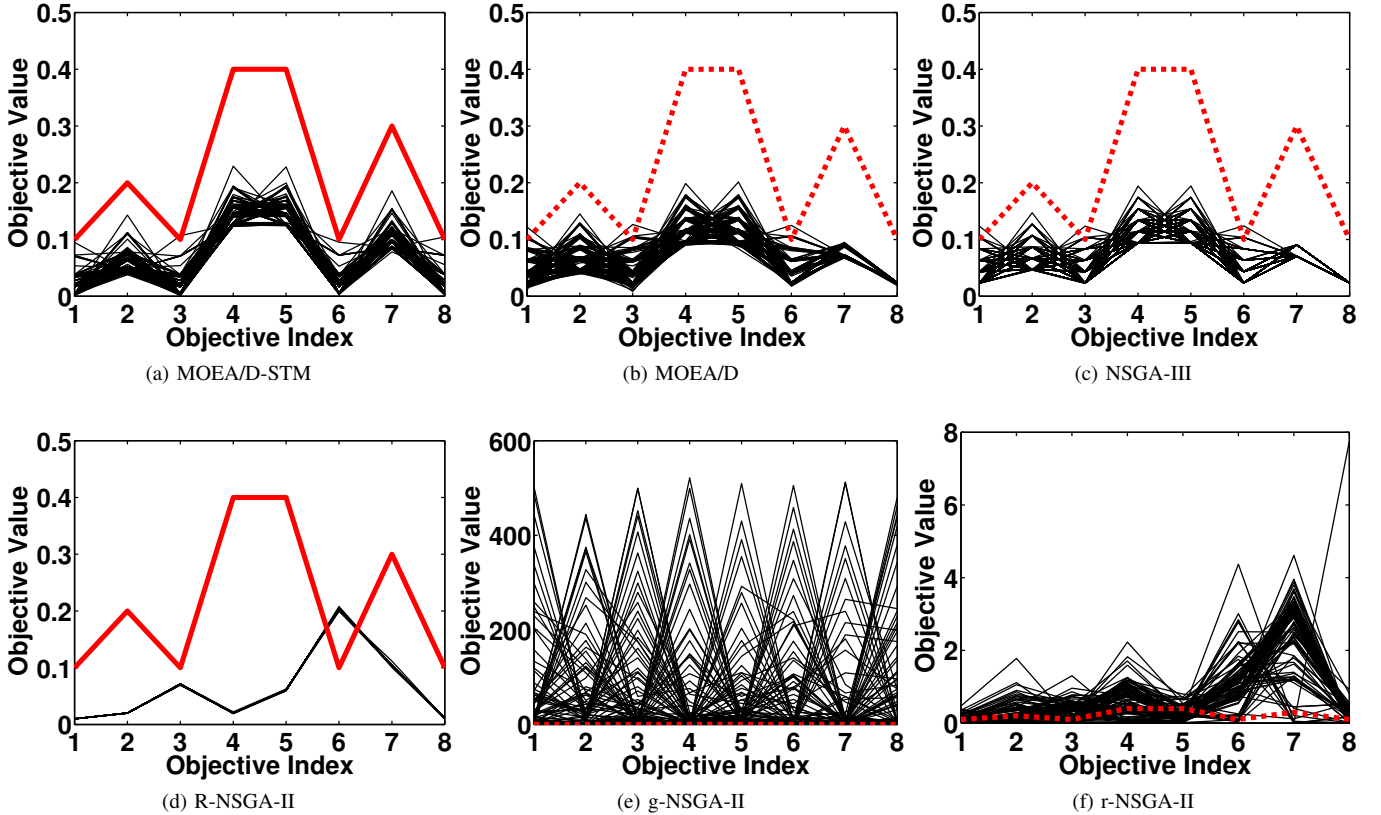
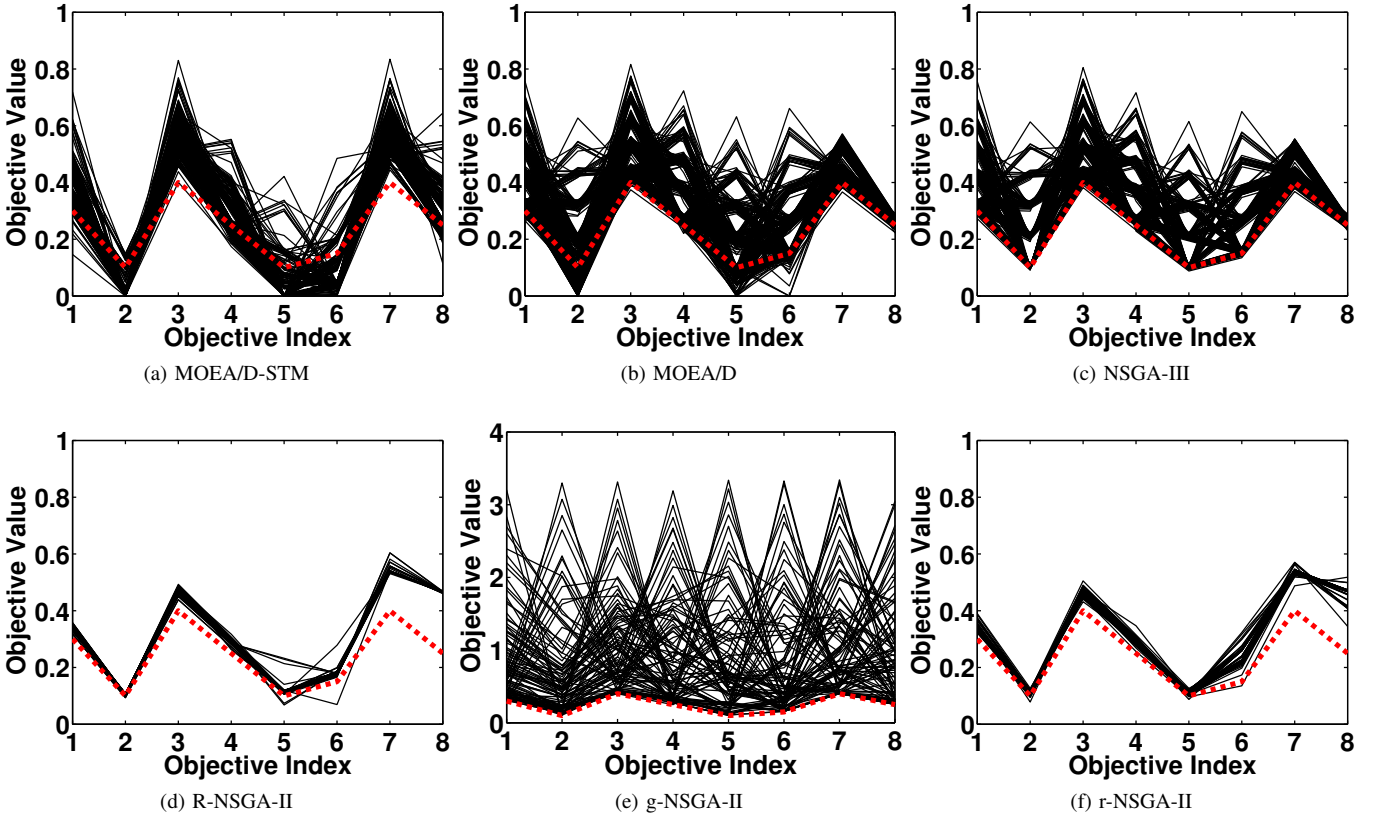
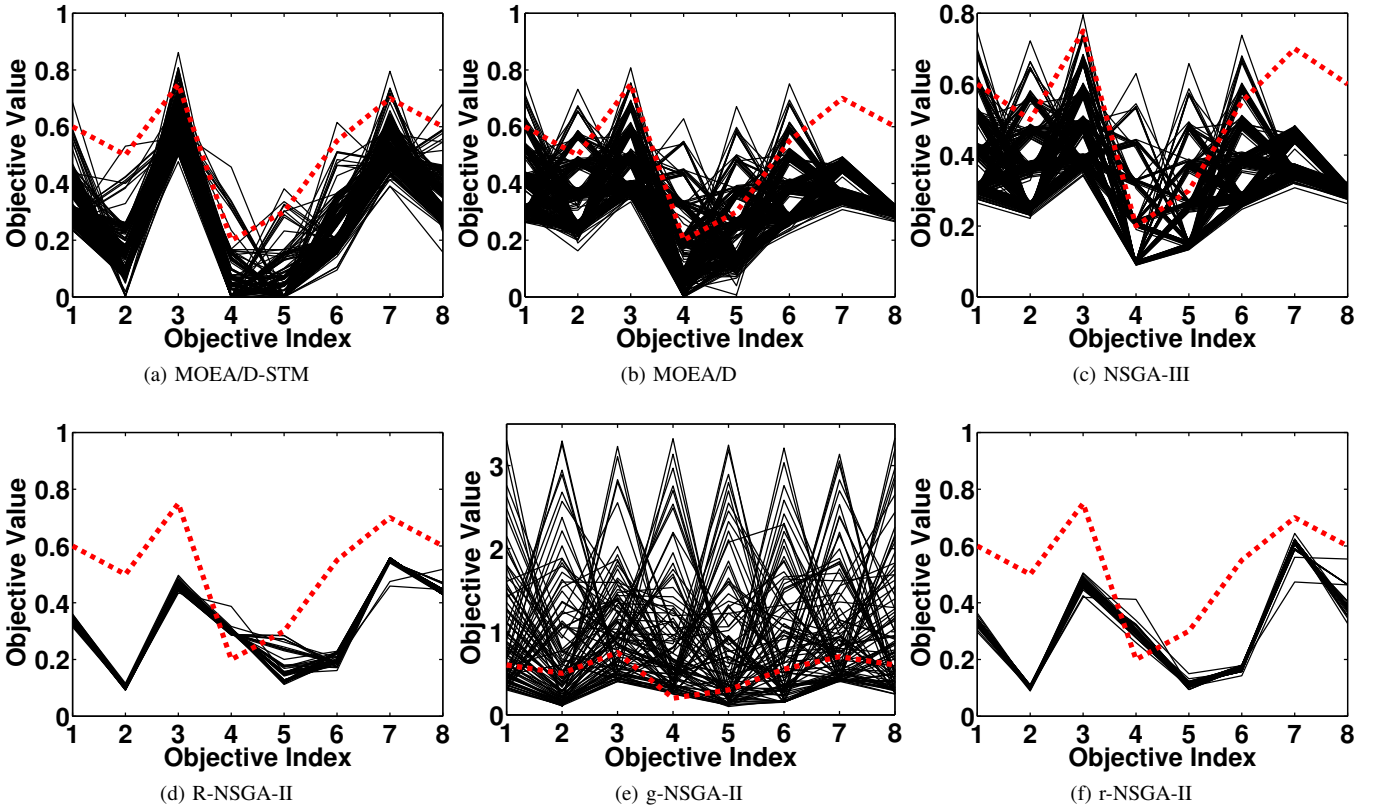


Fig. 20: Comparisons on 8-objective DTLZ1 where $\mathbf{z}^r = (0.1, 0.2, 0.1, 0.4, 0.4, 0.1, 0.3, 0.1)^T$.

Fig. 21: Comparisons on 8-objective DTLZ2 where $\mathbf{z}^r = (0.3, 0.1, 0.4, 0.25, 0.1, 0.15, 0.4, 0.25)^T$.Fig. 22: Comparisons on 8-objective DTLZ2 where $\mathbf{z}^r = (0.6, 0.5, 0.75, 0.2, 0.3, 0.55, 0.7, 0.6)^T$.

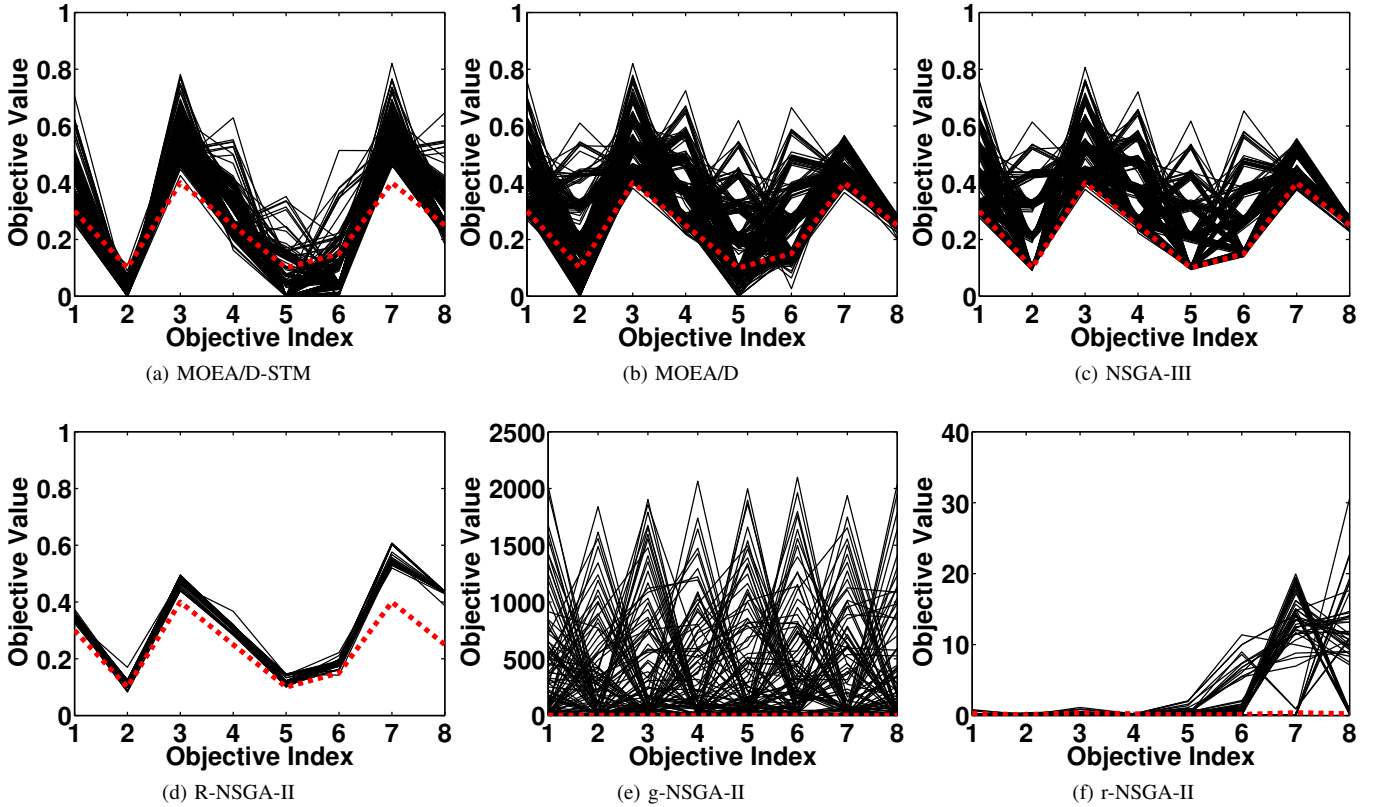


Fig. 23: Comparisons on 8-objective DTLZ3 where $\mathbf{z}^r = (0.3, 0.1, 0.4, 0.25, 0.1, 0.15, 0.4, 0.25)^T$.

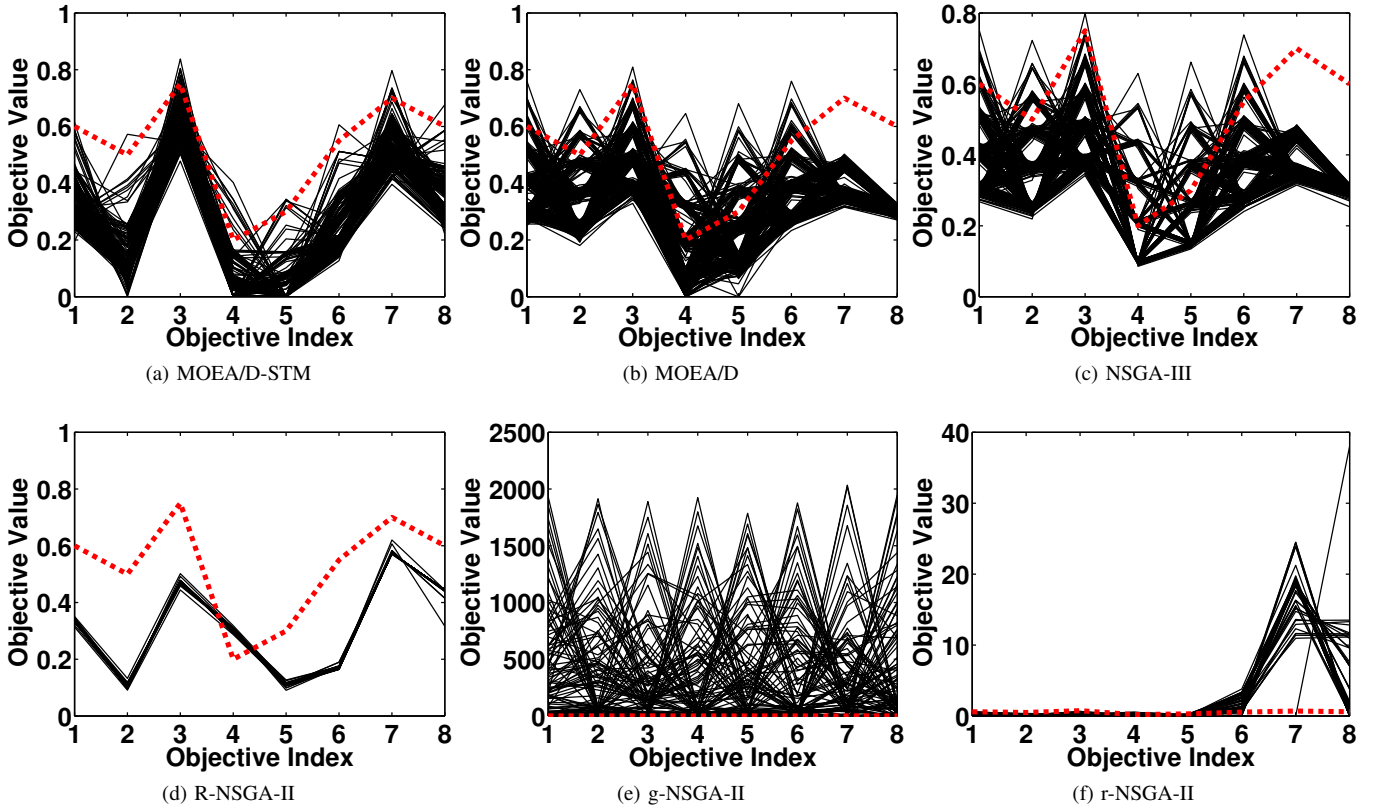


Fig. 24: Comparisons on 8-objective DTLZ3 where $\mathbf{z}^r = (0.6, 0.5, 0.75, 0.2, 0.3, 0.55, 0.7, 0.6)^T$.

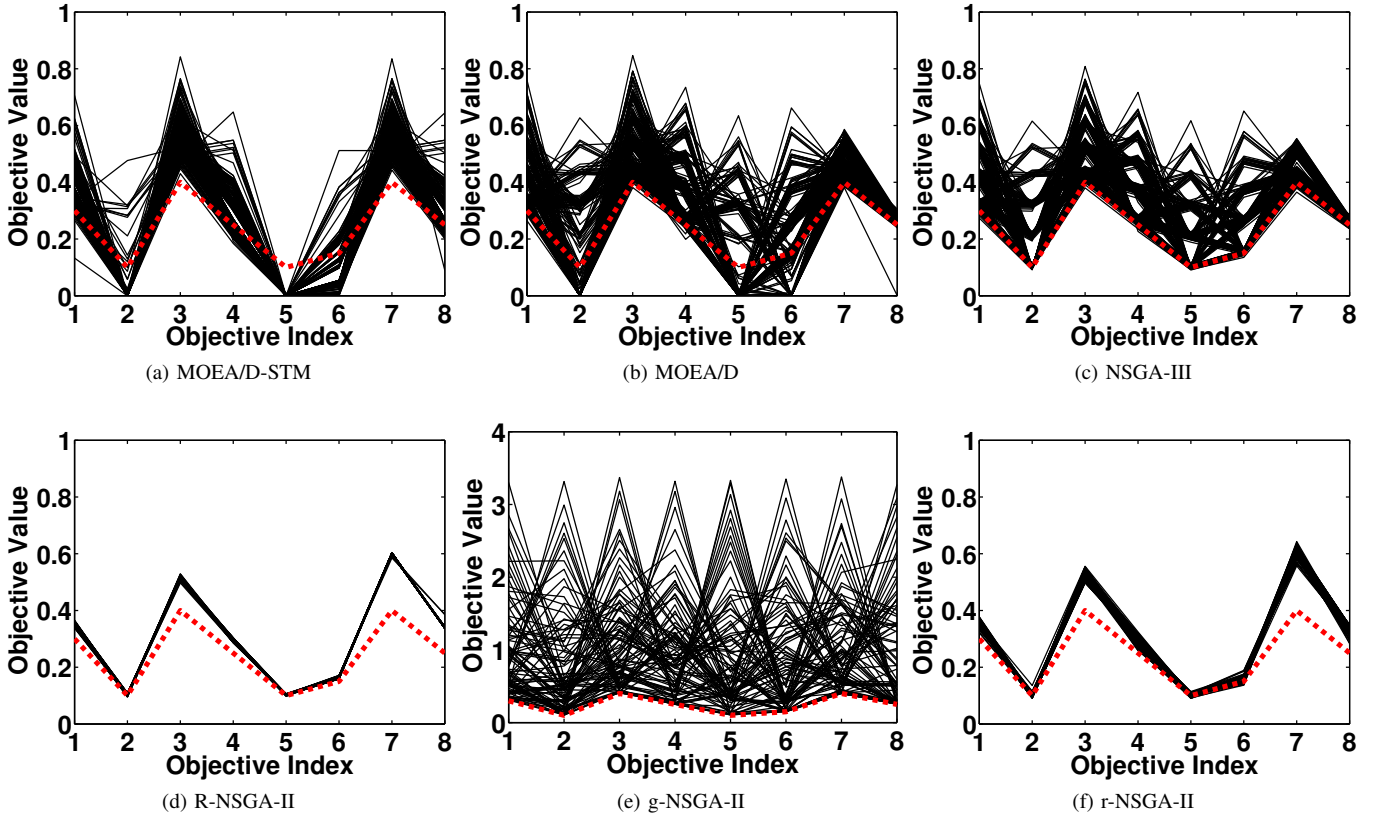


Fig. 25: Comparisons on 8-objective DTLZ4 where $\mathbf{z}^r = (0.3, 0.1, 0.4, 0.25, 0.1, 0.15, 0.4, 0.25)^T$.

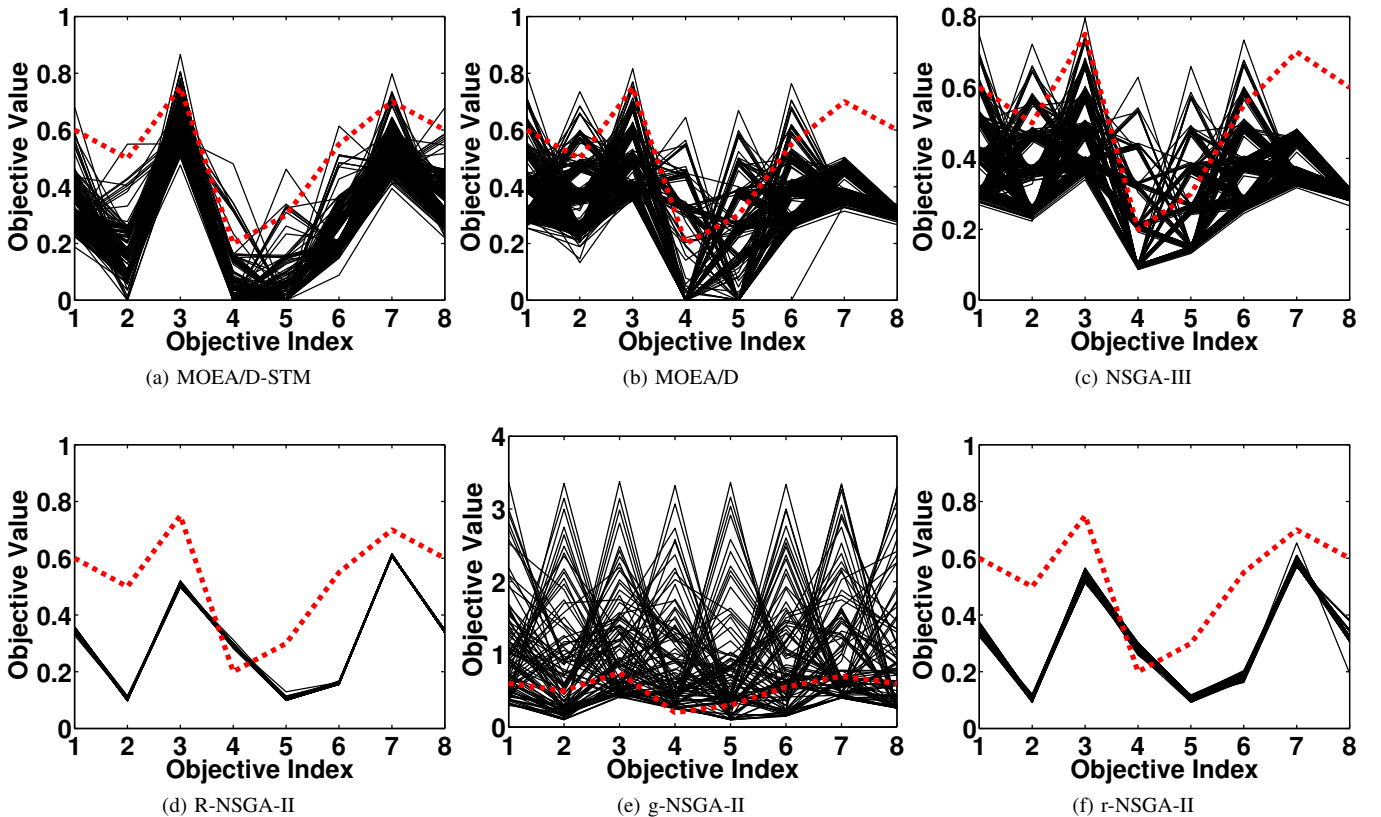


Fig. 26: Comparisons on 8-objective DTLZ4 where $\mathbf{z}^r = (0.6, 0.5, 0.75, 0.2, 0.3, 0.55, 0.7, 0.6)^T$.

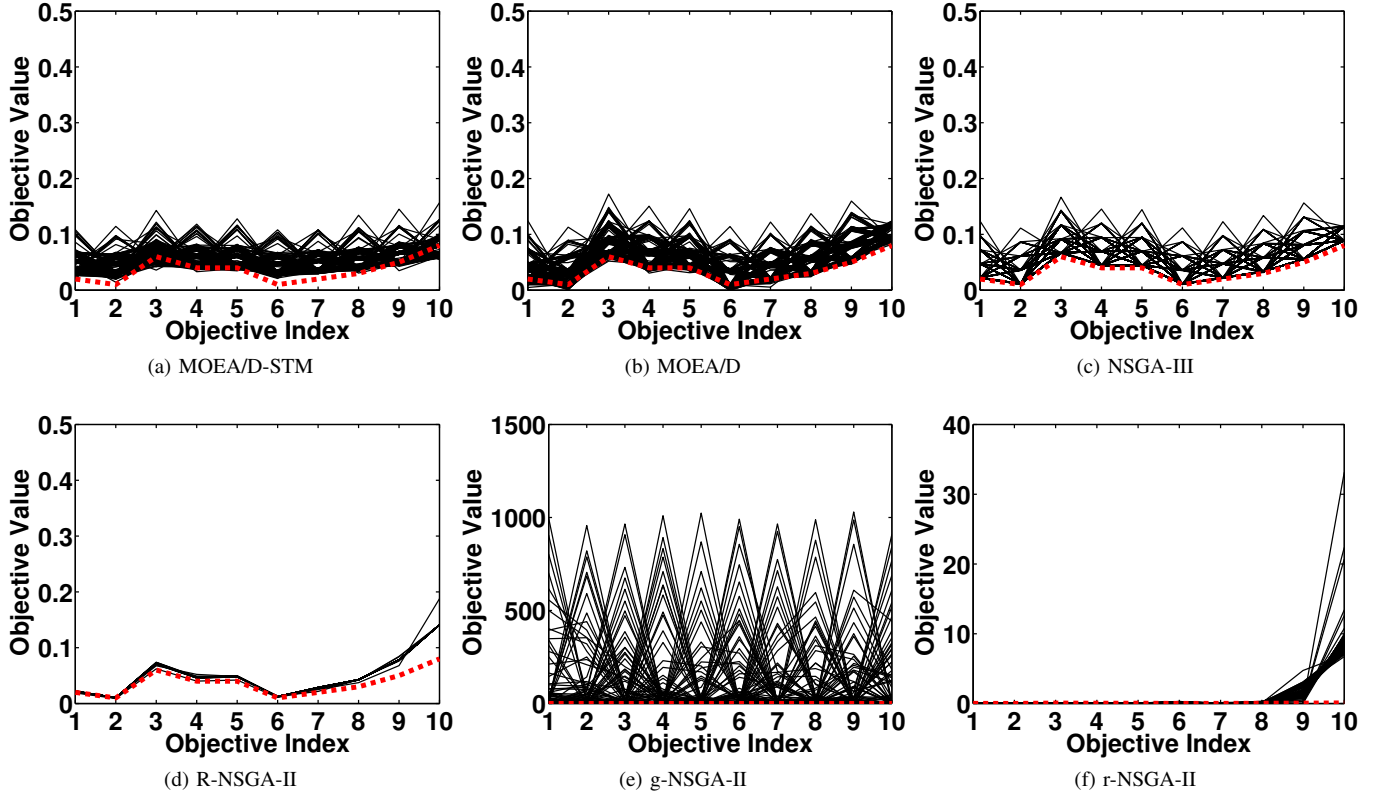


Fig. 27: Comparisons on 10-objective DTLZ1 where $\mathbf{z}^r = (0.02, 0.01, 0.06, 0.04, 0.04, 0.01, 0.02, 0.03, 0.05, 0.08)^T$.

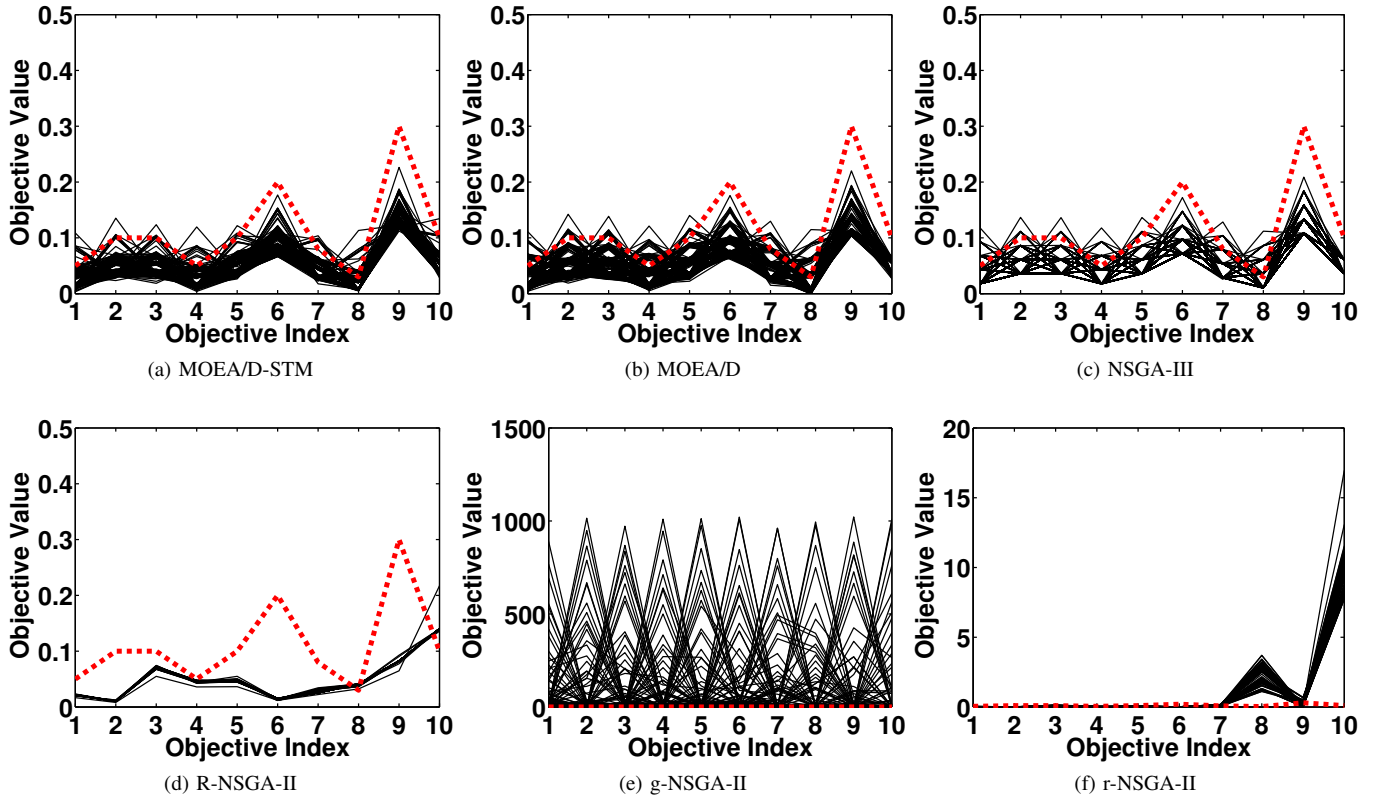


Fig. 28: Comparisons on 10-objective DTLZ1 where $\mathbf{z}^r = (0.05, 0.1, 0.1, 0.05, 0.1, 0.2, 0.08, 0.03, 0.3, 0.1)^T$.

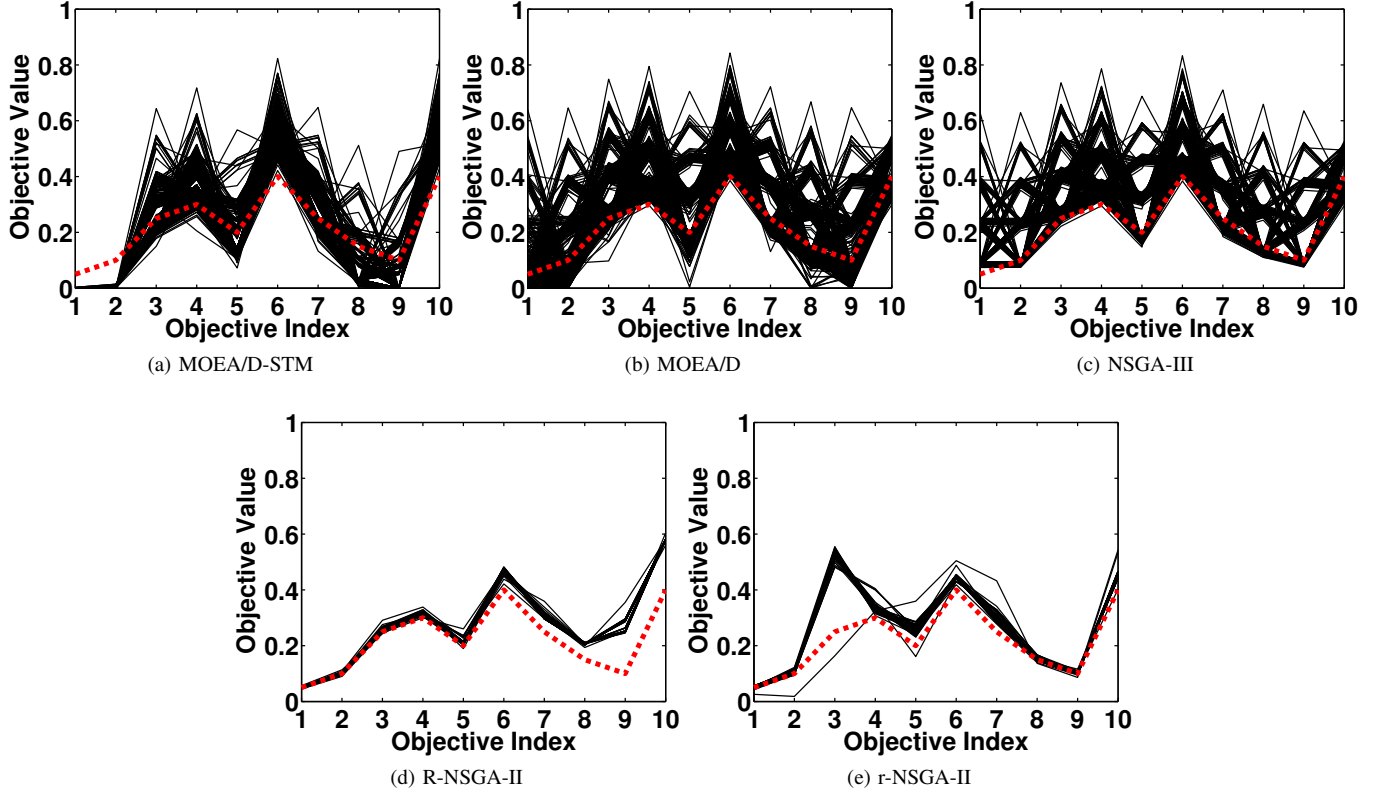


Fig. 29: Comparisons on 10-objective DTLZ2 where $\mathbf{z}^r = (0.05, 0.1, 0.25, 0.3, 0.2, 0.4, 0.25, 0.15, 0.1, 0.4)^T$.

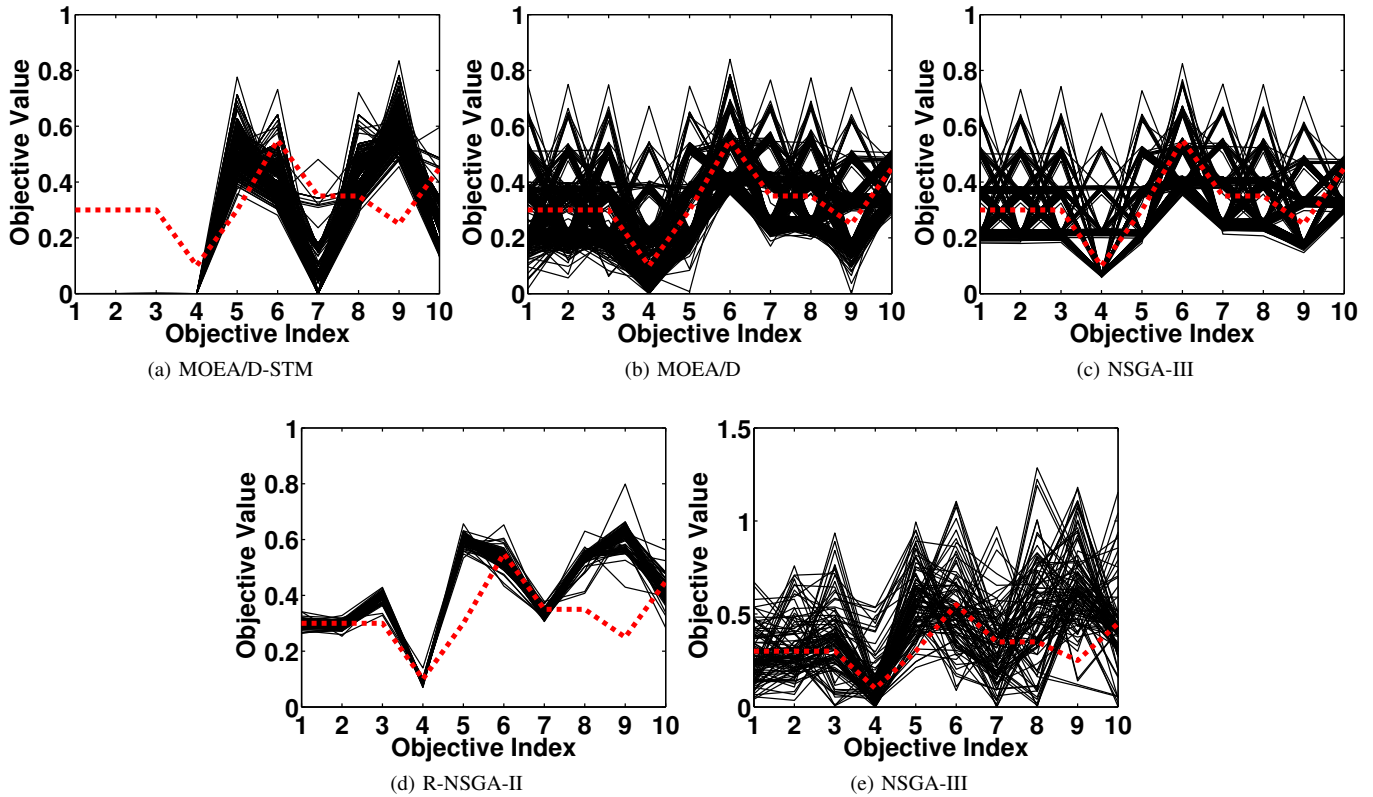


Fig. 30: Comparisons on 10-objective DTLZ2 where $\mathbf{z}^r = (0.3, 0.3, 0.3, 0.1, 0.3, 0.55, 0.35, 0.35, 0.25, 0.45)^T$.

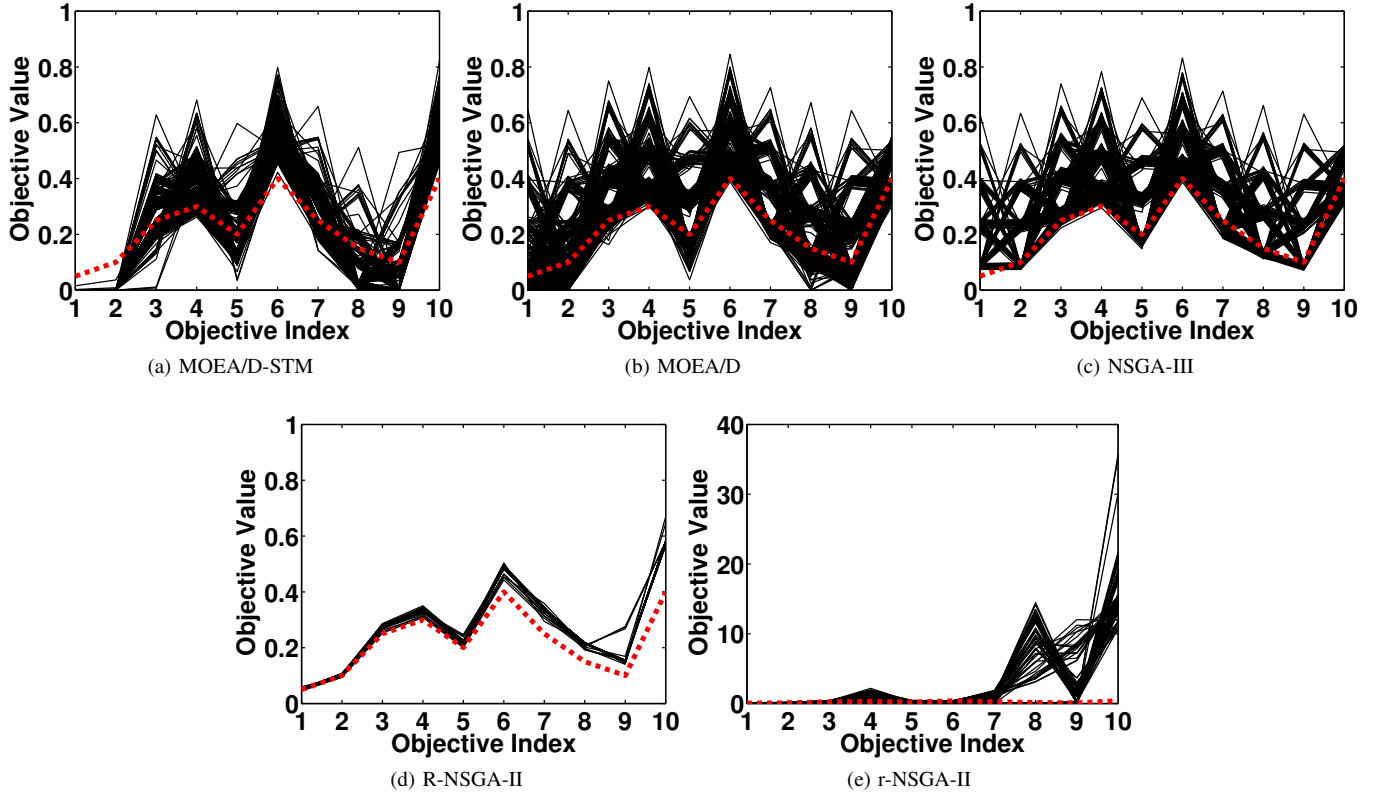


Fig. 31: Comparisons on 10-objective DTLZ3 where $\mathbf{z}^r = (0.05, 0.1, 0.25, 0.3, 0.2, 0.4, 0.25, 0.15, 0.1, 0.4)^T$.

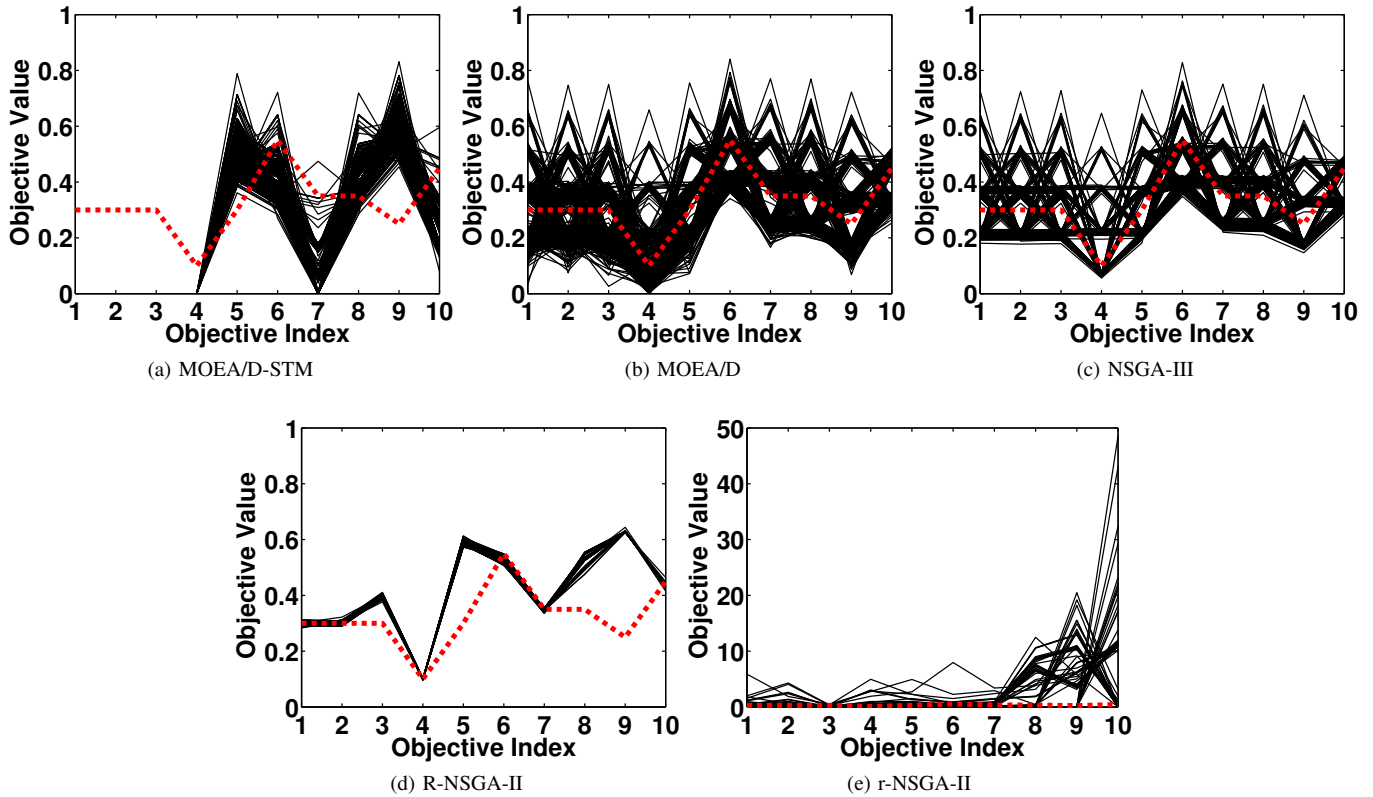


Fig. 32: Comparisons on 10-objective DTLZ3 where $\mathbf{z}^r = (0.3, 0.3, 0.3, 0.1, 0.3, 0.55, 0.35, 0.35, 0.25, 0.45)^T$.

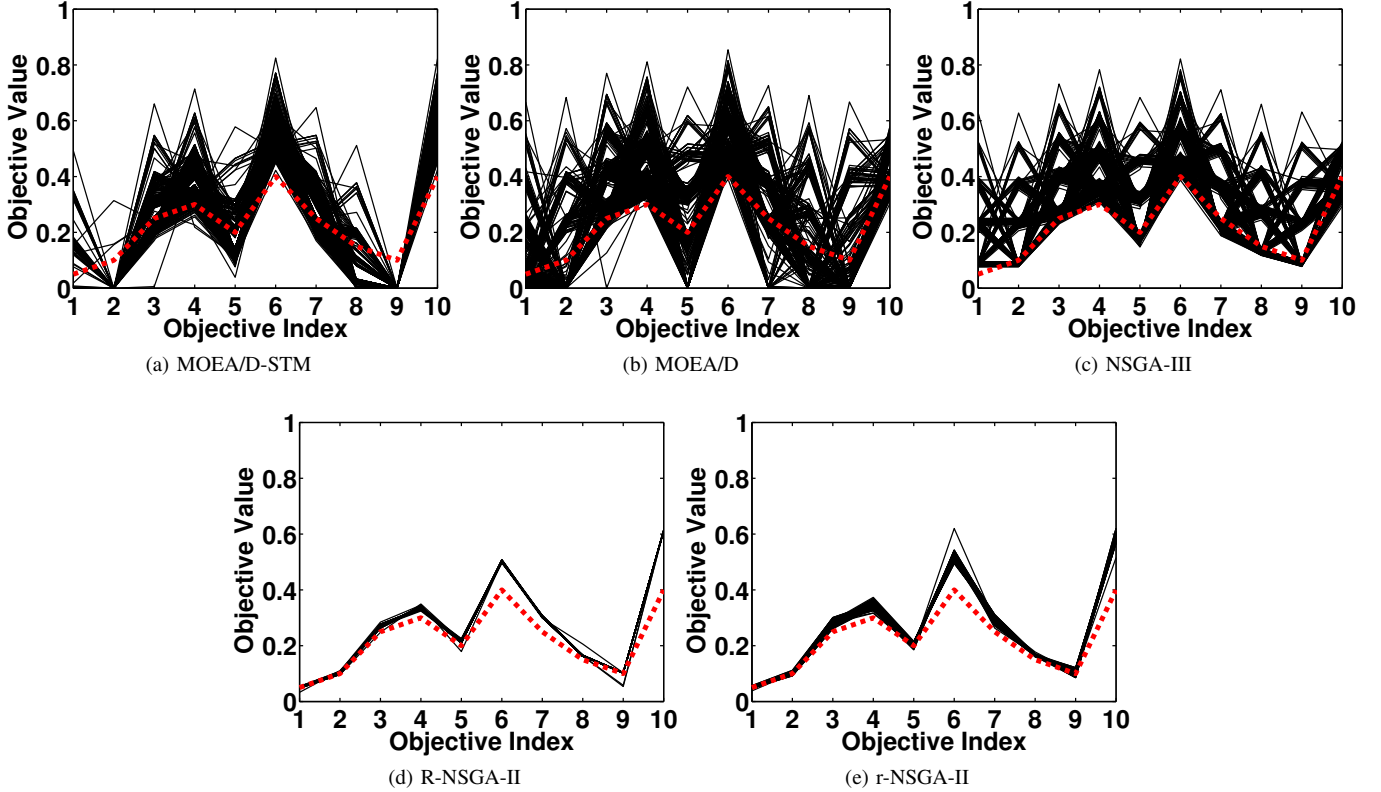


Fig. 33: Comparisons on 10-objective DTLZ4 where $\mathbf{z}^r = (0.05, 0.1, 0.25, 0.3, 0.2, 0.4, 0.25, 0.15, 0.1, 0.4)^T$.

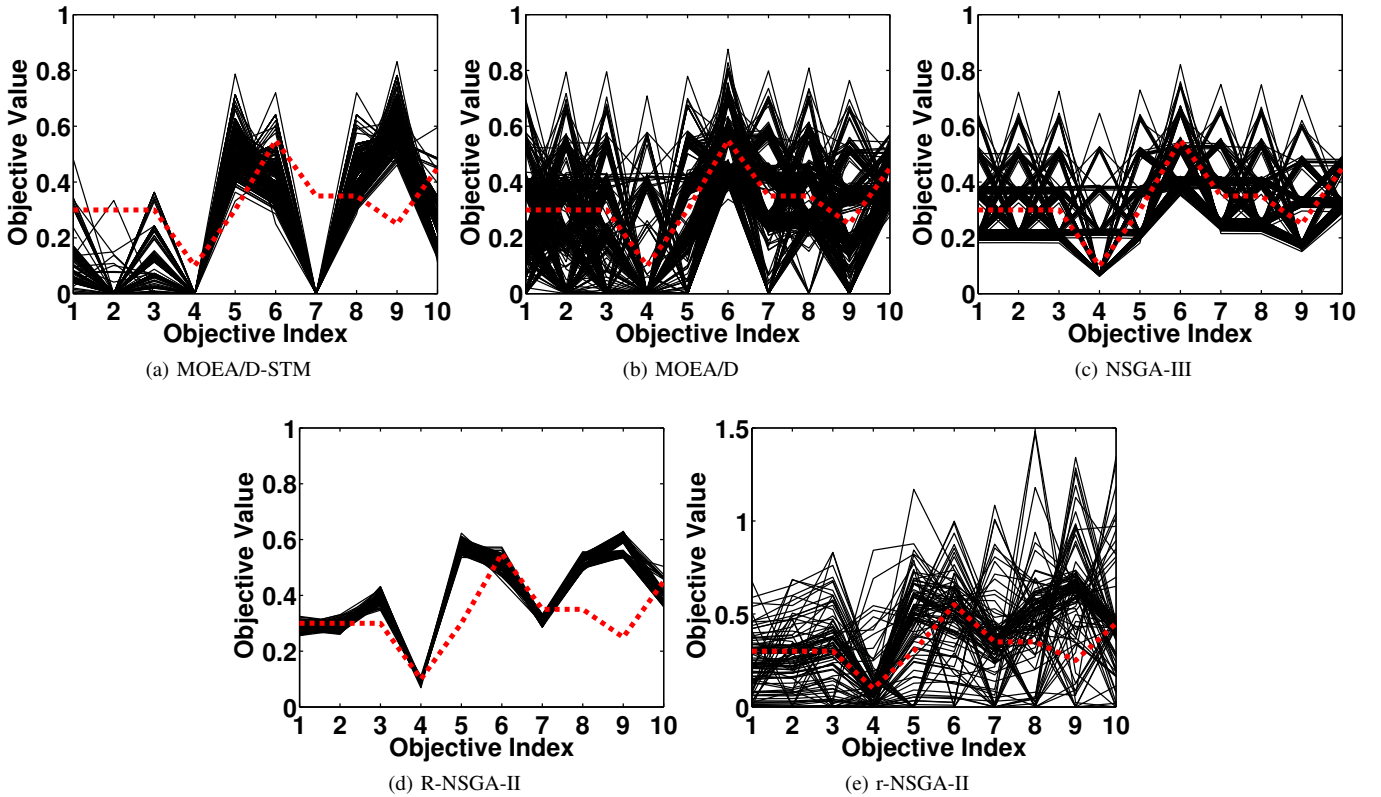
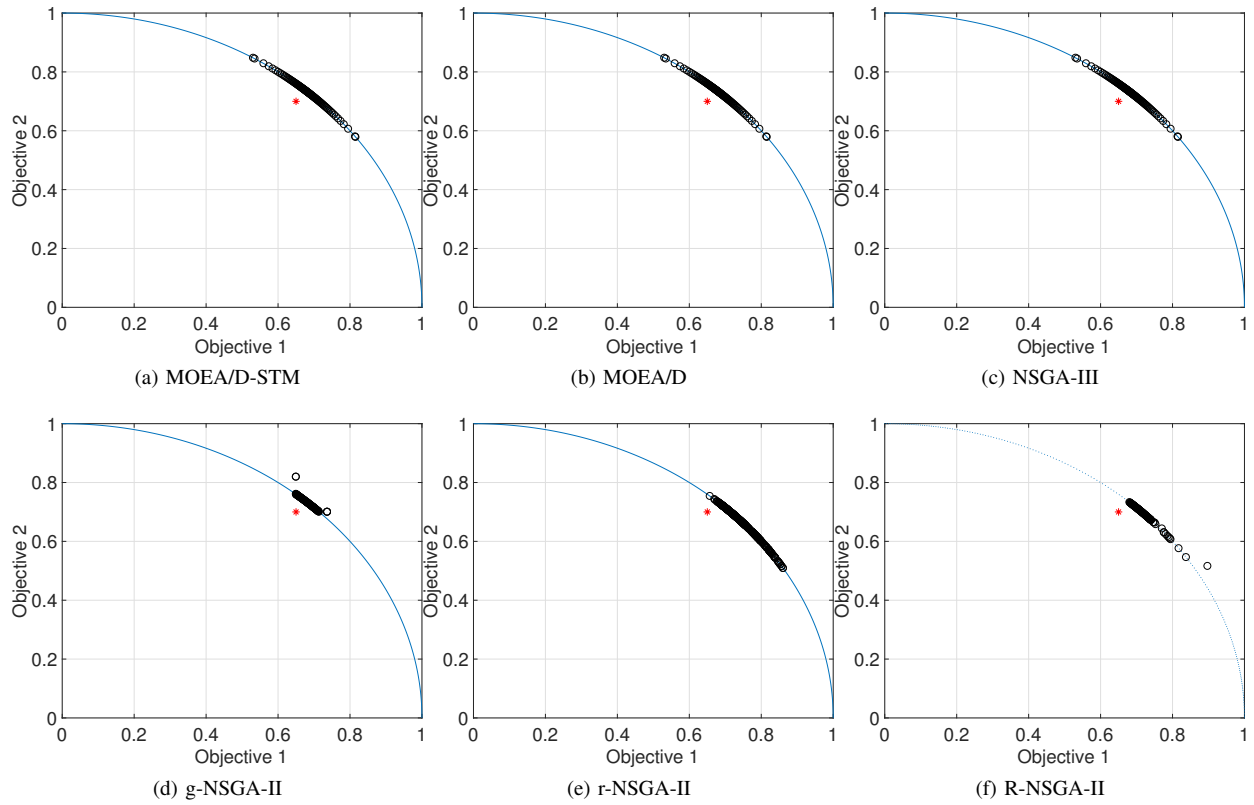
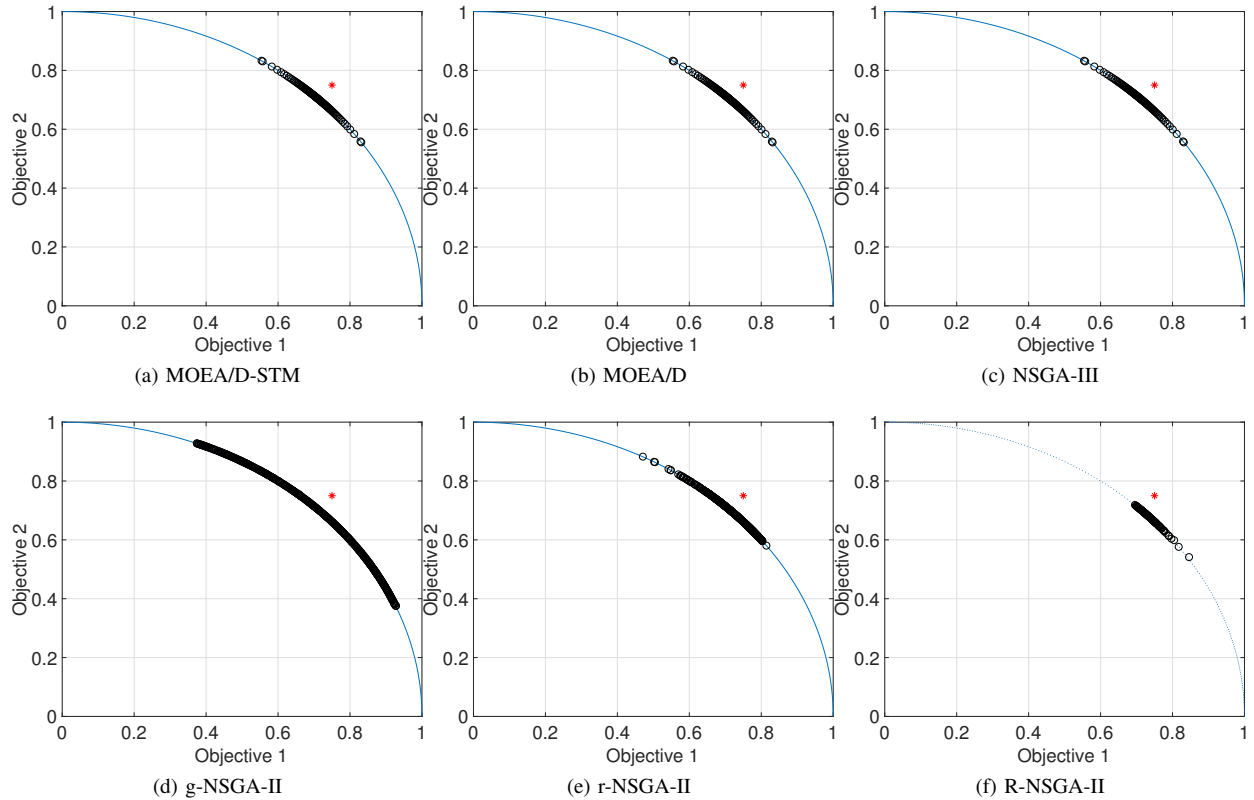
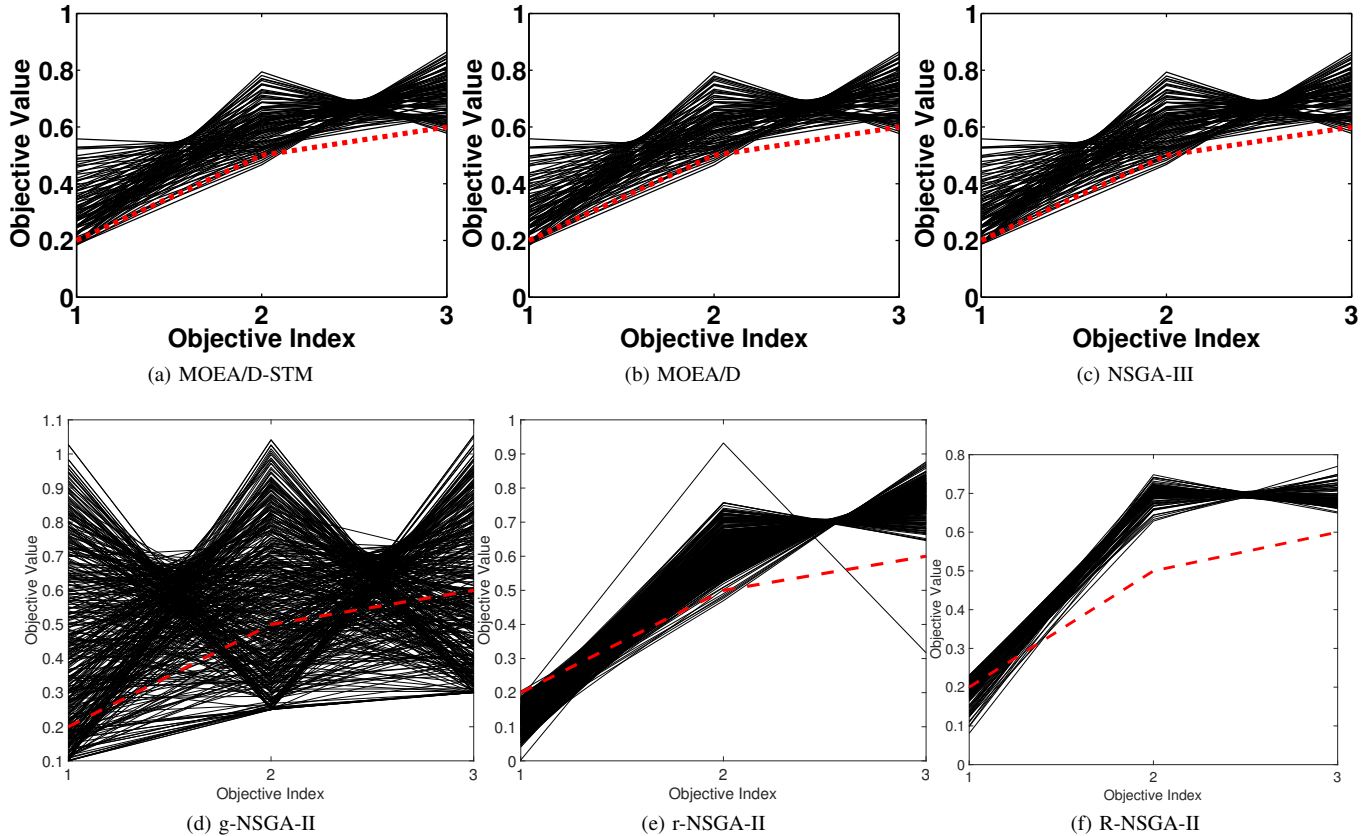
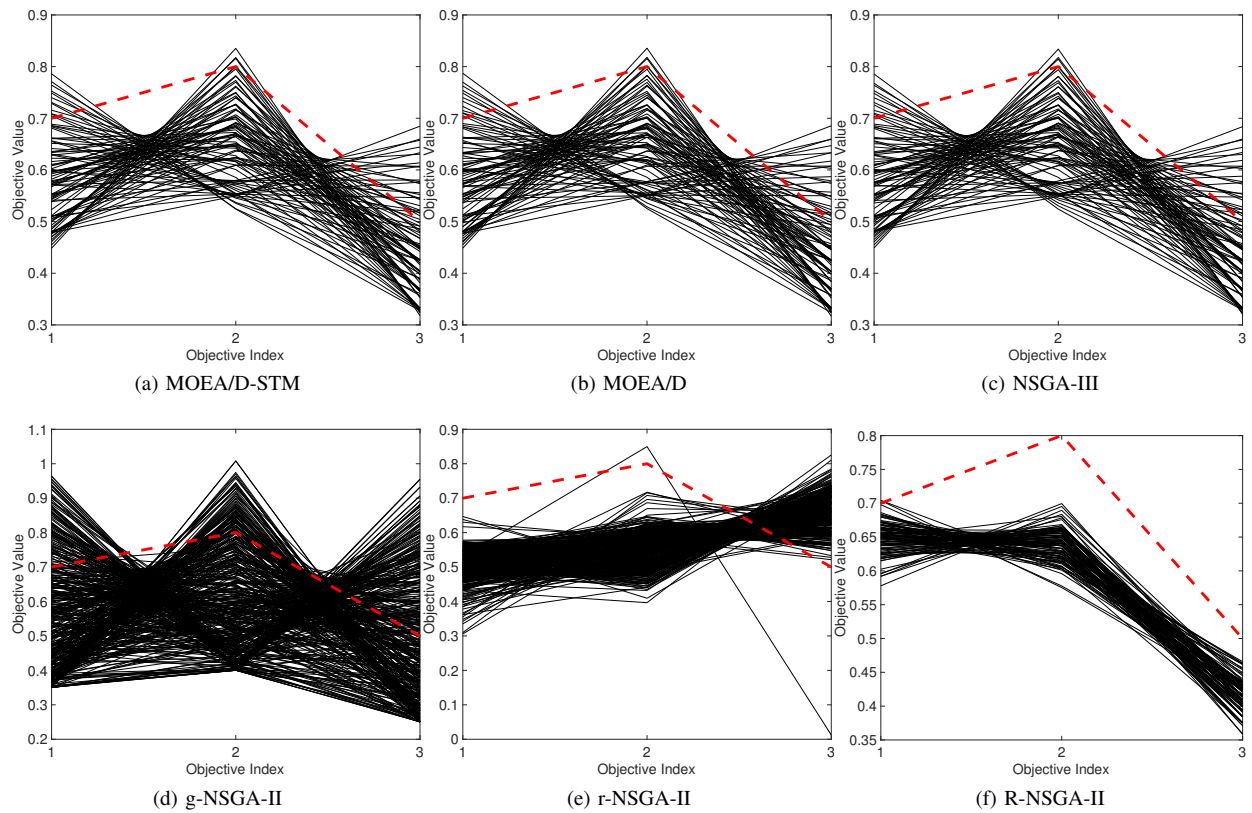
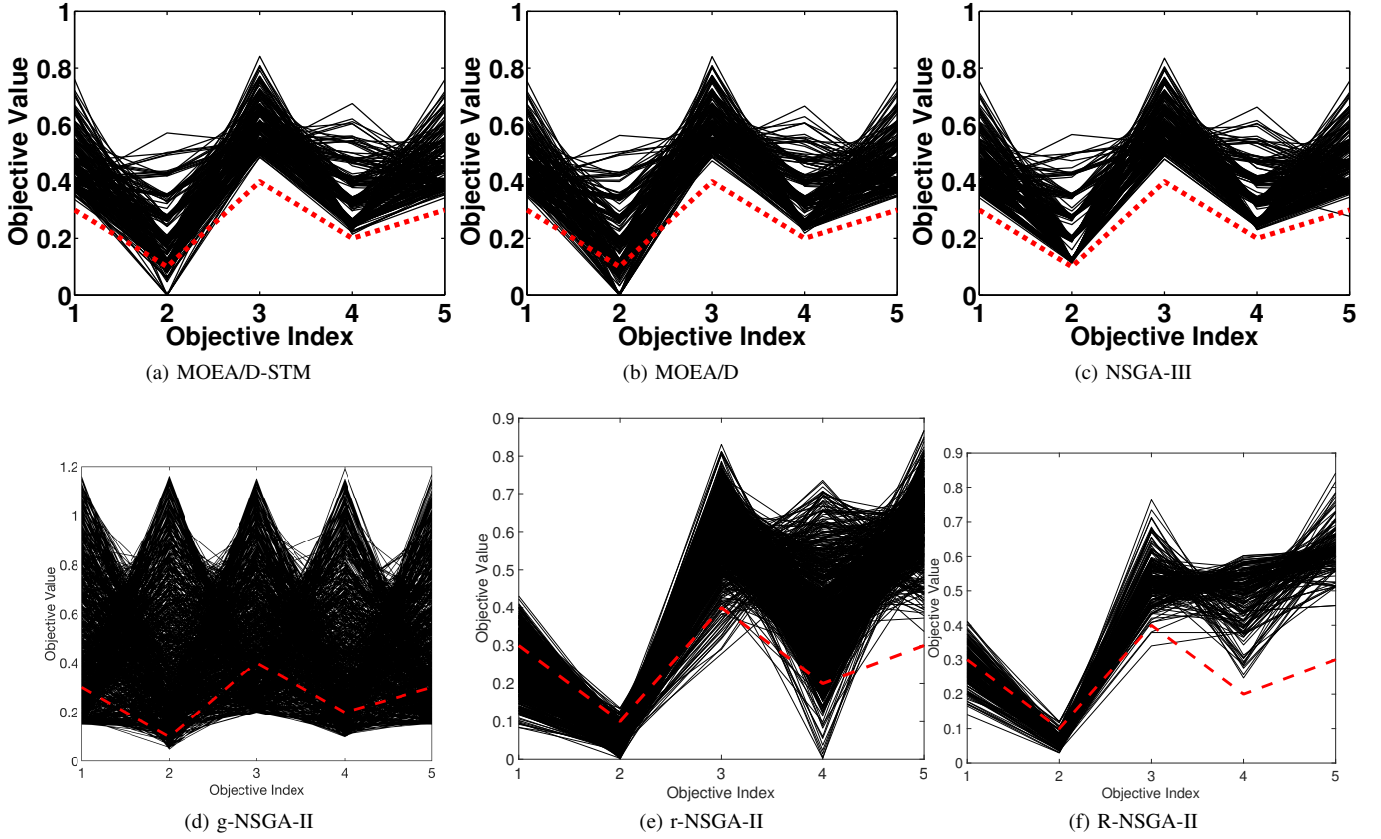
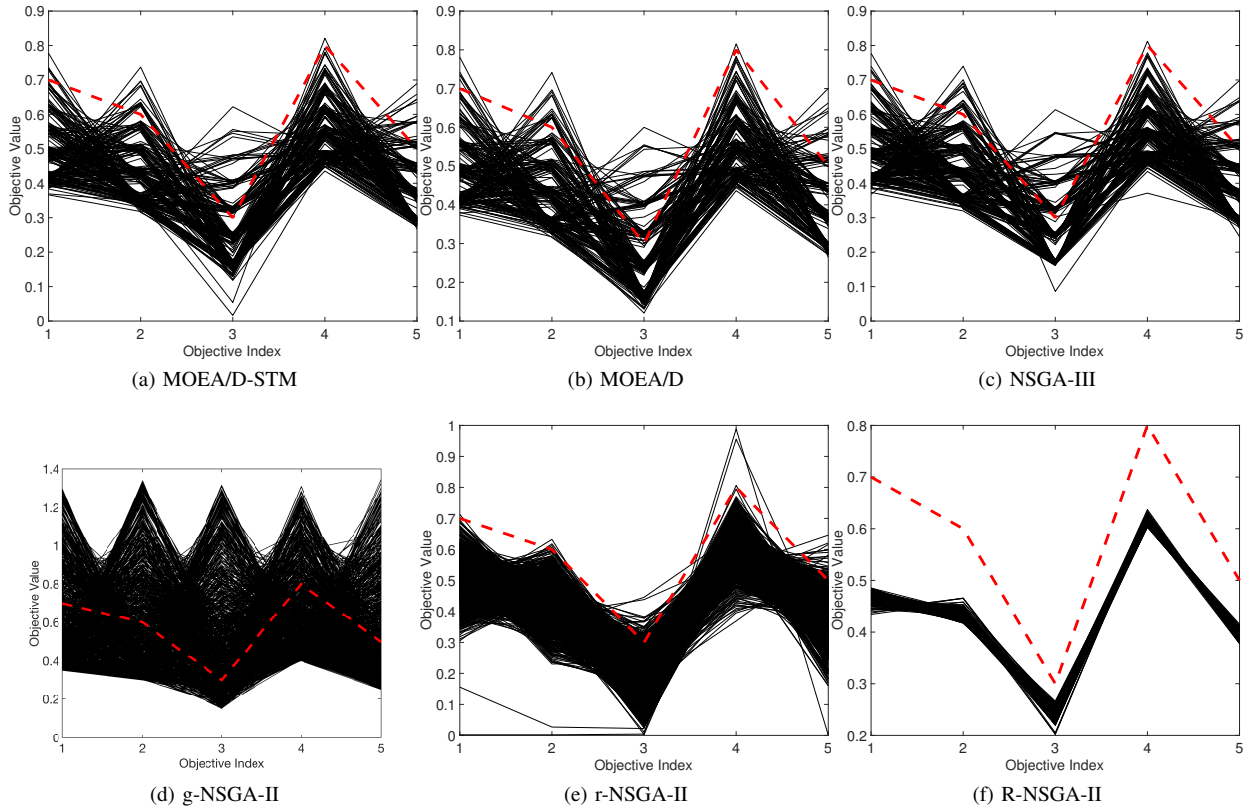


Fig. 34: Comparisons on 10-objective DTLZ4 where $\mathbf{z}^r = (0.3, 0.3, 0.3, 0.1, 0.3, 0.55, 0.35, 0.35, 0.25, 0.45)^T$.

Fig. 35: Comparisons on 2-objective WFG41 where $\mathbf{z}^r = (0.65, 0.7)^T$.Fig. 36: Comparisons on 2-objective WFG41 where $\mathbf{z}^r = (0.75, 0.75)^T$.

Fig. 37: Comparisons on 3-objective WFG41 where $\mathbf{z}^r = (0.2, 0.5, 0.6)^T$.Fig. 38: Comparisons on 3-objective WFG41 where $\mathbf{z}^r = (0.7, 0.8, 0.5)^T$.

Fig. 39: Comparisons on 5-objective WFG41 where $\mathbf{z}^r = (0.3, 0.1, 0.4, 0.2, 0.3)^T$.Fig. 40: Comparisons on 5-objective WFG41 where $\mathbf{z}^r = (0.7, 0.6, 0.3, 0.8, 0.5)^T$.

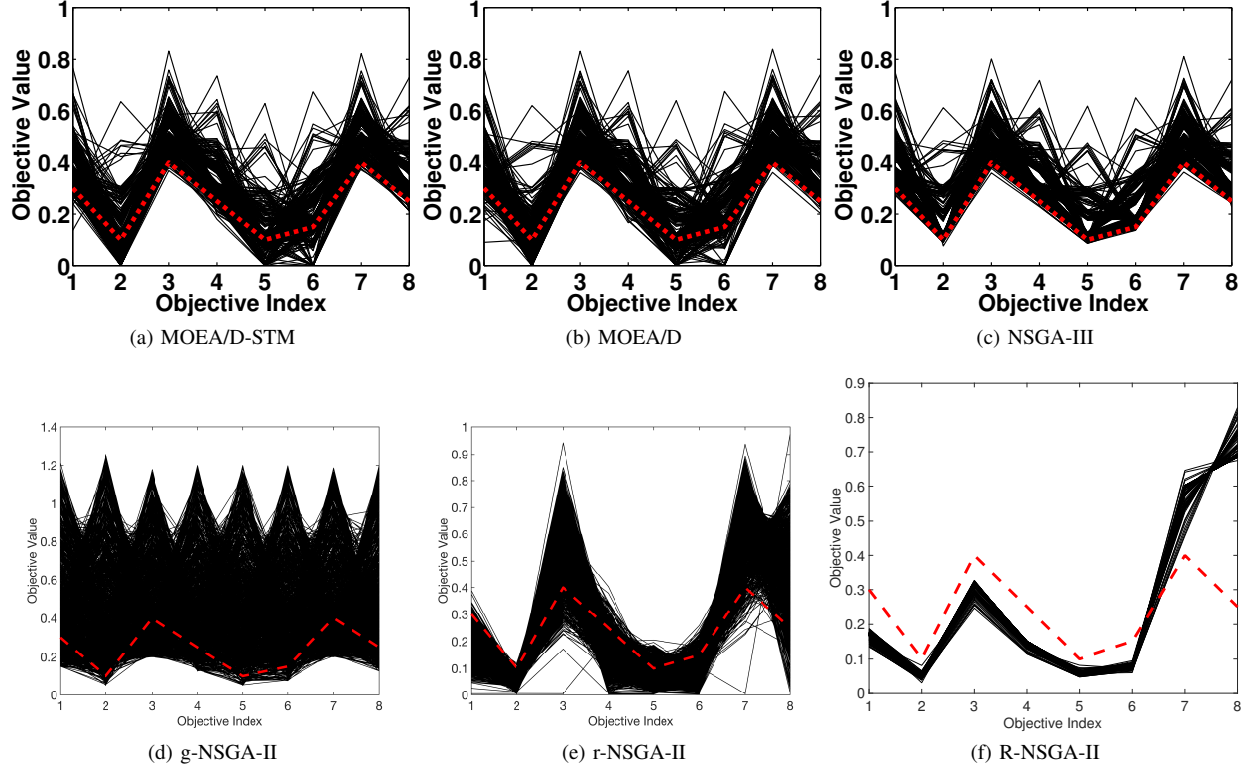


Fig. 41: Comparisons on 8-objective WFG41 where $\mathbf{z}^r = (0.3, 0.1, 0.4, 0.25, 0.1, 0.15, 0.4, 0.25)^T$.

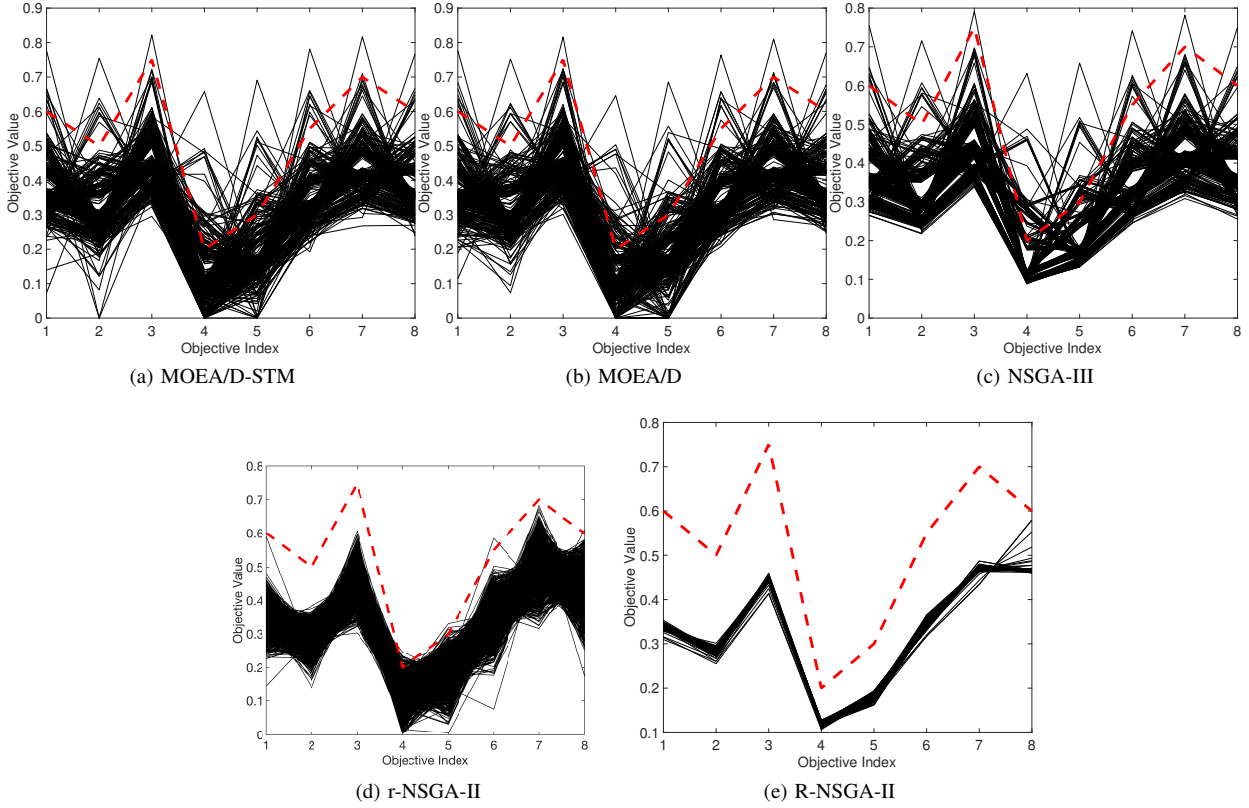


Fig. 42: Comparisons on 8-objective WFG41 where $\mathbf{z}^r = (0.6, 0.5, 0.75, 0.2, 0.3, 0.55, 0.7, 0.6)^T$.

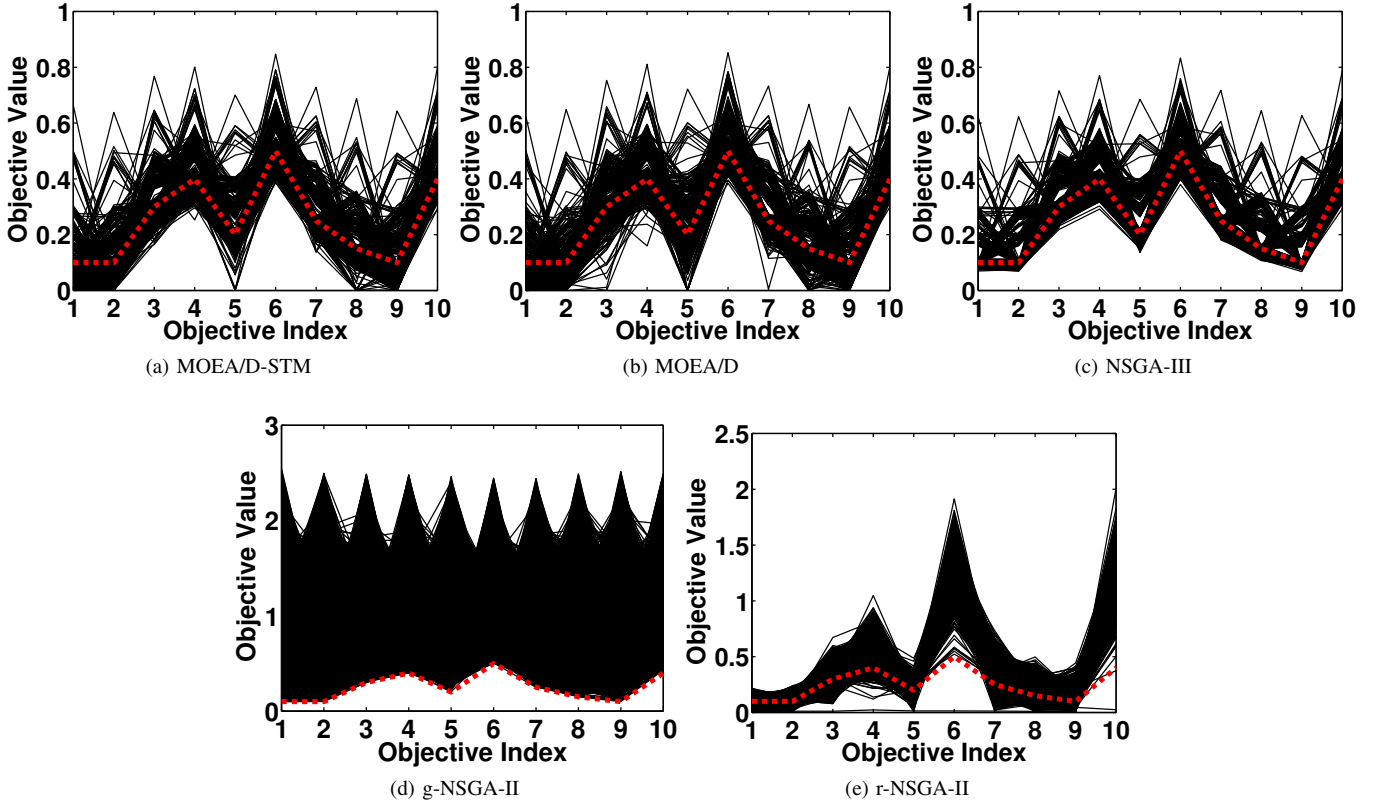


Fig. 43: Comparisons on 10-objective WFG41 where $\mathbf{z}^r = (0.1, 0.1, 0.3, 0.4, 0.2, 0.5, 0.25, 0.15, 0.1, 0.4)^T$.

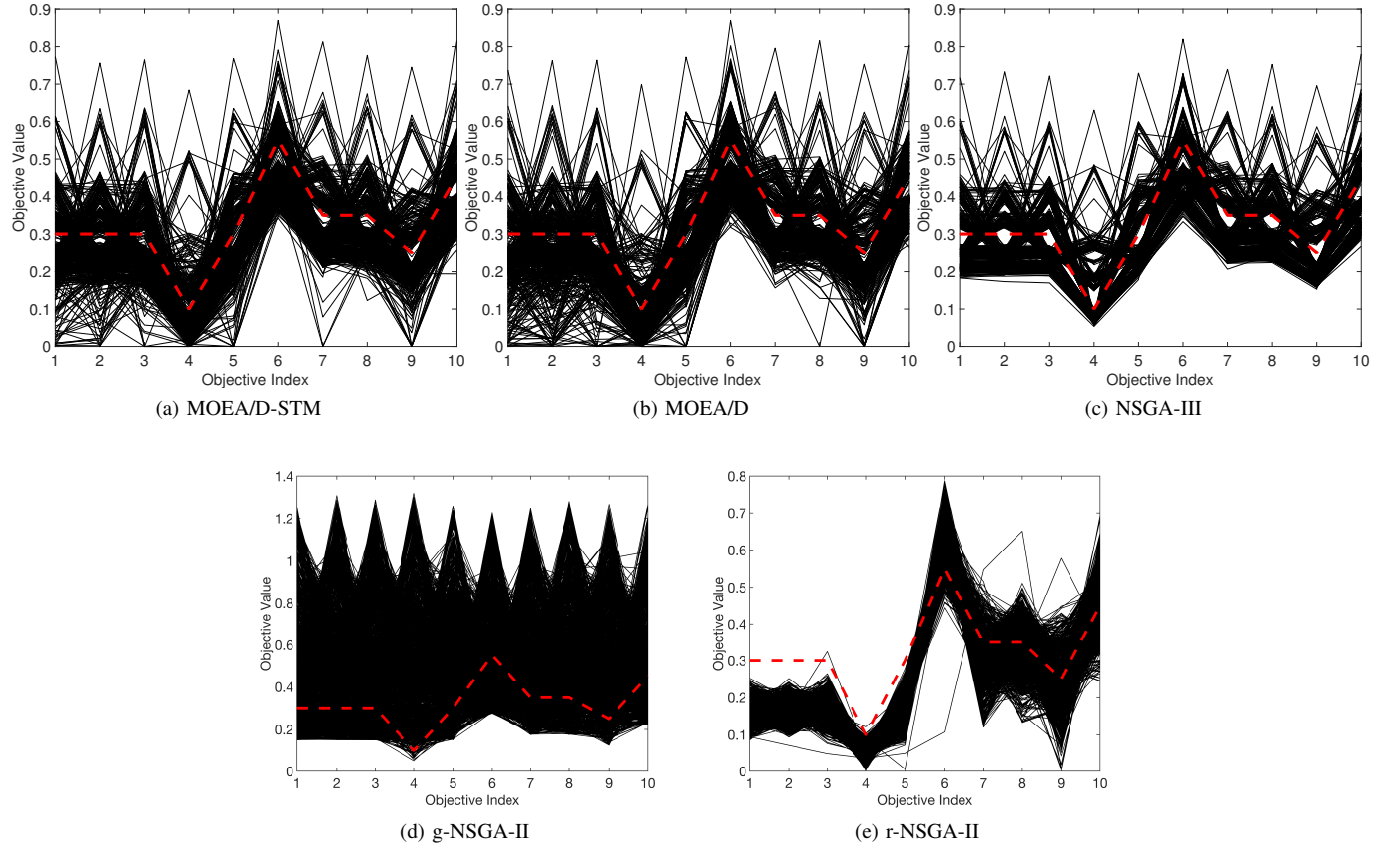
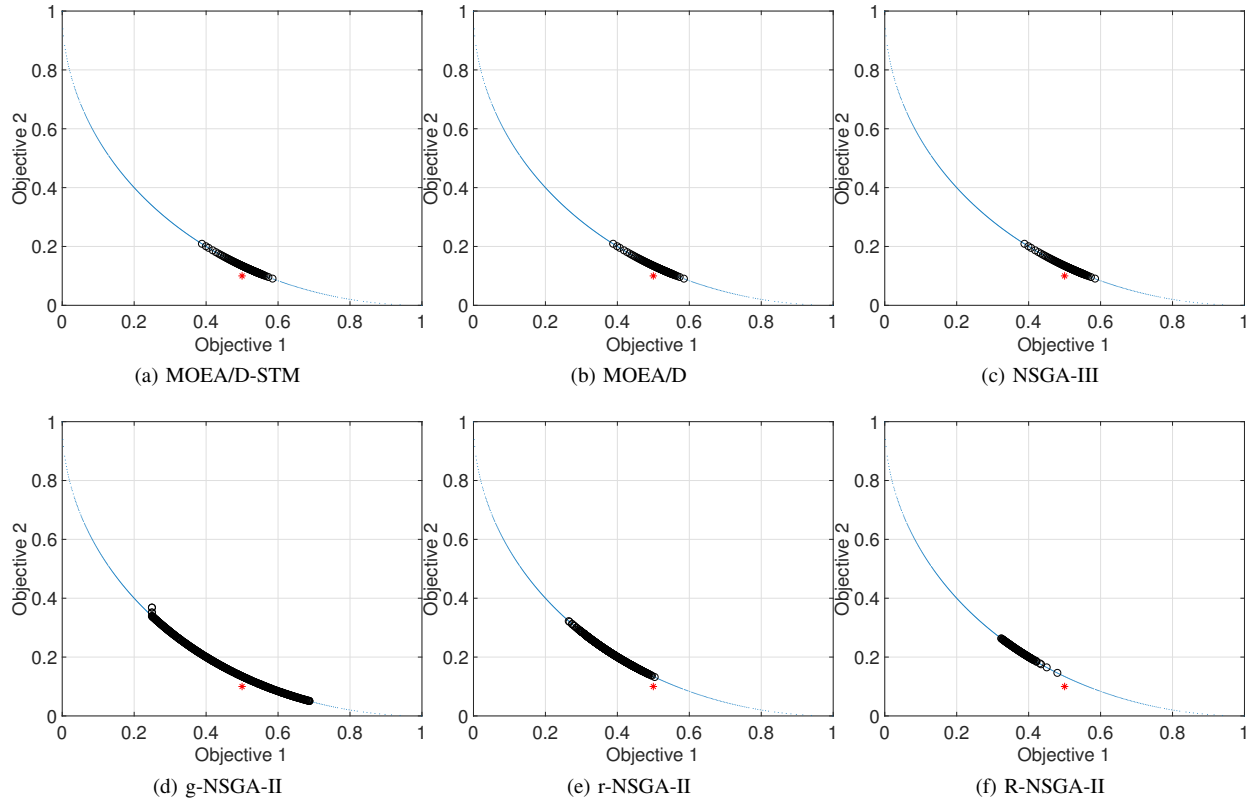
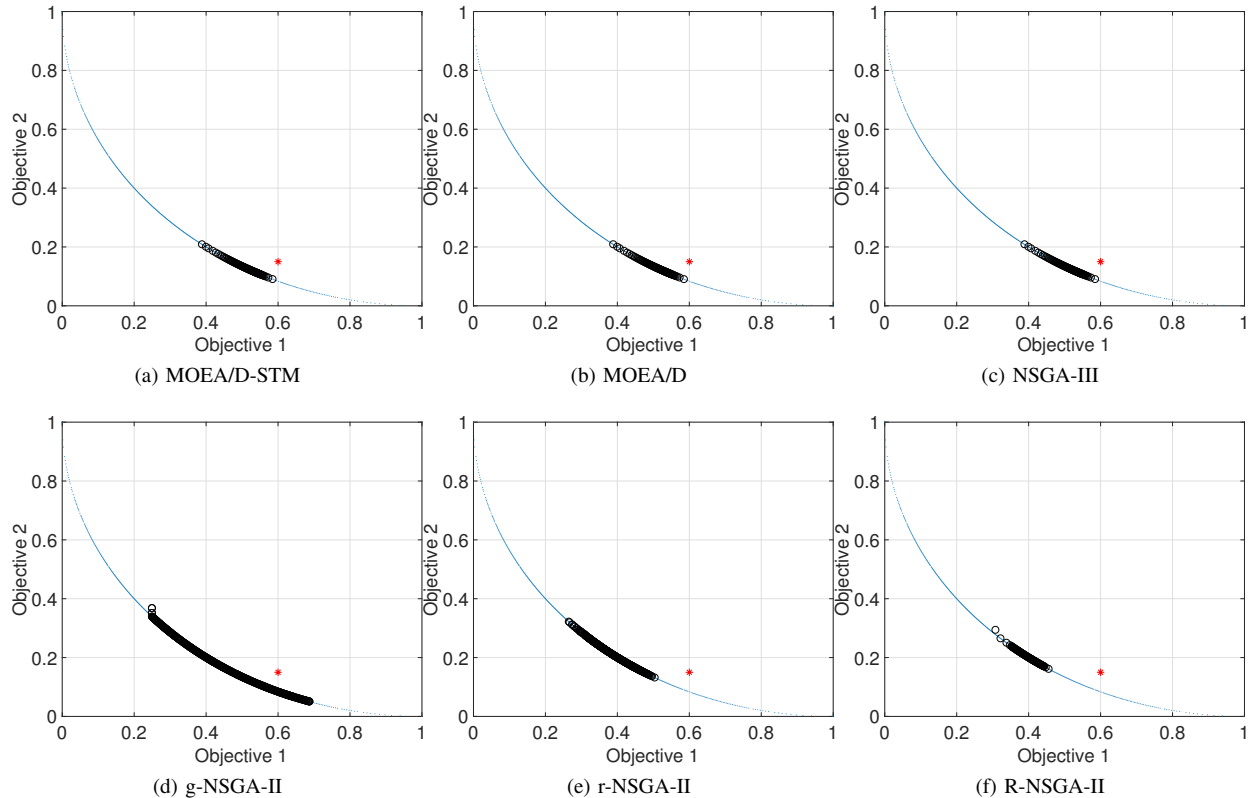
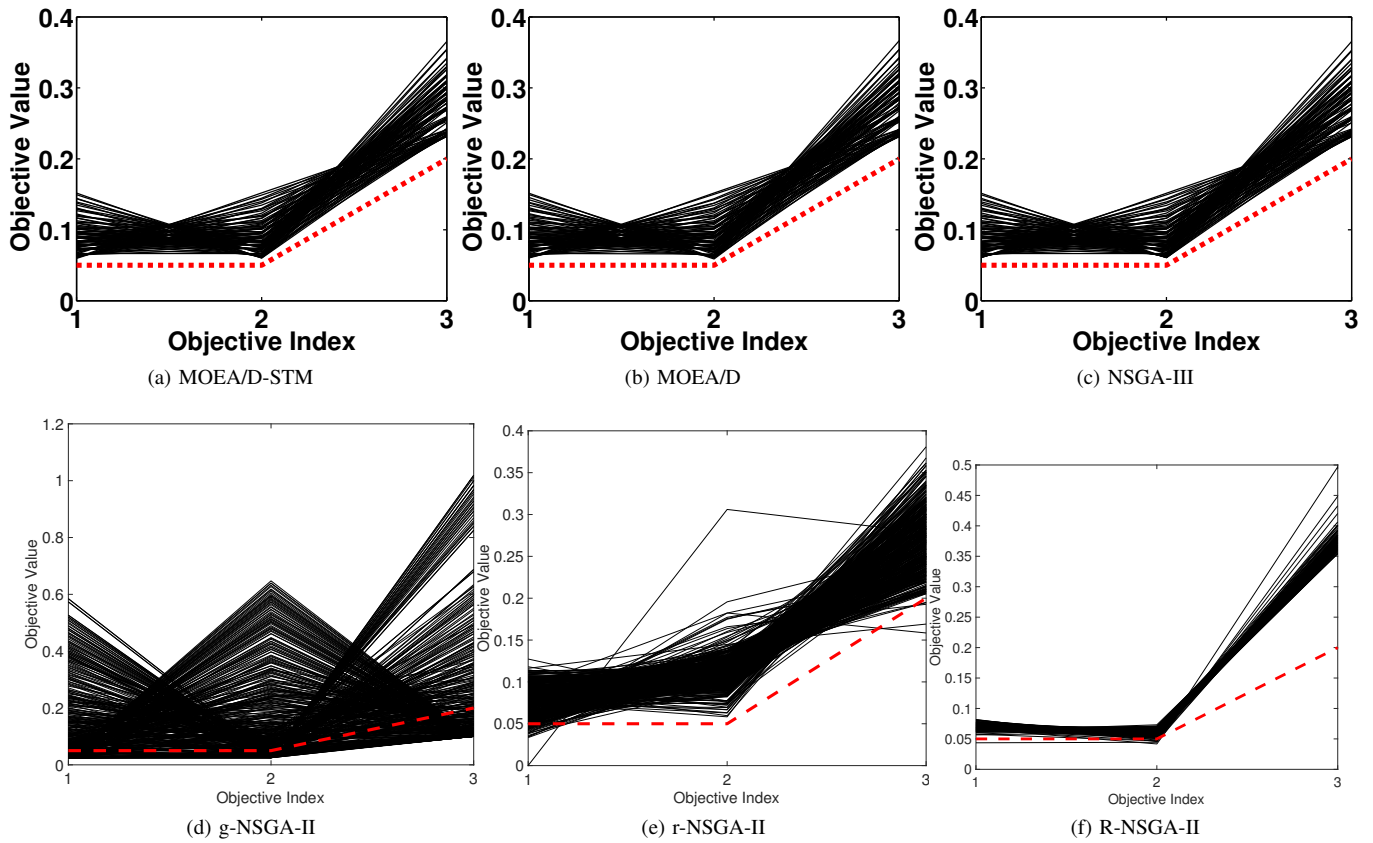
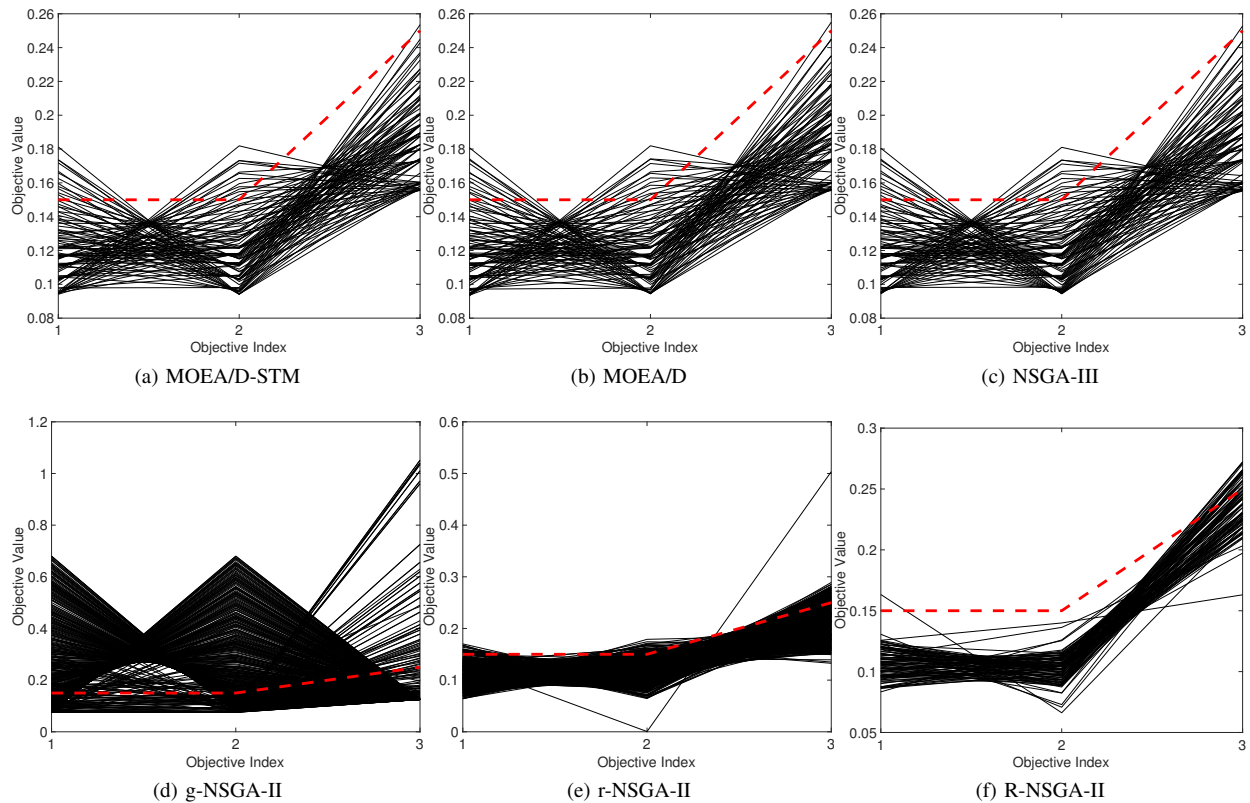


Fig. 44: Comparisons on 10-objective WFG41 where $\mathbf{z}^r = (0.3, 0.3, 0.3, 0.1, 0.3, 0.55, 0.35, 0.35, 0.25, 0.45)^T$.

Fig. 45: Comparisons on 2-objective WFG42 where $\mathbf{z}^r = (0.5, 0.1)^T$.Fig. 46: Comparisons on 2-objective WFG42 where $\mathbf{z}^r = (0.6, 0.15)^T$.

Fig. 47: Comparisons on 3-objective WFG42 where $\mathbf{z}^r = (0.05, 0.05, 0.2)^T$.Fig. 48: Comparisons on 3-objective WFG42 where $\mathbf{z}^r = (0.15, 0.15, 0.25)^T$.

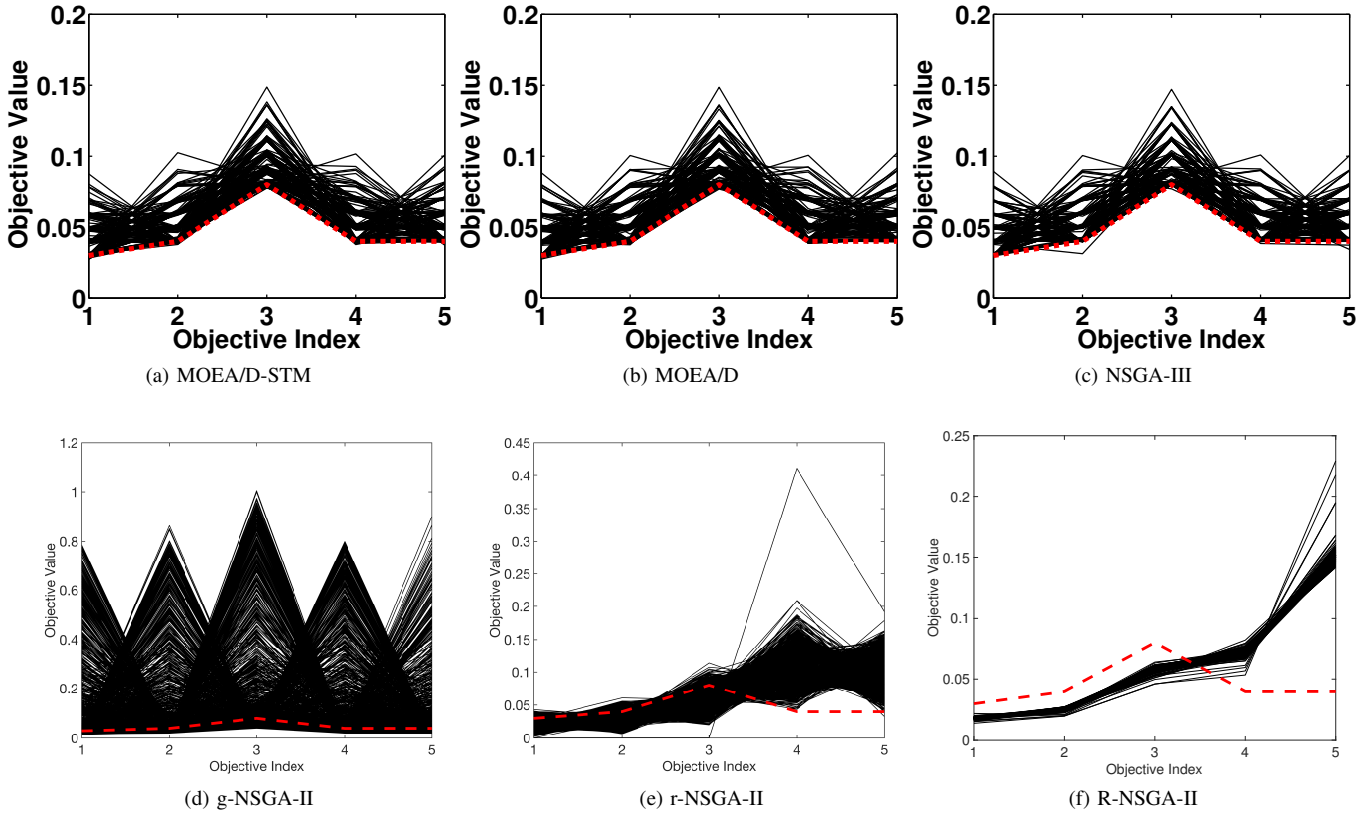


Fig. 49: Comparisons on 5-objective WFG42 where $\mathbf{z}^r = (0.03, 0.04, 0.08, 0.04, 0.04)^T$.

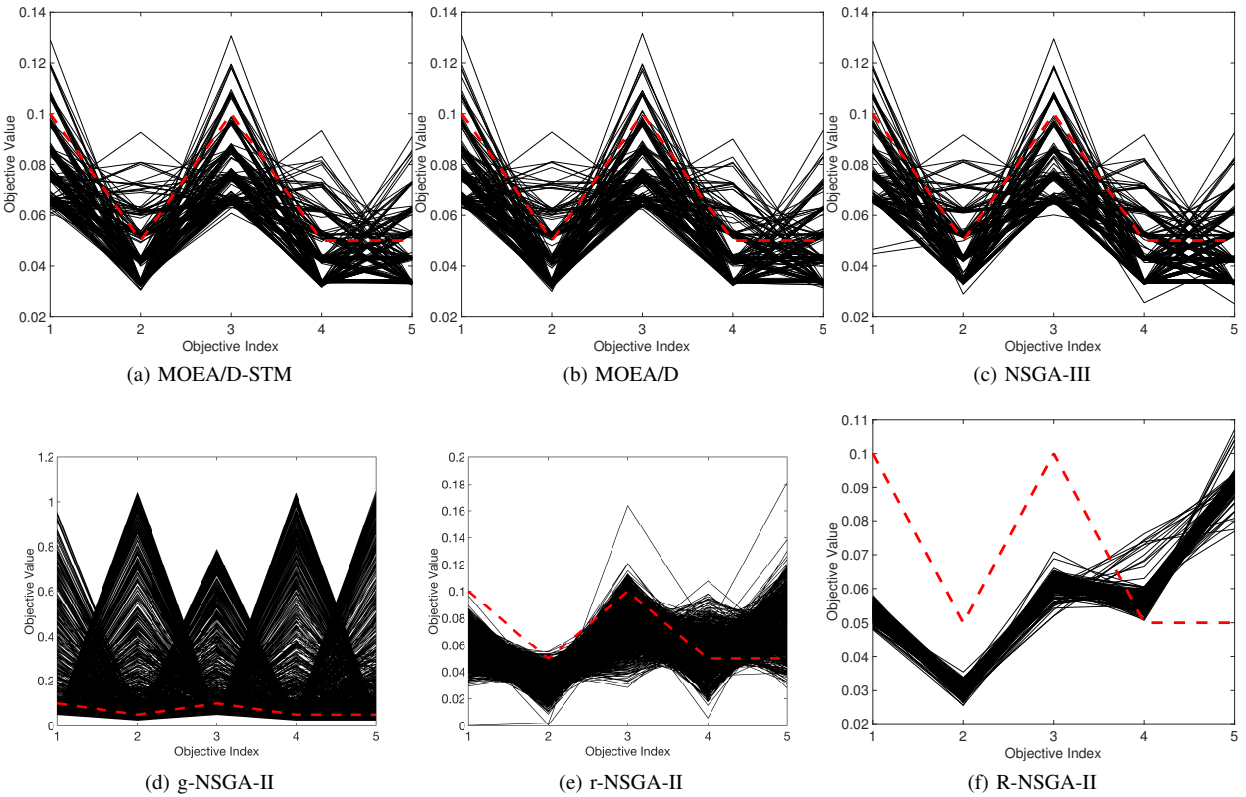


Fig. 50: Comparisons on 5-objective WFG42 where $\mathbf{z}^r = (0.1, 0.05, 0.1, 0.05, 0.05)^T$.

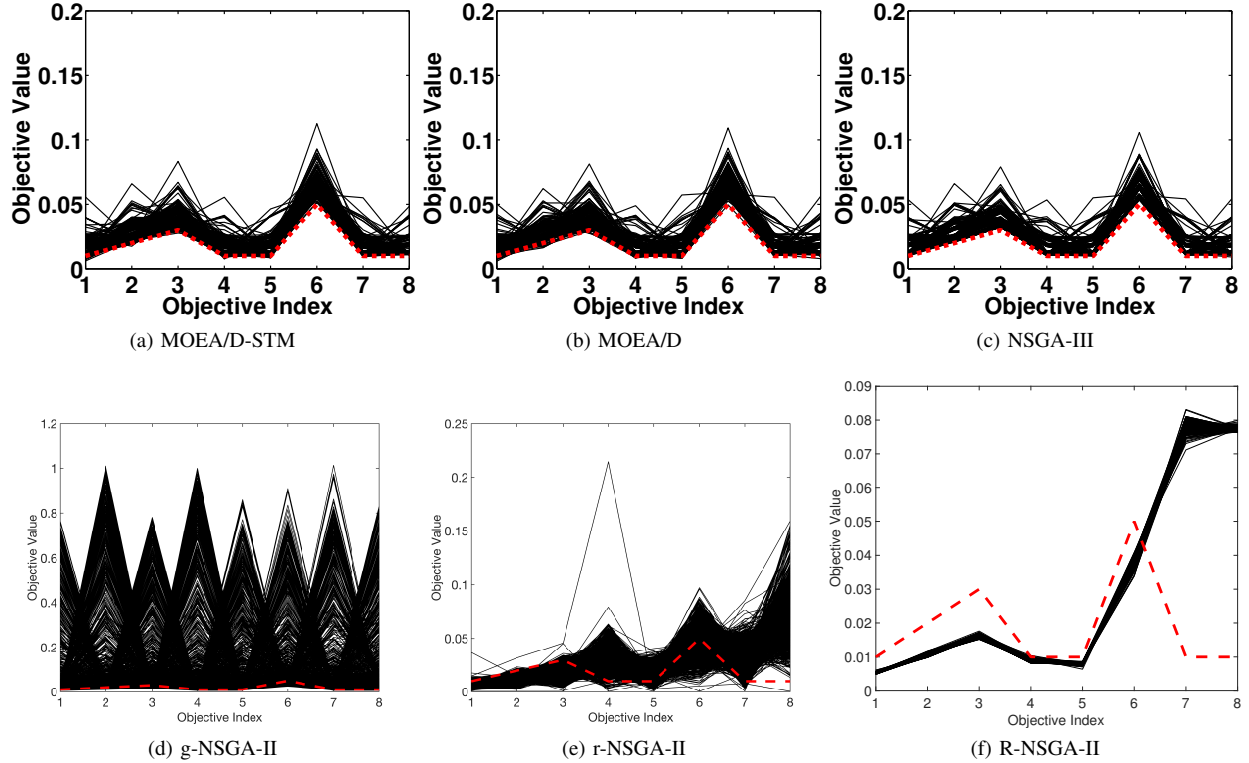


Fig. 51: Comparisons on 8-objective WFG42 where $\mathbf{z}^r = (0.01, 0.02, 0.03, 0.01, 0.01, 0.01, 0.05, 0.01, 0.01)^T$.

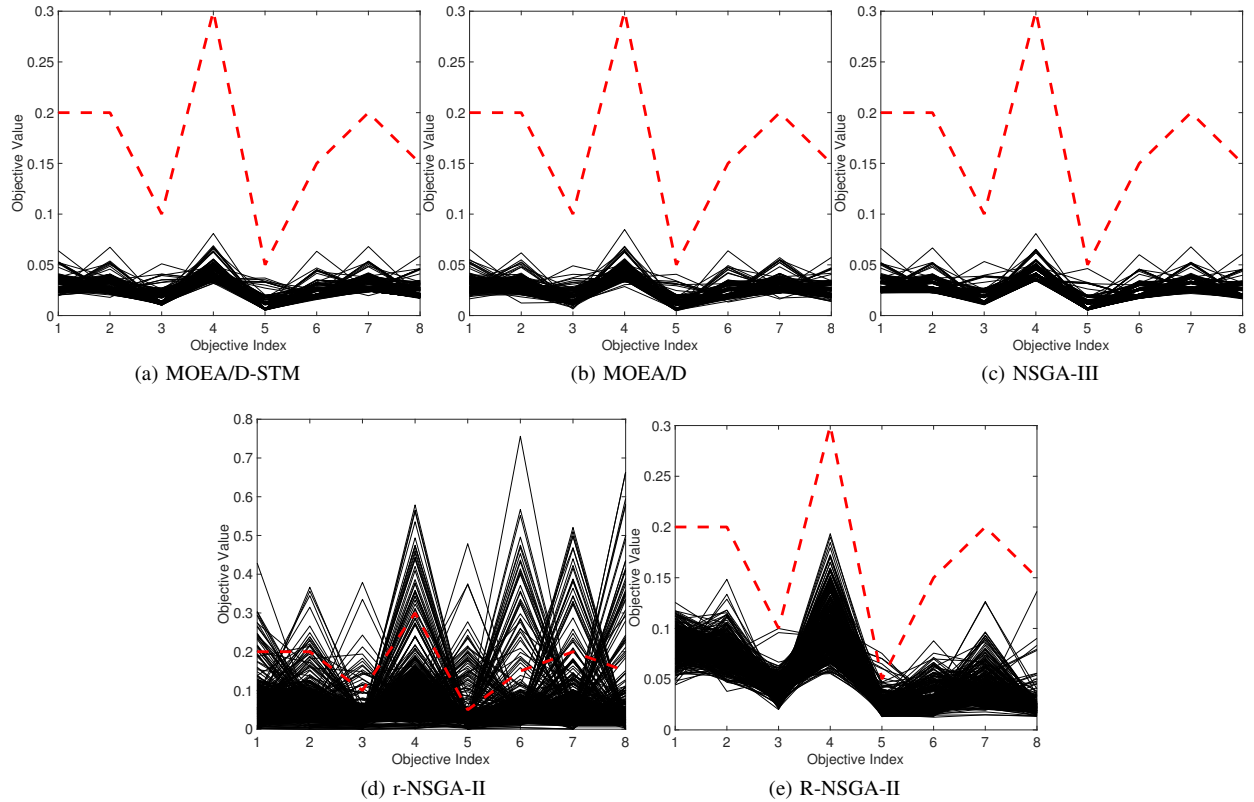


Fig. 52: Comparisons on 8-objective WFG42 where $\mathbf{z}^r = (0.2, 0.2, 0.1, 0.3, 0.05, 0.15, 0.2, 0.15)^T$.

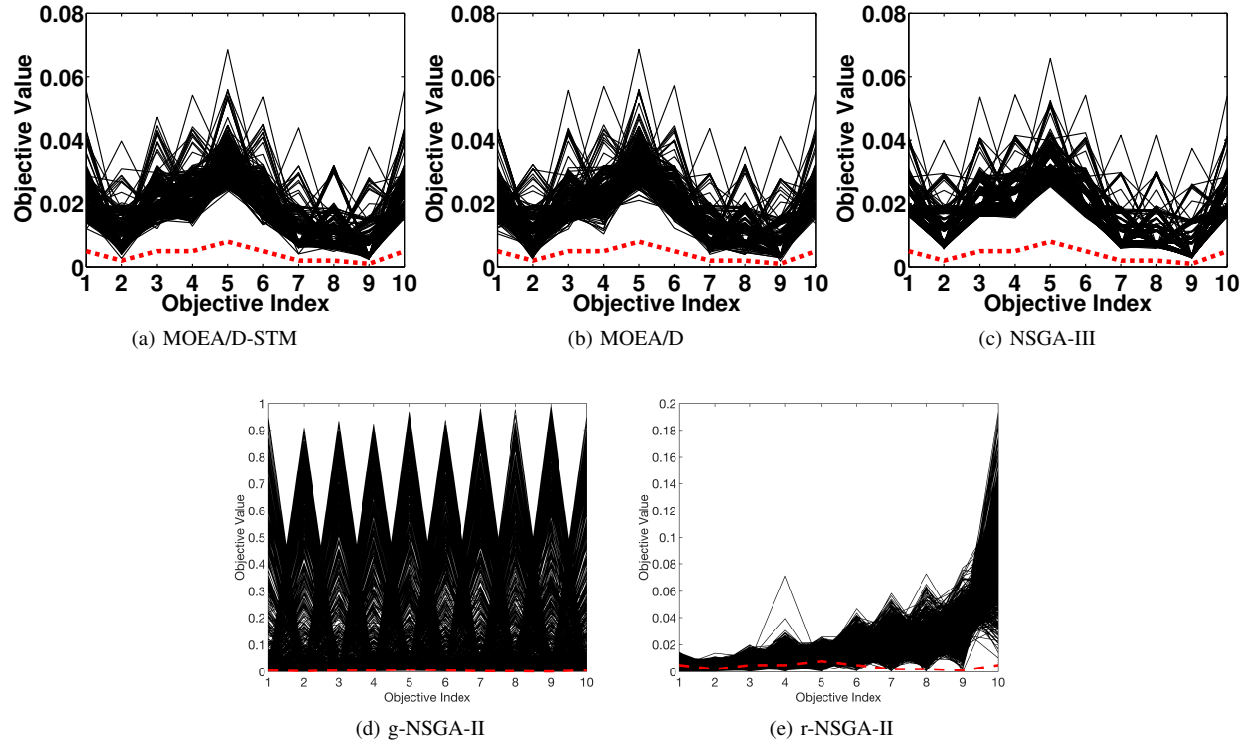


Fig. 53: Comparisons on 10-objective WFG42 where $\mathbf{z}^r = (0.005, 0.002, 0.005, 0.005, 0.008, 0.005, 0.005, 0.002, 0.002, 0.001, 0.005)^T$.

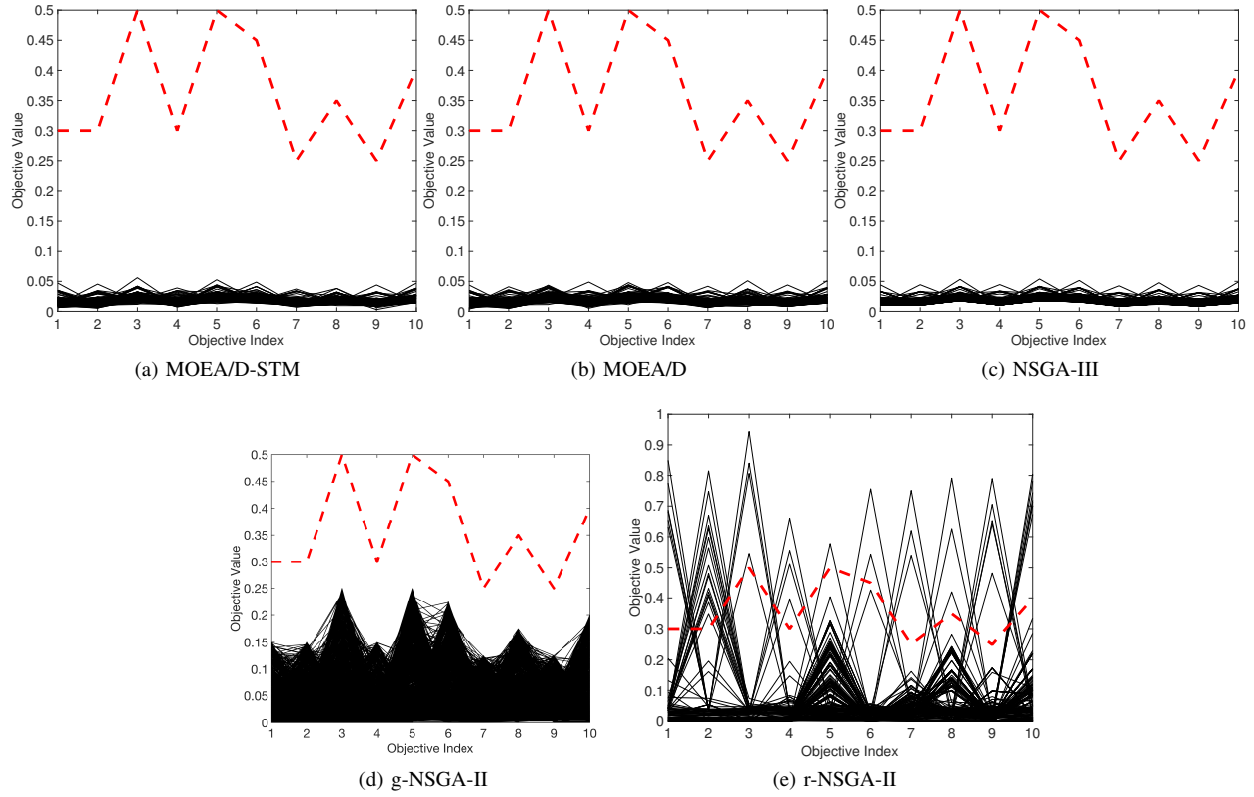


Fig. 54: Comparisons on 10-objective WFG42 where $\mathbf{z}^r = (0.3, 0.3, 0.5, 0.3, 0.5, 0.45, 0.25, 0.35, 0.25, 0.4)^T$.

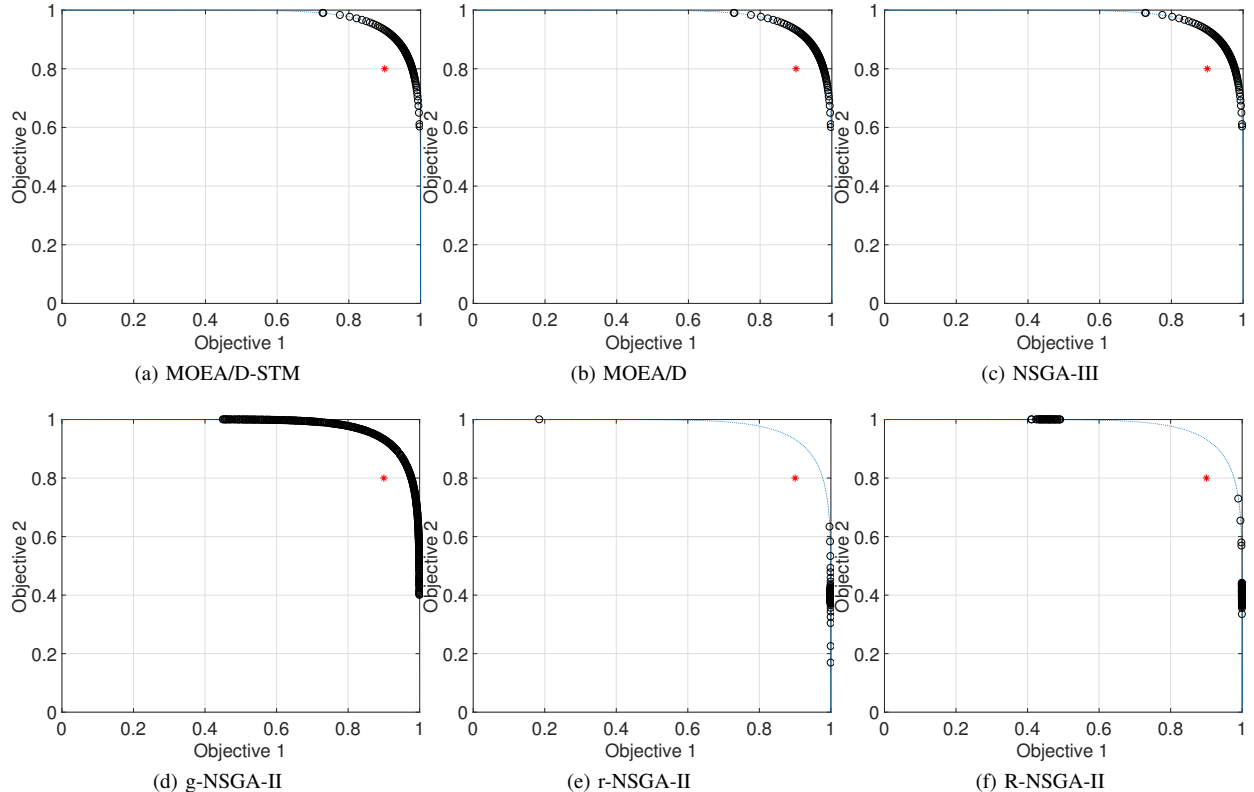
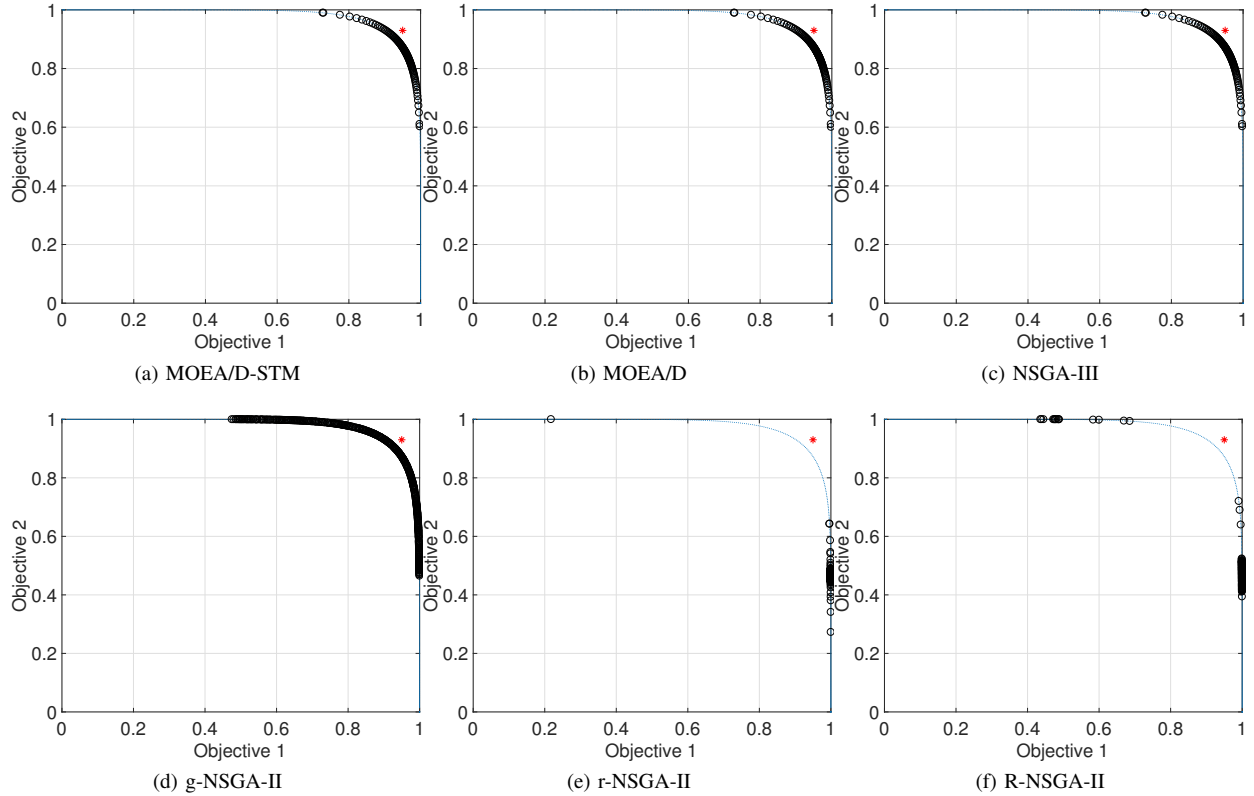
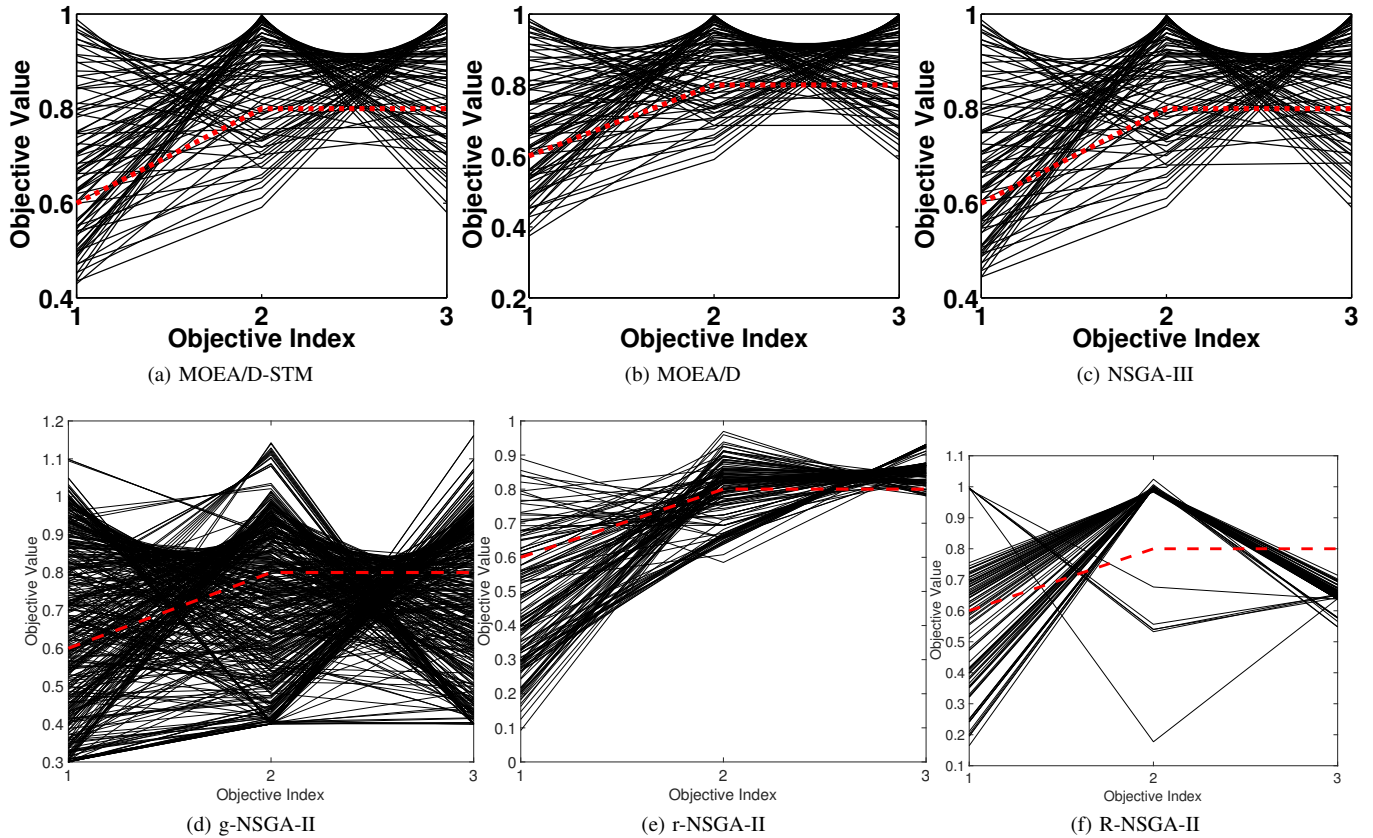
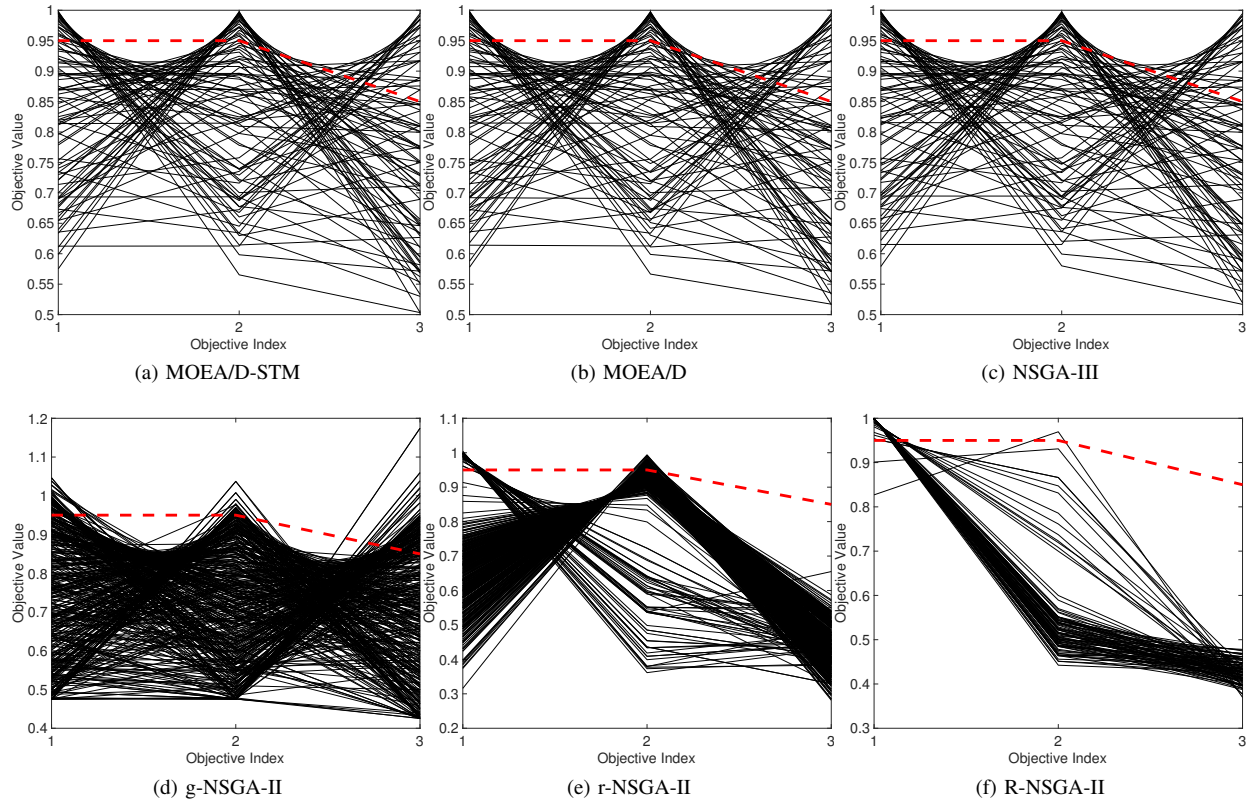
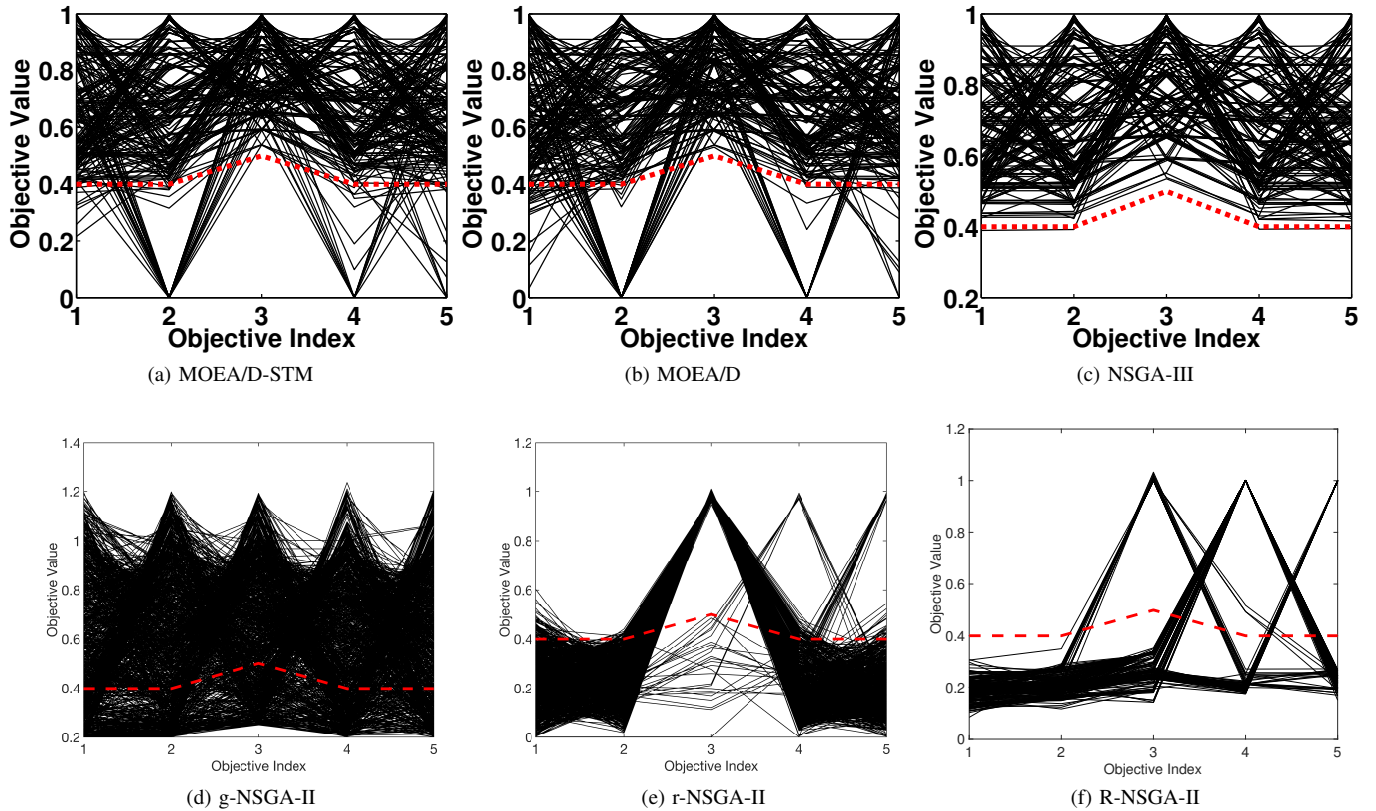
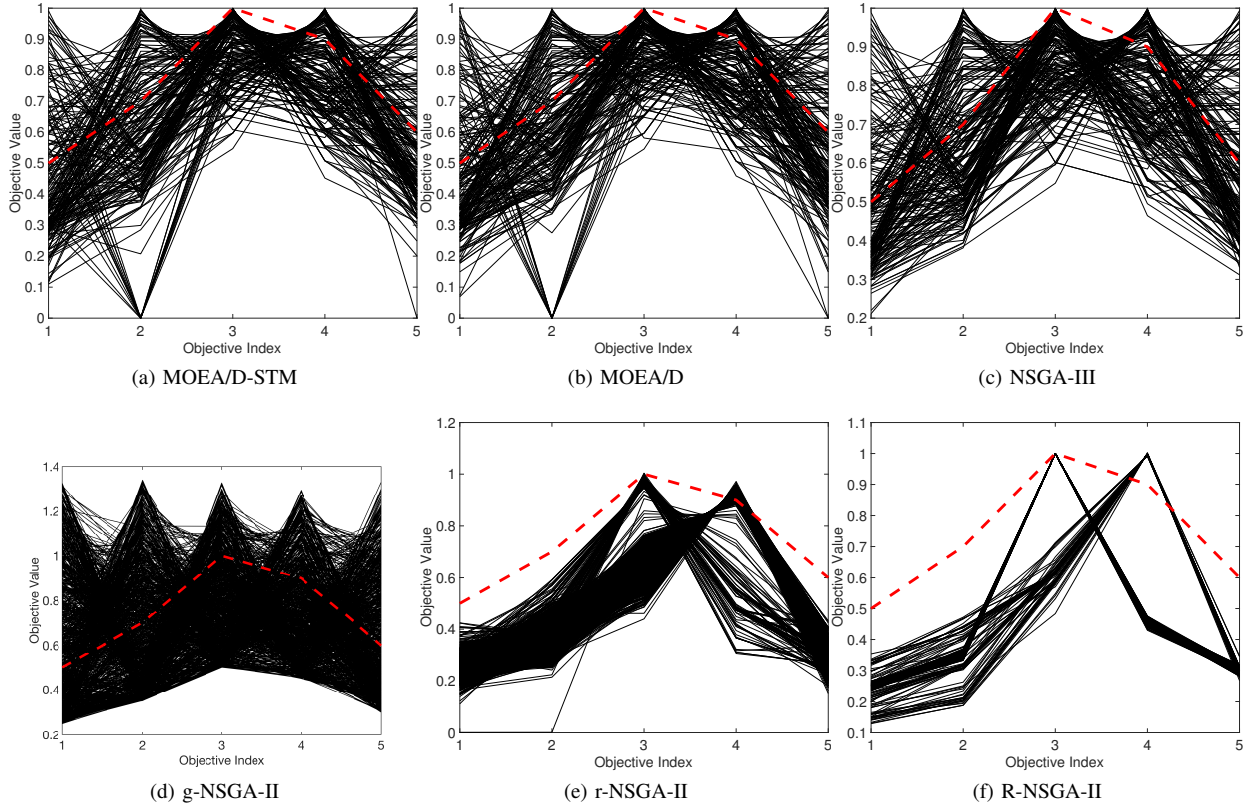
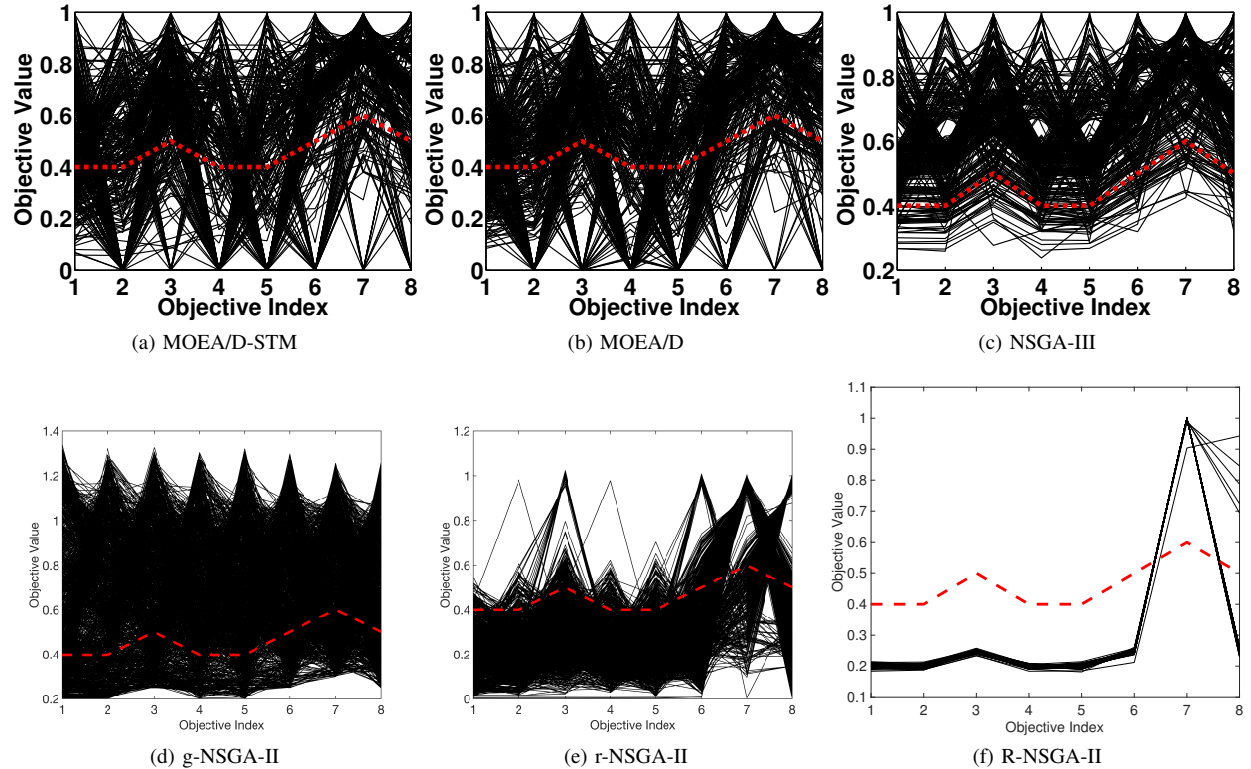


Fig. 55: Comparisons on 2-objective WFG43 where $\mathbf{z}^r = (0.9, 0.8)^T$.

Fig. 56: Comparisons on 2-objective WFG43 where $\mathbf{z}^r = (0.95, 0.93)^T$.Fig. 57: Comparisons on 3-objective WFG43 where $\mathbf{z}^r = (0.6, 0.8, 0.8)^T$.

Fig. 58: Comparisons on 3-objective WFG43 where $\mathbf{z}^r = (0.95, 0.95, 0.85)^T$.Fig. 59: Comparisons on 5-objective WFG43 where $\mathbf{z}^r = (0.4, 0.4, 0.5, 0.4, 0.4)^T$.

Fig. 60: Comparisons on 5-objective WFG43 where $\mathbf{z}^r = (0.5, 0.7, 1.0, 0.9, 0.6)^T$.Fig. 61: Comparisons on 8-objective WFG43 where $\mathbf{z}^r = (0.4, 0.4, 0.5, 0.4, 0.4, 0.5, 0.6, 0.5)^T$.

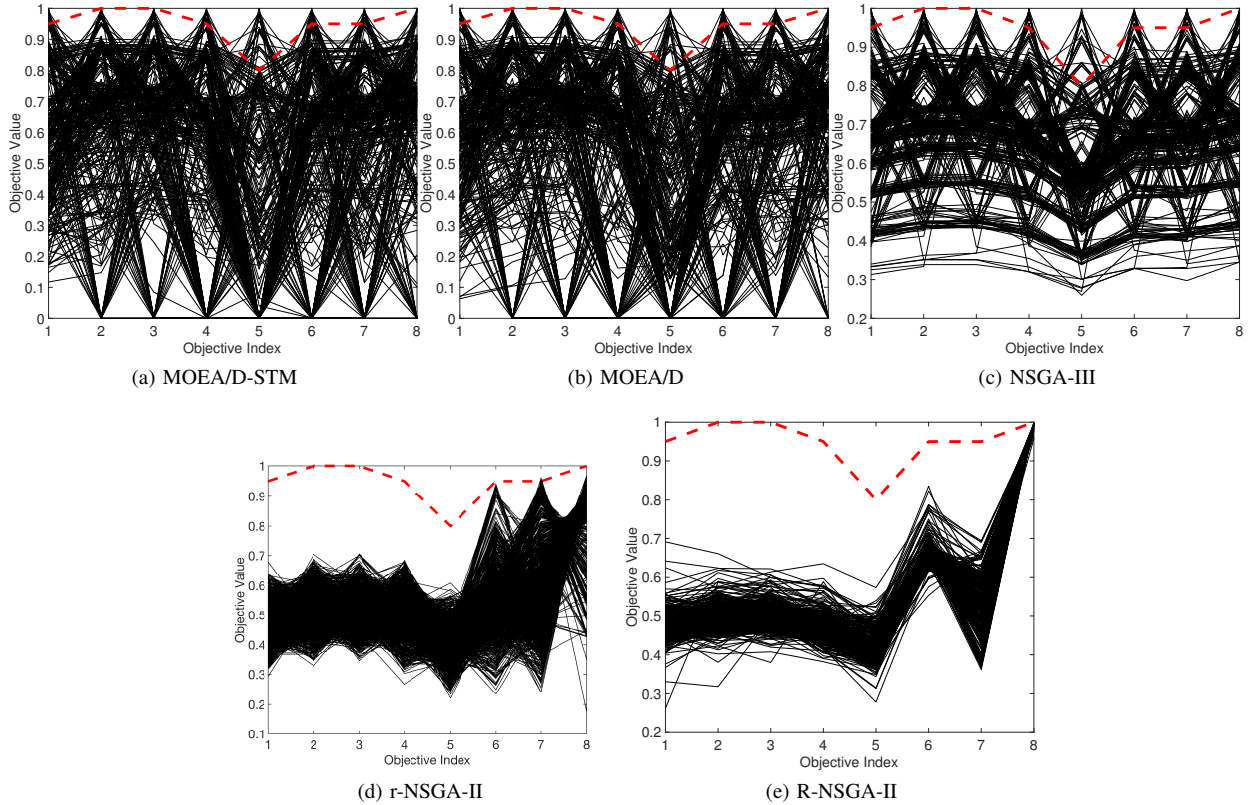


Fig. 62: Comparisons on 8-objective WFG43 where $\mathbf{z}^r = (0.95, 1.0, 1.0, 0.95, 0.8, 0.95, 0.95, 1.0)^T$.

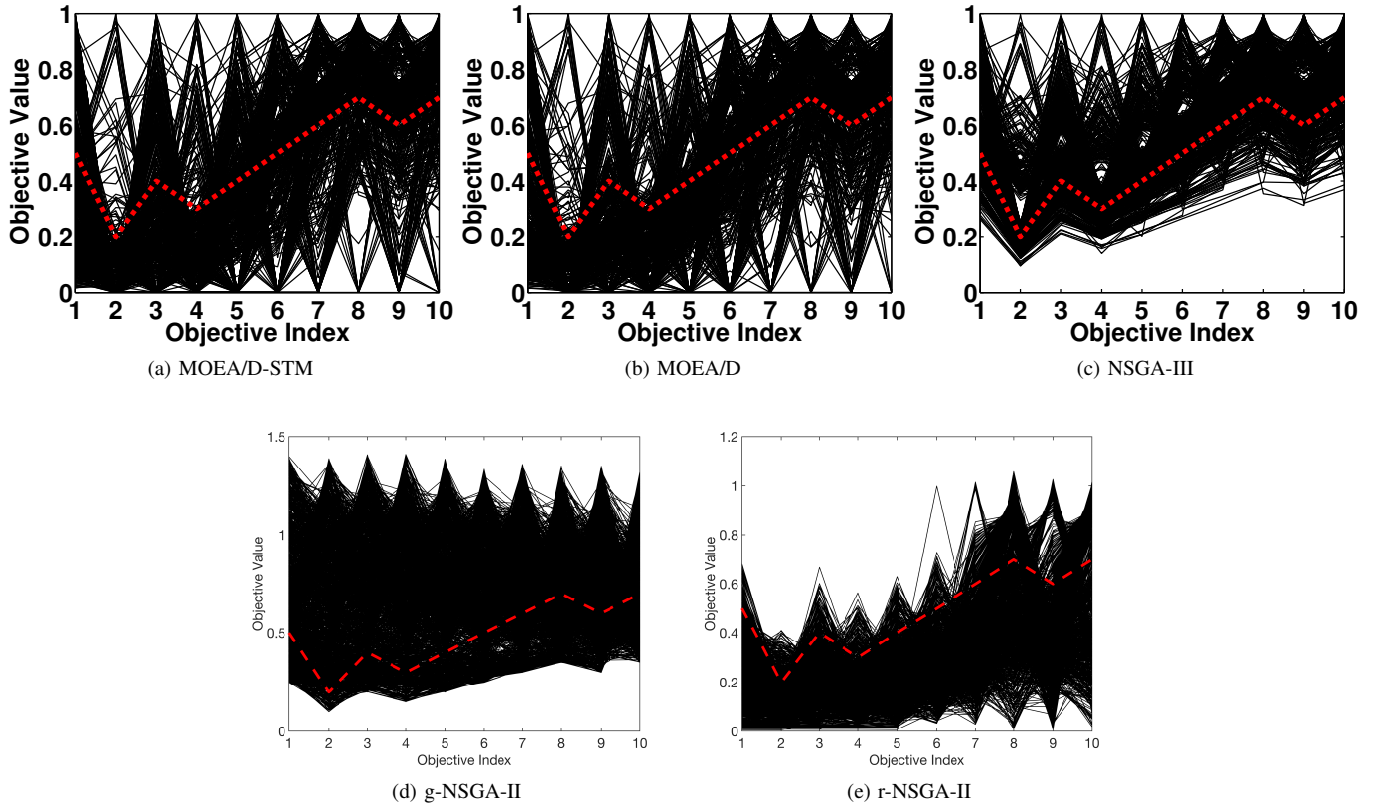


Fig. 63: Comparisons on 10-objective WFG43 where $\mathbf{z}^r = (0.5, 0.2, 0.4, 0.3, 0.4, 0.5, 0.6, 0.7, 0.6, 0.7)^T$.

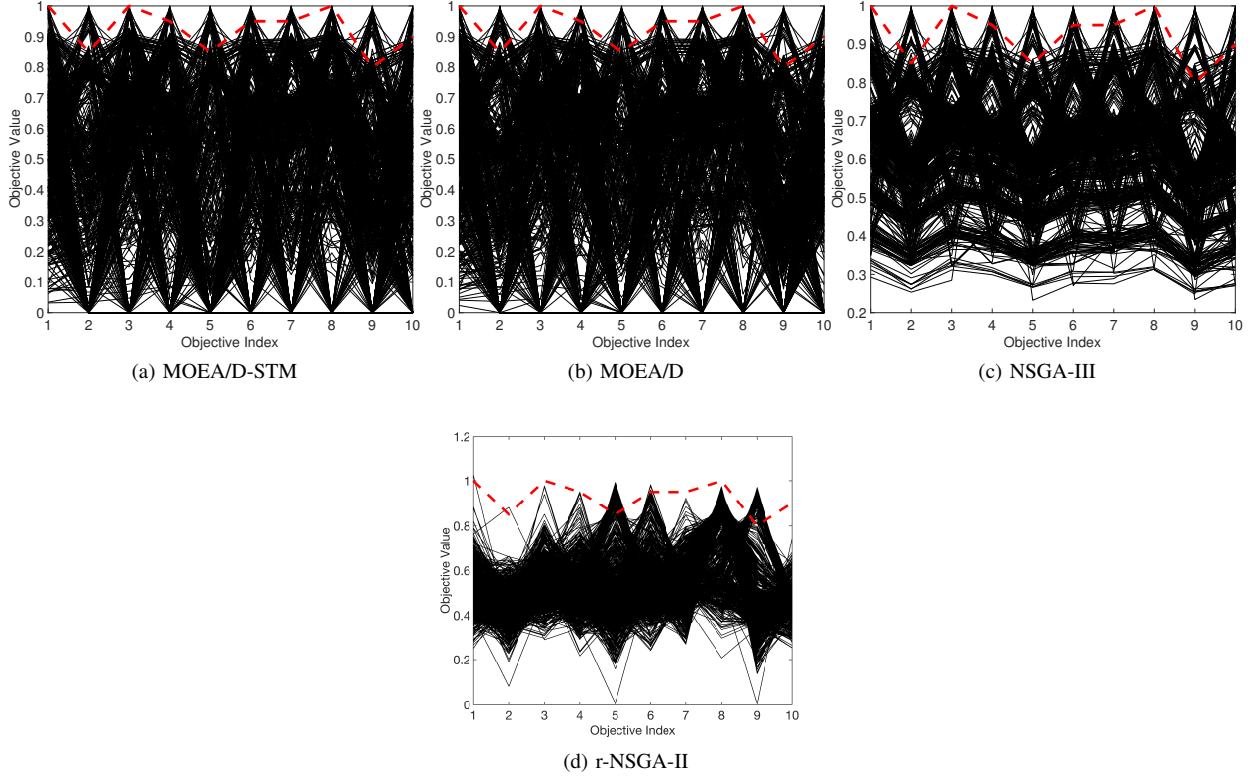


Fig. 64: Comparisons on 10-objective WFG43 where $\mathbf{z}^r = (1.0, 0.85, 1.0, 0.95, 0.85, 0.95, 0.95, 0.95, 1.0, 0.8, 0.9)^T$.

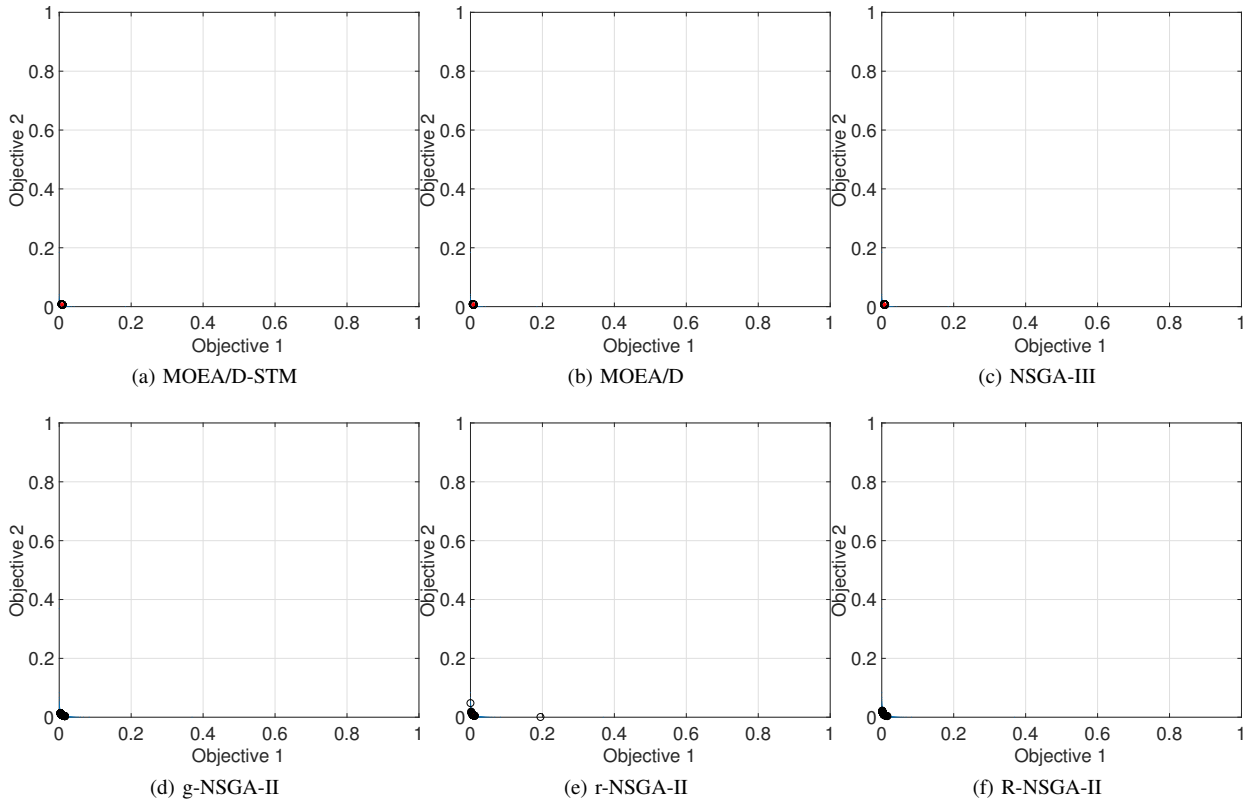
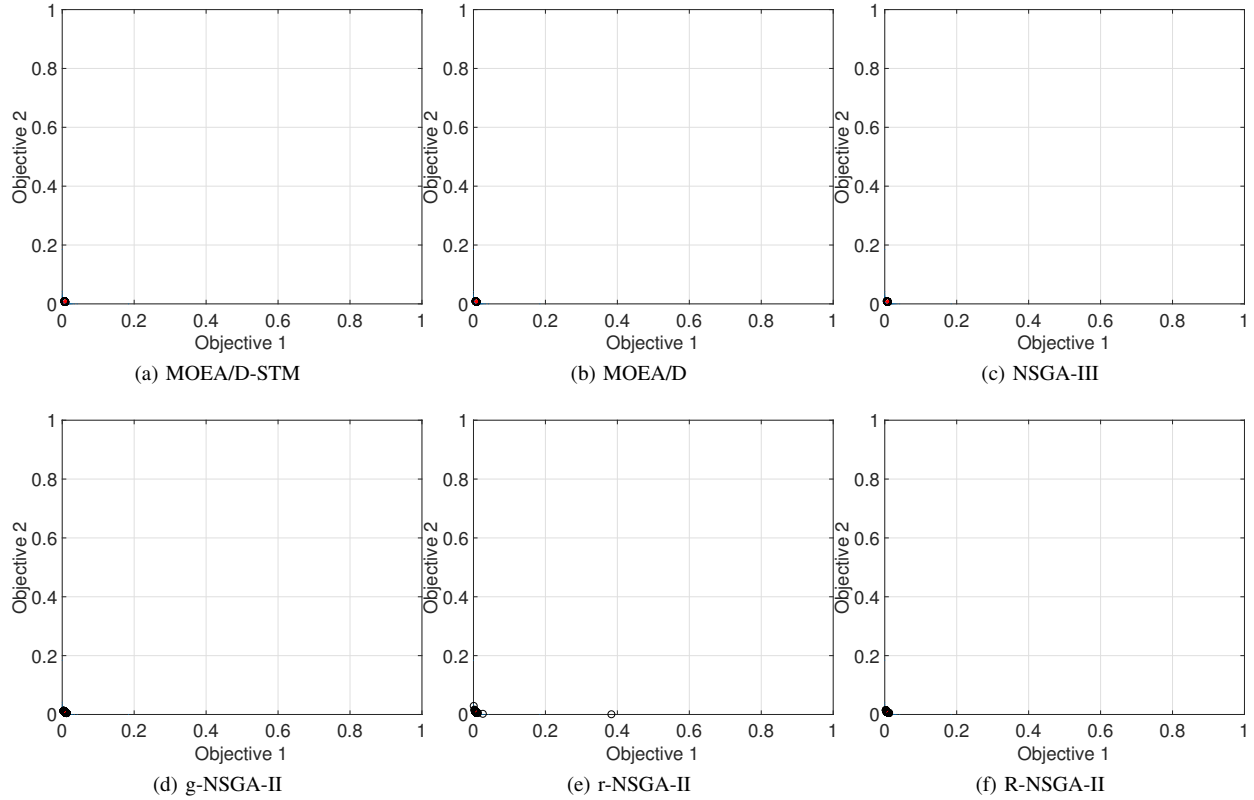
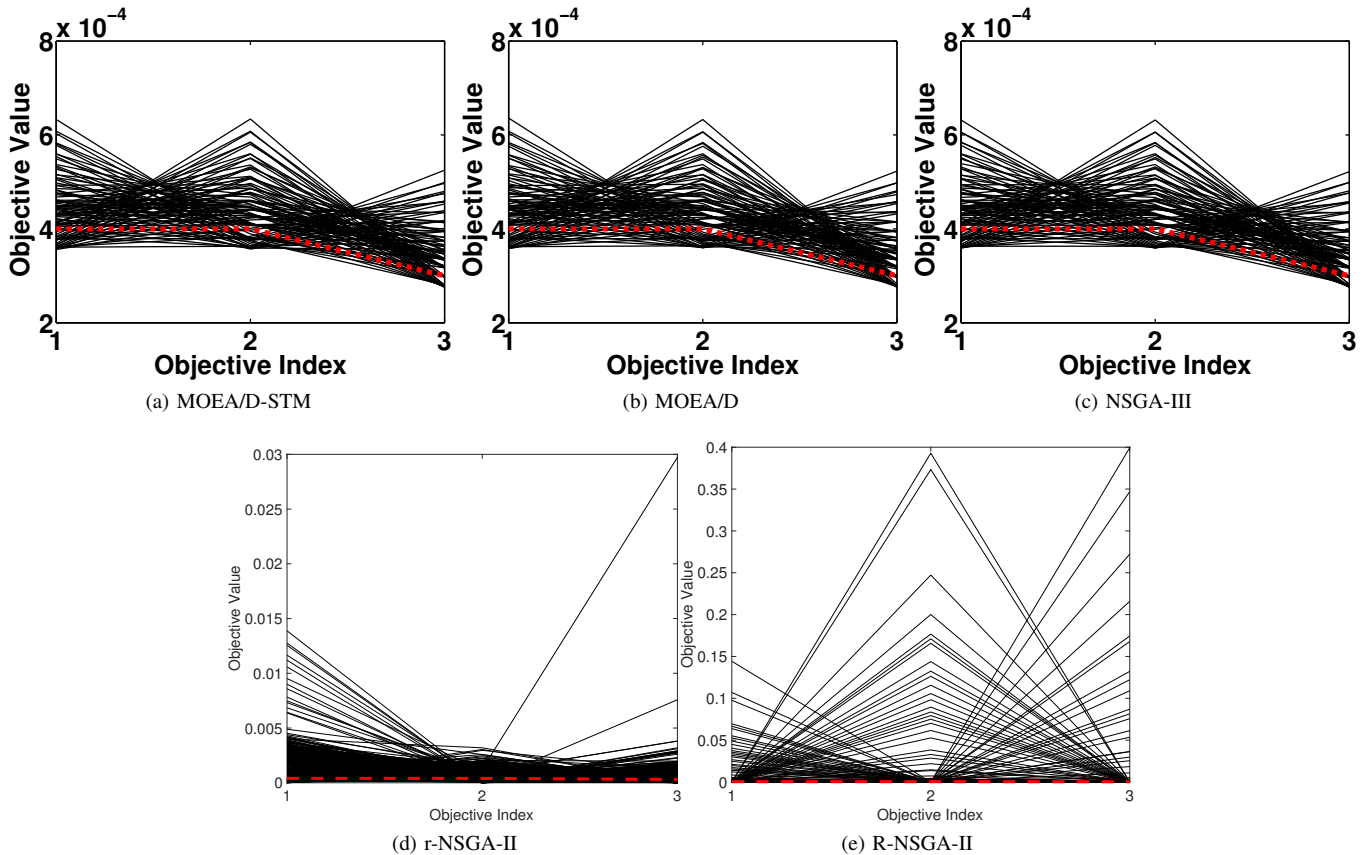


Fig. 65: Comparisons on 2-objective WFG44 where $\mathbf{z}^r = (0.008, 0.006)^T$.

Fig. 66: Comparisons on 2-objective WFG44 where $\mathbf{z}^r = (0.009, 0.008)^T$.Fig. 67: Comparisons on 3-objective WFG44 where $\mathbf{z}^r = (0.0004, 0.0004, 0.0003)^T$.

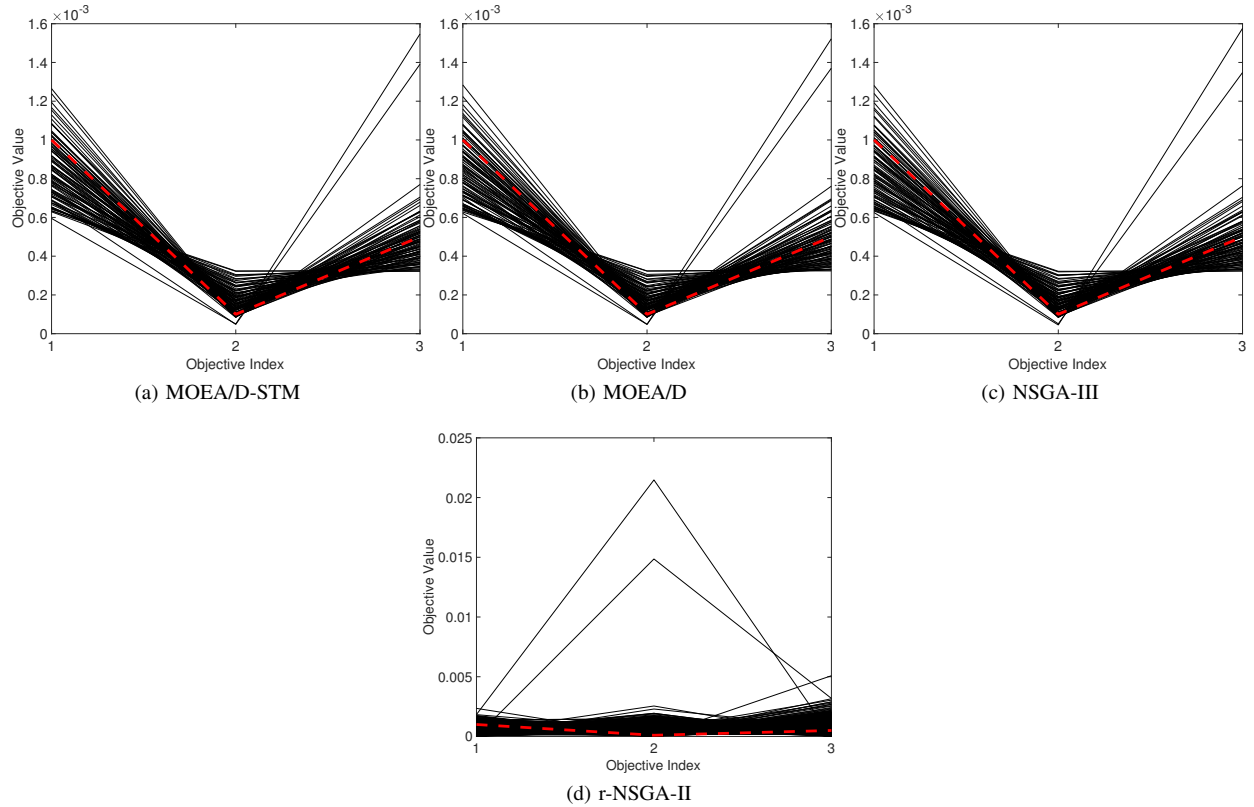


Fig. 68: Comparisons on 3-objective WFG44 where $\mathbf{z}^r = (0.001, 0.0001, 0.0005)^T$.

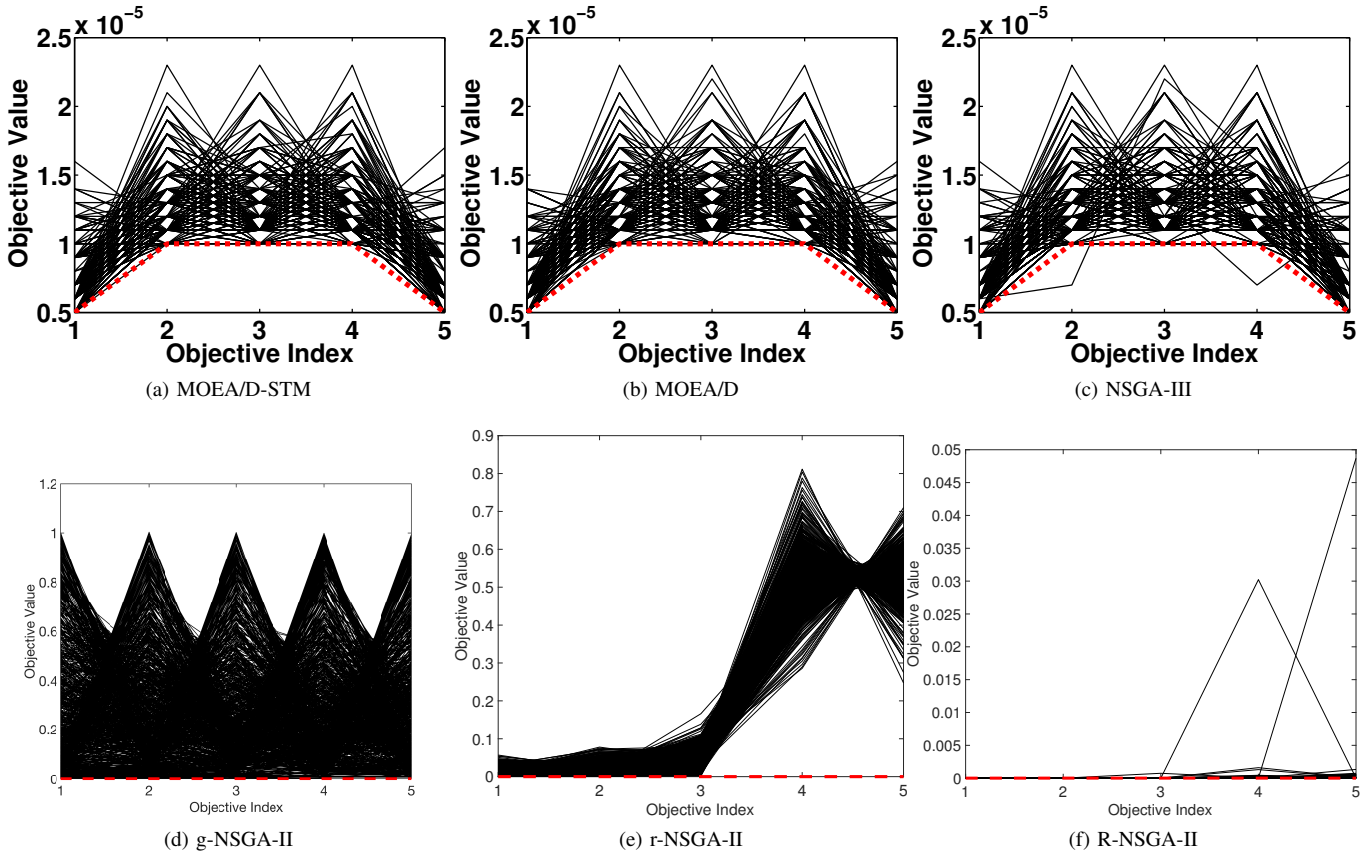


Fig. 69: Comparisons on 5-objective WFG44 where $\mathbf{z}^r = (0.000005, 0.00001, 0.00001, 0.00001, 0.000005)^T$.

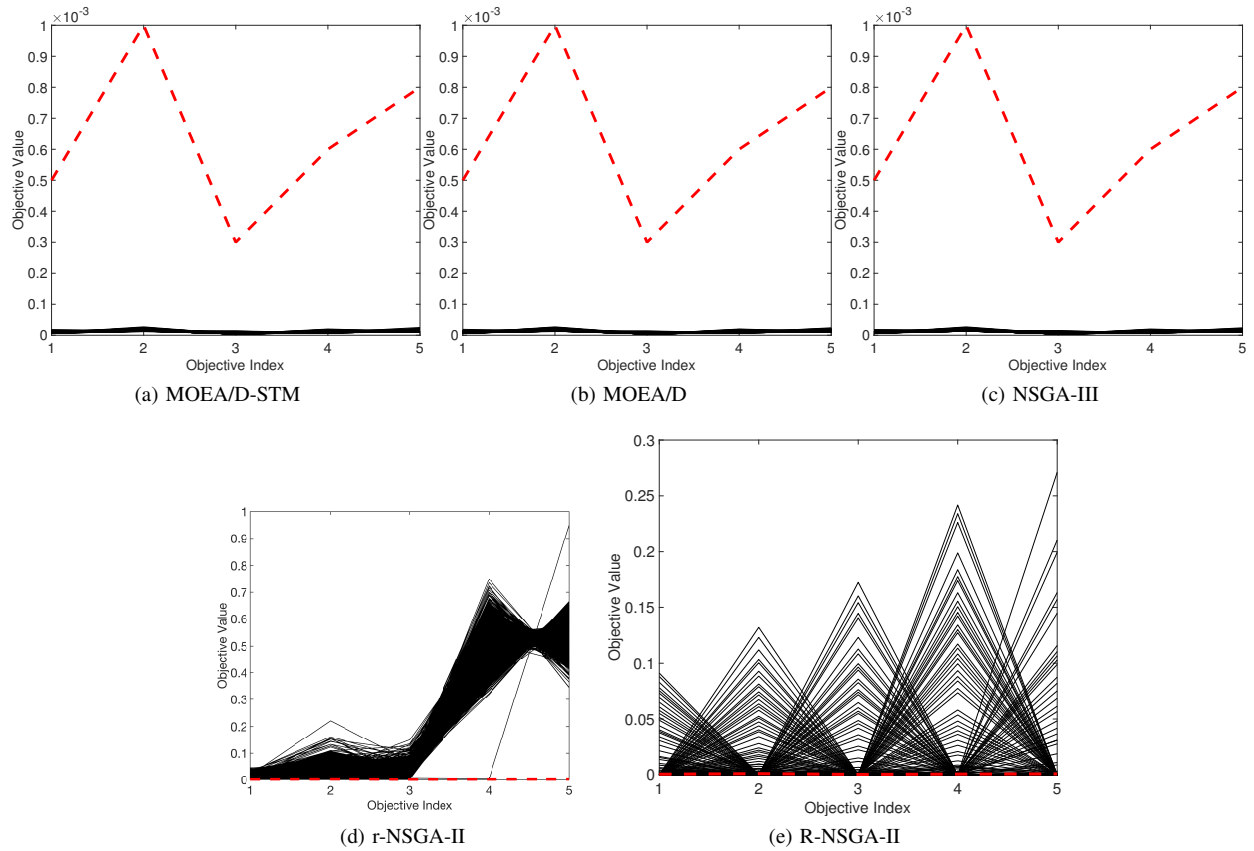


Fig. 70: Comparisons on 5-objective WFG44 where $\mathbf{z}^r = (0.0005, 0.001, 0.0003, 0.0006, 0.0008)^T$.

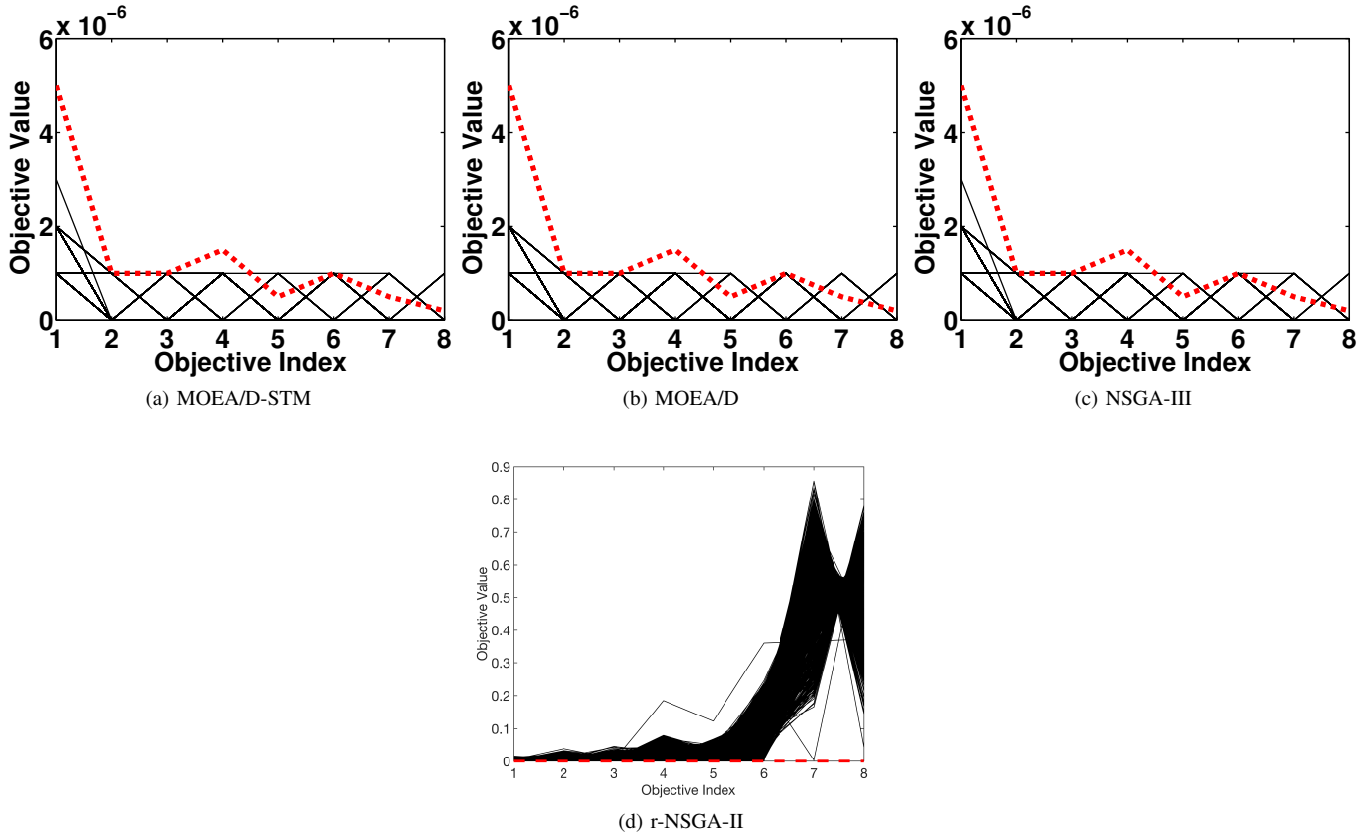


Fig. 71: Comparisons on 8-objective WFG44 where $\mathbf{z}^r = (0.000005, 0.000001, 0.000001, 0.0000015, 0.0000005, 0.000001, 0.0000005, 0.0000005)$

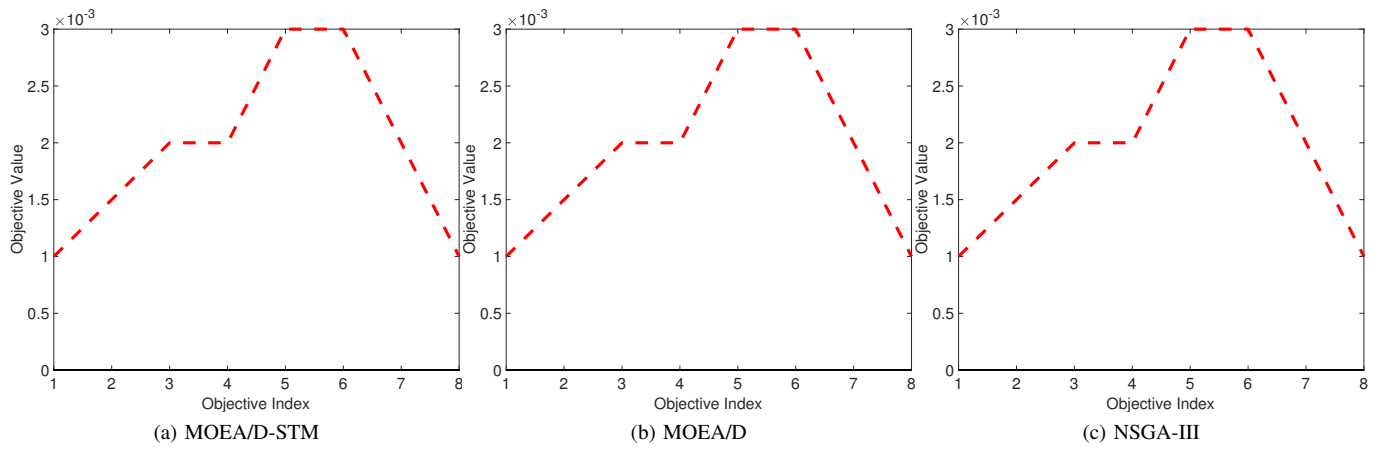


Fig. 72: Comparisons on 8-objective WFG44 where $\mathbf{z}^r = (0.001, 0.0015, 0.002, 0.002, 0.003, 0.003, 0.002, 0.001)^T$.

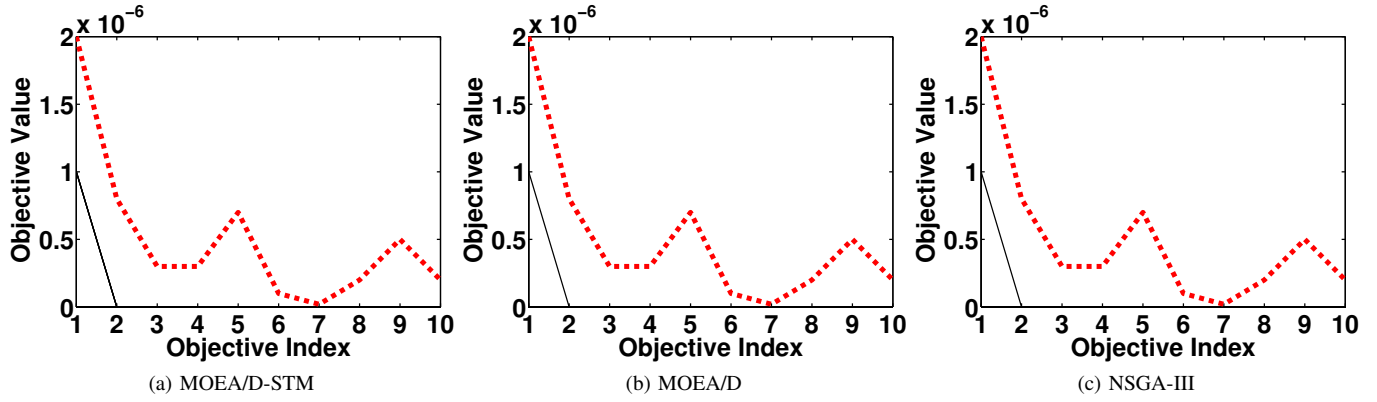


Fig. 73: Comparisons on 10-objective WFG44 where $\mathbf{z}^r = (0.000002, 0.0000008, 0.0000003, 0.0000003, 0.0000007, 0.0000001, 0.00000002)^T$.

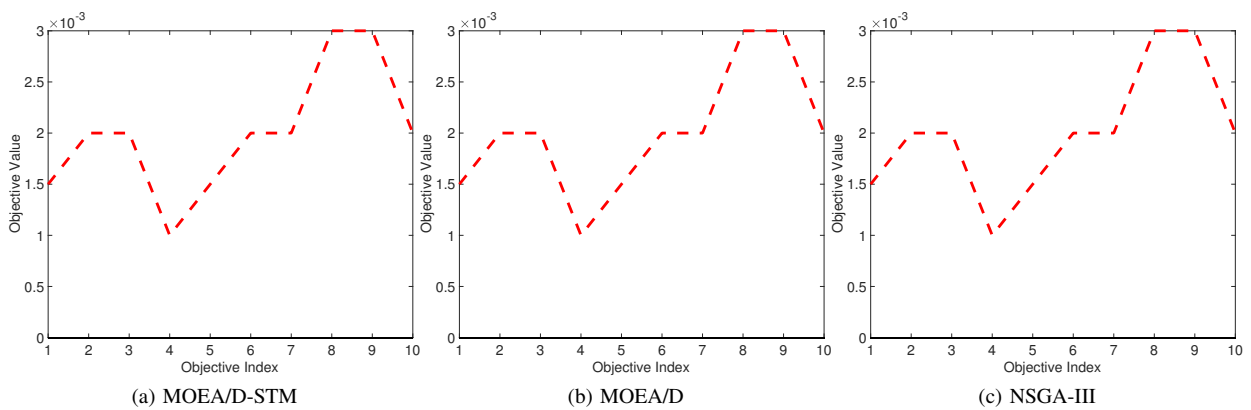
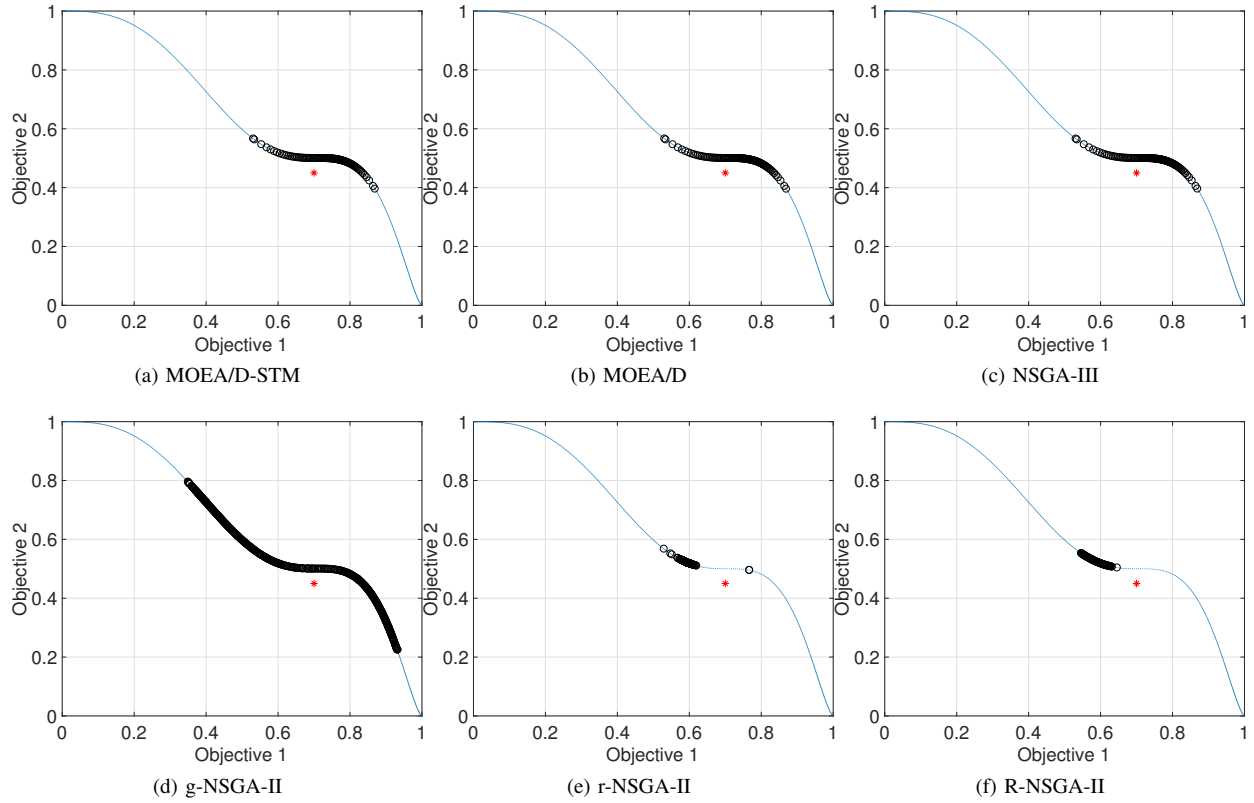
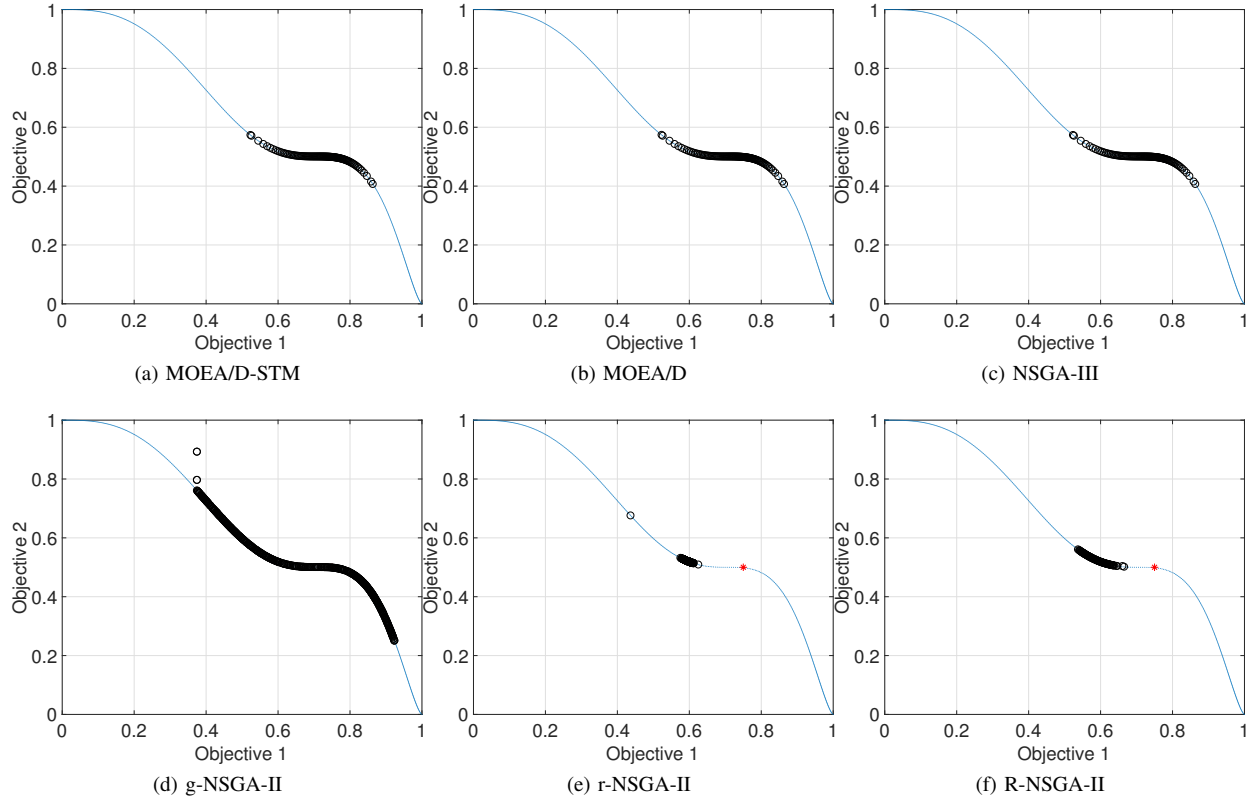
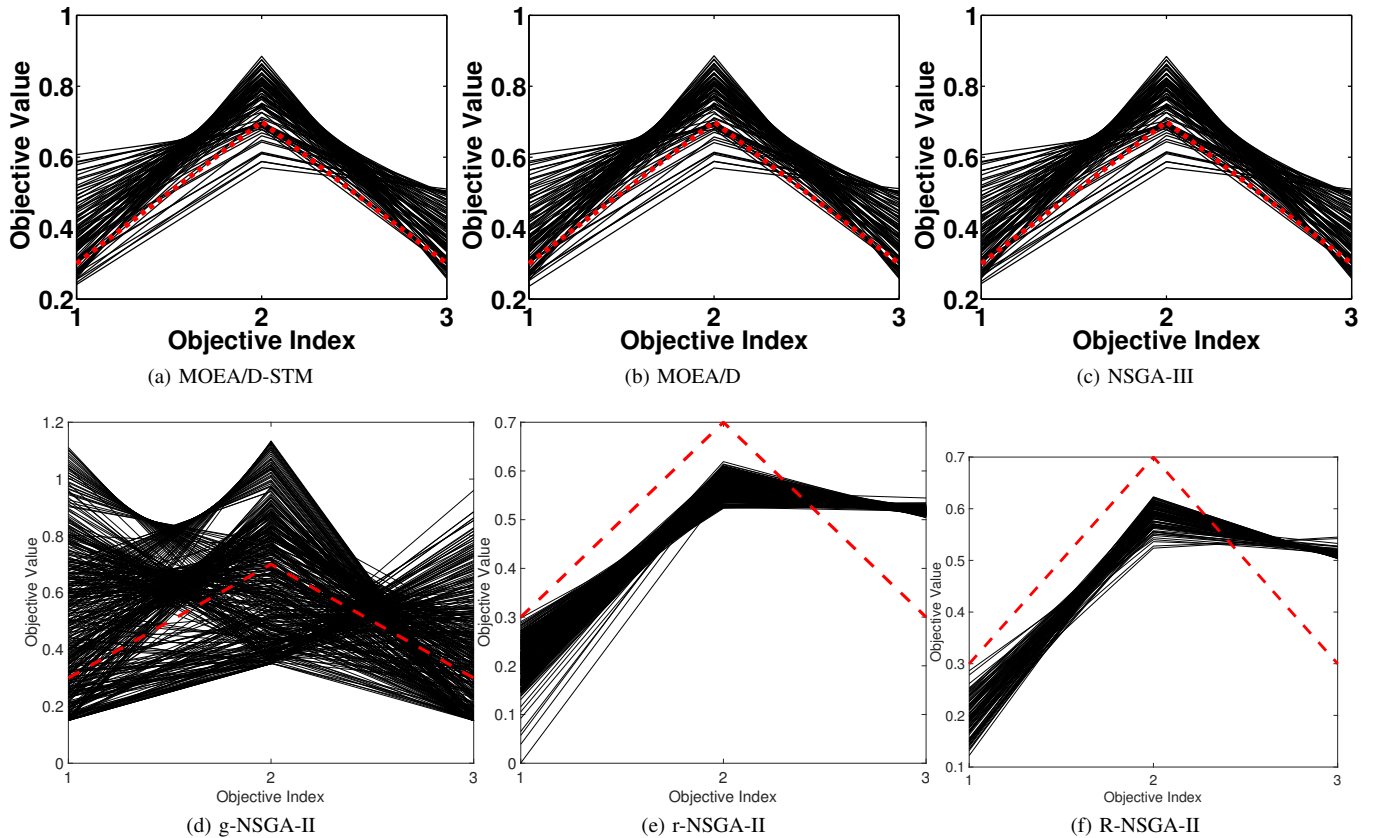
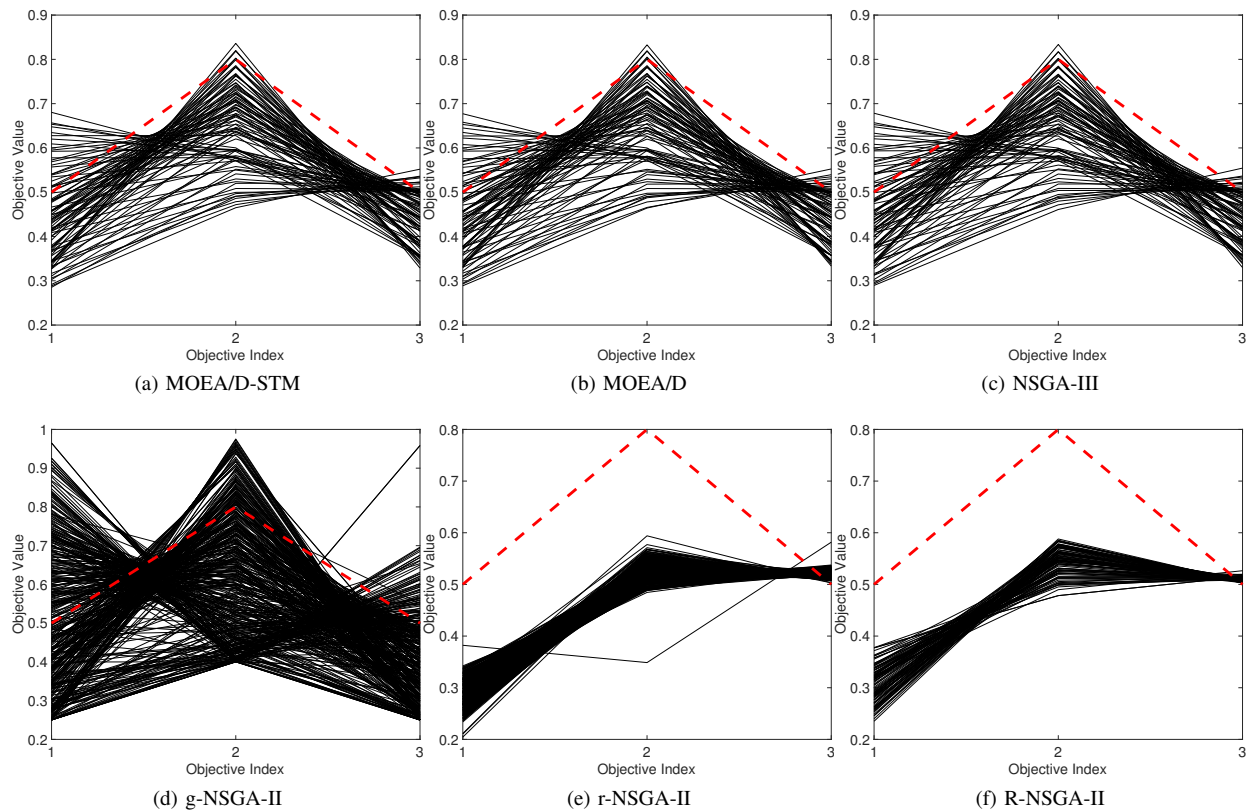
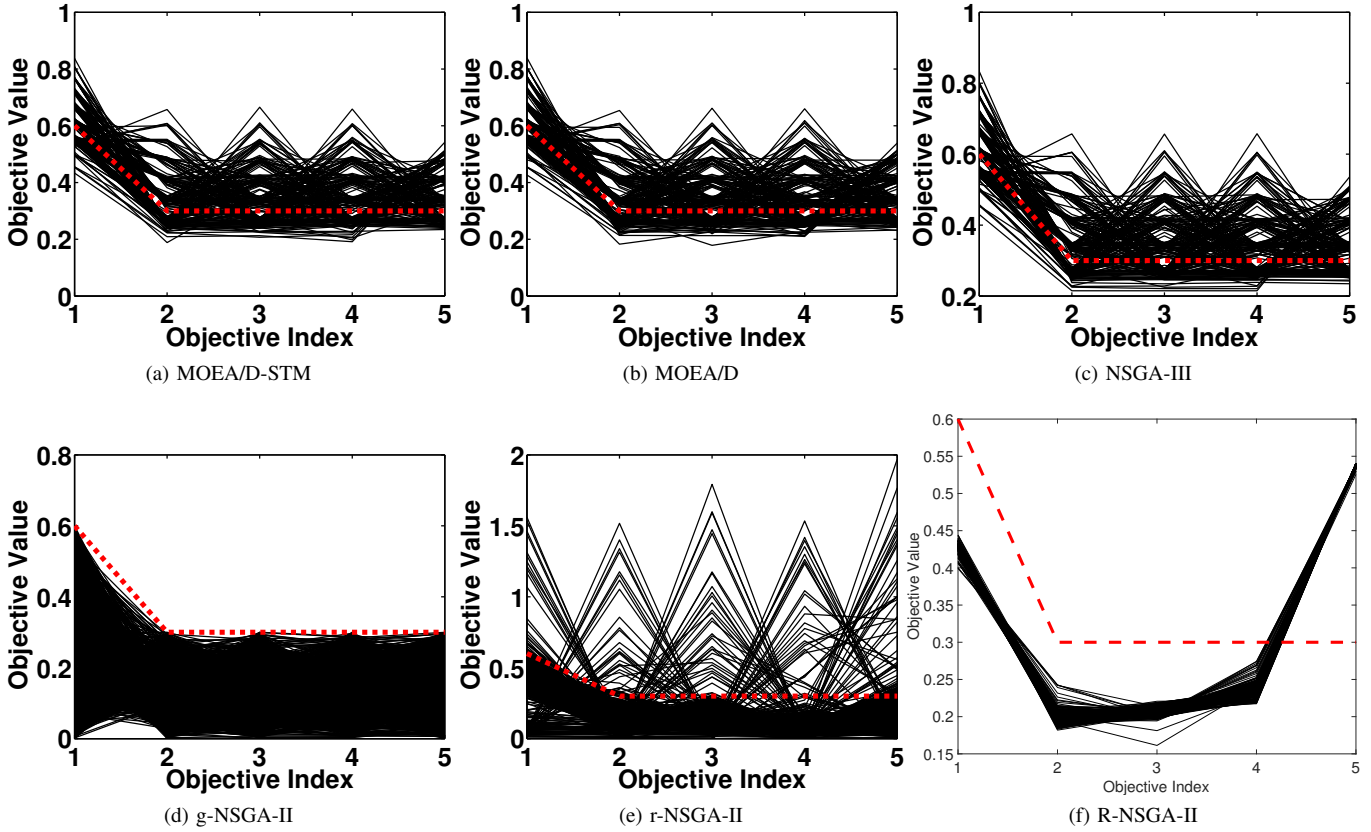
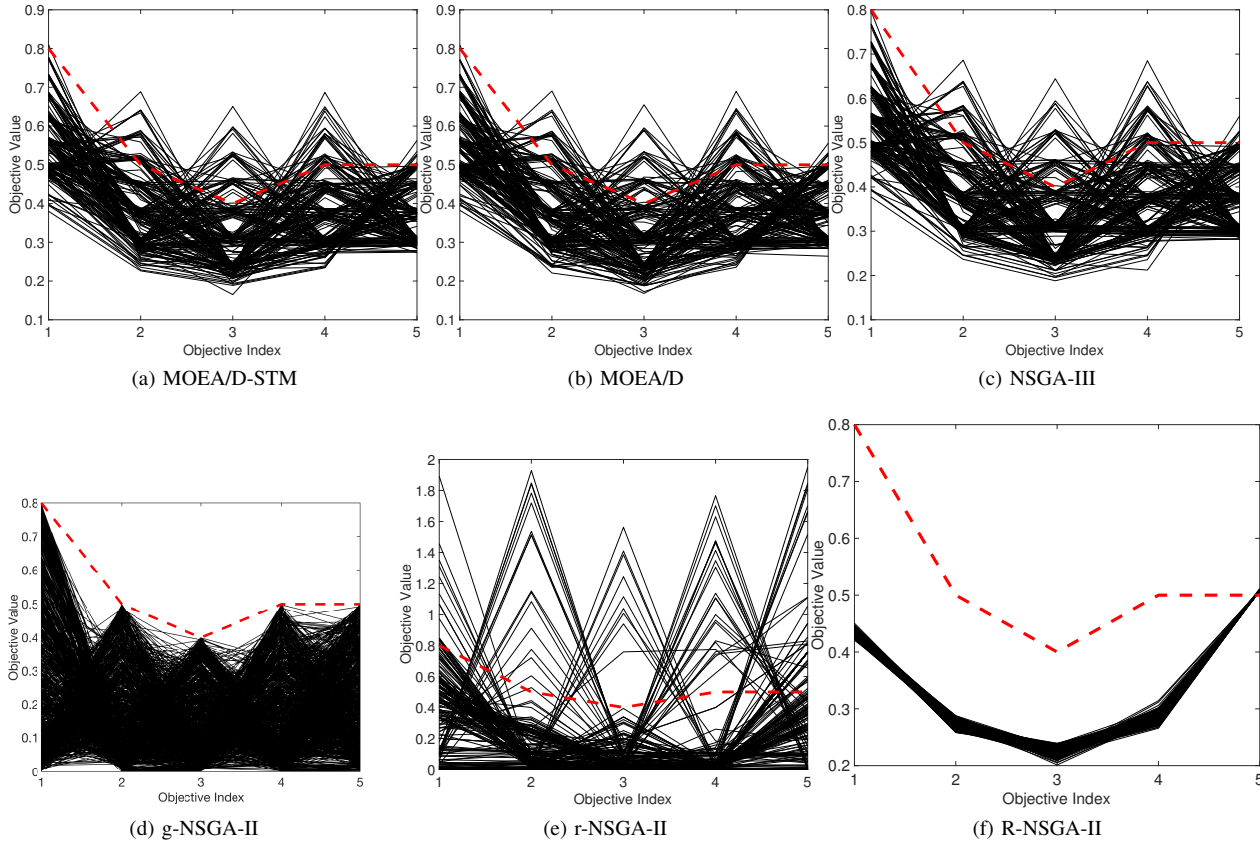


Fig. 74: Comparisons on 10-objective WFG44 where $\mathbf{z}^r = (0.0015, 0.002, 0.002, 0.001, 0.0015, 0.002, 0.002, 0.003, 0.003, 0.002)^T$.

Fig. 75: Comparisons on 2-objective WFG45 where $z^r = (0.7, 0.45)^T$.Fig. 76: Comparisons on 2-objective WFG45 where $z^r = (0.75, 0.5)^T$.

Fig. 77: Comparisons on 3-objective WFG45 where $\mathbf{z}^r = (0.3, 0.7, 0.3)^T$.Fig. 78: Comparisons on 3-objective WFG45 where $\mathbf{z}^r = (0.5, 0.8, 0.5)^T$.

Fig. 79: Comparisons on 5-objective WFG45 where $\mathbf{z}^r = (0.6, 0.3, 0.3, 0.3, 0.3)^T$.Fig. 80: Comparisons on 5-objective WFG45 where $\mathbf{z}^r = (0.8, 0.5, 0.4, 0.5, 0.5)^T$.

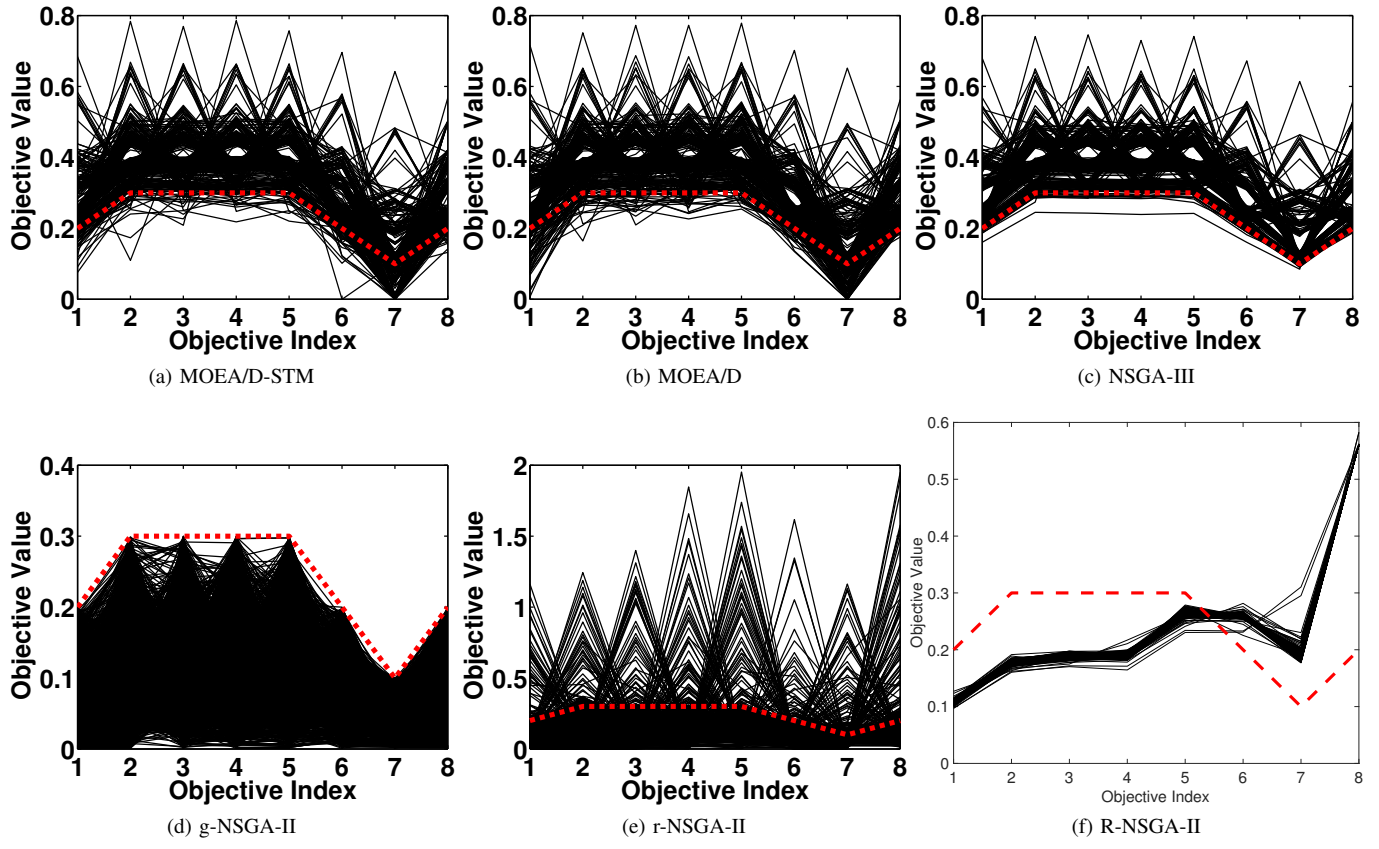


Fig. 81: Comparisons on 8-objective WFG45 where $\mathbf{z}^r = (0.2, 0.3, 0.3, 0.3, 0.3, 0.2, 0.1, 0.2)^T$.

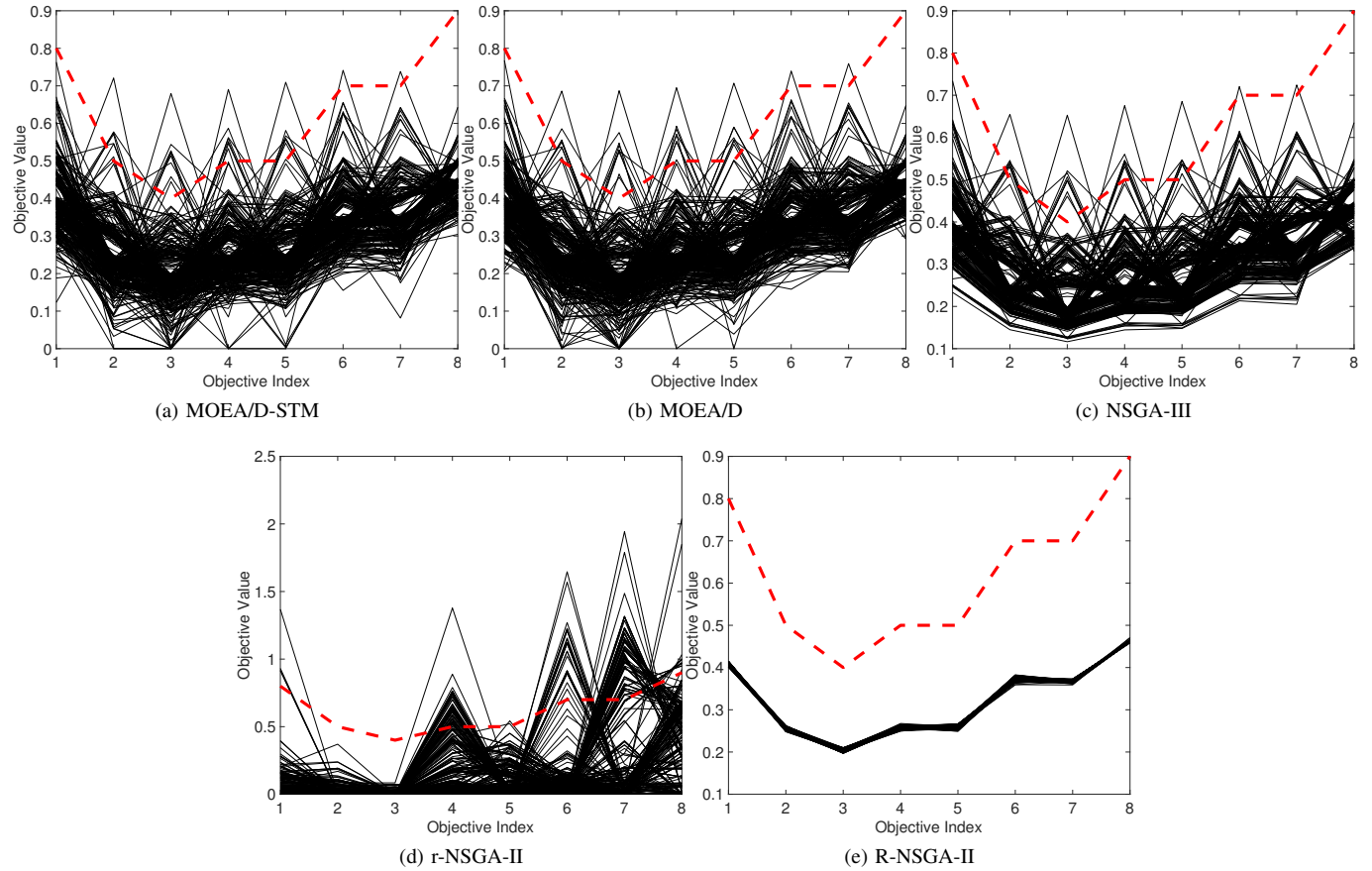


Fig. 82: Comparisons on 8-objective WFG45 where $\mathbf{z}^r = (0.8, 0.5, 0.4, 0.5, 0.5, 0.7, 0.7, 0.9)^T$.

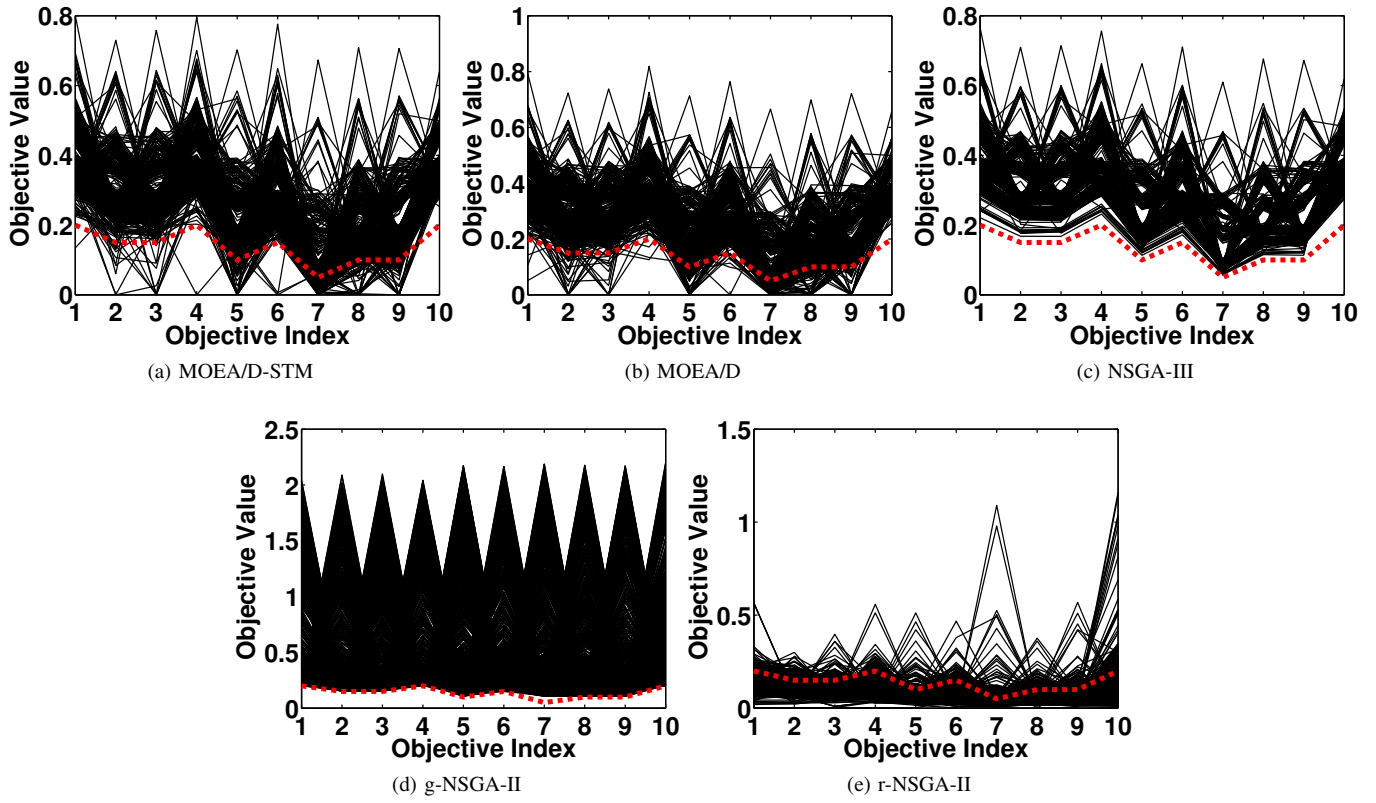


Fig. 83: Comparisons on 10-objective WFG45 where $\mathbf{z}^r = (0.2, 0.15, 0.15, 0.2, 0.2, 0.1, 0.15, 0.05, 0.1, 0.1, 0.2)^T$.

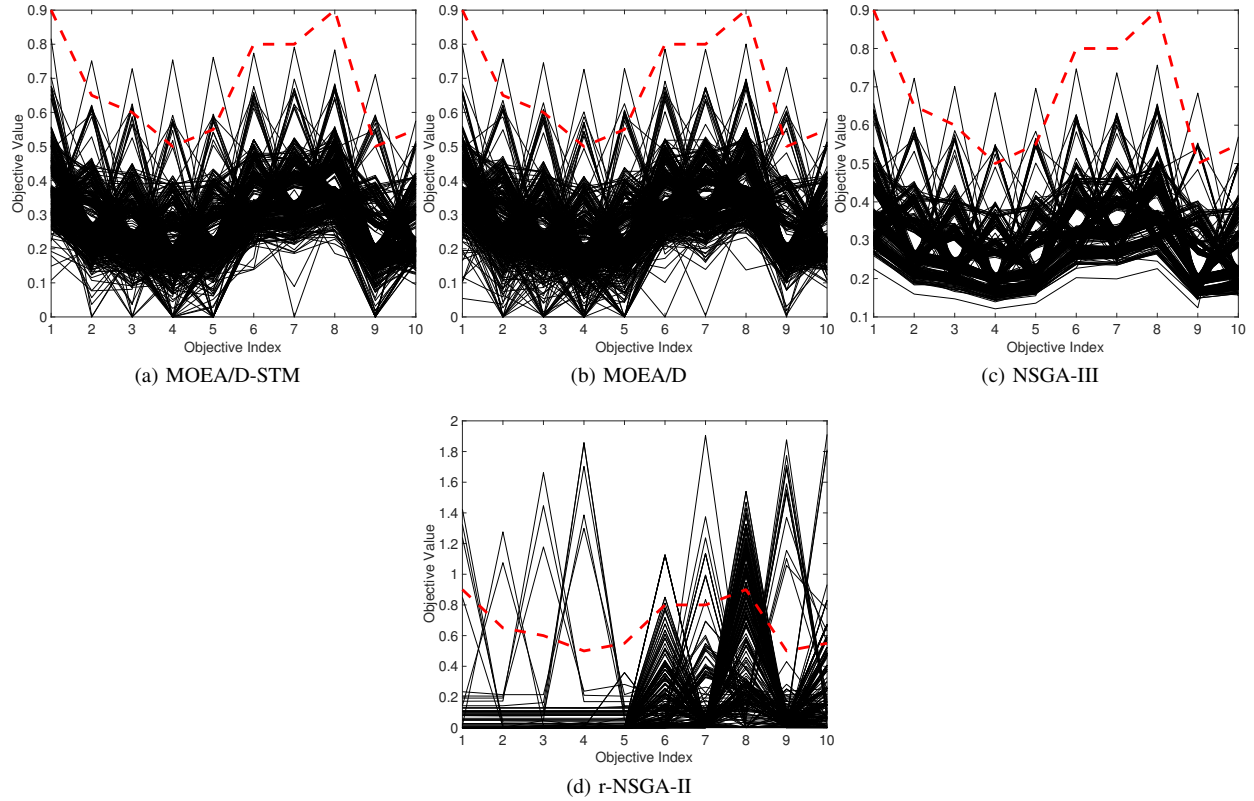


Fig. 84: Comparisons on 10-objective WFG45 where $\mathbf{z}^r = (0.9, 0.65, 0.6, 0.5, 0.55, 0.8, 0.8, 0.9, 0.5, 0.55)^T$.

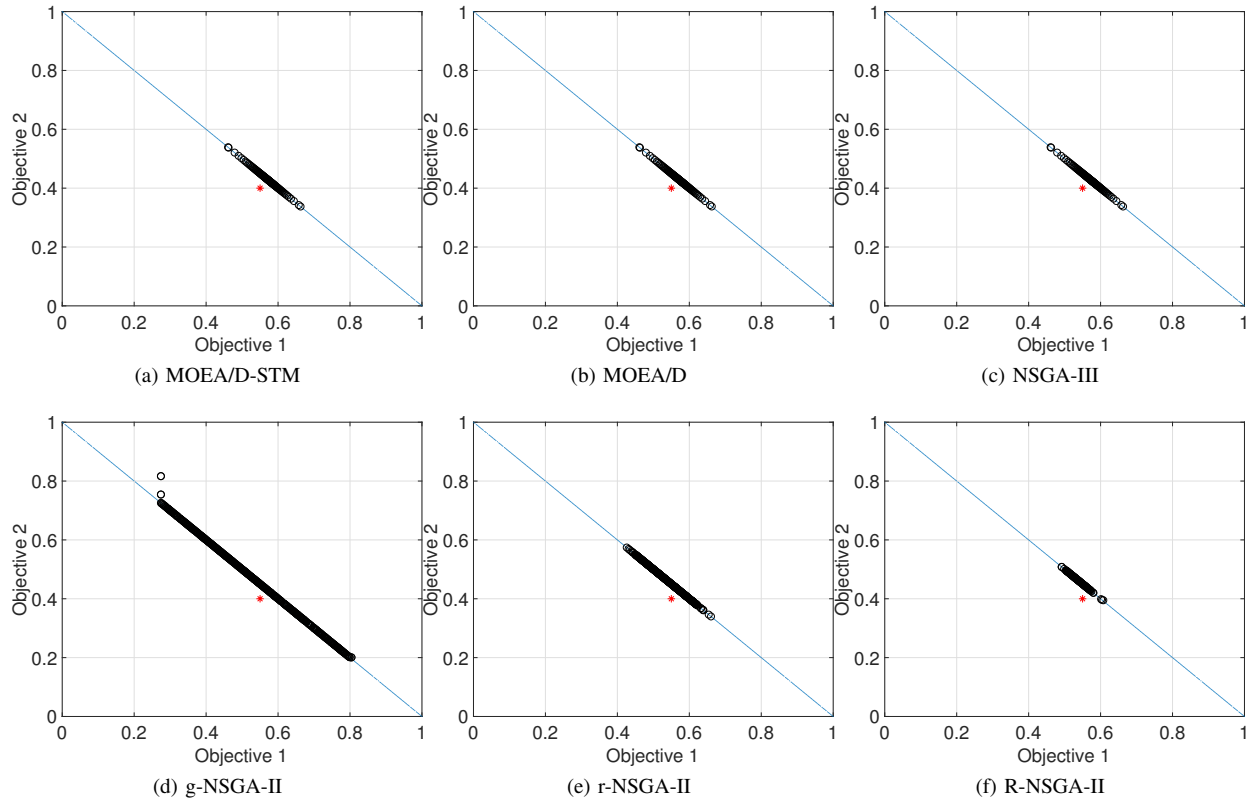
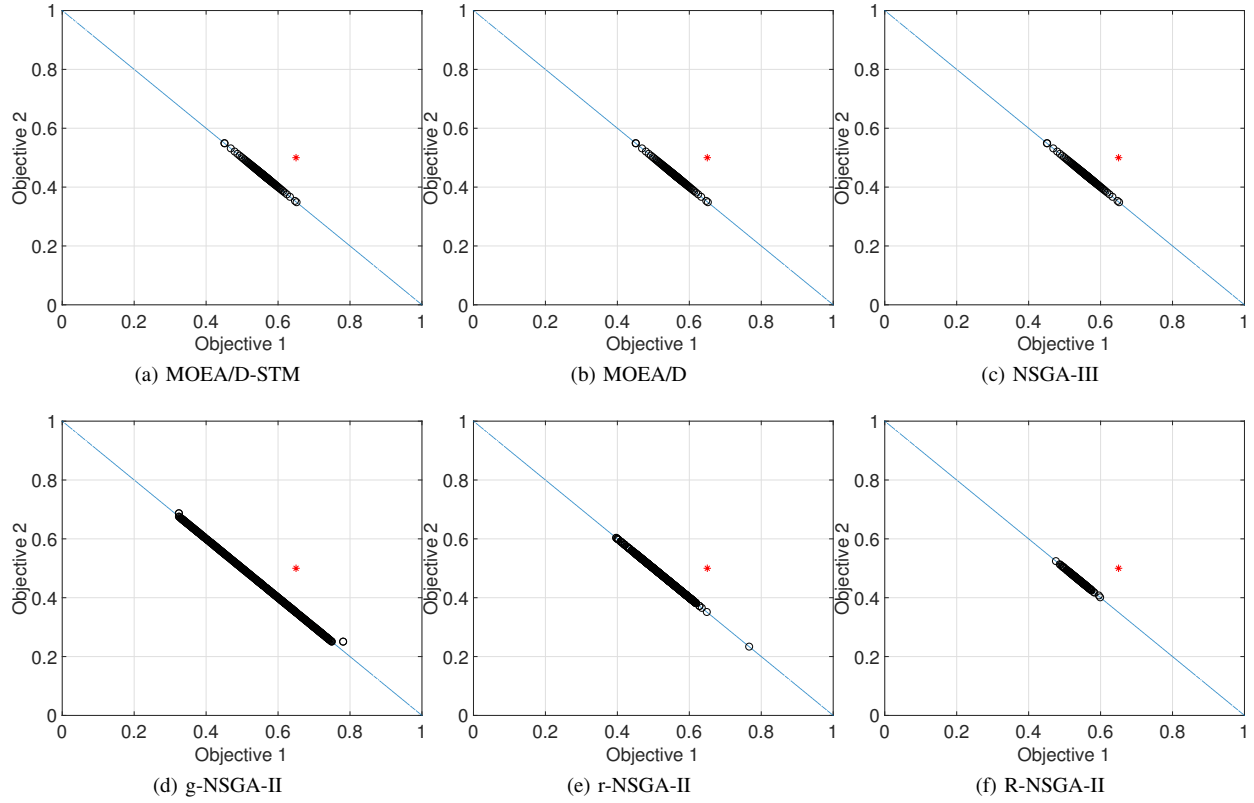
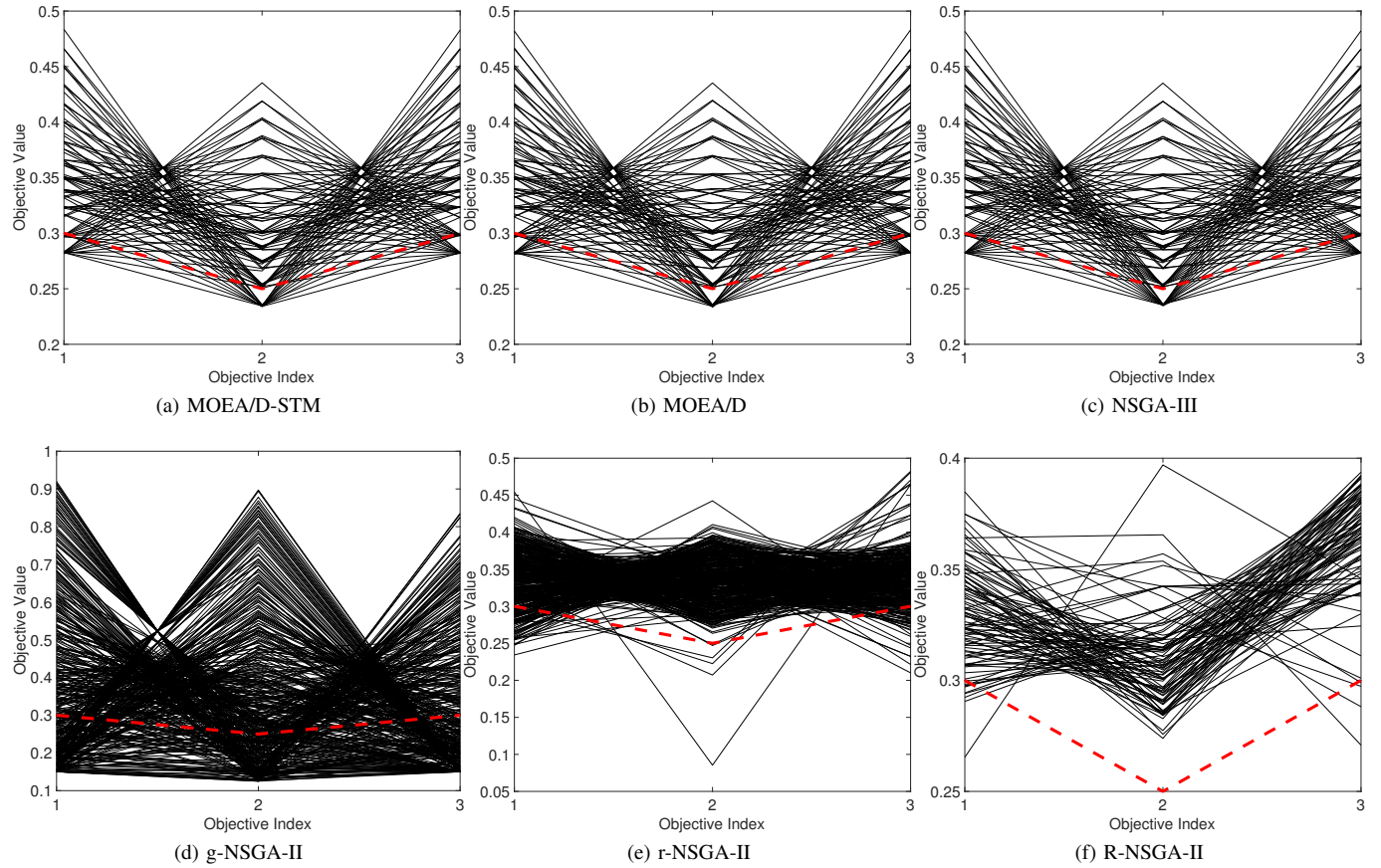
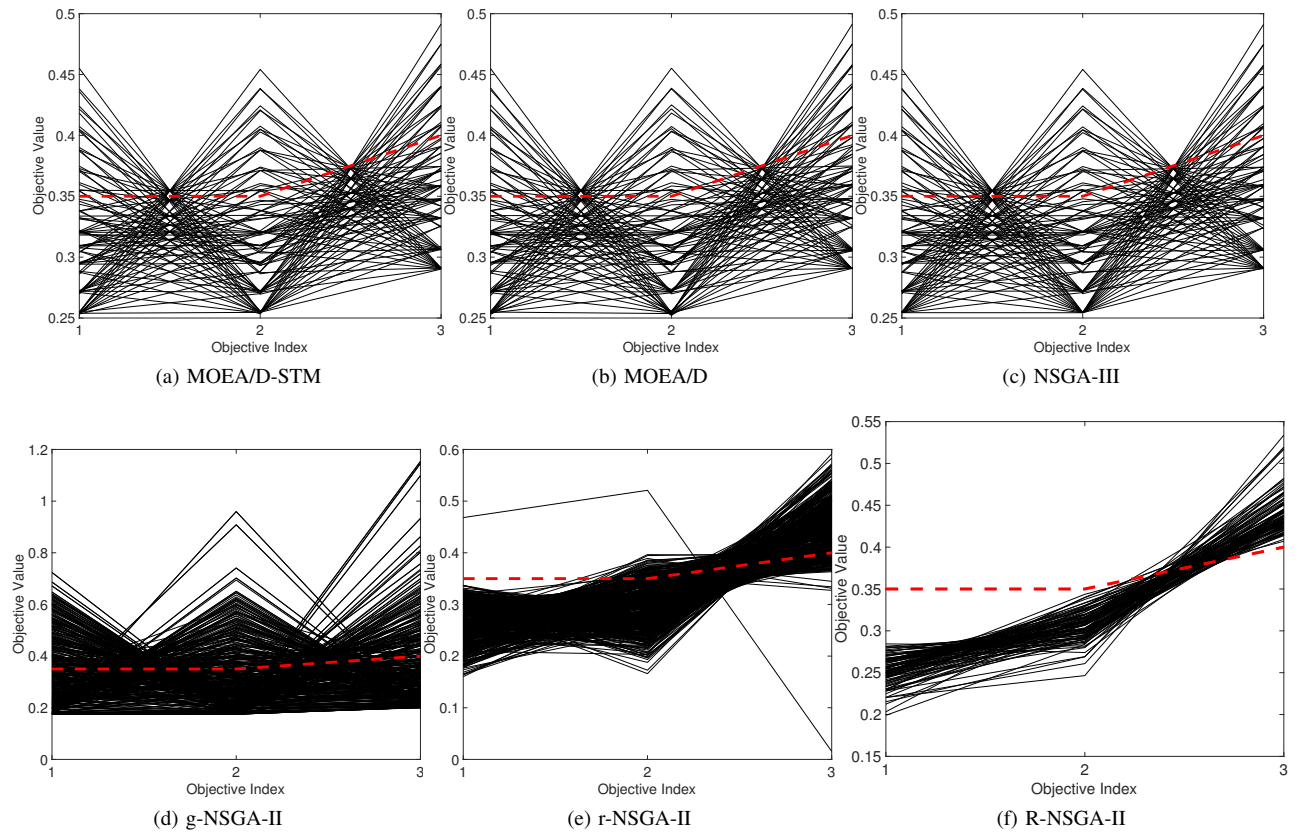
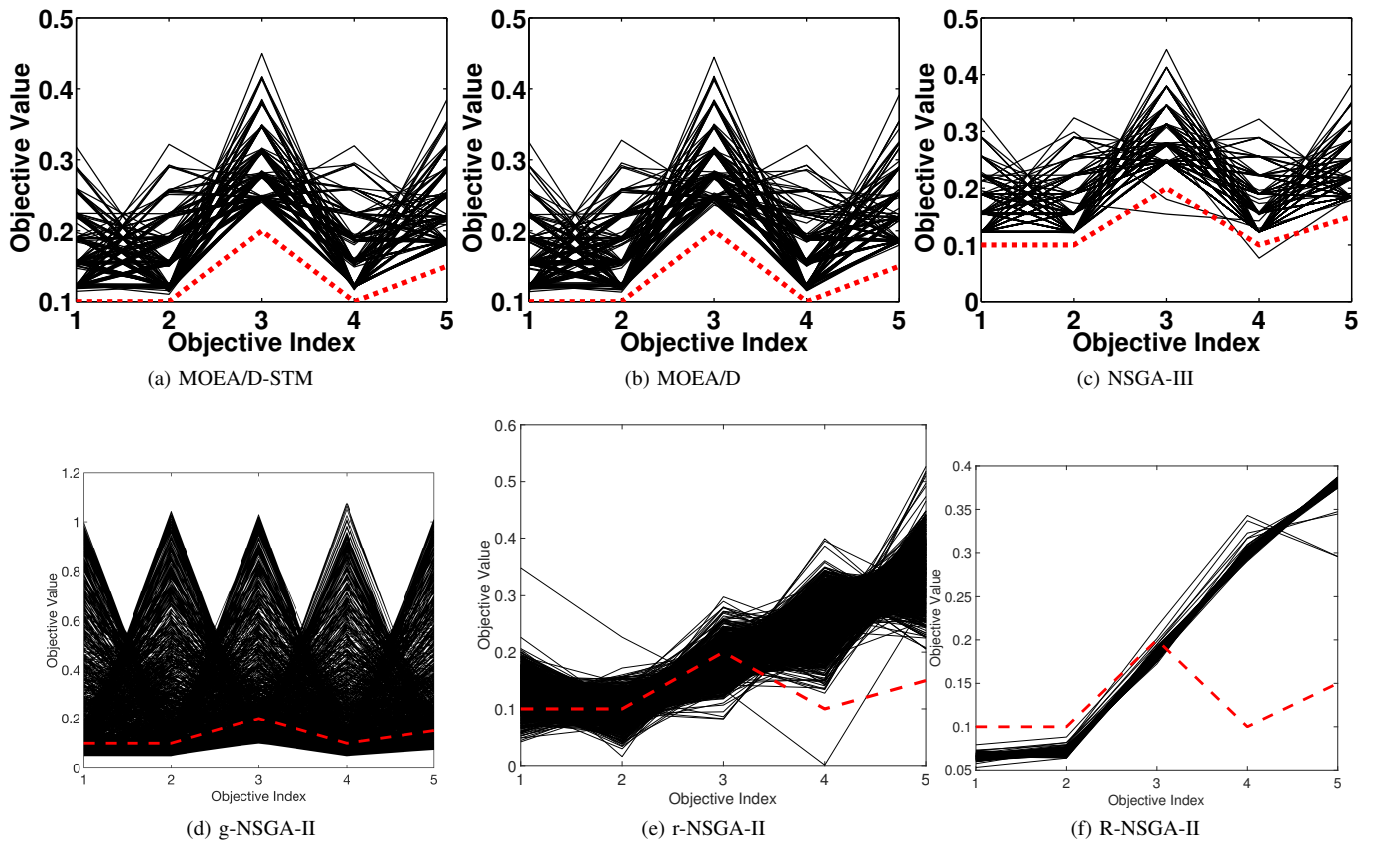
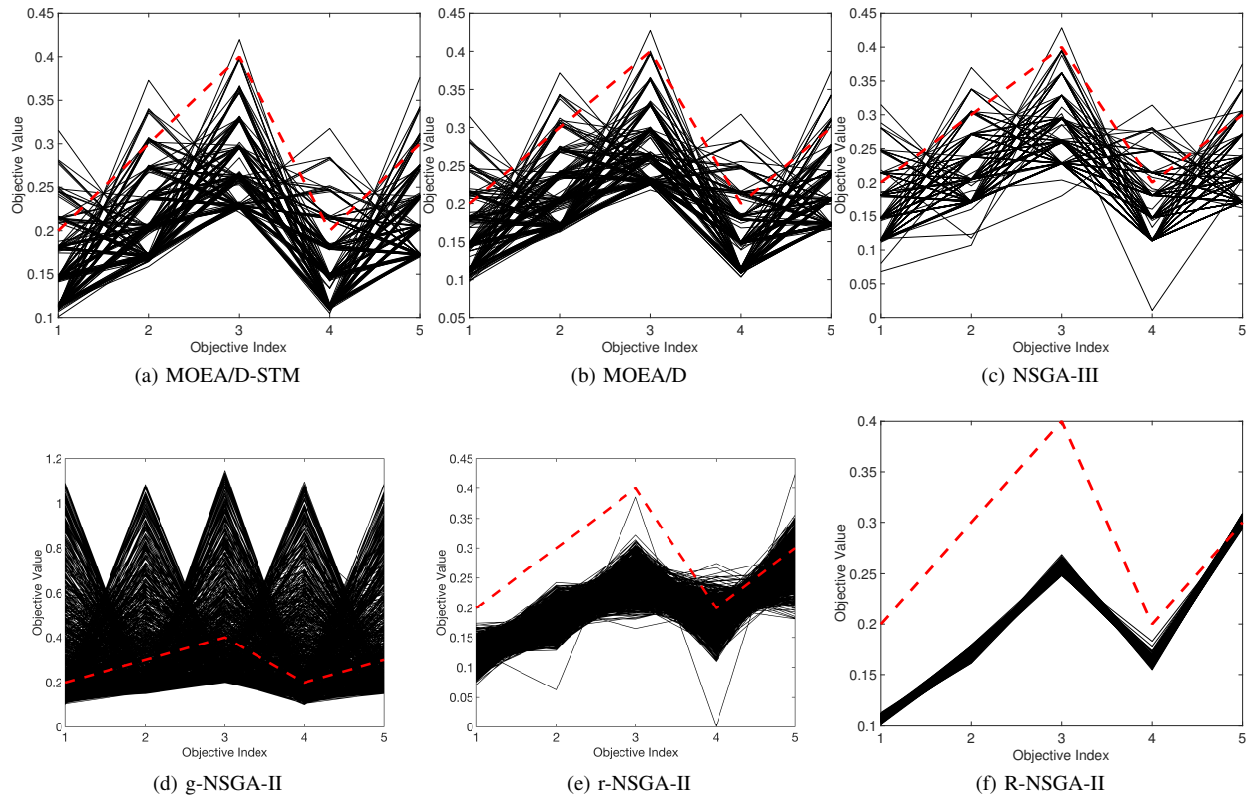
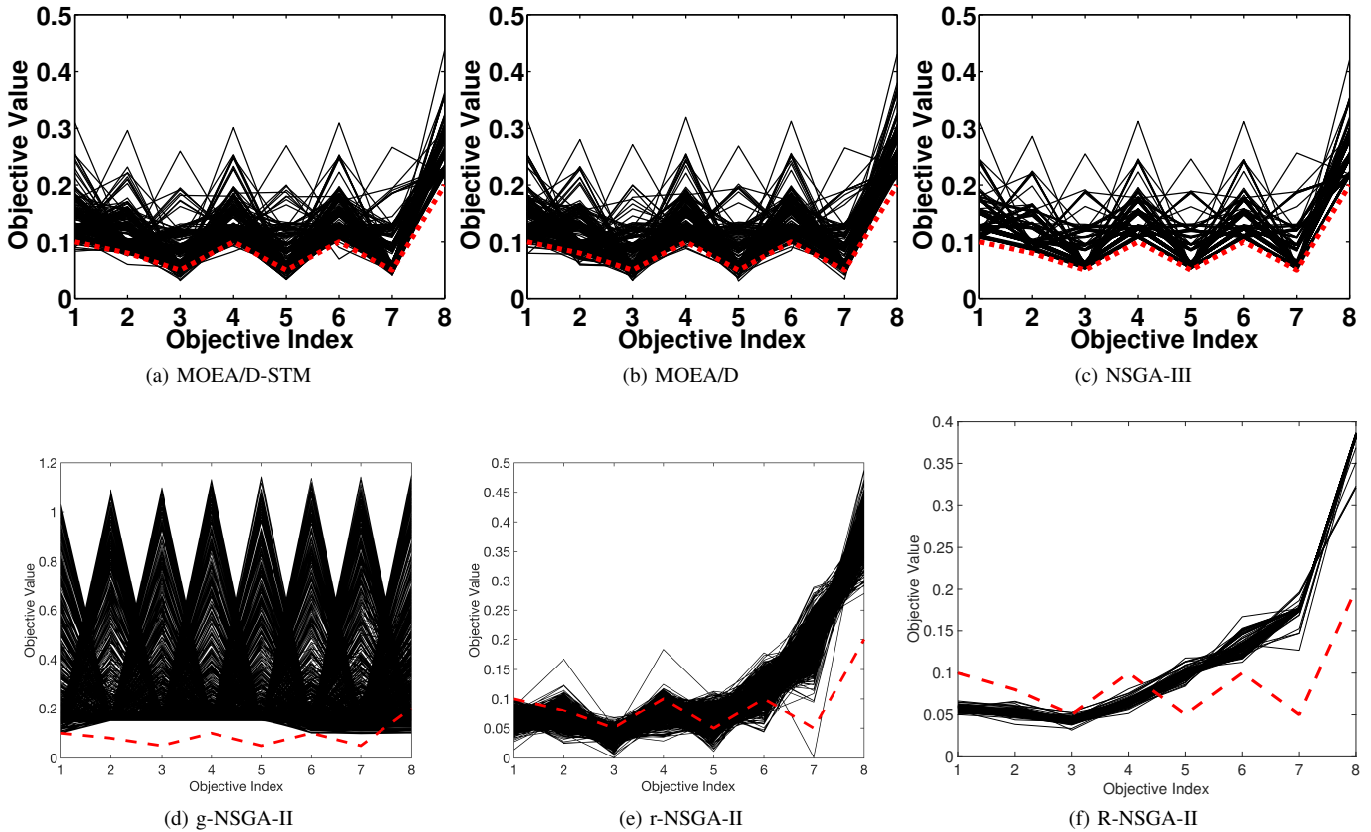


Fig. 85: Comparisons on 2-objective WFG46 where $\mathbf{z}^r = (0.55, 0.4)^T$.

Fig. 86: Comparisons on 2-objective WFG46 where $\mathbf{z}^r = (0.65, 0.5)^T$.Fig. 87: Comparisons on 3-objective WFG46 where $\mathbf{z}^r = (0.3, 0.25, 0.3)^T$.

Fig. 88: Comparisons on 3-objective WFG46 where $\mathbf{z}^r = (0.35, 0.35, 0.4)^T$.Fig. 89: Comparisons on 5-objective WFG46 where $\mathbf{z}^r = (0.1, 0.1, 0.2, 0.1, 0.15)^T$.

Fig. 90: Comparisons on 5-objective WFG46 where $\mathbf{z}^r = (0.2, 0.3, 0.4, 0.2, 0.3)^T$.Fig. 91: Comparisons on 8-objective WFG46 where $\mathbf{z}^r = (0.1, 0.08, 0.05, 0.1, 0.05, 0.1, 0.05, 0.2)^T$.

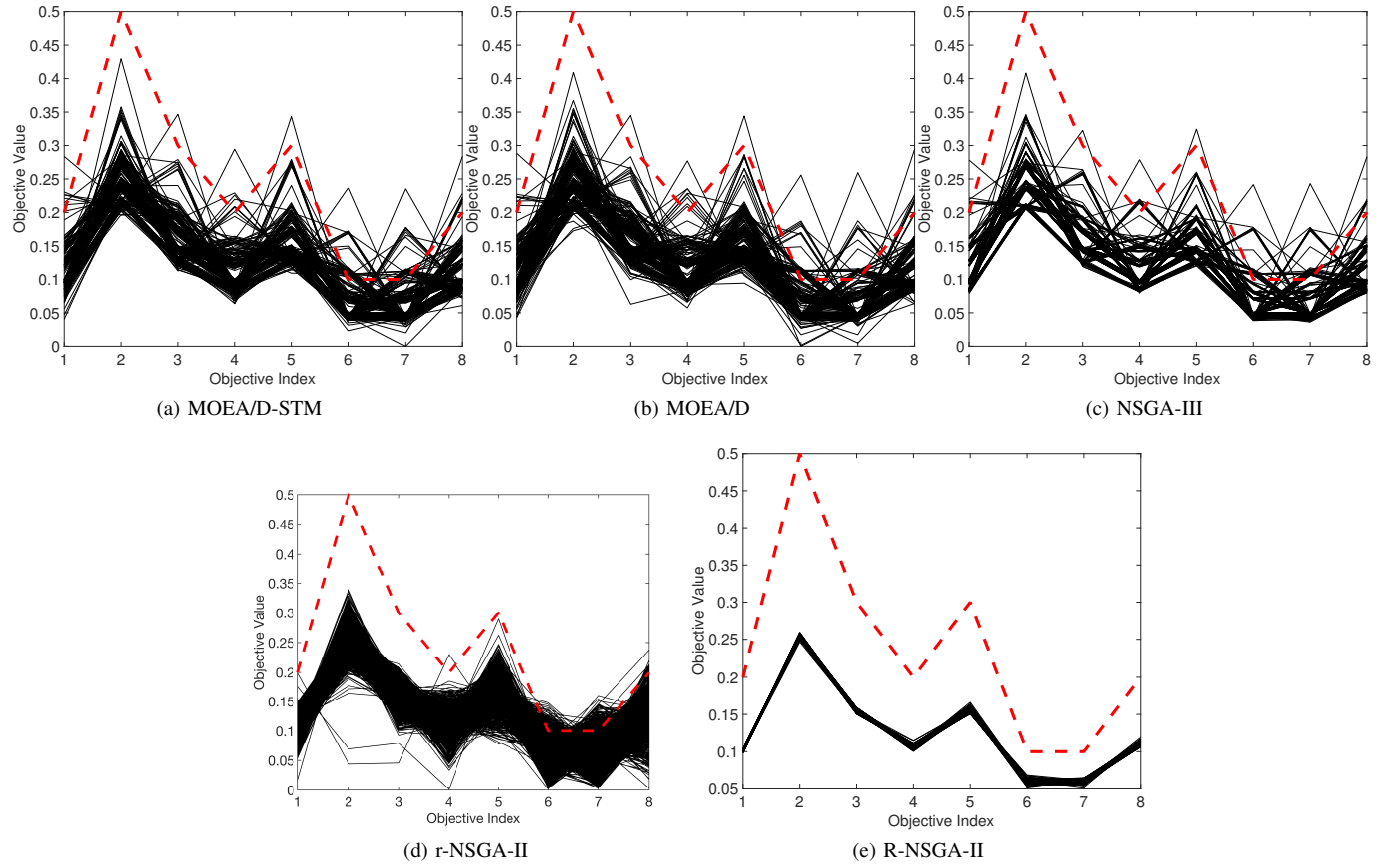


Fig. 92: Comparisons on 8-objective WFG46 where $\mathbf{z}^r = (0.2, 0.5, 0.3, 0.2, 0.3, 0.1, 0.1, 0.2)^T$.

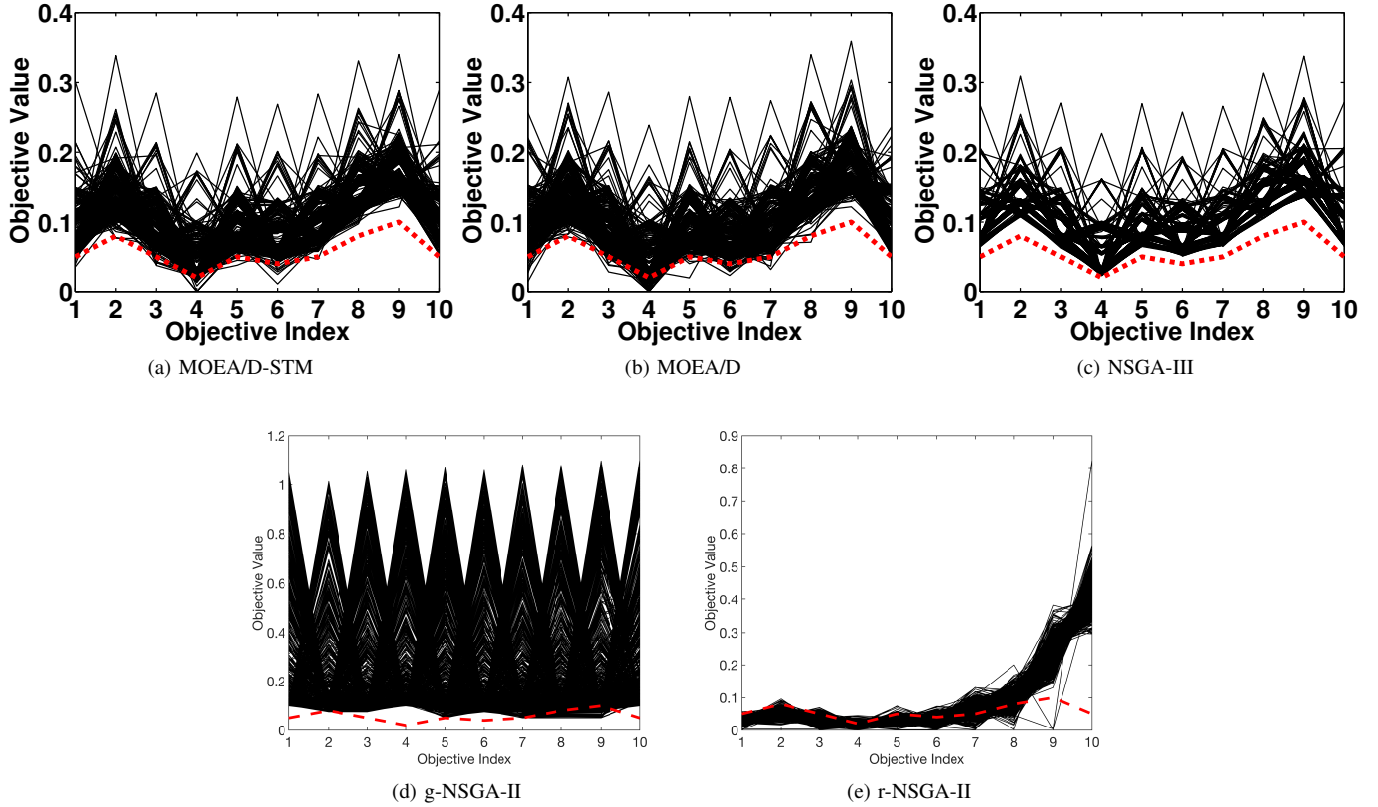


Fig. 93: Comparisons on 10-objective WFG46 where $\mathbf{z}^r = (0.05, 0.08, 0.05, 0.02, 0.05, 0.04, 0.05, 0.08, 0.1, 0.05)^T$.

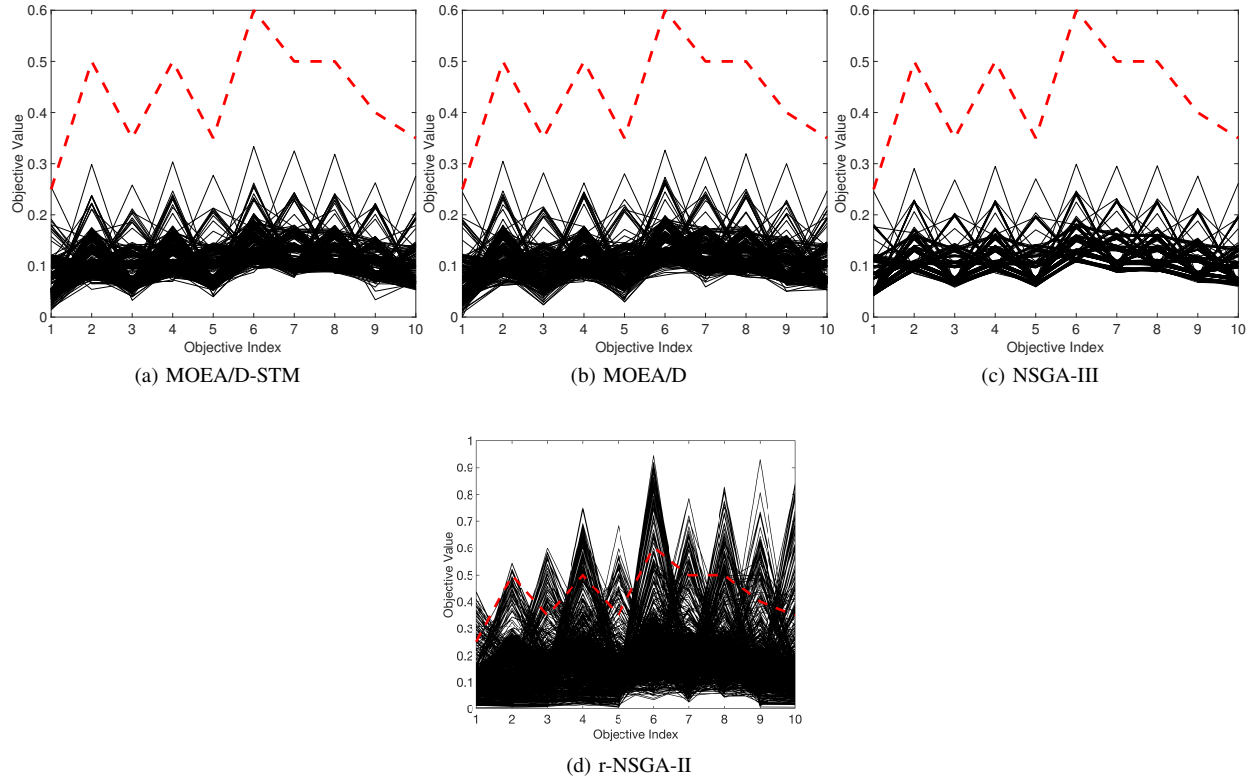


Fig. 94: Comparisons on 10-objective WFG46 where $\mathbf{z}^r = (0.25, 0.5, 0.35, 0.5, 0.35, 0.6, 0.5, 0.5, 0.4, 0.35)^T$.

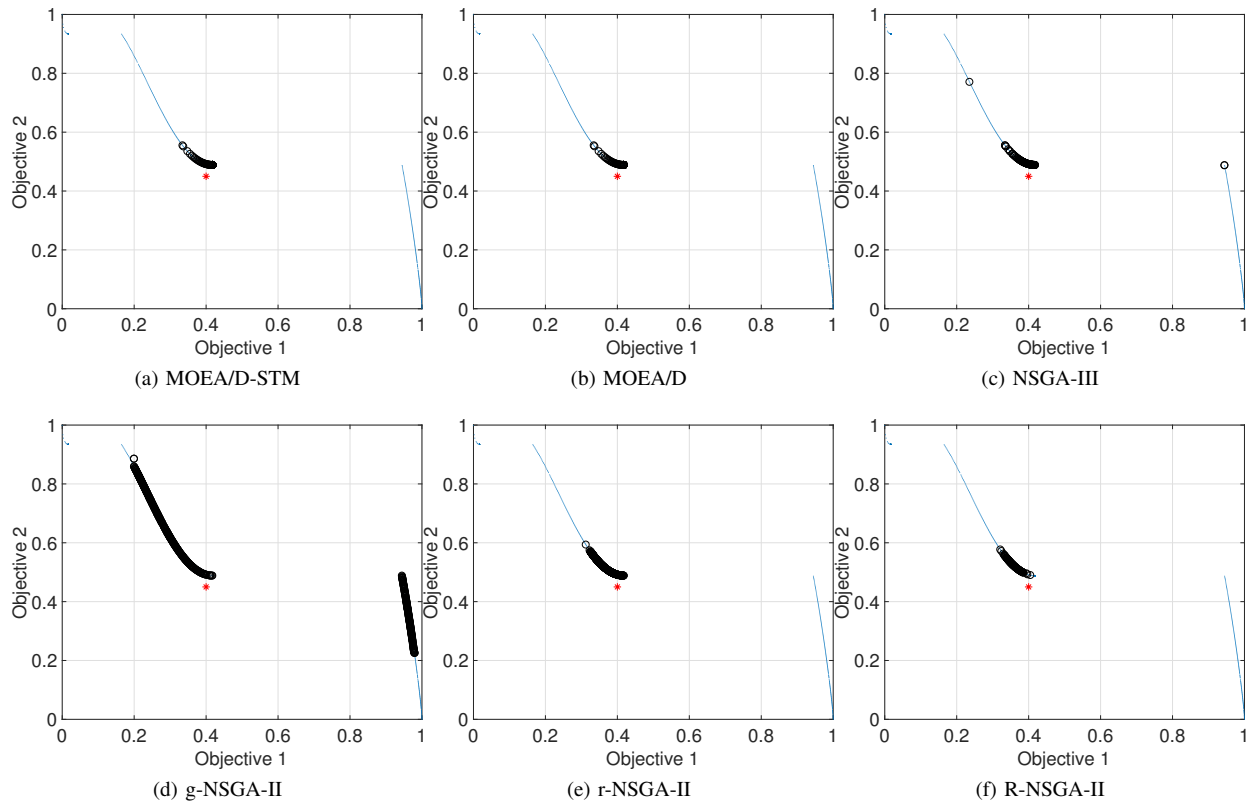


Fig. 95: Comparisons on 2-objective WFG47 where $\mathbf{z}^r = (0.4, 0.45)^T$.

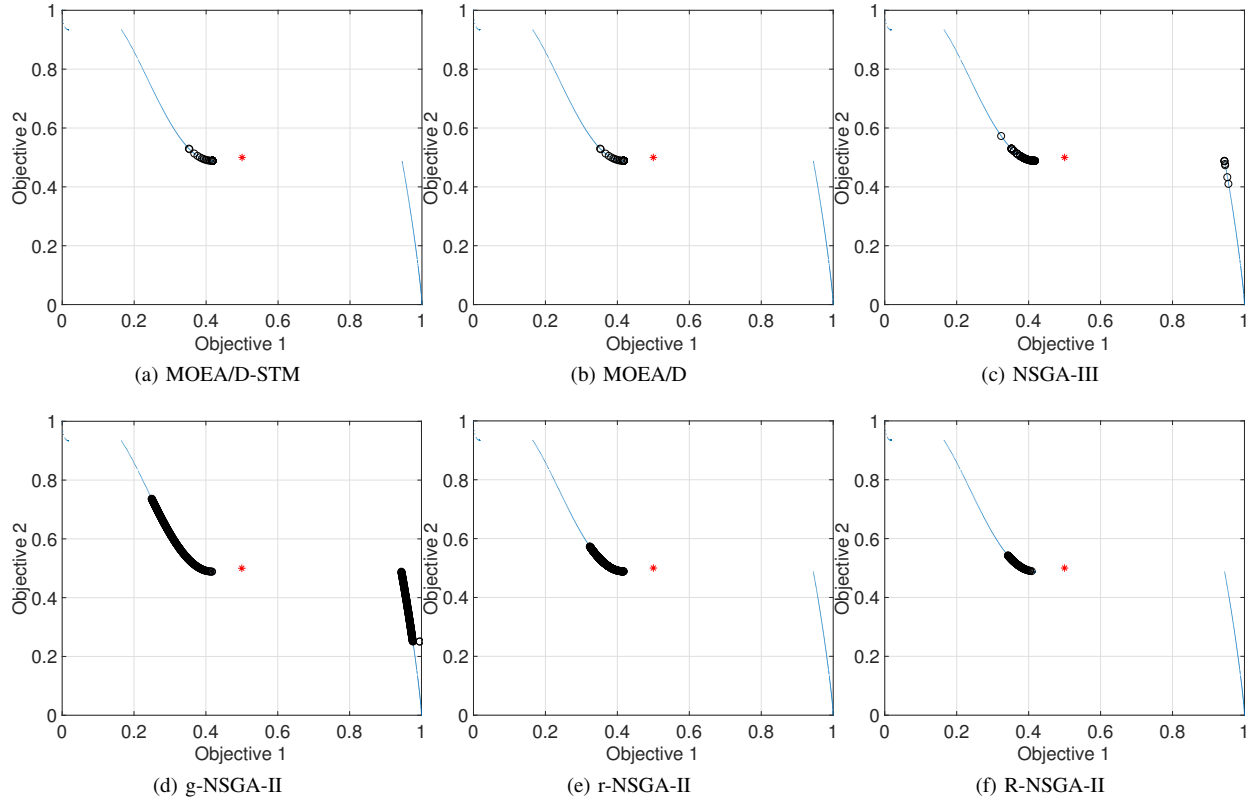
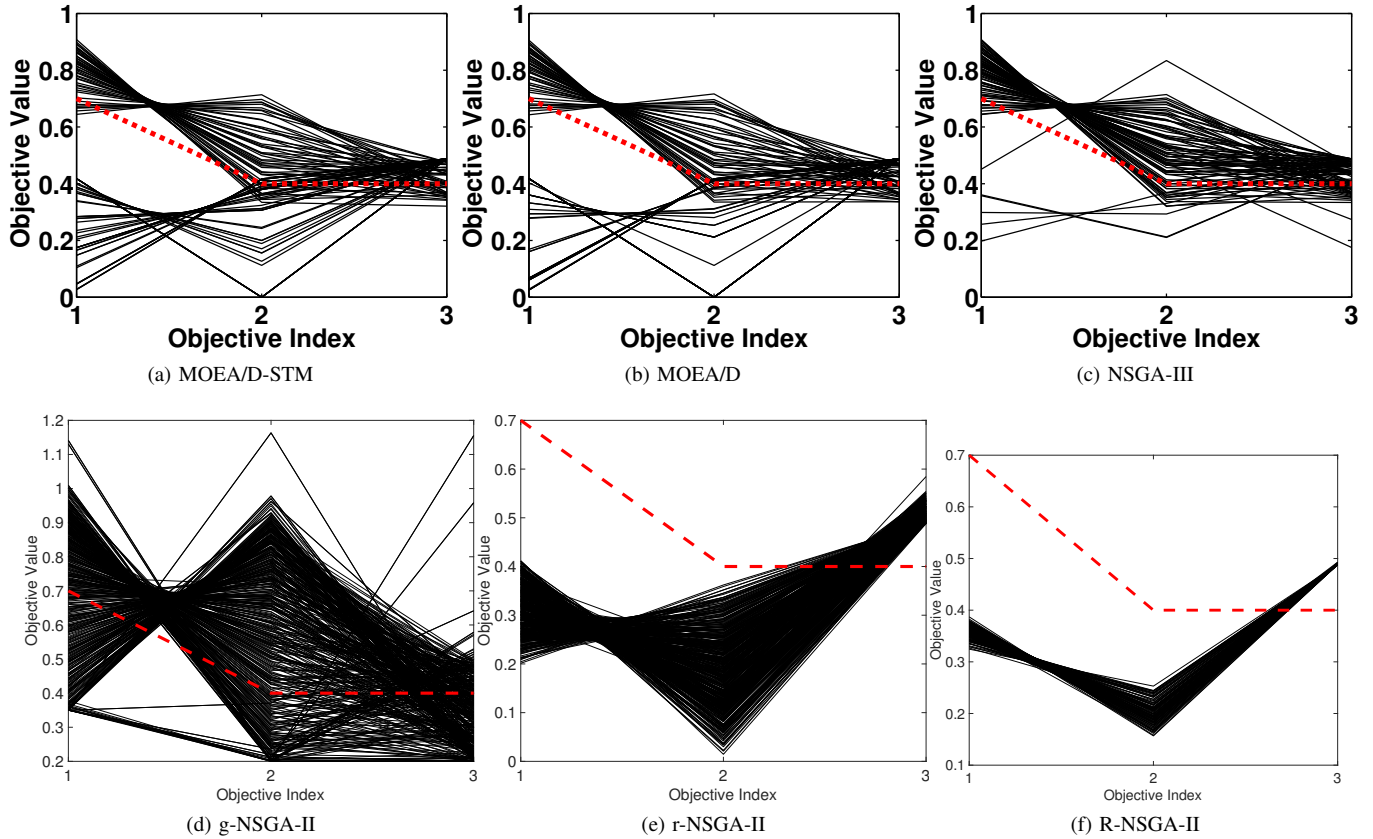
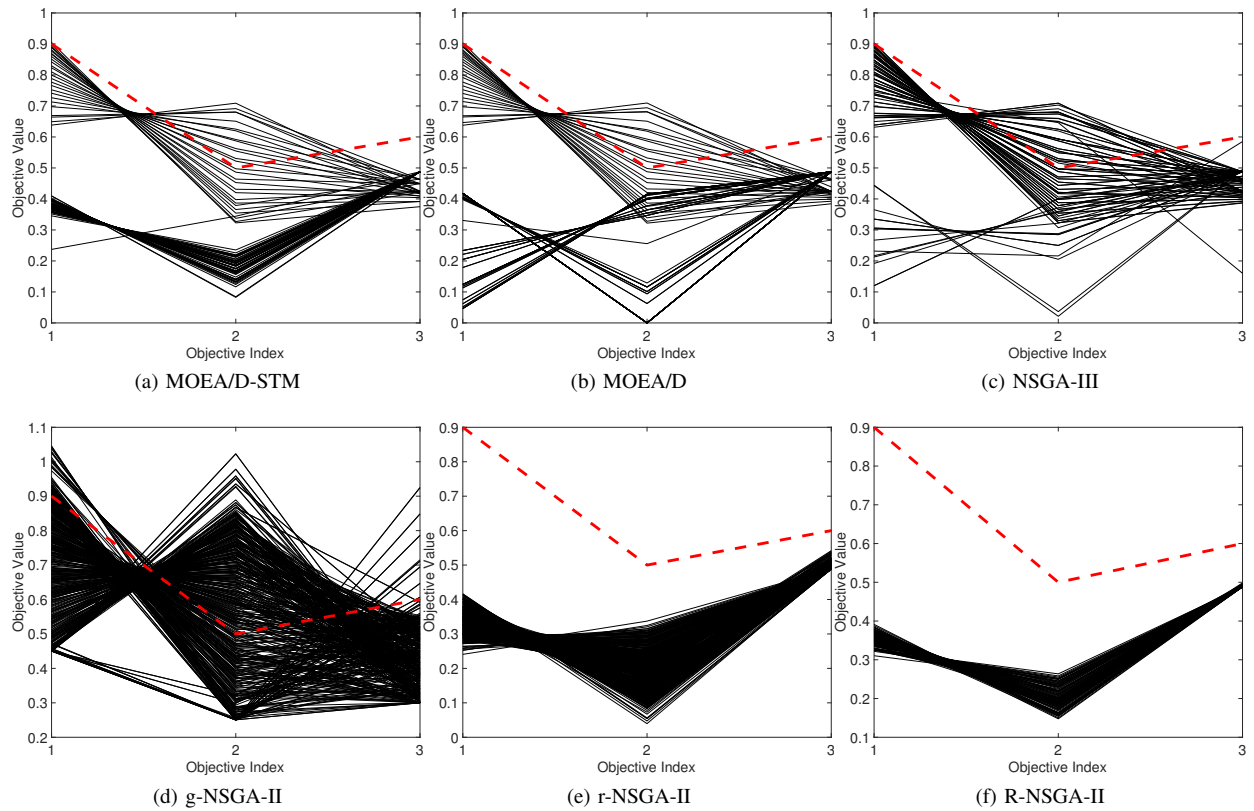
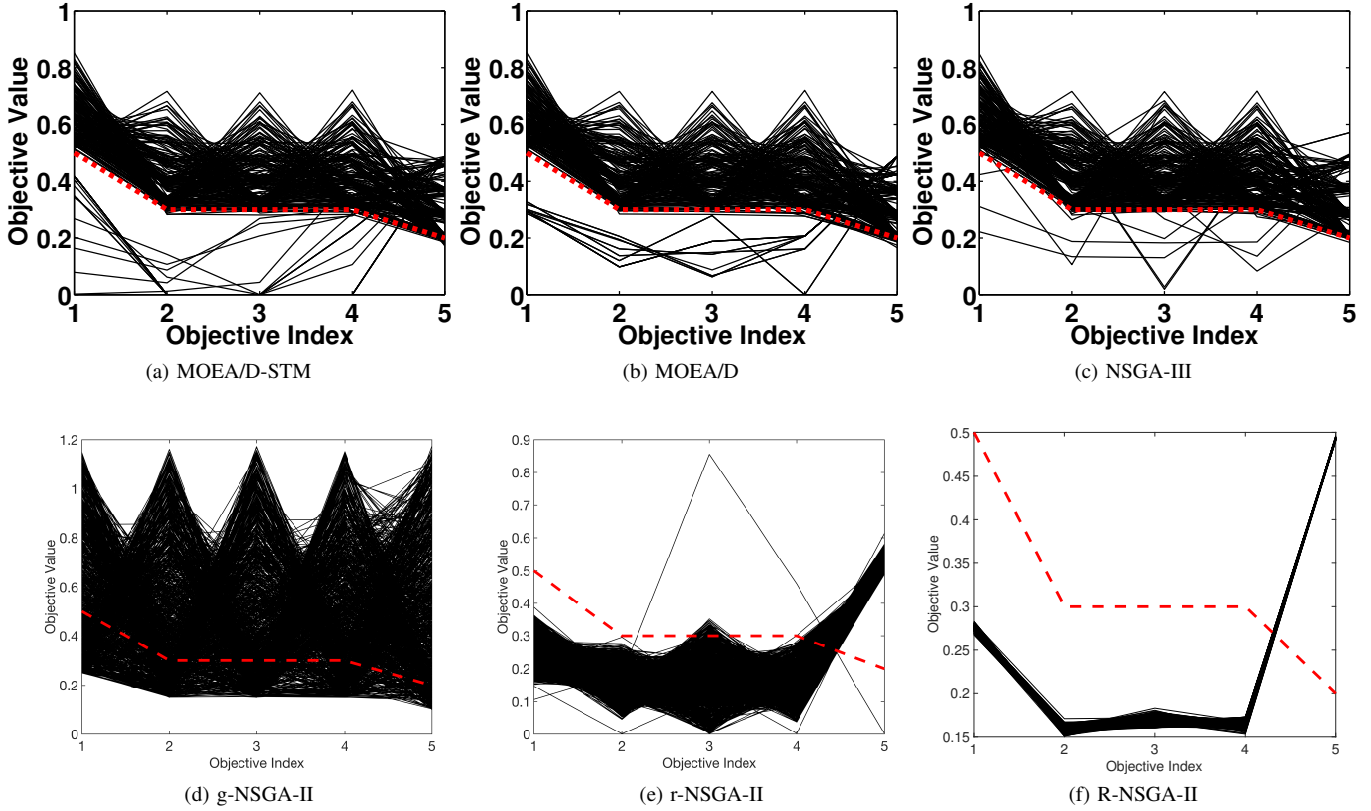
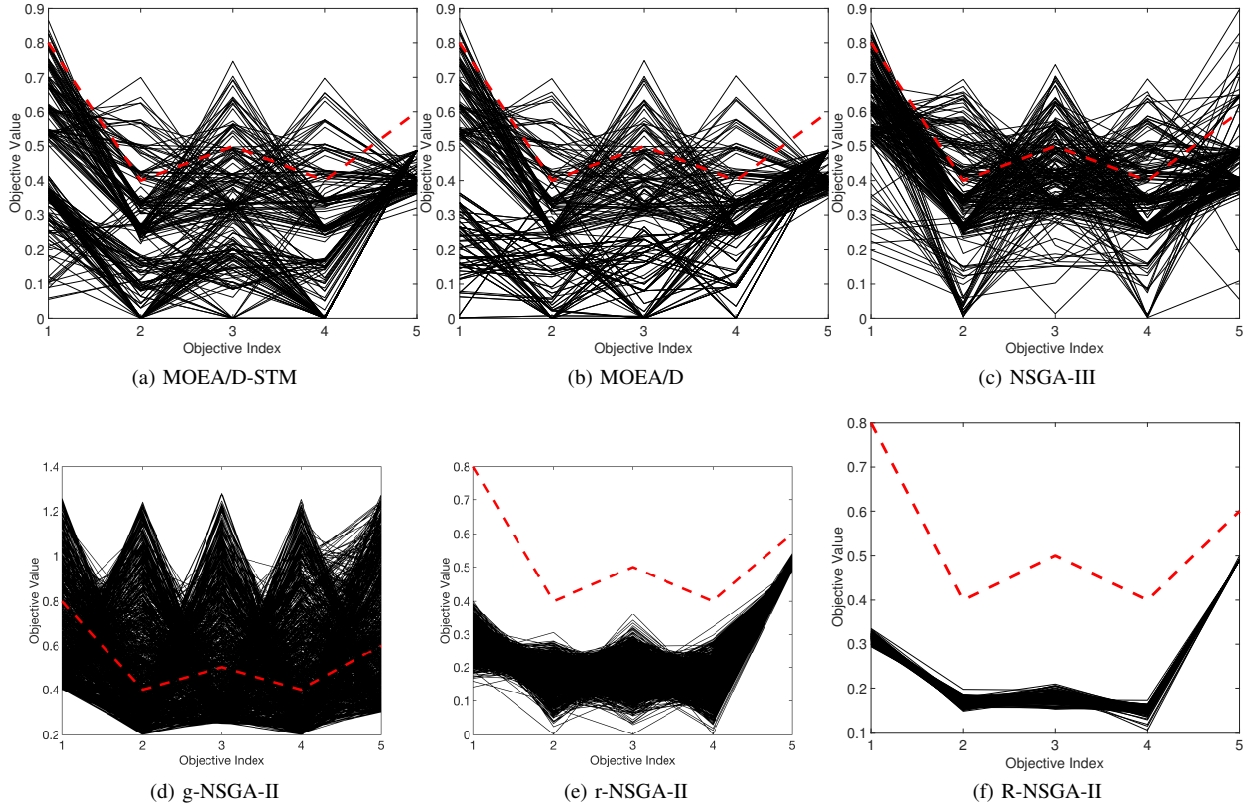


Fig. 96: Comparisons on 2-objective WFG47 where $\mathbf{z}^r = (0.5, 0.5)^T$.

REFERENCES

- [1] I. Das and J. E. Dennis, "Normal-Boundary Intersection: A new method for generating the pareto surface in nonlinear multicriteria optimization problems," *SIAM Journal on Optimization*, vol. 8, pp. 631–657, 1998.
- [2] J. J. Durillo, A. J. Nebro, C. A. C. Coello, J. García-Nieto, F. Luna, and E. Alba, "A study of multiobjective metaheuristics when solving parameter scalable problems," *IEEE Trans. Evolutionary Computation*, vol. 14, no. 4, pp. 618–635, 2010.
- [3] S. Huband, P. Hingston, L. Barone, and L. While, "A review of multiobjective test problems and a scalable test problem toolkit," *IEEE Trans. Evolutionary Computation*, vol. 10, no. 5, pp. 477–506, Oct. 2006.
- [4] H. Asafi, F. Jolai, M. Rabiee, and M. T. Araghi, "A hybrid NSGA-II and VNS for solving a bi-objective no-wait flexible flowshop scheduling problem," *The International Journal of Advanced Manufacturing Technology*, vol. 75, no. 5, pp. 1017–1033, 2014.

Fig. 97: Comparisons on 3-objective WFG47 where $\mathbf{z}^r = (0.7, 0.4, 0.4)^T$.Fig. 98: Comparisons on 3-objective WFG47 where $\mathbf{z}^r = (0.9, 0.5, 0.6)^T$.

Fig. 99: Comparisons on 5-objective WFG47 where $\mathbf{z}^r = (0.5, 0.3, 0.3, 0.3, 0.2)^T$.Fig. 100: Comparisons on 5-objective WFG47 where $\mathbf{z}^r = (0.8, 0.4, 0.5, 0.4, 0.6)^T$.

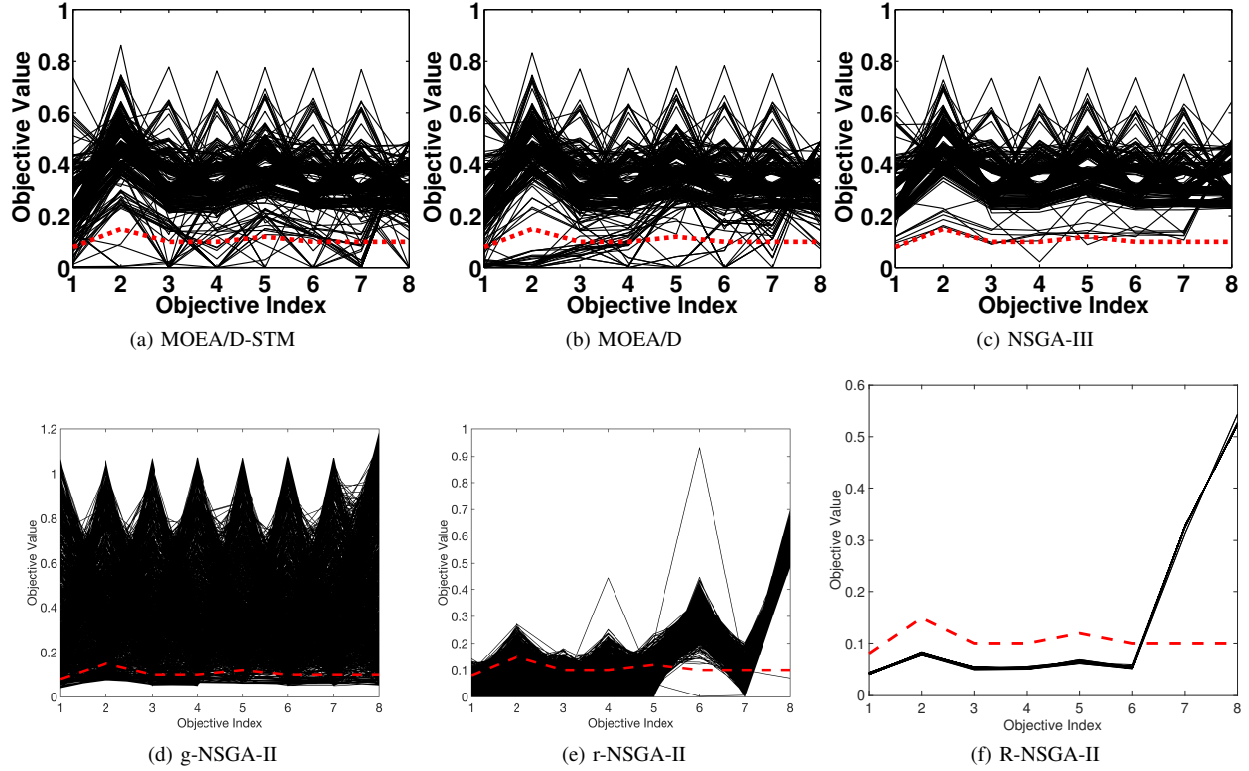


Fig. 101: Comparisons on 8-objective WFG47 where $\mathbf{z}^r = (0.08, 0.15, 0.1, 0.1, 0.12, 0.1, 0.1, 0.1)^T$.

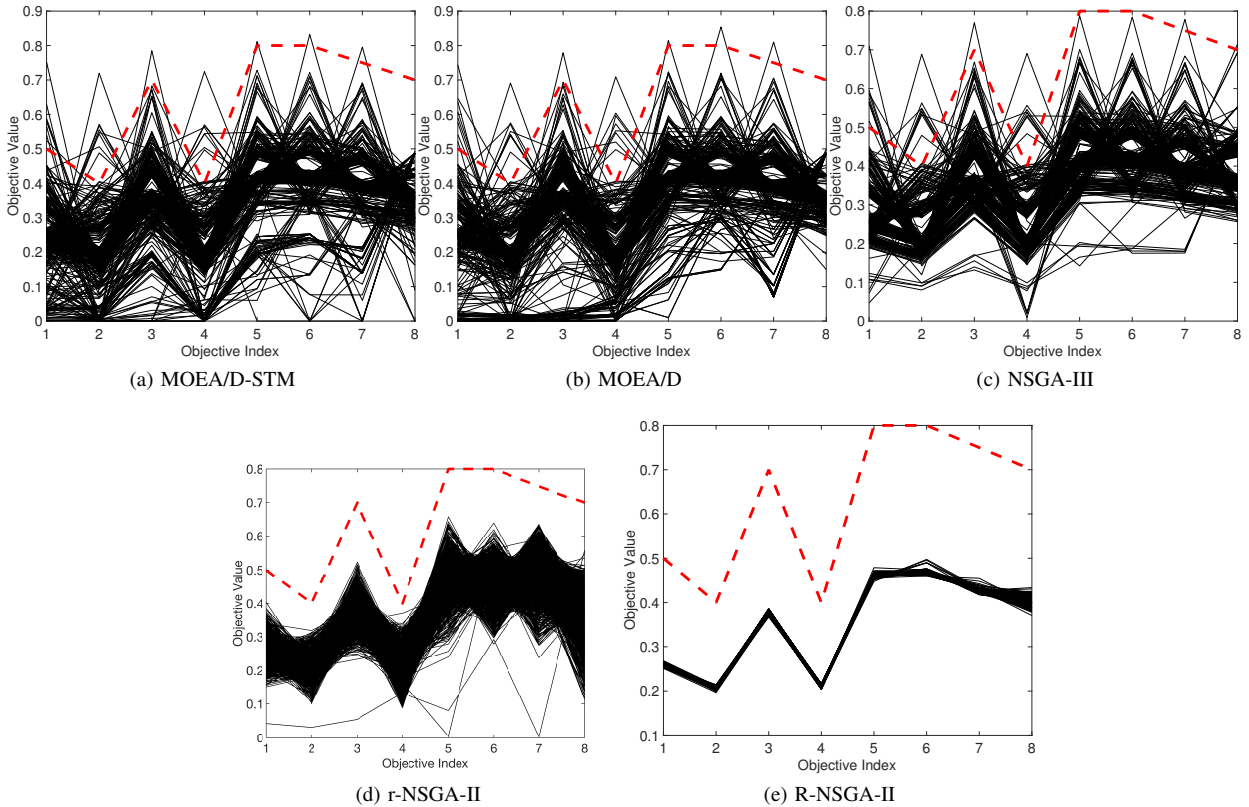


Fig. 102: Comparisons on 8-objective WFG47 where $\mathbf{z}^r = (0.5, 0.4, 0.7, 0.4, 0.8, 0.8, 0.75, 0.7)^T$.

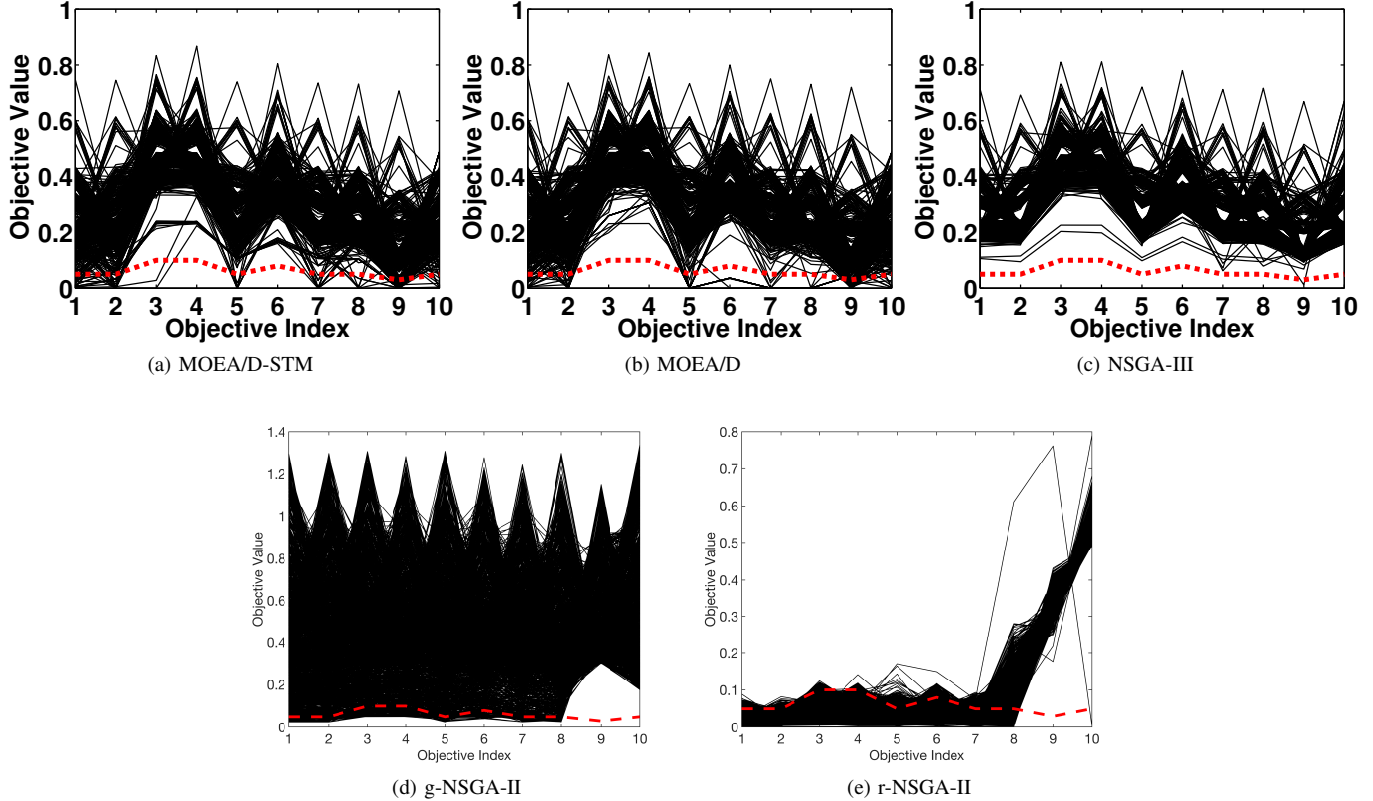


Fig. 103: Comparisons on 10-objective WFG47 where $\mathbf{z}^r = (0.05, 0.05, 0.1, 0.1, 0.05, 0.08, 0.05, 0.05, 0.03, 0.05)^T$.

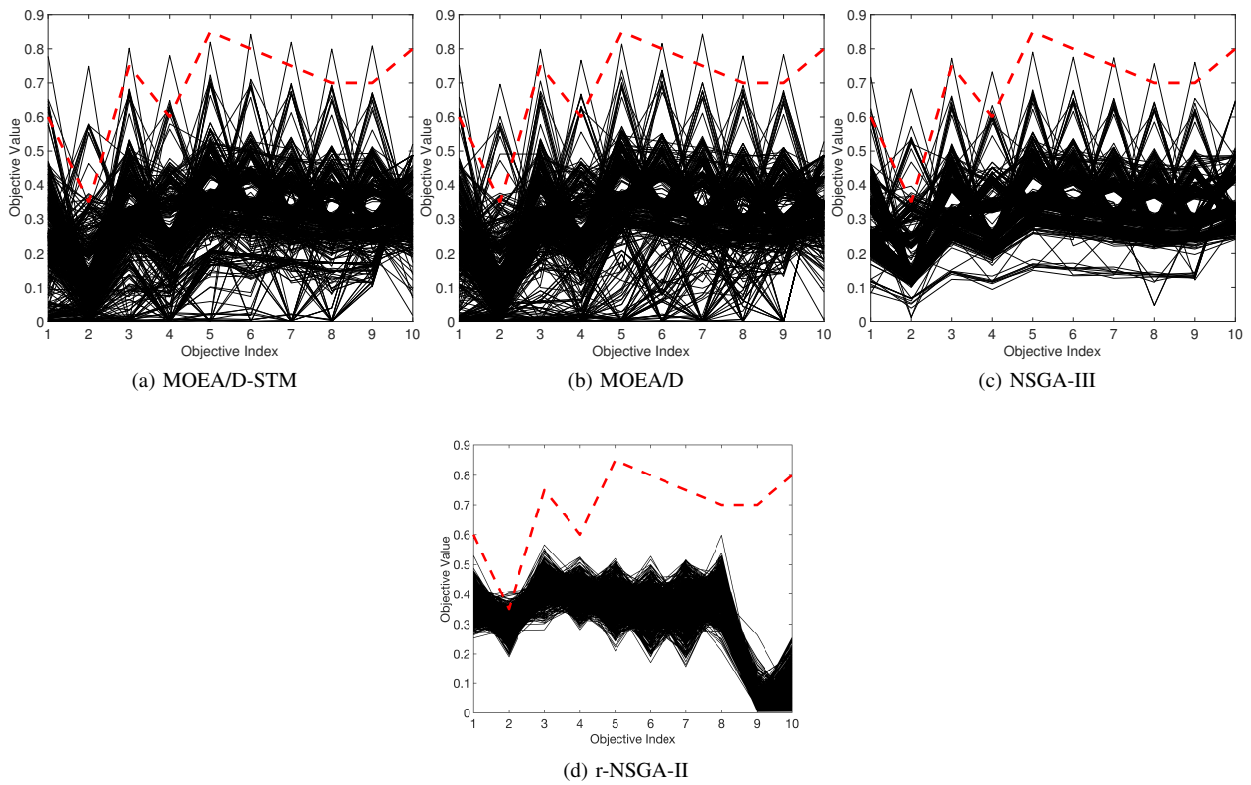


Fig. 104: Comparisons on 10-objective WFG47 where $\mathbf{z}^r = (0.6, 0.35, 0.75, 0.6, 0.85, 0.8, 0.75, 0.7, 0.7, 0.8)^T$.

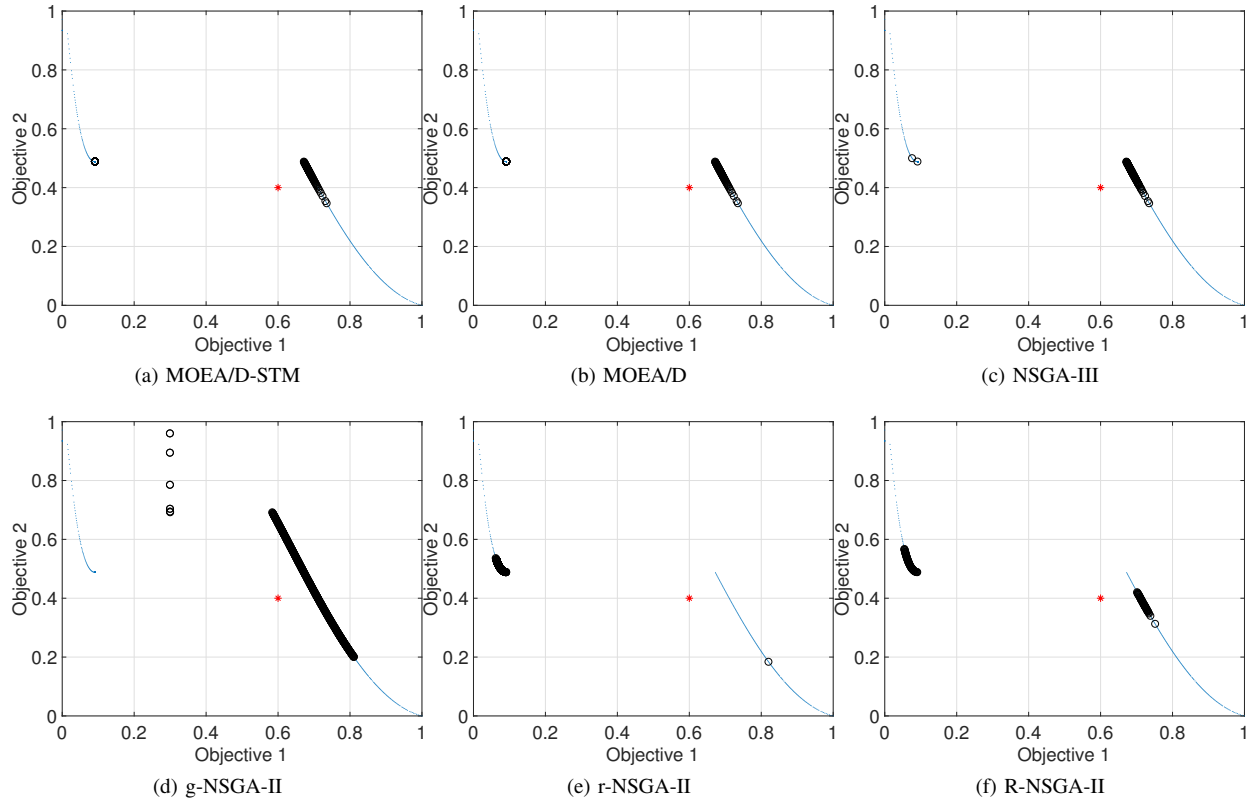


Fig. 105: Comparisons on 2-objective WFG48 where $\mathbf{z}^r = (0.6, 0.4)^T$.

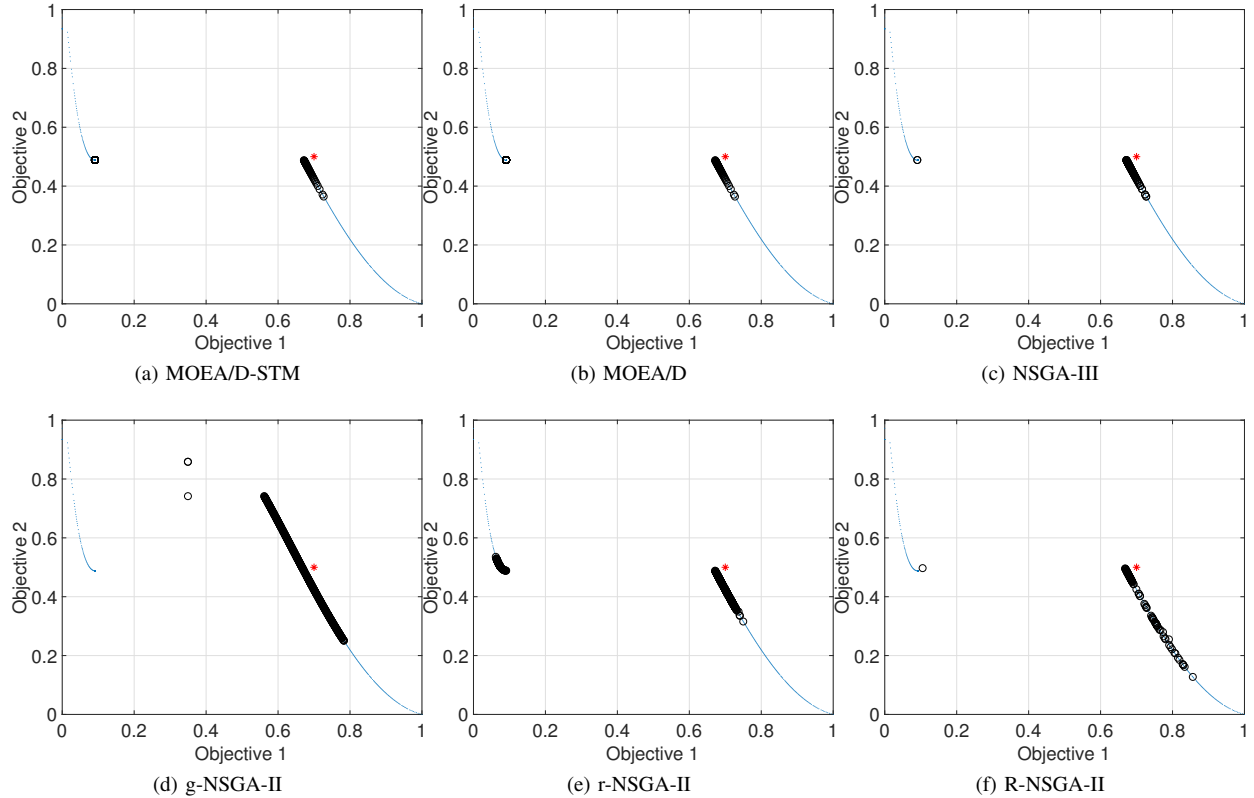
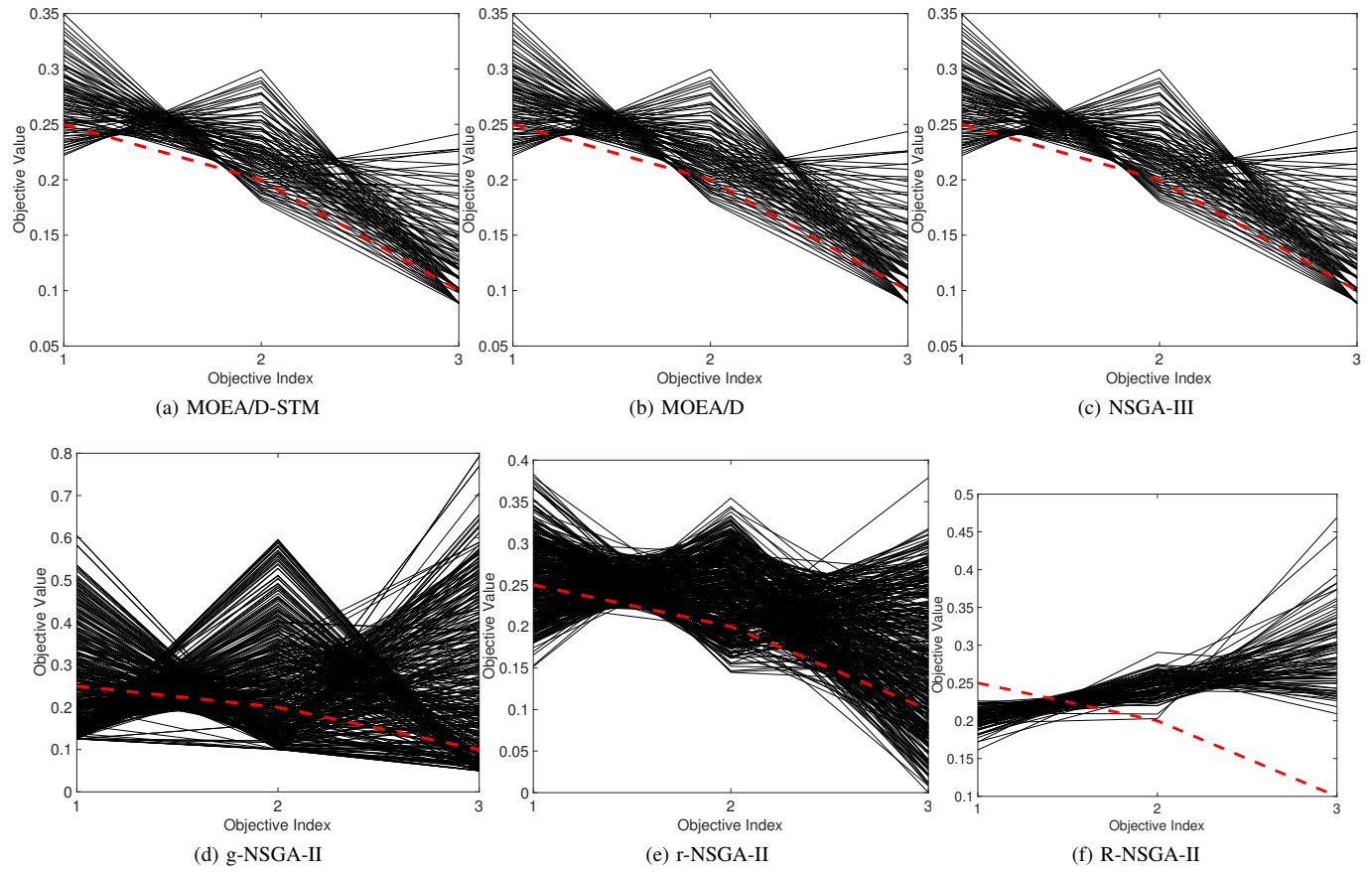
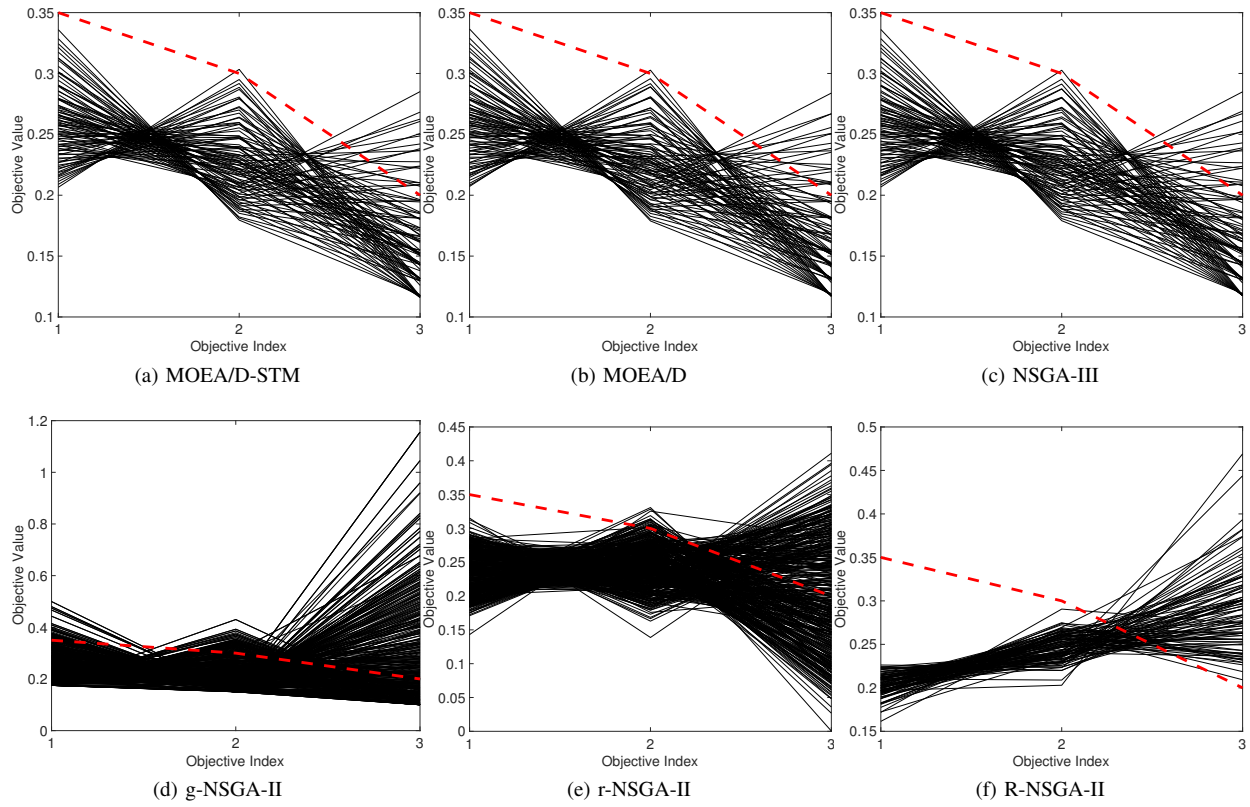


Fig. 106: Comparisons on 2-objective WFG48 where $\mathbf{z}^r = (0.7, 0.5)^T$.

Fig. 107: Comparisons on 3-objective WFG48 where $\mathbf{z}^r = (0.25, 0.2, 0.1)^T$.Fig. 108: Comparisons on 3-objective WFG48 where $\mathbf{z}^r = (0.35, 0.3, 0.2)^T$.

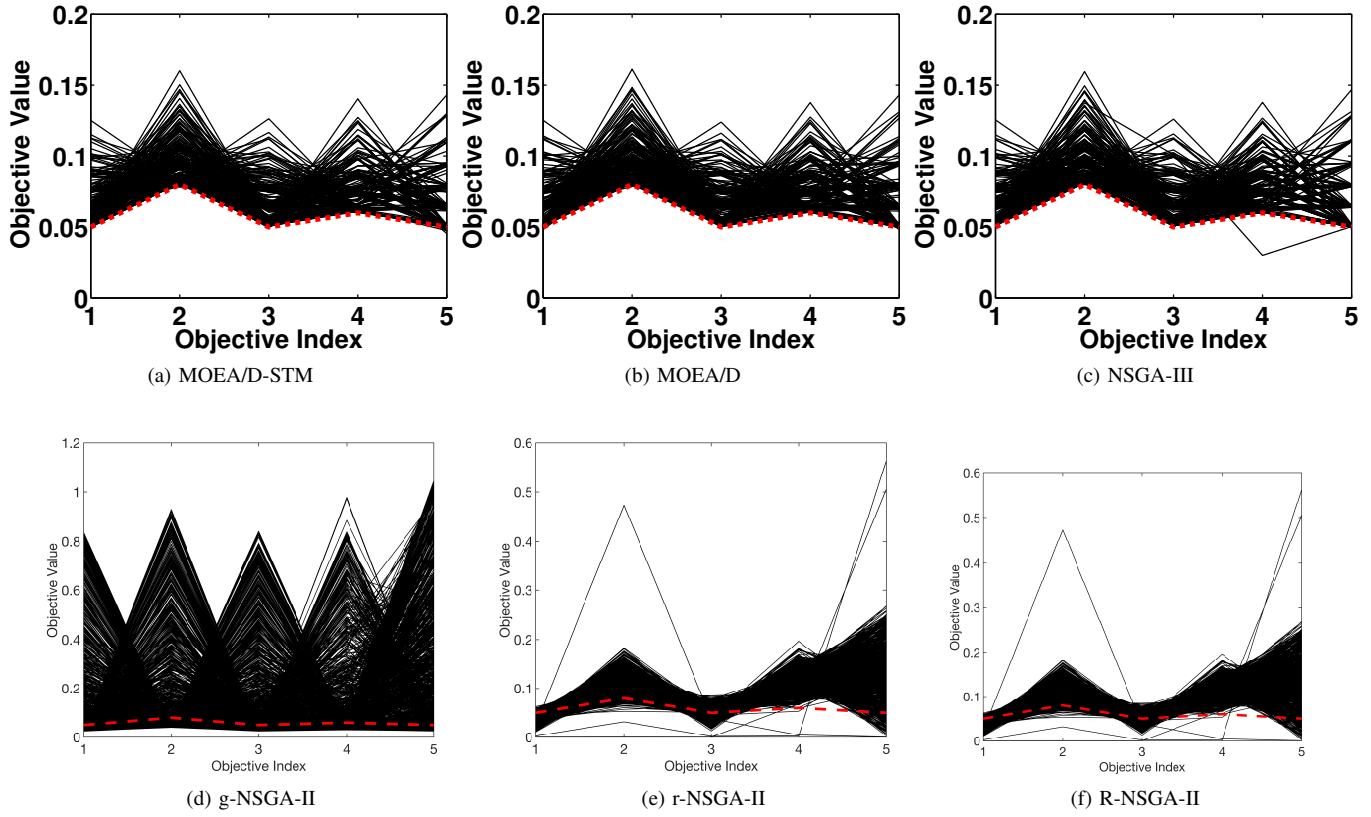


Fig. 109: Comparisons on 5-objective WFG48 where $\mathbf{z}^r = (0.05, 0.08, 0.05, 0.06, 0.05)^T$.

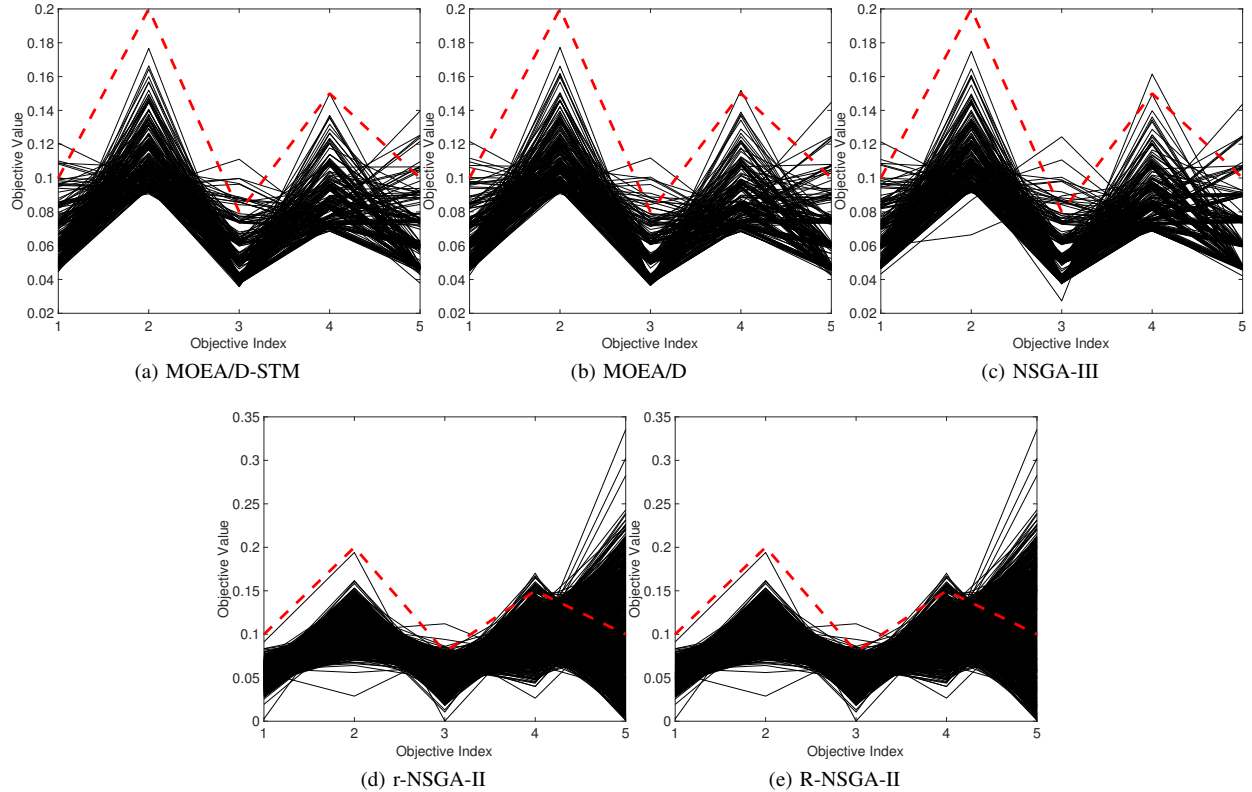


Fig. 110: Comparisons on 5-objective WFG48 where $\mathbf{z}^r = (0.1, 0.2, 0.08, 0.15, 0.1)^T$.

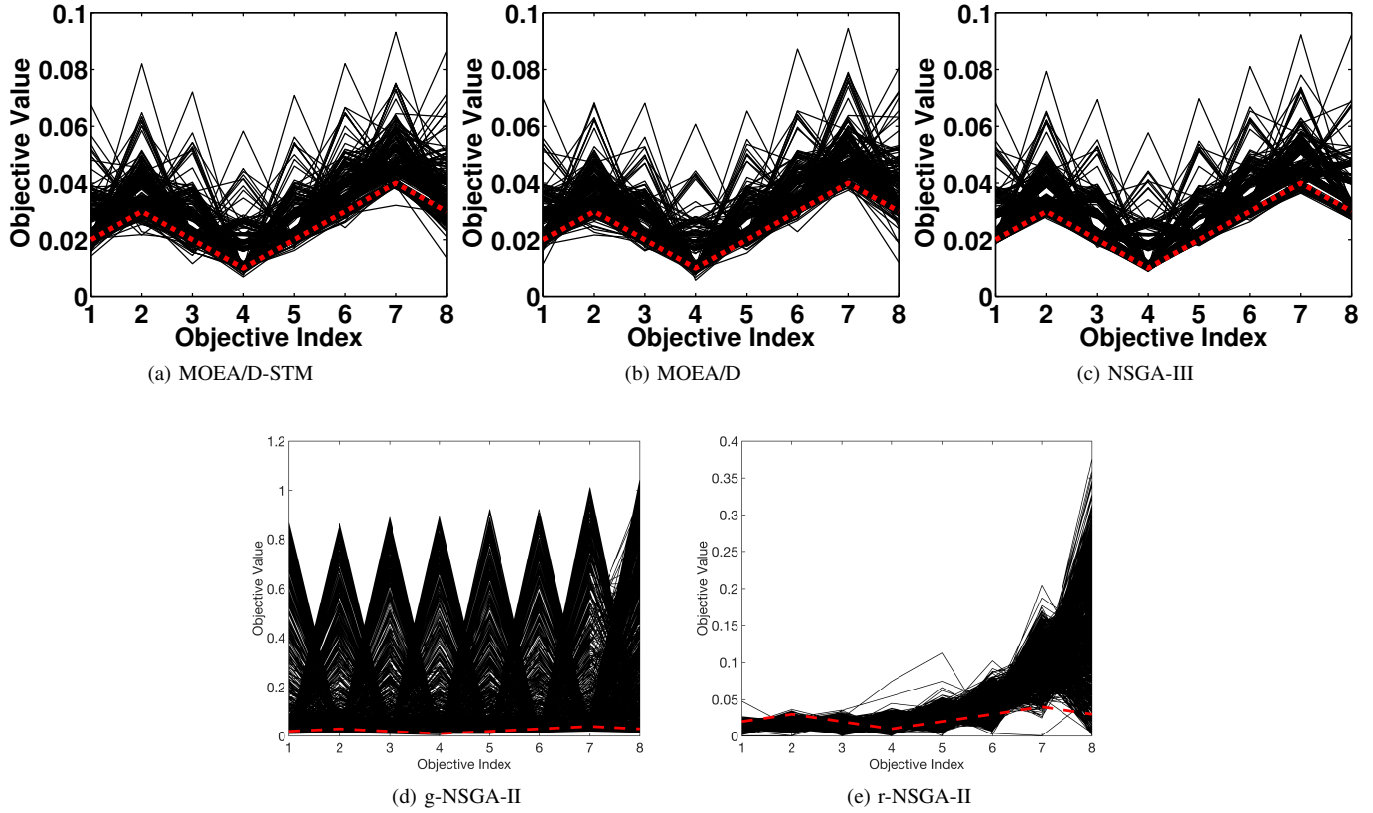


Fig. 111: Comparisons on 8-objective WFG48 where $\mathbf{z}^r = (0.02, 0.03, 0.02, 0.01, 0.02, 0.03, 0.04, 0.03)^T$.

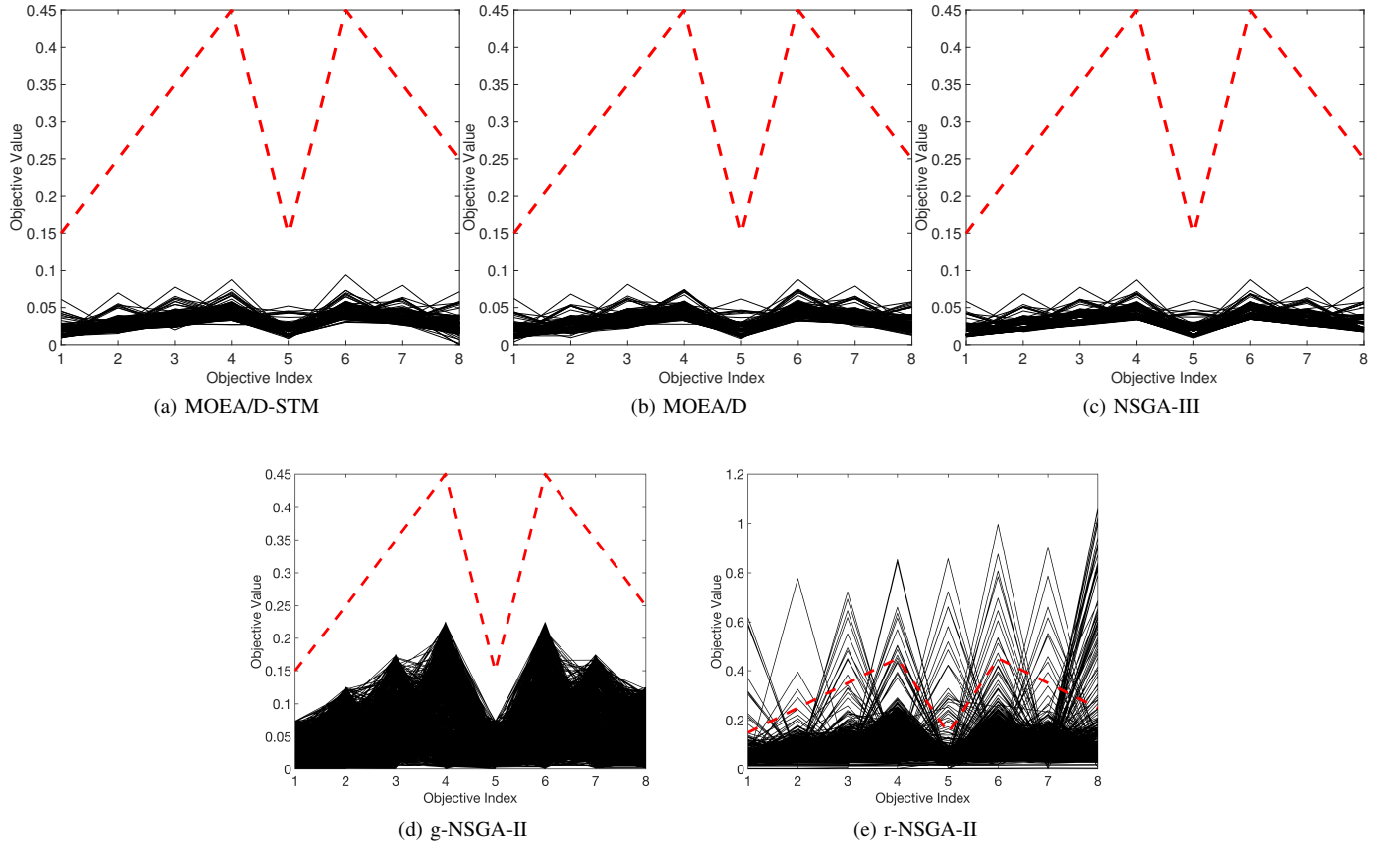


Fig. 112: Comparisons on 8-objective WFG48 where $\mathbf{z}^r = (0.15, 0.25, 0.35, 0.45, 0.15, 0.45, 0.35, 0.25)^T$.

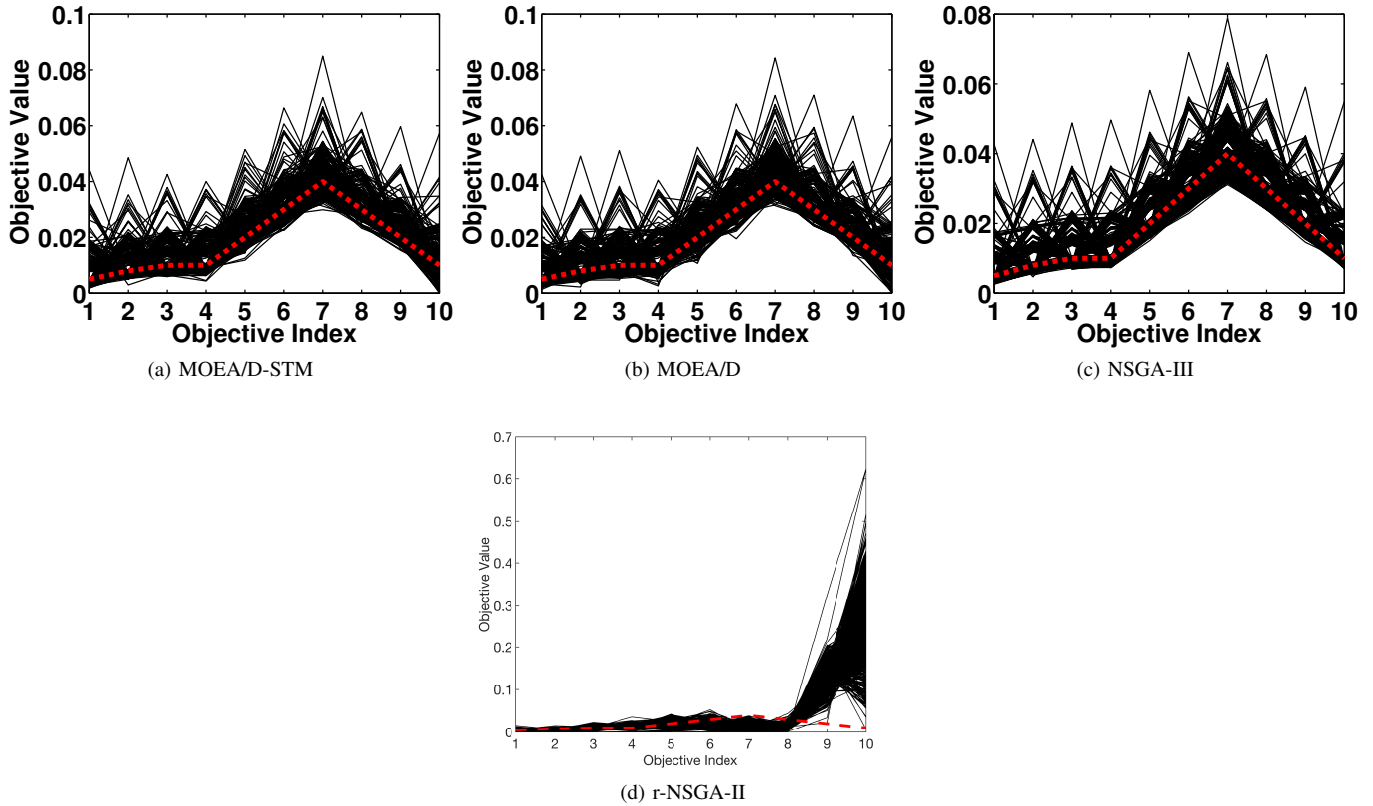


Fig. 113: Comparisons on 10-objective WFG48 where $\mathbf{z}^r = (0.005, 0.008, 0.01, 0.01, 0.02, 0.03, 0.04, 0.03, 0.02, 0.01)^T$.

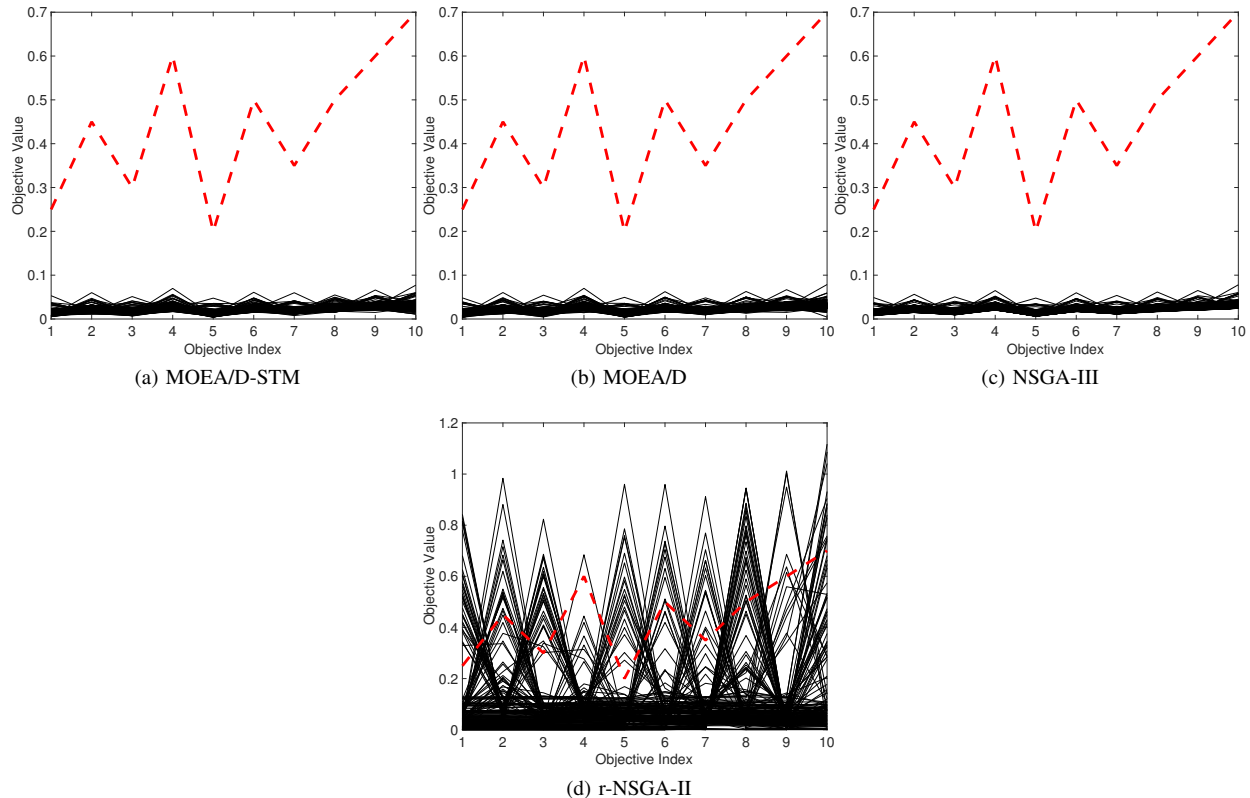


Fig. 114: Comparisons on 10-objective WFG48 where $\mathbf{z}^r = (0.25, 0.45, 0.3, 0.6, 0.2, 0.5, 0.35, 0.5, 0.6, 0.7)^T$.